

ลักษณะสมบัติและการแสดงออกของยีนโอ-เมทิลทรานส์เฟอเรสและบรอดคอมเพล็กซ์และโปรตีนในกุ้ง
กุลาดำ *Penaeus monodon*



นาย อรุณ บัวกลิ่น

ศูนย์วิทยทรัพยากร

วิทยานิพนธ์นี้เป็นส่วนหนึ่งของการศึกษาตามหลักสูตรปริญญาวิทยาศาสตรดุษฎีบัณฑิต

สาขาวิชาเทคโนโลยีชีวภาพ

คณะวิทยาศาสตร์ จุฬาลงกรณ์มหาวิทยาลัย

ปีการศึกษา 2553

ลิขสิทธิ์ของจุฬาลงกรณ์มหาวิทยาลัย

CHARACTERIZATION AND EXPRESSION OF O-METHYLTRANSFERASE
AND BROAD COMPLEX GENES AND PROTEINS IN THE GIANT TIGER
SHRIMP *Penaeus monodon*



Mr. Arun Buaklin

ศูนย์วิทยทรัพยากร
จุฬาลงกรณ์มหาวิทยาลัย

A Dissertation Submitted in Partial Fulfillment of the Requirements
for the Degree of Doctor of Philosophy of Science Program in Biotechnology

Faculty of Science

Chulalongkorn University

Academic Year 2010

Copyright of Chulalongkorn University

Thesis Title Characterization and expression of o-methyltransferase and broad complex genes and proteins in the giant tiger shrimp *Penaeus monodon*


By Mr. Arun Buaklin

Field of study Biotechnology

Thesis Advisor Professor Piamsak Menasveta, Ph.D.

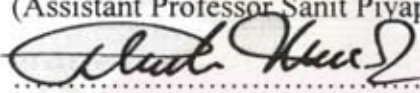
Thesis Co-advisor Sirawut Klinbunga, Ph.D.


Accepted by the Faculty of Science, Chulalongkorn University in Partial Fulfillment of the Requirements for the Doctoral Degree

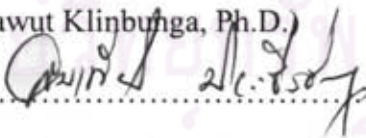
 Dean of the Faculty of Science
(Professor Supot Hannongbua, Dr.rer.nat.)


THESIS COMMITTEE

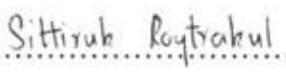
 Chairman
(Assistant Professor Sanit Piyapattanakorn, Ph.D.)

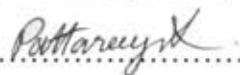
 Thesis Advisor
(Professor Piamsak Menasveta, Ph.D.)

 Thesis Co-advisor
(Sirawut Klinbunga, Ph.D.)

 Examiner
(Associate Professor Somkiat Piyatiratitivorakul, Ph.D.)

 Examiner
(Associate Professor Warawut Chulalaksananukul, Ph.D.)

 External Examiner
(Sittiruk Roytrakul, Ph.D.)

 External Examiner
(Pattareeya Ponza, Ph.D.)

นายอรุณ บัวกลิ่น: ลักษณะสมบัติและการแสดงออกของยีนโอ-เมทิลทรานส์เฟอเรส และบรอดคอมเพล็กซ์และโปรตีนในกุ้งกุลาดำ *Penaeus monodon* (CHARACTERIZATION AND EXPRESSION OF O-METHYLTRANSFERASE AND BROAD COMPLEX GENES AND PROTEINS IN THE GIANT TIGER SHRIMP *Penaeus monodon*.) อ.ที่ปรึกษาวิทยานิพนธ์หลัก : ศ.ดร.เปี่ยมศักดิ์ เมนะเศวต, อ.ที่ปรึกษาวิทยานิพนธ์ร่วม: ดร.ศิวารุณ กลิ่นนุหงา, 221 หน้า.

การหาลำดับนิวคลีโอไทด์และลักษณะสมบัติของยีนและโปรตีนที่เกี่ยวข้องกับการพัฒนารังไข่ เป็นจุดเริ่มต้นของความเข้าใจกลไกระดับโมเลกุลของการสมบูรณ์พันธุ์ของกุ้งกุลาดำ จึงหาลำดับนิวคลีโอไทด์ที่สมบูรณ์ของยีน *catechol-O-methyltransferase (PmCOMT)*, *farnesic-O-methyltransferase (PmFAMeT)*, *broad complex Z1 (PmBr-cZ1)* และ *broad complex Z4 (PmBr-cZ4)* โดยพบรูปแบบของยีน *PmCOMT* และ *PmBr-cZ4* เพียงรูปแบบเดียว และพบว่า *PmCOMT* และ *PmBr-cZ1* มี 2 รูปแบบของยีน นอกจากนี้ยังพบว่ายีน *PmCOMT* ประกอบด้วย 3 intron (ขนาด 194, 111 และ 361 คู่เบส) 2 exon (ขนาด 143 และ 147 คู่เบส)

เมื่อตรวจสอบการแสดงออกของยีนดังกล่าวด้วยวิธี quantitative real-time PCR พบว่ายีน *PmCOMT* มีระดับการแสดงออกที่ไม่แตกต่างกันในรังไข่ของกุ้งกุลาดำแม่พันธุ์ธรรมชาติปกติและกุ้งกุลาดำที่ตัดก้านตา ($P > 0.05$) และพบว่ายีน *PmFAMeT* มีระดับการแสดงออกที่สูงขึ้นในรังไข่ระยะที่สี่ของกุ้งกุลาดำแม่พันธุ์ปกติ ($P < 0.05$) แต่มีระดับการแสดงออกที่ไม่แตกต่างกันในรังไข่ของกุ้งกุลาดำที่ตัดก้านตา ($P > 0.05$) ส่วนระดับการแสดงออกของยีน *PmBr-cZ1* นั้นลดลงในรังไข่ระยะที่สองและสามของกุ้งกุลาดำปกติ ($P < 0.05$) โดยการตัดก้านตามีผลให้การแสดงออกของยีนนี้เพิ่มขึ้น ($P < 0.05$) ในขณะที่ยีน *PmBr-cZ4* มีระดับการแสดงที่ลดลงในระยะที่สี่ในกุ้งกุลาดำแม่พันธุ์ปกติ ($P < 0.05$) และการตัดก้านตามีผลให้การแสดงออกของยีนนี้ลดลง ($P < 0.05$)

ตรวจสอบผลของซีโรโทนิน (5-HT) โปรเจสเตรโรน และ 20-hydroxyysteriod (20-E) ต่อการแสดงออกของยีนดังกล่าวในกุ้งแม่พันธุ์ตัดพันธุ์และกุ้งเลี้ยงขนาดวัยรุ่น พบว่าระดับการแสดงออกของยีน *PmFAMeT* จะเพิ่มขึ้นประมาณ 50 เท่า หลังถูกฉีดด้วย 5-HT เป็นเวลา 1 ชั่วโมง ($P < 0.05$) แต่ไม่พบระดับการแสดงออกที่แตกต่างกันของยีนต่างๆในกุ้งกุลาดำแม่พันธุ์ที่ถูกกระตุ้นด้วยโปรเจสเตรโรน แต่พบว่าการฉีด 20E ส่งผลให้ระดับการแสดงออกของยีน *PmCOMT* ในรังไข่ของกุ้งวัยรุ่นลดลง ($P < 0.05$) แต่ส่งผลให้ยีน *PmFAMeT*, *PmBr-cZ1* และ *PmBr-cZ4* มีการแสดงออกที่สูงขึ้น ($P < 0.05$)

เมื่อตรวจสอบตำแหน่งการแสดงออกของยีนที่สนใจในรังไข่ของกุ้งกุลาดำด้วยวิธี *in situ hybridization* พบว่า *PmCOMT*, *PmFAMeT*, *PmBr-cZ1* และ *PmBr-cZ4* มีตำแหน่งการแสดงออกของ mRNA ในส่วนของไฮโปทาลามัสของเซลล์ไข่ระยะ previtellogenesis โดยพบการแสดงออกของยีน *PmCOMT* ในส่วนของไฮโปทาลามัสของ follicular cell และ ไฮโปเนียอีกด้วย

สร้างโปรตีนลูกผสมของ *PmCOMT*, *PmFAMeT-H* และ *PmFAMeT-S* ในแบคทีเรีย และผลิตโพลีโคลอนแอนติบอดีของโปรตีนดังกล่าวในกระต่าย เมื่อตรวจสอบระดับการแสดงออกของโปรตีนในรังไข่ของกุ้งกุลาดำ พบว่าโปรตีน *PmCOMT* มีระดับการแสดงออกในรังไข่ระยะที่หนึ่งและสองสูงกว่าในรังไข่ระยะที่สามและสี่ ในขณะที่พบระดับการแสดงออกของโปรตีน *PmFAMeT* ในรังไข่ระยะที่หนึ่งและสอง แต่ไม่พบการแสดงออกในรังไข่ระยะที่สามและสี่ของกุ้งแม่พันธุ์ธรรมชาติ และพบว่าในกุ้งวัยรุ่นมีแถบโปรตีน *PmFAMeT* ขนาด 32 และ/หรือ 37 kDa โดยพบเฉพาะแถบโปรตีนขนาด 37 kDa ในรังไข่ของกุ้งแม่พันธุ์ธรรมชาติ

ผลจาก immunohistochemistry พบโปรตีน *PmCOMT* ในส่วนไฮโปทาลามัสของไข่ระยะที่หนึ่งและสอง แต่พบ *PmCOMT* ในคอติคูลารอดของไข่ระยะที่สามและสี่ของกุ้งกุลาดำแม่พันธุ์ปกติและกุ้งกุลาดำที่ตัดก้านตา ส่วนโปรตีน *PmFAMeT* นั้นพบว่ายูอยู่ในส่วนคอติคูลารอดของไข่ระยะที่สามและสี่ในทั้งกุ้งกุลาดำแม่พันธุ์ปกติและกุ้งกุลาดำที่ตัดก้านตา โดยไม่พบโปรตีนนี้ในรังไข่ระยะที่หนึ่งและสอง ผลการทดลองบ่งชี้ว่ายีนและโปรตีน *PmCOMT*, *PmFAMeT*, *PmBr-cZ1* และ *PmBr-cZ4* มีหน้าที่สำคัญเกี่ยวกับการพัฒนาไข่ของกุ้งกุลาดำ นอกจากนี้ยังพบว่ารูปแบบการแสดงออกของยีน *PmFAMeT*, *PmBr-cZ1* และ *PmBr-cZ4* สามารถใช้เป็นชีวเครื่องหมายสำหรับติดตามการพัฒนาไข่และรังไข่ของกุ้งกุลาดำ

สาขาวิชา.....เทคโนโลยีชีวภาพ.....ลายมือชื่อ.....อรุณ บัวกลิ่น.....
ปีการศึกษา....2553.....ลายมือชื่อ อ.ที่ปรึกษาวิทยานิพนธ์หลัก.....
ลายมือชื่อ อ.ที่ปรึกษาวิทยานิพนธ์ร่วม.....

497 38632 23 : MAJOR BIOTECHNOLOGY

KEYWORDS : *Penaeus monodon* / GIANT TIGER SHRIMP / PmFAMeT / PmCOMT / BROAD COMPLEX

ARUN BUAKLIN : CHARACTERIZATION AND EXPRESSION OF O-METHYLTRANSFERASE AND BROAD COMPLEX GENES AND PROTEINS IN THE GIANT TIGER SHRIMP *Penaeus monodon*. THESIS ADVISOR : PROF.PIAMSAK MENASVETA, Ph.D., THESIS CO-ADVISOR : SIRAWUT KLINBUNGA, Ph.D., 221 pp.

Identification and characterization of genes and proteins involved in ovarian development are the initial step necessary for understanding molecular mechanisms of reproductive maturation in the giant tiger shrimp (*Penaeus monodon*). The full length cDNAs of catechol-O-methyltransferase (PmCOMT), farnesoic-O-methyltransferase (PmFAMeT), broad complex Z1 (PmBr-cZ1) and broad complex Z4 (PmBr-cZ4) were successfully characterized. Only a single form of PmFAMeT and PmBr-cZ4 was found but two isoforms were observed in PmFAMeT (PmFAMeT-l and PmFAMeT-s) and PmBr-cZ1 (PmBr-cZ1-l and PmBr-cZ1-s). In addition, genomic organization of PmCOMT (3 exons of 194, 111 and 361 bp and 2 introns of 143 and 147 bp) was also isolated.

Quantitative real-time PCR indicated that the expression level PmCOMT was not significantly different during ovarian development in both intact and eyestalk-ablated *P. monodon* broodstock ($P > 0.05$). PmFAMeT mRNA was significantly up-regulated at stage IV ovaries in intact wild broodstock ($P < 0.05$). In contrast, its expression level was not significantly different during ovarian development of eyestalk-ablated broodstock ($P > 0.05$). In intact wild broodstock, PmBr-cZ1 was significantly down-regulated at stages II and III ovaries ($P < 0.05$) and returned to the basal level at stage IV ovaries and after spawning. Eyestalk ablation resulted in its up-regulation at stage IV ovaries of *P. monodon* broodstock. The level of PmBr-cZ4 mRNA was down-regulated at stage IV ovaries of intact *P. monodon* broodstock ($P < 0.05$). Nevertheless, this transcript was up-regulated at stage IV ovaries of eyestalk-ablated broodstock ($P > 0.05$).

Effects of serotonin (5-HT), progesterone (P4) and 20-hydroxysteroid (20E) on expression of these genes in domesticated shrimp were examined. Serotonin administration immediately elevated the expression level of FAMEt approximately 50 fold at 1 hpi ($P < 0.05$). In contrast, progesterone had no effects on expression of these genes ($P > 0.05$). The expression levels of PmCOMT (at 6 hpi), PmBr-cZ1 (at 168 hpi) and PmBr-cZ4 (at 168 hpi) in ovaries of juvenile *P. monodon* was significantly decreased following 20E treatment ($P < 0.05$).

In situ hybridization revealed that PmFAMeT, PmBr-cZ1 and PmBr-cZ4 transcripts were localized in cytoplasm of previtellogenic oocytes while PmCOMT mRNA was clearly observed in the cytoplasm of follicular cells, oogonia and previtellogenic oocytes.

Recombinant protein of PmCOMT, PmFAMeT-l and PmFAMeT-s were successfully expressed *in vitro*. The polyclonal antibody against each recombinant protein was produced. Western blot analysis indicated more preferentially expressed of PmCOMT in previtellogenic and vitellogenic ovaries than that in early cortical rod and mature ovaries of *P. monodon*. PmFAMeT was found in ovaries of juveniles and stages I and II ovaries of broodstock. Interestingly, juvenile shrimp possessed either 32 kDa, 37 kDa or both positive bands whereas only a 37 kDa band owing to posttranslational modifications of ovarian FAMEt was observed in stages I and II ovaries of shrimp broodstock.

Immunohistochemistry revealed the positive signals of the PmCOMT protein in cytoplasm of previtellogenic and vitellogenic oocytes. Subsequently, the positive signals were observed in cortical rods of stages III and IV oocytes in both intact and eyestalk-ablated broodstock. Interestingly, the PmFAMeT protein was detected in stages III and IV oocytes but not in stage I and II oocytes of *P. monodon* broodstock. Taken the information together PmCOMT, PmFAMeT, PmBr-cZ1 and PmBr-cZ4 gene products seem to play the important role on ovarian development and PmFAMeT, PmBr-cZ1 and PmBr-cZ4, in particular, may be used as the bioindicators for monitoring progression of oocyte/ovarian maturation in *P. monodon*.

Field of Study : Biotechnology Student's Signature Arun Buaklin

Academic Year : 2010 Advisor's Signature [Signature]

Co-Advisor's Signature [Signature]

ACKNOWLEDGEMENTS

I would like to express my deepest sense of gratitude to my advisor, Professor Dr. Piamsak Menasveta and my co-advisor, Dr. Sirawut Klinbunga for their guidance, encouragement, valuable suggestion and supports throughout my study.

My sincere gratitude is also extended to Assist. Prof. Dr. Sanit Piyapattanakorn, Assoc. Prof. Dr. Somkiat Piyateeratitivorakul, Assoc. Prof. Dr. Warawut Chulalaksananukul, Dr. Sittiruk Roytrakul and Dr. Pattareeya Ponza for serving as thesis committee and for providing useful suggestions and recommendations of my thesis.

I would particularly like to thank Dr. Sage Chaiyapechara for his critical suggestion on the review of shrimp endocrinology. I wish to acknowledge the Center of Excellent in Marine Biotechnology, Aquatic Molecular Genetics and Biotechnology, National Center for Genetic Engineering and Biotechnology (BIOTEC), National Science and Technology Development Agency (NSTDA) for facilities required by the experiments and Thailand Graduate Institute of Science and Technology (TGIST) for my scholarship.

Thanks are also express to all my friends in Sukhothai Wittayakom, Biotechnology of Chiang Mai University (CMU) and Chulalongkorn University (CU) for their kind friendships.

Finally, I would like to express my deepest gratitude to my parents, my brother and my sister for their love, care, understanding and encouragement extended throughout my study.

CONTENTS

	Page
THAI ABSTRACT.....	iv
ENGLIST ABSTRACT.....	v
ACKNOWLEDGMENTS.....	vi
CONTENTS.....	vii
LIST OF TABLES.....	xv
LIST OF FIGURES.....	xvii
LIST OF ABBREVIATIONS.....	xix
CHAPTER I INTRODUCTION.....	1
1.1 Background information and objectives of this thesis.....	4
1.2 Objective of this thesis.....	4
1.3 General introduction.....	6
1.4 Taxonomy of <i>P. monodon</i>	6
1.5 Morphology.....	7
1.6 Female reproductive system.....	7
1.6.1 Morphology of female reproductive system.....	8
1.6.2 Ovarian development.....	12
1.7 Vitellogenesis and oocyte maturation.....	13
1.8 Hormonal control of shrimp and Female reproductive hormone..	13
1.8.1 Hormonal control of shrimp.....	16
1.8.2 Female reproductive hormone.....	16
1.8.2.1 Eyestalk hormone.....	18
1.8.2.2 Ecdysteroids.....	20
1.8.2.3 Vertebrate-type steroid hormones.....	23
1.8.2.4 Prostaglandins and other eicosanoids.....	23
1.9 Molecular technique used for studies in this thesis.....	26
1.9.1 PCR.....	27

	Page
1.9.2 Reverse Transcription-polymerase chain reaction (RT-PCR) and semiquantitative RT-PCR.....	27
1.9.3 Rapid Amplification of cDNA End-polymerase chain reaction	28
1.9.4 Genome walk analysis.....	29
1.9.5 DNA sequencing.....	34
1.9.6 Quantitative real-time PCR.....	34
1.9.7 <i>In situ</i> hybridization.....	37
1.10 Effects of <i>O</i> -methyltransferase and ecdysteroids on ovarian.....	39
1.10.1.1 Catechol- <i>O</i> -methylation (COMT).....	39
1.10.1.2 Farnesoic acid- <i>O</i> -methyltransferase (FAMeT).....	41
1.10.2 Broad-Complex (Br-c).....	47
CHAPTER II MATERIALS AND METHODS.....	51
2.1 Experimental animals.....	51
2.2 Nucleic acid extraction.....	52
2.2.1 Genomic DNA extraction.....	52
2.2.2 RNA extraction.....	53
2.2.3 Preparation of DNase I-free total RNA.....	53
2.3 Measuring concentration of nucleic acids by spectrophotometry	54
2.4 Agarose gel electrophoresis.....	54
2.5 Isolation and characterization of the full length cDNA and genomic DNA using rapid amplification of cDNA ends - Polymerase chain reaction (RACE-PCR) and genome walking technique...	55
2.5.1 RACE-PCR.....	55
2.5.1.1 Preparation of the 5' and 3' RACE-PCR template.....	55
2.5.1.2 RACE-PCR and cloning of amplification products....	56

	Page
2.5.2 Genome walking analysis.....	56
2.5.2.1 Digestion of genomic DNA	58
2.5.2.2 Ligation of genomic DNA to GenomeWalker	58
2.5.2.3 PCR-based genomic DNA walking.....	59
2.5.2.4 Overlapping PCR of genomic <i>PmCOMT</i>	59
.. 2.6 Cloning of PCR-amplified DNA.....	60
2.6.1 Elution of DNA from agarose gels.....	60
2.6.2 Ligation of PCR product to pGEM-T easy vector.....	61
2.6.3 Preparation of competent cells.....	61
2.6.4 Transformation of the ligation product to E.coli host cells	61
2.6.5 Detection of recombinant clone by colony PCR.....	62
2.6.6 Isolation and digestion of recombinant plasmid DNA.....	62
2.6.7 DNA sequencing.....	63
2.7 Phylogenetic analysis.....	63
2.8 RT-PCT and tissue distribution analysis of P _{COMT} , P _{FAMeT} , P _{mBr-C Z1} and P _{mBr-C Z4}	64
2.8.1 Primer design.....	64
2.8.2 First strand cDNA synthesis.....	64
2.8.3 RT-PCR analysis.....	65
2.8.4 Tissue distribution analysis by RT-PCR.....	65
2.9 Semi-quantitative RT-PCR.....	66
2.9.1 Primers.....	66

	Page
2.9.3 Determination of PCR conditions.....	66
2.9.4 Primer concentration.....	67
2.9.5 MgCl ₂ concentration.....	67
2.9.6 Cycle number	67
2.9.7 Gel electrophoresis and quantitative analysis.....	67
2.10 Effects of dopamine and serotonin on expression of genes in Ovaries of juvenile <i>P. monodon</i>	68
2.10.1 Dopamine administration.....	68
2.10.2 Serotonin administration.....	69
2.10.3 Data analysis.....	69
2.11 Quantitative real-time PCR of PmCOMT, PmFAMeT, PmBr-C Z1 and PmBr-C Z4 in ovaries of <i>P. monodon</i>	69
2.11.1 Experimental animals.....	69
2.11.1.1 Intac wild and domesticated <i>P. monodon</i> used for expression analysis of various genes during ovarian	69
2.11.1.2 Serotonin administration.....	70
2.11.1.3 Progesterone administration.....	70
2.11.1.4 20 β -hydroxyecdysone administration.....	70
2.11.2 Primer design and construction of the standard curve.....	71
2.11.3 Quantitative real-time PCR analysis.....	71
2.12 In situ hybridization (ISH).....	72
2.12.1 Sample preparation.....	73

	Page
2.12.2 Preparation of cRNA probes.....	74
2.12.3 Synthesis of the cRNA probes.....	74
2.12.4 Dot blot analysis.....	75
2.12.5 Hybridization and detection.....	75
2.13 <i>In vitro</i> expression of recombinant protein using the bacterial....	75
2.13.1 Primer design.....	77
2.13.2 Construction of recombinant plasmid in cloning and expres	78
2.13.3 Expression of recombinant proteins.....	79
2.13.4 Purification of recombinant proteins.....	79
2.13.5 Peptide sequencing of recombinant proteins.....	79
2.13.5.1 In-gel digestion.....	79
2.13.5.2 NanoLC-MS/MS.....	80
2.13.5.3 Database searches.....	80
2.13.6 Polyclonal antibody production and western blot analysi	81
2.14 Immunohistochemistry.....	81
CHAPTER III RESULTS.....	82
3.1 Isolation and characterization of the full length cDNA of <i>COMT</i>	
<i>,PmFAMeT</i> and <i>PmBr-c</i> genes in <i>P. monon</i>	82
3.1.1 Total RNA extraction and first strand synthesis.....	82

	Page
3.1.3 Characterization of full length cDNA of <i>PmFAMeT</i>	82
3.1.4 Characterization of the full length cDNA of <i>PmBr-c</i> gene...	86
3.1.4.1 <i>PmBr-cZl</i>	93
3.1.4.2 <i>PmBr-CZ4</i> genes	99
3.2 Characterization of the genomic organization <i>PmCOMT</i> by using Genome Walking Technique.....	104
3.3 Phylogenetic analysis	107
3.3.1 Phylogenetic analysis of <i>PmCOMT</i>	109
3.4. Determination of expression profile and tissue distribution of <i>PmCOMT</i> , <i>PmFAMeT</i> , <i>PmBr-CZl</i> and <i>PmBr-CZ4</i> genes	109
3.4.1 Determination of expression profile of <i>PmCOMT</i> , <i>PmFAMeT</i> <i>PmBr-cZl</i> and <i>PmBr-cZ4</i> genes in <i>P. monodon</i> by RT-PCR...	117
3.4.2 Tissue distribution analysis of <i>PmCOMT</i> , <i>PmFAMeT</i> , <i>PmBr-</i> <i>cZl</i> and <i>PmBr-cZ4</i> genes in <i>P. monodon</i> examined by RT-PCR..	117
3.4.2.1 <i>PmCOMT</i>	118
3.4.2.2 <i>PmFAMeT</i>	118
3.4.2.2 <i>PmBr-cZl</i>	119
3.4.2.4 <i>PmBr-cZ4</i>	120
3.4.3 Expression levels of <i>PmCOMT</i> and <i>PmFAMeT</i> during ovarian development of wild <i>P. monodon</i> examined by semi..	120
3.4.3.1 Optimization of PCR conditions	121

	Page
3.4.3.2 The expression profiles of <i>PmCOMT</i> and <i>PmFAMeT</i> in ovaries of <i>P. monodon</i> following dopamine and serotonin	122
3.4.3.2 Dopamine administration.....	122
3.4.3.2 Serotonin administration.....	127
3.5 Quantitative real-time PCR analysis of <i>PmCOMT</i> , <i>PmFAMeT</i> ,	129
3.5.1 Expression profiles of <i>COMT</i> during ovarian development..	130
3.5.2 Expression profiles of <i>FAMeT</i> during ovarian development..	132
3.5.3 Expression profiles of <i>Br-cZ1</i> during ovarian development..	135
3.5.4 Expression profiles of <i>Br-cZ4</i> during ovarian development ..	138
3.6 Effects of 5-HT, progesterone and 20 β -hydroxyecdysone administration on transcription of reproduction-related genes in ovaries ...	140
3.6.1 Effects of 5-HT administration on transcription of <i>PmCOMT</i> , <i>PmFAMeT</i> , <i>PmBr-cZ1</i> and <i>PmBr-cZ4</i> in ovaries of domesticated ..	140
3.6.2 Effects of progesterone administration on transcription of <i>COMT</i> , <i>PmFAMeT</i> , <i>PmBr-cZ1</i> and <i>PmBr-cZ4</i> in ovaries.....	151
3.6.2.1 18-month-old shrimp.....	151
3.6.2.1 14-month-old domesticated broodstock.....	151
3.7 Localization of all genes and protein in ovaries of <i>P. monodon</i>	156
3.7.1 Localization of all genes in ovaries of <i>P. monodon</i>	156
3.7.1.1 Quantification of the cRNA probe.....	156
3.7.1.2 <i>In situ</i> hybridization (ISH).....	158
3.8 <i>In vitro</i> expression of recombinant using the bacterial expression .	168

	Page
3.8.2 Optimization of conditions for an <i>in vitro</i> expression	175
3.8.3 Cell localization of recombinant protein.....	181
3.8.4 Purification of recombinant protein.....	185
3.8.5 Peptide sequencing of purified recombinant protein.....	187
3.8.6 The production of polyclonal antibodies against	187
3.8.7 Expression profiles of COMT, PFAMeT-I and FAMeT-s proteins during ovarian development of <i>P. monodon</i>	189
3.9 Localization of all proteins in ovaries of <i>P. monodon</i>	190
CHAPTER IV DISCUSSION.....	197
CHAPTER V CONCLUSION.....	206
REFERENCES.....	208
APPENDICES.....	219
BIOGRAPHY.....	221

LIST OF TABLES

	Page
Table 1.1 Export of the giant tiger shrimp from Thailand during 2002-2007	5
Table 1.2 A summary on the ovarian maturation stages in <i>P. monodon</i> based on histological studies (Tan-Fermin.J.D., and Pudadera. R.A., 1989).....	11
Table 2.1 Primer sequences for the first strand cDNA synthesis and RACE-PCR.....	56
Table 2.2 The gene specific primer (GSP1), their sequences and T _m of COMT, FAMeT and Br-C gene.	57
Table 2.3 Composition of 5'-RACE-PCR.....	58
Table 2.4 Composition of 3'-RACE-PCR.....	58
Table 2.5 The gene specific primer (GSP1), their sequences and T _m of PmCOMT, PmFAMeT, PmBr-C Z1 and PmBr-C Z4 gene for RT-PCR and Tissue distribution analysis.....	68
Table 2.6 Nucleotide sequences and T _m of primers used for quantitative real-time PCR of PmCOMT, PmFAMeT , PmBr-C Z1, PmBr-C Z4 and EF1	76
Table 2.7 Nucleotide sequences and T _m of primers for synthesis of the cRNA probes of PmCOMT, PmFAMeT, PmBrCZ1 and PmBrCZ4.....	77
Table 3.1 Relative expression level of <i>PmCOMT</i> in ovaries and testes of <i>P. monodon</i>	132
Table 3.2 Relative expression level of <i>PmFAMeT</i> ovaries and testes of <i>P. monodon</i>	110
Table 3.3 Relative expression level of <i>PmBr-cZ1</i> ovaries and testes of <i>P. monodon</i>	111
Table 3.4 Relative expression level of <i>PmBr-C Z4</i> in ovaries and testes of <i>P. monodon</i>	114
Table 3.5 Optimized MgCl ₂ and primer concentrations, number of amplification cycles and thermal profiles for semi-quantitative RT-PCR of <i>EF1-α</i> , <i>PmCOMT</i> and <i>PmFAMeT</i> in ovaries of <i>P. monodon</i>	121
Table 3.6 Time course relative expression levels of <i>PmCOMT</i> and <i>PmFAMeT</i> in different ovarian stages of intact <i>P. monodon</i>	124
Table 3.7 Time course relative expression levels of <i>PmCOMT</i> and <i>PmFAMeT</i> in different ovarian stages of eyestalk-ablated <i>P. monodon</i>	126
Table 3.8 Time course relative expression levels of <i>PmCOMT</i> and <i>PmFAMeT</i> in ovaries of <i>P. monodon</i> treated with dopamine at 10 ⁻⁶ M/shrimp.....	127
Table 3.9 Time course relative expression levels of <i>PmCOMT</i> and <i>PmFAMeT</i> in ovaries of <i>P. monodon</i> juveniles treated serotonin (50 ug/g body weight).....	128

	Page
Table 3.10 Relative expression levels of <i>PmCOMT</i> in different ovarian stages of wild (A) and domesticated (B) <i>P. monodon</i> female broodstock.....	135
Table 3.11 Relative expression levels of <i>PmFAMeT</i> in different ovarian stages of wild (A) and domesticated (B) <i>P. monodon</i> female broodstock.....	135
Table 3.12 Relative expression levels of <i>PmBr c ZI</i> in different ovarian stages of wild (A) and domesticated (B) <i>P. monodon</i> female broodstock.....	138
Table 3.13 Relative expression levels of <i>PmBr-cZ4</i> in different ovarian stages of wild (A) and domesticated (B) <i>P. monodon</i> females....	141
Table 3.14 Time course relative expression levels of <i>PmCOMT</i> in ovaries of 18-month-old <i>P. monodon</i> treated with serotonin (50 µg/g body weight).....	142
Table 3.15 Time course relative expression levels of <i>PmFAMeT</i> in ovaries of 18-month-old <i>P. monodon</i> treated with serotonin (50 µg/g body weight).....	143
Table 3.16 Time course relative expression levels of <i>PmBr-cZI</i> in ovaries of 18-month-old <i>P. monodon</i> treated with serotonin (50 µg/g body weight).....	144
Table 3.17 Time course relative expression levels of <i>PmBr-cZ4</i> in ovaries of juvenile <i>P. monodon</i> treated with serotonin (50 µg/g body weight).....	145
Table 3.18 Time course relative expression levels of <i>PmCOMT</i> in ovaries of 18-month-old <i>P. monodon</i> treated with progesterone (0.1 µg/g body weight).....	146
Table 3.19 Time course relative expression levels of <i>PmFAMeT</i> in ovaries of 18-month-old <i>P. monodon</i> treated with progesterone (0.1 µg/g body weight).....	147
Table 3.20 Time course relative expression levels of <i>PmCOMT</i> in ovaries of 14-month-old <i>P. monodon</i> treated with progesterone (0.1µg/g body weight).....	148
Table 3.21 Time course relative expression levels of <i>PmFAMeT</i> in ovaries of 14-month-old <i>P. monodon</i> treated with progesterone (0.1 µg/g body weight).....	149
Table 3.22 Time course relative expression levels of <i>PmBr-cZI</i> in ovaries of 14- month-old <i>P. monodon</i> treated with progesterone (0.1 µg/g body eight).....	150
Table 3.23 Time course relative expression levels of <i>PmBr-cZ4</i> in ovaries of 14-month-old <i>P. monodon</i> treated with progesterone (0.1µg/g body weight).....	151
Table 3.24 Time course relative expression levels of <i>PmCOMT</i> in ovaries of cultured <i>P. monodon</i> juveniles treated with 20E(1µg/g body weight).....	152

	Page
Table 3.25 Time course relative expression levels of <i>PmFAMeT</i> in ovaries of cultured <i>P. monodon</i> juveniles treated with 20E(1µg/g body weight).....	153
Table 3.26 Time course relative expression levels of <i>PmBr-cZ1</i> in ovaries of cultured <i>P. monodon</i> juveniles treated with 20E (1µg/g body weight).....	154
Table 3.27 Time course relative expression levels of <i>PmBr-cZ4</i> in ovaries of cultured <i>P. monodon</i> juveniles treated with 20E (1 µg/g body weight).....	155
Table 3.28 A summary for localization of <i>PmCOMT</i> , <i>PmFAMeT</i> , <i>PmBr-cZ1</i> and <i>PmBr-cZ4</i> transcripts in ovaries of intact and eyestalk-ablated <i>P. monodon</i> broodstock determined by <i>in situ</i> hybridization.....	167
Table 3.29 Titters of anti-PmCOMT after the rabbit was immunized rPmCOMT for 4 times.....	188
Table 3.30 Titters of anti-PmFAMeT-I after the rabbit was immunized rPmFAMeT-I for 5 times.....	188
Table 3.31 Titters of anti-PmFAMeT-s after the rabbit was immunized rPmFAMeT-s for 3 times.....	188

LIST OF FIGURES

FIGURE		Page
Figure 1.1	Lateral view of the external morphology of <i>P. monodon</i>	7
Figure 1.2	Lateral view of the internal anatomy of a female <i>P. monodon</i> .	8
Figure 1.3	The illustration of an ovary extending the entire length of prawn (a) and complete ovaries of <i>P. monodon</i> females scored from stages II to IV (b). Note the color change that is due to an increasing carotenoid content.....	9
Figure 1.4	The location and anatomy of each stage of <i>P. monodon</i> ovary	11
Figure 1.5	Schematic diagram of the endocrine control of vitellogenesis in shrimp, MF:methyl farnesoate, MOIH:mandibular organ inhibiting hormone, Vg:vitellogenin.....	14
Figure 1.6	Diagram illustrating the hormonal controls of physiological processes of penaeid shrimp.....	15
Figure 1.7	diagram to show complexity of controls in endocrine controlling growth and maturation in female crustacean.....	16
Figure 1.8	Major endocrine and neuro-endocrine structures of generalized female crustacean. Included are the organs important for female reproduction, the eyestalk sinus gland x-organ, the mandibular organ, Y-organ, and thoracic ganglion.(Laufer et al.).....	17
Figure 1.9	The reproduction cycle of crustacean	18
Figure 1.10	The biologically active ecdysteroid.....	19
Figure 1.11	The chemical structures of ecdysteroids and methyl farnesoate (MF).....c.....	20
Figure 1.12	The malonate pathway and juvenile hormone biosynthesis in insects	21
Figure 1.13	General illustration of the polymerase chain reaction (PCR) for amplifying DNA.....	23
Figure 1.14	Mechanism of a SMART™ technology cDNA synthesis. First-strand synthesis is primed using a modified oligo (dT) primer	25
Figure 1.15	A flow chart illustrating the GenomeWalk analysis protocol.	26
Figure 1.16	The <i>O</i> -methylation of the catechol substrate catalysed by COMT.	30
Figure 1.17	Complexities of estrogen metabolism. Abbreviations used. ST;sulfotranferase, GT:glucosyltransferase, EAT:estrogen acyltransferase, 17β-HSD:17βhydroxysteroid dehydrogenase, COMT:catechol- <i>O</i> -methyltransferase and P450:cytochrome P450.....	32

FIGURE	Page
Figure 1.18 Models for the regulation of glue, early, and late gene transcription by the BR-C+ and E74' functions.....	40
Figure 2.1 The pET-15b vector map	48
Figure 3.1 A 0.8% ethidium bromide-stained agarose gel showing the quality of RNA from ovaries (Lanes = 1 - 6) of <i>P. monodon</i> . Lanes M is λ /Hind III marker.....	64
Figure 3.2 Nucleotide sequence of a COMT homologue from haemocyte cDNA library of <i>P. monodon</i> . The positions of sequences primers were illustrated in boldface and underlined and start codon were illustrated in boldface, respectively. (A) and BlastX results of nucleotide sequence of a COMT homologue from EST (B).....	65
Figure 3.3 The 3' RACE-PCR of <i>PmCOMT</i> (lanes 1) and a 100 bp (lanes m) DNA ladder were used as the markers.....	65
Figure 3.4 Nucleotide sequence of 3'UTR of COMT was generated by 3'RACE PCR primary primer and upm. The positions of sequencing primers are illustrated in boldface and underlined...	66
Figure 3.5 The full length cDNA of <i>COMT</i> (A), BlastX result of <i>COMT</i> and Coding nucleotides and deduced amino acids of <i>COMT</i> (C). Nucleotide sequences illustrating organization of <i>PmCOMT</i> genes. Coding nucleotides and deduced amino acids of each exon are capitalized.. Start and stop codons are illustrated in boldface and underlined. The catechol- <i>O</i> -Methyltransferase domain is highlighted. Polyadenylation signals (AATAAA) are underlined.....	66
Figure 3.6 Schematic diagrams of <i>PmCOMT</i> gene (A) and deduced proteins (B).....	67
Figure 3.7 Partial nucleotide sequence of a FAMEt from <i>P. monodon</i> . The positions of sequences primers were illustrated in boldface and underlined (A) and BlastX results of nucleotide sequence of a FAMEt homologue from partial cDNA of <i>P. monodon</i> ...	67
Figure 3.8 5'and 3' RACE-PCR of <i>PmFAMEt</i> (lanes 1 and 2, respectively) and a 100 bp (lanes m) DNA ladder were used as the markers. Nucleotide sequence of 5'UTR of PmFAMEt was generated by 5'RACE PCR secondary primer and nested upm.....	68
Figure 3.9 Nucleotide sequence of 3'UTR of <i>PmFAMEt</i> was generated by 3'RACE PCR primary primer and upm. The positions of sequencing primers are illustrated in boldface and underlined..	68

FIGURE	Page
Figure 3.10 Full length cDNA combination between 5'RACE, 3'RACE and parcial cDNA sequence of <i>P. monodon</i> (A) The positions of sequencing primers are illustrated in boldface and underlined. And results of nucleotide sequence of a FAMeT homologue from partial cDNA of <i>P. monodon</i> (B).....	69
Figure 3.11 Nucleotide sequence of <i>PmFAMeT-l</i> (A) and <i>PmFAMeT-s</i> (B) was generated by RT-PCR primer And results of nucleotide sequence of a FAMeT homologue from partial cDNA of <i>P. monodon</i> (C).....	69
Figure 3.12 Nucleotide sequence of <i>PmFAMeT-l</i> (A), <i>PmFAMeT-s</i> (B) and amino acid alignment of PmFAMeT-l and PmFAMeT-s (C)...	74
Figure 3.13 The full length cDNA and deduced amino acids of <i>PmFAMeT-l</i> (A) and <i>PmFAMeT-s</i> (B) which are different according to a pentapeptide (EGRGS, undelined)(C). The start and stop codons are boldfaced and undelined. The poly A additional signal (AATAAA) is boldfaced, italicized and underlined. Crustacean FAMeT domains (positions 8 - 138 and 144 – 278) in the deduced FAMeT are highlighted. The diagram representing PmFAMeT is also illustrated.....	75
Figure 3.14 Schematic diagrams of PmFAMeT deduced proteins.....	77
Figure 3.15 Nucleotide sequence of a BrC-Z1 homologue. The positions of sequences primers were illustrated in boldface and underlined (A) and BlastX results of nucleotide sequence of a BrC-Z1 homologue from EST (B).....	78
Figure 3.16 Nucleotide sequence of 5'UTR of <i>PmBr-C Z1</i> was generated by 5'RACE PCR using secondary primer and upm.....	79
Figure 3.17 Nucleotide sequence of 3'UTR of <i>PmBr-C Z1</i> was generated by 3'RACE PCR using secondary primer and upm, sequenced with M13R. The positions of sequencing primers are illustrated in boldface and underlined.....	81
Figure 3.18 Nucleotide sequence of 5'UTR of <i>PmBr-C Z1</i> was generated by 5'RACE PCR using secondary primer and upm, sequenced with M13F. The positions of sequencing primers are illustrated in boldface and underlined.....	84
Figure 3.19 Nucleotide sequence of 3'UTR of <i>PmBr-C Z1</i> was generated by 3'RACE PCR using secondary primer and upm, sequenced with 3BRCZ1-F. The positions of sequencing primers are illustrated in boldface and underlined.....	86
Figure 3.20 Nucleotide sequence of a PmBr-C Z1-l.....	87

Figure 3.22	Nucleotide sequence of 5'UTR-2 of PmBr-C Z1 was generated by 5'RACE PCR using secondary primer and upm, sequenced with M13F. The positions of sequencing primers are illustrated in boldface and underlined.....	91
Figure 3.23	Nucleotide sequence of a <i>PmBr-C Z1-s</i>	93
Figure 3.24	The full length cDNA of <i>BrC-Z1-s</i> (a) and <i>Z1-l</i> (b) (The start and stop codons are illustrated in boldface. The poly A additional signal site are underlined. And the glycosylation site are red and amino acid alignment of <i>BrC-Z1-s</i> and <i>Z1-l</i>	94
Figure 3.25	Schematic diagrams of PmBr-C Z1-l (A) and PmBr-C Z1-s (B) deduced proteins.....	96
Figure 3.26	Nucleotide sequence of a BrC-Z4 homologue. The positions of sequences primers were illustrated in boldface and underlined (A) and BlastX results of nucleotide sequence of a BrC-Z4 homologue from EST (B).....	97
Figure 3.27	Nucleotide sequence of 5'UTR-2 of PmBr-C Z4 was generated by 5'RACE PCR using secondary primer and upm, sequenced with M13F. The positions of sequencing primers are illustrated in boldface and underlined.....	97
Figure 3.28	Nucleotide sequence of 5'UTR-2 of PmBr-C Z4 was generated by 5'RACE PCR using secondary primer and upm, sequenced with M13R. The positions of sequencing primers are illustrated in boldface and underlined.....	97
Figure 3.29	The full length cDNA of BrC-Z4 (A), BlastX result of BrC-Z4 and Coding nucleotides and deduced amino acids of BrC-Z4 (B).....	98
Figure 3.30	The full length cDNA of <i>PmBrC-Z4</i> (The start and stop codons are illustrated in boldface. The poly A additional signal site are underlined. And the glycosylation site are red.....	98
Figure 3.31	32 The alignment BTB domained of <i>PmBrC-Z1-s</i> , <i>PmBr-C Z1-l</i> and <i>PmBr-C Z4</i>	99
Figure 3.32	5'PCR product of PmCOMT was generated by 5'Genome walking using secondary primer and AP2. The product of <i>Alu</i> I, <i>Dra</i> I, <i>Hae</i> III <i>Stu</i> I, and <i>Rsa</i> I mini-libraries (lanes 1 – 4) amplified with forward gene-specific and the adapter primer (AP2).	101
Figure 3.33	PCR phe 5'PCR product of PmCOMT was generated by 5'Genome walking using secondary primer and AP2. The product of <i>Alu</i> I, <i>Dra</i> I, <i>Hae</i> III <i>Stu</i> I, and <i>Rsa</i> I mini-libraries (lanes 1 – 4) amplified with forward gene-specific and the adapter primer (AP2).....	103

FIGURE	Page
Figure 3.34 Nucleotide sequence of <i>PmCOMT</i> was generated by 5'Genome walking using secondary primer and AP2, sequenced with M13F. The positions of sequencing primers are illustrated in boldface and underlined.....	104
Figure 3.35 Nucleotide sequence of <i>PmCOMT</i> was generated by RT-PCR. The positions of sequencing primers are illustrated in boldface and underlined.....	105
Figure 3.46 Nucleotide sequences illustrating organization of <i>PmCOMT</i> genes. Coding nucleotides and deduced amino acids of each exon are capitalized. Introns are italicized and illustrated with lower letters. Start and stop codons are illustrated in boldface and underlined. The catechol- <i>O</i> -Methyltransferase domain is highlighted. Polyadenylation signals (AATAAA) are underlined.....	105
Figure 3.37 Schematic diagrams of PmCOMT cDNA and gene. The complete PmCOMT cDNA were obtained by RACE-PCR. Genomic DNA fragments of PmCOMT were obtained from both genome walking analysis and overlapping PCR amplification. Noncoding regions are represented by solid bars. Introns (with numbers) are gray-shaded. Primers used for amplification of genomic PmCOMT and corresponding clones are illustrated.....	106
Figure 3.38 Multiple alignments (A) and bootstrapped neighbor-joining trees illustrating relationships between PmCOMT and catechol- <i>O</i> -methyltransferase domain-containing protein 1 (B) of various taxa. Values at the node represent the percentage of times that the particular node occurred in 1000 trees generated by bootstrapping the original aligned sequences.....	106
Figure 3.39 A brootstrapped neighbor-joining tree illustrating phylogenetic relationships of <i>catechol-O-methyltransferase (COMT)</i> and <i>farnesoic-O-methyltransferase (FAMeT)</i> of various taxa..	108
Figure 3.40 RT-PCR of <i>PmCOMT</i> using the first strand cDNA from ovaries of cultured juveniles (lanes 1 - 4, A) and wild broodstock (lanes 5 - 8, A) and testes cultured juveniles (lanes 9 - 12, A) and wild broodstock (lanes 13 - 16, A) <i>P. monodon</i> . <i>EF-1α</i> was successfully amplified from the same template (B). Lanes M and N are a 100 bp DNA marker and the negative control (without cDNA template), respectively.....	110
Figure 3.41 Histograms showing the relative expression profiles of <i>PmCOMT</i> in testes of cultured juveniles (JNTT), testes of wild broodstock (BSTT), ovaries of cultured juveniles (JNOV) and ovaries of wild broodstock (BSOV) <i>P. monodon</i>	111

FIGURE	Page
Figure 3.52 Time-course relative expression levels of <i>PmCOMT</i> in ovaries of 18 months old after serotonin injection (50 µg/g body weight) at 1, 2, 3, 6, 12, 24, 48 and 72 hpt (<i>N</i> = 4 for each stage). Shrimp injected with absolute ethanol and 0.85% saline solution at 0 hour post injection (hpi) were included as the vehicle control for 5-HT.....	112
Figure 3.53 Time-course relative expression levels of <i>PmFAMeT</i> in ovaries of 18 months old after serotonin injection (50 µg/g body weight) at 1, 2, 3, 6, 12, 24, 48 and 72 hpt (<i>N</i> = 4 for each stage). Shrimp injected with absolute ethanol and 0.85% saline solution at 0 hour post injection (hpi) were included as the vehicle control for 5-HT.....	113
Figure 3.54 Time-course relative expression levels of <i>PmCOMT</i> in ovaries of 18 months old at 12, 24 and 48 hours post injection (hpi) of progesterone (1 µg/g body weight; <i>N</i> = 4 for each stage).....	113
Figure 3.55 Time-course relative expression levels of <i>PmFAMeT</i> in ovaries of 18 months old at 12, 24 and 48 hours post injection (hpi) of progesterone (1 µg/g body weight; <i>N</i> = 4 for each stage). Shrimp injected with absolute ethanol and 0.85% saline solution at 0 hour post injection (hpi) were included as the vehicle control for progesterone.....	114
Figure 3.56 Template of <i>in situ</i> hybridization probe of <i>PmFAMeT</i> was amplified from the first strand cDNA of ovaries of <i>P. monodon</i> (A), The SP6 (antisense,1B) and T7 (sense, 2B) probe of <i>PmFAMeT</i> (B) and dot blot hybridization of antisense, sense of <i>PmFAMeT</i> and control RNA (C).....	115
Figure 3.57 Template of <i>in situ</i> hybridization probe of <i>PmBr-C ZI</i> was amplified from the first strand cDNA of ovaries of <i>P. monodon</i> (A) and The SP6 (antisense,1B) and T7 (sense, 2B) probe of <i>PmBr-C ZI</i> (B) and dot blot hybridization of antisense, sense of <i>PmBr-C ZI</i> and control RNA (C).....	116
Figure 3.58 Template of <i>in situ</i> hybridization probe of <i>PmBr-C Z4</i> was amplified from the first strand cDNA of ovaries of <i>P. monodon</i> (A) and The SP6 (antisense,1B) and T7 (sense, 2B) probe of <i>PmBr-C Z4</i> (B) and and dot blot hybridization of antisense, sense of <i>PmBr-C Z4</i> and control RNA (C).....	117
Figure 3.59 Template of <i>in situ</i> hybridization probe of <i>PmCOMT</i> was digested the full length plasmid of <i>PmCOMT</i> with NcoI (for SP6 probe, 2A) and APa I (for T7 probe, 3A), lane M=marker 100bp, m=lamda Hind III, 1=undigested plasmid of <i>PmCOMT</i> (A), and The SP6 (antisense,1B) and T7 (sense, 2B) probe of <i>PmCOMT</i> (B) and dot blot hybridization of antisense, sense of <i>PmCOMT</i> and control RNA (C).....	119

FIGURE	Page
Figure 3.60 Localization of <i>PmCOMT</i> transcript during ovarian development of normal <i>P. monodon</i> broodstock visualized by in situ hybridization using the antisense(A-C), sense probe(D-E) and conventional HE staining was carried out for identification of oocyte stages(F-G). EP =early previtellogenic oocytes; ECR =early cortical rod oocytes; CR=cortical rod oocytes; LCR=late cortical rod oocytes; Vg=vitellogenic oocyte.....	120
Figure 3.61 Localization of <i>PmCOMT</i> transcript during ovarian development of eyestalk-ablated <i>P. monodon</i> broodstock visualized by in situ hybridization using the antisense(A-d), sense probe(E) and conventional HE staining was carried out for identification of oocyte stages(F-G). EP =early previtellogenic oocytes; ECR =early cortical rod oocytes; CR=cortical rod oocytes; LCR=late cortical rod oocytes; Vg=vitellogenic oocyte; Fl=follicular layers.....	120
Figure 3.62 Localization of <i>PmFAMeT</i> transcript during ovarian development of normal <i>P. monodon</i> broodstock visualized by in situ hybridization using the antisense(A-C), sense probe(D) and conventional HE staining was carried out for identification of oocyte stages(E). EP =early previtellogenic oocytes; ECR =early cortical rod oocytes; CR=cortical rod oocytes; LCR=late cortical rod oocytes; Vg=vitellogenic oocyte.....	121
Figure 3.63 Localization of <i>PmFAMeT</i> transcript during ovarian development of eyestalk-ablated <i>P. monodon</i> broodstock visualized by in situ hybridization using the antisense(A-d), sense probe(E) and conventional HE staining was carried out for identification of oocyte stages(F-G). EP =early previtellogenic oocytes; ECR =early cortical rod oocytes; CR=cortical rod oocytes; LCR=late cortical rod oocytes; Vg=vitellogenic oocyte; Fl=follicular layers.....	121
Figure 3.64 Localization of <i>PmBr-C ZI</i> transcript during ovarian development of intact <i>P. monodon</i> broodstock visualized by in situ hybridization using the antisense(A-C), sense probe(D-E) and conventional HE staining was carried out for identification of oocyte stages(F-G). EP =early previtellogenic oocytes; ECR =early cortical rod oocytes; CR=cortical rod oocytes; LCR=late cortical rod oocytes; Vg=vitellogenic oocyte.....	122
Figure 3.65 Localization of <i>PmBr-C ZI</i> transcript during ovarian development of eyestalk-ablated <i>P. monodon</i> broodstock visualized by in situ hybridization using the antisense(A-C), sense probe(D-E) and conventional HE staining was carried out for identification of oocyte stages(F-G). EP =early previtellogenic oocytes; ECR =early cortical rod oocytes; CR=cortical rod oocytes; LCR=late cortical rod oocytes.....	122

FIGURE	Page	
Figure 3.66	Localization of <i>PmBr-C Z4</i> transcript during ovarian development of intact <i>P. monodon</i> broodstock visualized by in situ hybridization using the antisense(A-D), sense probe(E-G) and conventional HE staining was carried out for identification of oocyte stages(H). EP =early previtellogenic oocytes; ECR =early cortical rod oocytes; CR=cortical rod oocytes; LCR=late cortical rod oocytes; Vg=vitellogenic oocyte.....	123
Figure 3.67	Localization of <i>PmBr-C Z4</i> transcript during ovarian development of eyestalk-ablated <i>P. monodon</i> broodstock visualized by in situ hybridization using the antisense(A-D), sense probe(E-G) and conventional HE staining was carried out for identification of oocyte stages(H). EP =early previtellogenic oocytes; ECR =early cortical rod.....	123
Figure 3.68	RT-PCR of the full length of <i>PmCOMT</i> used as ovaries (lane 1) and haemocyte (lane 2) as a template (A) and the ORF of <i>PmCOMT</i> overhang with Nde I- Bam HI-6His tag (lane 1) (B).....	161
Figure 3.69	Nucleotide sequence of the full length <i>PmCOMT</i> (A) was generated by start-stop primer. And BlastX results of nucleotide sequence of a <i>PmCOMT</i> homologue(B).....	165
Figure 3.70	Nucleotide sequence of the ORF of <i>PmCOMT</i> overhang with Nde I- Bam HI-6His tag was sequenced with <i>PmCOMT</i> -ORF/ Nde I-F (A). And BlastX results of nucleotide sequence of the ORF of <i>PmCOMT</i> overhang with Nde I- Bam HI-6His tag ..	166
Figure 3.71	RT-PCR of the full length of <i>PmFAMeT- 1</i> (lane 1,A) and <i>PmFAMeT-s</i> (lane 2B) used as ovaries as a template, the ORF of <i>PmFAMeT- 1</i> (lane 1,A) and <i>PmFAMeT-s</i> (lane 2,B) overhang with Nde I- Bam HI-6His tag and the digestion of ORF of <i>PmFAMeT- 1</i> (lane 1,C) and <i>PmFAMeT-s</i> (lane 2,C) overhang with Nde I- Bam HI-6His tag with Xho II.....	166
Figure 3.72	Nucleotide sequence of the full length of <i>PmFAMeT-1</i> was sequenced with M13 F (A) M13 R(B). The combined full length of <i>PmFAMeT-1</i> (C) and BlastX results of nucleotide sequence of a <i>PmFAMeT-1</i> homologue(D).....	167
Figure 3.73	Nucleotide sequence of the full length of <i>PmFAMeT-s</i> was sequenced with M13 F (A) M13 R(B). The combined full length of <i>PmFAMeT-s</i> (C) and BlastX results of nucleotide sequence of a <i>PmFAMeT-s</i> homologue(D).....	168
Figure 3.74	Nucleotide sequence of the ORF of <i>PmFAMeT-1</i> overhang with Nde I- Bam HI-6His tag was sequenced with <i>PmCFAMeT</i> -ORF/ Nde I-F (A). And BlastX results of nucleotide sequence of the ORF of <i>PmFAMeT-1</i> overhang with Nde I- Bam HI-6His tag (B).....	169

FIGURE	Page
Figure 3.75 Nucleotide sequence of the ORF of PmFAMeT-s overhang with Nde I- Bam HI-6His tag was sequenced with T7F (A). And BlastX results of nucleotide sequence of the ORF of PmFAMeT-s overhang with Nde I- Bam HI-6His tag (B).....	170
Figure 3.76 In vitro expression of (r)PmCOMT of <i>P. monodon</i> clone 1-3 at 1 and 6 hours after induction with 0.4 mM IPTG(lanes 1-7), respectively A pET 15-b vector in <i>E. coli</i> BL21-CodonPlus (DE3)-RIPL(lane 8) and <i>E. coli</i> BL21-CodonPlus (DE3)-RIPL(lane 9)analyzed by SDS-PAGE (A)and Western blot (B).	170
Figure 3.77 In vitro expression of (r)PmFAMeT-1 of <i>P. monodon</i> clone 1-3 at 1 and 6 hours after induction with 0.4 mM IPTG(lanes 1-7), respectively A pET 15-b vector in <i>E. coli</i> BL21-CodonPlus (DE3)-RIPL(lane 8) and <i>E. coli</i> BL21-CodonPlus (DE3)-RIPL(lane 9)analyzed by SDS-PAGE (A)and Western blot (B).	171
Figure 3.78 In vitro expression of (r)PmFAMeT-s of <i>P. monodon</i> clone 1-3 at 1 and 6 hours after induction with 0.4 mM IPTG(lanes 1-7), respectively A pET 15-b vector in <i>E. coli</i> BL21-CodonPlus (DE3)-RIPL(lane 8) and <i>E. coli</i> BL21-CodonPlus (DE3)-RIPL(lane 9)analyzed by SDS-PAGE (A)and Western blot (B).	171
Figure 3.79 In vitro expression of (r)PmCOMT of <i>P. monodon</i> at 0.4,0. 6, 0.8, and 1 mM IPTG after 3 hr (lane 1-4, respectively) and 6 hr (lane 5-8, respectively) after IPTG induction, respectively, and A pET 15-b vector in <i>E. coli</i> BL21-CodonPlus (DE3)-RIPL(lane 9) analyzed by SDS-PAGE	172
Figure 3.80 In vitro expression of (r)PmFAMeT-1 of <i>P. monodon</i> at 0.4,0. 6, 0.8, and 1 mM IPTG after 3 hr (lane 1-4, respectively) and 6 hr (lane 5-8, respectively) after IPTG induction, respectively, and A pET 15-b vector in <i>E. coli</i> BL21-CodonPlus (DE3)-RIPL(lane 9) analyzed by SDS-PAGE	173
Figure 3.81 In vitro expression of (r)PmFAMeT-s of <i>P. monodon</i> at 0.4,0. 6, 0.8, and 1 mM IPTG after 3 hr (lane 1-4, respectively) and 6 hr (lane 5-8, respectively) after IPTG induction, respectively, and A pET 15-b vector in <i>E. coli</i> BL21-CodonPlus (DE3)-RIPL(lane 9) analyzed by SDS-PAGE	173
Figure 3.82 In vitro expression of (r)PmCOMT of <i>P. monodon</i> at 0, 1, 2, 3, 6, 12, and 24 hours after induction with 0.4 mM IPTG(lanes 1-7), A pET 15-b vector in <i>E. coli</i> BL21-CodonPlus (DE3)-RIPL(lane 8) and <i>E. coli</i> BL21-CodonPlus (DE3)-RIPL(lane 9) analyzed by SDS-PAGE (A) and Western blot (B).....	174
Figure 3.83 In vitro expression of (r)PmFAMeT-1 of <i>P. monodon</i> at 0, 1, 2, 3, 6, 12, and 24 hours after induction with 0.4 mM IPTG(lanes 1-7), A pET 15-b vector in <i>E. coli</i> BL21-CodonPlus (DE3)-RIPL(lane 8) and <i>E. coli</i> BL21-CodonPlus (DE3)-RIPL(lane 9) analyzed by SDS-PAGE (A) and Western blot (B).....	175

FIGURE	Page
Figure 3.84 In vitro expression of (r)PmFAMeT-s of <i>P. monodon</i> at 0, 1, 2, 3, 6, 12, and 24 hours after induction with 0.4 mM IPTG(lanes 1-7), A pET 15-b vector in <i>E. coli</i> BL21-CodonPlus (DE3)-RIPL(lane 8) and <i>E. coli</i> BL21-CodonPlus (DE3)-RIPL(lane 9) analyzed by SDS-PAGE (A) and Western blot (B).....	176
Figure 3.85 In vitro expression of (r)PmCOMT of <i>P. monodon</i> culture at 37 °C for 3 hours after induction with 0.4 mM IPTG. Lane 1=whole cell, lane 2=insoluble and lane 3=soluble analyzed by SDS-PAGE (A) and Western blot (B).....	177
Figure 3.86 In vitro expression of (r)PmCOMT of <i>P. monodon</i> culture at 25 °C for 3 hours after induction with 0.4 mM IPTG. Lane 1=whole cell, lane 2=insoluble and lane 3=soluble analyzed by SDS-PAGE (A) and Western blot (B).....	178
Figure 3.87 In vitro expression of (r)PmFAMeT-l of <i>P. monodon</i> culture at 37 °C for 3 hours after induction with 0.4 mM IPTG. Lane 1=whole cell, lane 2=insoluble and lane 3=soluble analyzed by SDS-PAGE (A) and Western blot (B).....	178
Figure 3.88 In vitro expression of (r)PmFAMeT-l of <i>P. monodon</i> culture at 25 °C for 3 hours after induction with 0.4 mM IPTG. Lane 1=whole cell, lane 2=insoluble and lane 3=soluble analyzed by SDS-PAGE (A) and Western blot (B).....	179
Figure 3.89 In vitro expression of (r)PmFAMeT-s of <i>P. monodon</i> culture at 37 °C for 3 hours after induction with 0.4 mM IPTG. Lane 1=whole cell, lane 2=insoluble and lane 3=soluble analyzed by SDS-PAGE (A) and Western blot (B).....	179
Figure 3.90 In vitro expression of (r)PmFAMeT-s of <i>P. monodon</i> culture at 25 °C for 3 hours after induction with 0.4 mM IPTG. Lane 1=whole cell, lane 2=insoluble and lane 3=soluble analyzed by SDS-PAGE (A) and Western blot (B).....	180
Figure 3.91 Purification of (r)PmCOMT were purified in denaturing condition after culture at 37 °C for 3 hours and after induction with 0.4 mM IPTG were analyzed by SDS-PAGE (A,B) and Western blot (C,B).....	181
Figure 3.92 Purification of (r)PmFAMeT-l were purified in denaturing condition after culture at 37 °C for 3 hours and after induction with 0.4 mM IPTG were analyzed by SDS-PAGE (A,B) and Western blot (C,B).....	182
Figure 3.93 Purification of (r)PmFAMeT-s were purified in denaturing condition after culture at 37 °C for 3 hours and after induction with 0.4 mM IPTG were analyzed by SDS-PAGE (A,B) and Western blot (C,B).....	183

FIGURE	Page	
Figure 3.94	In vitro expression of (r)PmFAMeT-s of <i>P. monodon</i> at 0, 1, 2, 3, 6, 12, and 24 hours after induction with 0.4 mM IPTG(lanes 1-7), A pET 15-b vector in <i>E. coli</i> BL21-CodonPlus (DE3)-RIPL(lane 8) and <i>E. coli</i> BL21-CodonPlus (DE3)-RIPL(lane 9) analyzed by SDS-PAGE (A) and Western blot (B).....	176
Figure 3.95	In vitro expression of (r)PmCOMT of <i>P. monodon</i> culture at 37 °C for 3 hours after induction with 0.4 mM IPTG. Lane 1=whole cell, lane 2=insoluble and lane 3=soluble analyzed by SDS-PAGE (A) and Western blot (B).....	177
Figure 3.96	In vitro expression of (r)PmCOMT of <i>P. monodon</i> culture at 25 °C for 3 hours after induction with 0.4 mM IPTG. Lane 1=whole cell, lane 2=insoluble and lane 3=soluble analyzed by SDS-PAGE (A) and Western blot (B).....	178
Figure 3.97	In vitro expression of (r)PmFAMeT-l of <i>P. monodon</i> culture at 37 °C for 3 hours after induction with 0.4 mM IPTG. Lane 1=whole cell, lane 2=insoluble and lane 3=soluble analyzed by SDS-PAGE (A) and Western blot (B).....	178
Figure 3.98	In vitro expression of (r)PmFAMeT-l of <i>P. monodon</i> culture at 25 °C for 3 hours after induction with 0.4 mM IPTG. Lane 1=whole cell, lane 2=insoluble and lane 3=soluble analyzed by SDS-PAGE (A) and Western blot (B).....	179
Figure 3.99	In vitro expression of (r)PmFAMeT-s of <i>P. monodon</i> culture at 37 °C for 3 hours after induction with 0.4 mM IPTG. Lane 1=whole cell, lane 2=insoluble and lane 3=soluble analyzed by SDS-PAGE (A) and Western blot (B).....	179
Figure 3.100	In vitro expression of (r)PmFAMeT-s of <i>P. monodon</i> culture at 25 °C for 3 hours after induction with 0.4 mM IPTG. Lane 1=whole cell, lane 2=insoluble and lane 3=soluble analyzed by SDS-PAGE (A) and Western blot (B).....	180
Figure 3.102	Purification of (r)PmCOMT were purified in denaturing condition after culture at 37 °C for 3 hours and after induction with 0.4 mM IPTG were analyzed by SDS-PAGE (A,B) and Western blot (C,B).....	181
Figure 3.102	Purification of (r)PmFAMeT-l were purified in denaturing condition after culture at 37 °C for 3 hours and after induction with 0.4 mM IPTG were analyzed by SDS-PAGE (A,B) and Western blot (C,B).....	182
Figure 3.103	Purification of (r)PmFAMeT-s were purified in denaturing condition after culture at 37 °C for 3 hours and after induction with 0.4 mM IPTG were analyzed by SDS-PAGE (A,B) and Western blot (C,B).....	183

FIGURE	Page
Figure 3.111 The insoluble protein of (r)PmCOMT, (r)PmFAMeT-s and (r)PmFAMeT-l were purified in denaturing condition after culture at 37 °C for 3 hours and after induction with 0.4 mM IPTG were analyzed by SDS-PAGE (A) and Western blot (B).	184
Figure 3.112 Western blot analysis of anti-COMT(1:300) in different stage of female shrimp.....	187
Figure 3.113 Western blot analysis of anti-FAMeT-l (1:300) in different stage of female shrimp.....	188
Figure 3.114 Immunohistochemical localization of PmCOMT protein in ovaries of intact broodstock P. monodon (C-D). The blocking solution(A) and normal sera (B)were used as negative and positive control conventional HE staining (A) was carried out for identification of oocyte stages.....	189
Figure 3.115 Immunohistochemical localization of PmCOMT protein in ovaries of eyestalk-ablated broodstock P. monodon (C-D). The blocking solution(A) and normal sera (B)were used as negative and positive control conventional HE staining (A) was carried out for identification of oocyte stages.....	189
Figure 3.116 Immunohistochemical localization of PmFAMeT-l protein in ovaries of intact broodstock P. monodon (C-D). The blocking solution(A) and normal sera (B)were used as negative and positive control conventional HE staining (A) was carried out for identification of oocyte stages.....	190
Figure 3.117 Immunohistochemical localization of PmFAMeT-l protein in ovaries of eyestalk-ablated broodstock P. monodon (C-D). The blocking solution(A) and normal sera (B)were used as negative and positive control conventional HE staining (A) was carried out for identification of oocyte stages.....	190
Figure 3.118 Immunohistochemical localization of PmFAMeT-s protein in ovaries of eyestalk-ablated broodstock P. monodon (C-D). The blocking solution(A) and normal sera (B)were used as negative and positive control conventional HE staining (A) was carried out for identification of oocyte stages.....	191
Figure 3.119 Immunohistochemical localization of PmFAMeT-s protein in ovaries of eyestalk-ablated broodstock P. monodon (C-D). The blocking solution(A) and normal sera (B)were used as negative and positive control conventional HE staining (A) was carried out for identification of oocyte stages.....	191

LIST OF ABBREVIATIONS

bp	base pair
°C	degree celcius
dATP	deoxyadenosine triphosphate
dCTP	deoxycytosine triphosphate
dGTP	deoxyguanosine triphosphate
dTTP	deoxythymidine triphosphate
DNA	deoxyribonucleic acid
HCl	hydrochloric acid
IPTG	isopropyl-thiogalactoside
Kb	kilobase
M	Molar
MgCl ₂	magnesium chloride
mg	milligram
ml	milliliter
mM	millimolar
ng	Nanogram
OD	optical density
PCR	polymerase chain reaction
RNA	Ribonucleic acid
RNase A	Ribonuclease A
rpm	revolution per minute
RT	reverse transcription
SDS	sodium dodecyl sulfat
Tris	tris(hydroxyl methyl) aminomethane
µg	microgram
µl	microlitre
µM	micromolar
UV	ultraviolet

CHAPTER I

INTRODUCTION

1.1 Background information and objectives of this thesis

The giant tiger shrimp (*Penaeus monodon*) was an economically important cultured species in Thailand. The annual production was approximately 225,000 metric tons in 2002, but has significantly decreased owing to the outbreak of diseases since 2003. Farming of *P. monodon* in Thailand relies entirely on wild-caught broodstock for supply of juveniles because reproductive maturation success of captive *P. monodon* female is extremely low. The high demand on wild female broodstock leads to overexploitation of the natural populations of *P. monodon* in Thai waters (Klinbunga et al., 1999; Khamnamtong et al., 2005). The lack of high quality wild and/or domesticated broodstock of *P. monodon* has caused a significant decrease in its farmed production since the last several years (Limsuwan, 2004). Reduced degrees of reproductive maturation in captive *P. monodon* broodstock have limited the potential of genetic improvement resulted in remarkably slow domestication and selective breeding programs of *P. monodon* in Thailand (Withyachumnarnkul et al., 1998; Clifford and Preston, 2006; Preechaphol et al., 2007).

Several biotechnological areas including investigation of genetic variation (identification of stocks) and genome structure, controls of reproduction and growth, domestication of strains exhibiting required economically important traits (e.g. specific pathogen resistant, SPR and/or fast growing strains) are thought to have significant impact in the industry of this species. The domestication and selective breeding programs of *P. monodon* would provide a more reliable supply of seed stock and the improvement of their production efficiency. The use of selectively bred stocks having improved culture performance (e.g. disease resistance and/or other commercially desired traits) rather than the reliance on wild-caught stocks is a major determinant of sustainability of the shrimp industry. Despite the potential benefits, the domestication of *P. monodon* has been

remarkably slow in Thailand and is still at the initial stage because the previous stocks (Withyachumnarnkul et al., 1998) were recently collapsed by WSSV infection.

The development of oocytes consists of a series of complex cellular events, in which different genes express to ensure the proper development of oocytes and to store transcripts and proteins as maternal factors for early embryogenesis (Qiu *et al.*, 2005). Different biotechnological approaches, for example; injection of vertebrate steroid hormones, neurotransmitters and ecdysteroids (Benzie 1998; Okumura, 2004) and the use of specially formulated feed (Harrison, 1990) have been applied to induce the ovarian maturation of female shrimp but results are inconsistent owing to limited knowledge on genetic and hormonal control of penaeid species (Okumura, 2004).

Maturation of female shrimp is controlled by several neuropeptides (Okumura, 2004). It has been proposed that ovarian and oocyte development is controlled by gonad stimulating hormone (GSH also called vitellogenin stimulating hormone, VSH) and gonad inhibiting hormone (GIH also called vitellogenin inhibiting hormone, VIH). In addition, ecdysteroids and methyl farnesoate represent two major endocrine signaling molecules in crustaceans that regulate many aspects of their development, growth, and reproduction.

O-methyltransferase (OMT) is ubiquitously present in diverse organisms and plays an important regulatory role in growth, development, reproduction and defense mechanisms in plants and animals. Two kinds of OMT; farnesoic acid-*O*-methyltransferase (FAMeT) and catechol-*O*-methyltransferase (COMT) were identified according to their selectivity to methyl acceptors.

Methyl farnesoate (MF) is structurally related to the insect juvenile hormone and believed to be synthesized by the mandibular organ (MO). MF has been implicated in the regulation of crustacean development and reproduction in conjunction with eyestalk molt inhibiting hormones and ecdysteroids (Laufer et al., 1987; Lam Hui, 2008). The incubation of ovarian tissue with MF and the addition of MF to the diet stimulate ovarian development of *Procambarus clarkii* (Laufer et al.1998). However, no significant effects were detected in the American lobster (*Homarus americanus*) and the giant freshwater

prawn (*Macrobrachium rosenbergii*) when MF was injected into the females (Tsukimura *et al.*, 1993; Wilder *et al.*, 1994) but the inhibitory effects were observed in tadpole shrimp, *Troops longicaudatus* (Tsukimura *et al.* 2006). Accordingly, the actual physiological function of MF on ovarian development of *P. monodon* is still not understood and should be examined.

Crustacean FAMEt catalyses methylation of farnesoic acid (FA) to produce isoprenoid methyl farnesoate (MF) at the final step of the MF biosynthetic pathway whereas COMT catalyses the transfer of the methyl group from *S*-adenosyl-methionine (SAM) to the hydroxyl group of catechol compounds. Thus, COMT plays an important role in the catabolism and *O*-methylation of endogenous catecholamines, such as dopamine and noradrenaline, in brains of animals.

In addition, ecdysteroids are known as the molting hormone in crustaceans and insects. In crustaceans, the inactive forms are secreted and converted to 20-hydroxyecdysone by the Y-organ. Ecdysteroids stimulate vitellogenesis in some insects. The broad-complex (BR-C), one of the ecdysteroid-responsive genes, is a key member of 20-hydroxyecdysone regulatory hierarchy that coordinates changes in gene expression during *Drosophila* metamorphosis (Bayer, *et al.*, 1996). The BR-C gene family can be divided into 4 isoforms; BR-C Z1, Z2, Z3 and Z4 that share an amino-terminal common core domain alternatively spliced to four distinct carboxyl-terminal domains bearing pairs of zinc fingers of the C₂H₂ type (DiBello. *et al.*,1991; Bayer *et al.*,1996) and a highly conserved amino-terminal domain called the BTB/POZ domain. (Zollman *et al.*, 1994)

Progress in genetic and biotechnology researches in penaeid shrimps have been slow because a lack of knowledge on fundamental aspects of their endocrinology and reproductive biology (Benzie, 1998). Therefore, molecular mechanisms and functional involvement of reproduction-related genes and proteins in ovarian development of *P. monodon* is necessary for better understanding of the reproductive maturation of *P. monodon* to resolve the major constraint of this economically important species in captivity which, in turn, provide the long term benefit for domestication and selective

breeding programs of this economically important species (Preechaphol et al., 2007; Klinbunga et al., 2009).

1.2 Objectives of this thesis

The objectives of this thesis were isolation and characterization of the full length cDNA and genomic DNA of *COMT*, *FAMeT* and *Br-c* genes in *P. monodon* and their expression levels of genes and/or protein during different stages of ovarian development of *P. monodon*. Localization of genes and/or protein during different stages of ovarian development of *P. monodon* is determined by *in situ* hybridization and/or immunohistochemistry.

1.3 General introduction

The giant tiger shrimp (*Penaeus monodon*) is one of the most economically important penaeid species in South East Asia. Farming of *P. monodon* has achieved a considerable economic and social importance in the region, constituting a significant source of income and employment.

In Thailand, *P. monodon* had been intensively cultured for more than two decades. Approximately 60% of the total shrimp production is from cultivation. Shrimp farms and hatcheries are scattered along the coastal areas of Thailand where southern provinces (Nakorn Sri Thammarat and Surat Thani) are the majority and those in the east (Chanthaburi) and central regions (Samut Sakhon and Samut Songkhram) comprise the minority in terms of number. The intensive farming system had been used for *P. monodon* farming activity resulting in consistent increase in the production (Department of Fisheries, 1999).

The increased demand of *P. monodon* in world markets has elevated the expansion of shrimp industry and activity of this important species. The culture of *P. monodon* is basically a two-step process composed of a broodstock-hatchery phase for producing seed or postlarvae and a grow-out phase usually in earthen culture ponds for on-growing of fry to marketable size (where a nursery for rearing of postlarvae to larger juveniles is incorporated).

Table 1.1 Export of the giant tiger shrimp from Thailand during 2002-2007

Country	2002		2003		2004		2005		2006		2007	
	Quantity (MT)	Value (MB)	Quantity (MT)	Value (MB)	Quantity (MT)	Value (MB)	Quantity (MT)	Value (MB)	Quantity (MT)	Value (MB)	Quantity (MT)	Value (MB)
USA	97681.81	36,011.41	89115.28	29,032.87	58365.2	17,206.75	29116.62	17,206.75	34537.23	8,847.42	7979.91	1,909.64
Japan	16644.6	13,813.33	33235.52	11,916.87	27977.27	9,586.59	20182.85	9,586.59	15,709.39	3,832.31	3711.32	1,067.25
Canada	6455.76	3,890.48	11216.47	3,412.09	6490.03	2,072.25	3249.37	2,072.25	2798.61	744.95	1762.16	462.68
Singapore	5251.66	3,138.86	3317.14	1,258.13	3383.18	537.88	1933.5	537.88	1580.11	236.31	401.47	63.53
Taiwan	4917.65	1,276.86	3051.77	799.44	2964.62	564.58	1673.65	564.58	607.7	170.12	692.69	194.78
Australia	4481.25	1,326.06	4817.5	1,252.31	2418.19	1,042.02	2097.76	1,042.02	1418.36	445.05	658.54	225.13
Hong Kong	1365.12	533.26	1437.54	340.42	1396.98	409.93	1026.84	409.93	921.88	256.91	1569	365.91
China	1649.23	352.68	992.91	214.54	833.1	162.66	1003	162.66	710.7	85.65	1629.74	235.57
U. Kingdom	661.07	210.81	184.23	64.11	505.76	181.63	161.79	181.63	241.91	70.54	242.4	73.46
Total	180,615.81	63,822.73	160,986.48	51,524.10	118,343.12	16,629.05	69,168.96	16,629.05	64,565.41	16,178.85	23,933.1	5,922.11

Source: http://www.fisheries.go.th/foreign/doc/excel/export_backtiger.xls

The success of the shrimp industry in Thailand has resulted in the steadily increased income for the nation. This has also elevated the quality of life for Thai farmers. The reasons for this are supported by several factors including the appropriate farming areas without the serious disturbing from typhoons or cyclone, small variable of seawater during seasons, and ideal soils for pond construction.

Thailand has become the world's leader in shrimp exports. The largest export markets for Thai black tiger shrimp are the United States and Japan. The remaining important markets are Canada, Asian countries, Australia and others (Table 1.1). However, the industry has consistently encountered production losses from infectious diseases, particularly from white spot syndrome virus (WSSV), yellow head virus (YHV) and *Vibrio* sp., environmental degradation and overexploitation of high quality natural female broodstock for seed production (Browdy, 1998). As a result, Thai shrimp export decreased from 181,050 in 2002 to only 69,412 in 2005 (Table 1.2).

1.4 Taxonomy of *P. monodon*

Penaeid shrimps are taxonomically recognized as members the largest phylum in the animal kingdom, the Arthropoda. This group of animals is characterized by the presence of paired appendages and a protective cuticle or exoskeleton that covers the whole animal. The taxonomic definition of the giant tiger shrimp, *P. monodon* is as follows (Bailey-Brook and Moss, 1992): a member of Phylum Arthropoda; Subphylum Crustacea; Class Malacostraca; Subclass Eumalacostraca; Order Decapoda; Suborder Natantia; Infraorder Penaeidea; Superfamily Penaeoidea; Family Penaeidae Rafinesque, 1985; Genus *Penaeus* Fabricius, 1798; Subgenus *Penaeus*. The scientific name of this species is *Penaeus monodon* (Fabricius, 1798) and the common name is giant tiger prawn or black tiger shrimp.

1.5 Morphology

The external morphology of penaeid shrimp is distinguished by a cephalothorax with a characteristic hard rostrum, and by a segmented abdomen (Fig. 1.1). Most organs are located in cephalothorax, while the body muscles are mainly in the abdomen. The

internal morphology of penaeid shrimp is outlined by Fig. 1.2. Penaeids and other arthropods have an open circulatory system and, therefore, the blood and the blood cells are called hemolymph and hemocytes, respectively.

1.6 Female reproductive system

1.6.1 Morphology of female reproductive system

The female reproductive system consists of paired ovaries, paired oviducts and a single thelycum. The first two are internal and the last is an external organ. The ovaries are partly fused, bilaterally symmetrical bodies extending in the mature female for almost its entire length, from the cardiac region of the stomach to the anterior portion of the telson. In cephalothorax region the organ bears a slender anterior lobe and five finger-like lateral projections (King, 1948). A pair of lobes, one from each ovary, extends over the length of the abdomen. The anterior lobes lie close to the esophagus and cardiac region of the stomach. The lateral lobes are located dorsally in the large mass of the hepatopancreas and ventrally in the pericardial chamber. The abdominal extensions lie dorsa-lateral to the intestine and ventro-lateral to the dorsal abdominal artery. The oviducts origins at the tips of the sixth lateral lobes and descend to the external genital apertures hidden in the ear-like lobes of the coxopods of the third pair of pereopods.

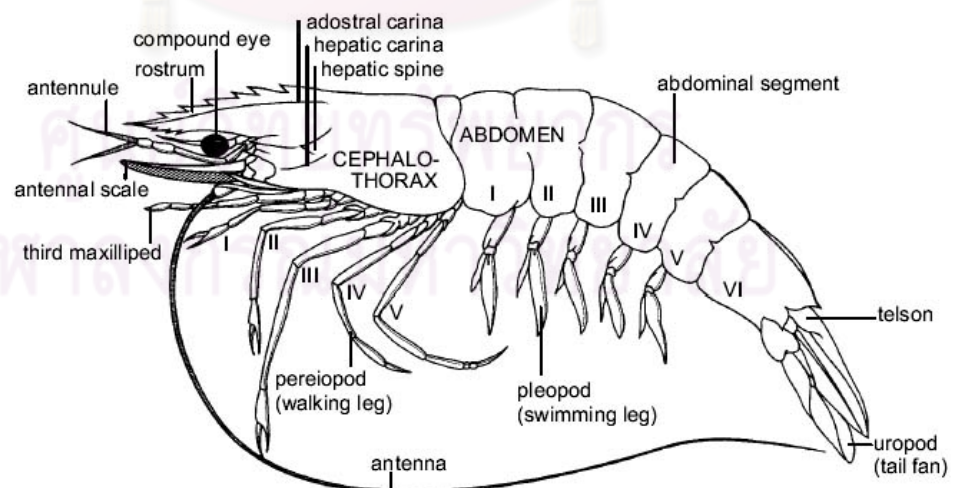


Figure 1.1 Lateral view of the external morphology of *P. monodon*. (Primavera, 1990)

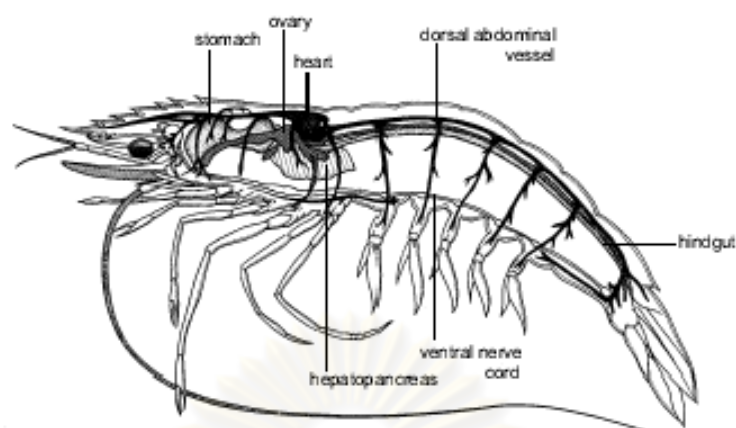


Figure 1.2 Lateral view of the internal anatomy of a female *P. monodon* (Primavera, 1990).

1.6.2 Ovarian development

The average *P. monodon* broodstock varies according to geographic location. Female wild broodstock are normally range from 110 g to 160 g. However, large females, those over 150 grams, which are assumed to be older females, often do not perform well in hatcheries. The ovary lies dorsal to the gut and extends from the cephalothorax (head and thorax region) along the entire length of the tail as shown in Figure 4. The ovaries are paired, but partially fused in the cephalothorax region which consists of a number of lateral lobes. The ovarian development is divided in 4 phases according to its histological features and germ cell association as shown in Figure 1.3. It consists of stages I (undeveloped phase or spent phase), II (proliferative phase), III (premature phase) and IV (mature phase) ovaries.

The stage I ovaries (Figure 1.4A) are comprised of a connective tissue capsule surrounding a soft vascular area containing future eggs, called oogonia, and accessory cells, also called follicle or nurse cells. The undifferentiated oogonia exists the germinative zone of the ovaries and became oogonia that divided mitotically and enter the meiotic prophase.



Figure 1.3 The illustration of ovaries that extend the entire length of shrimp (a) and complete ovaries of *P. monodon* females categorized as stages II to IV (b). Note the color changes are due to an increasing carotenoid content (<http://www.aims.au/pages/reseach/mdef/mdef-00.html>).

The stage II ovaries (Figure 1.4b) contain the majority of previtellogenic oocytes characterized by accumulation of ribosomes and the development of rough endoplasmic reticulums. The developing eggs are increasing in size and they are not as yet producing yolk.

In the stage III ovaries (Figure 1.4c), the majority of oocytes are vitellogenic oocytes governed by the process of vitellogenesis in which yolk proteins (vitellin) are recruited and made within the oocytes. Vitellin is the common form of yolk stored in oocytes and is a nutrient source for developing embryos. Vitellgenin is the precursor

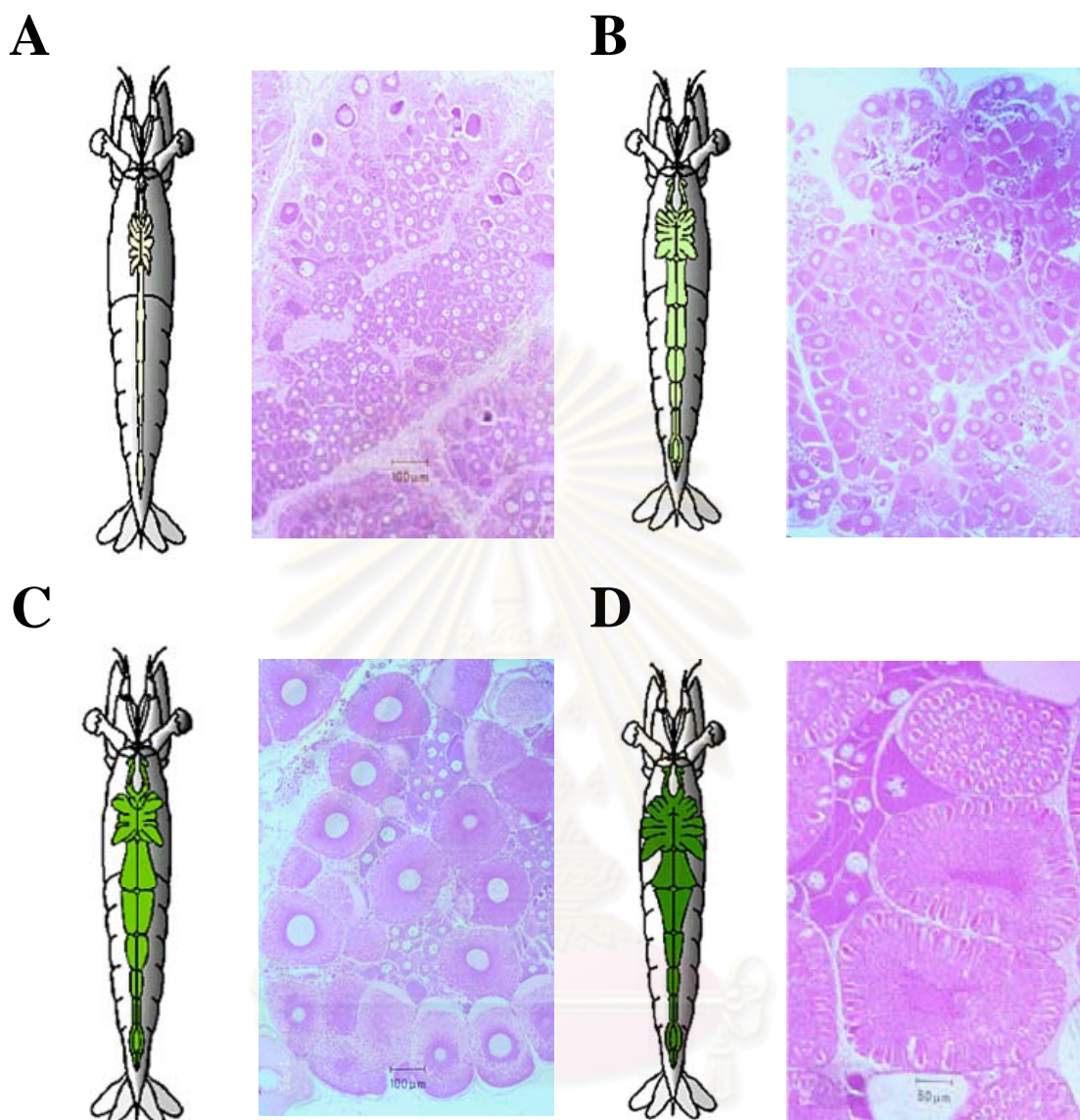


Figure 1.4 Different ovarian development stages of *P. monodon*. **Panel A.**, the underdeveloped ovaries (Stage I), **B.**, the developing stage (Stage II), **C.**, the nearly ripe stage (Stage III) and **D.**, the ripe stage (Stage IV) (www.aims.gov.au/.../mdef/images/fig01-4a.gif).

Table 1.2 A summary on the ovarian maturation stages in *P. monodon* based on histological studies (Tan-Fermin and Pudadera 1989)

Oocyte stage/component	Qualitative methods			
	Histology	Histochemistry		
		Mallory	AB-PAS	SB
P:previtellogenic				
a) oocyte	-oogonia and primary oocytes			
1) Nucleus	-chromatin nucleolus and/or perinucleolus stage; single to several nucleoli in nucleoplasm			
2) Cytoplasm	-clear	Basophilic	(-)	(-)
b) follicle cells	-rectangular or cuboidal in shape, if present in oocytes > 55µm	Basophilic		
V:vitellogenic				
a) oocyte	-			
1) Nucleus	chromatin materials evenly distributed in nucleoplasm			
2) Cytoplasm	-as in stage P plus oocytes which contain yolky substances in cytoplasm	Red, blue	Magenta	Black
b) follicle cells	-flattened in shape		Light blue	
C; cortical rod				
a) oocytes	-as in stage P plus oocytes with yolky substances and cortical rods in cytoplasm			
1) nucleus	- chromatin materials evenly distributed in nucleoplasm			
2) cytoplasm	- yolky substances in granules	Red, blue	Magenta	Black
3) cortical rods	-spherical or elongated near periphery and extends towards nucleus	Red, blue, purple	Blue near periphery, red towards nucleus	(-)
b) Follicle cells	-spindle-shaped or not distinguishable			
S; spent				
a) oocytes	-remaining oocytes with yolky cortical rods -thicker layers of follicle cells retracted to one side -darkly-stained, irregularly-shaped primary oocytes			
b) follicle cells	-rectangular or cuboidal in shape when enveloping oocytes			

AB-PAS: alcian blue-periodic acid-Schiff. SB: Sudan black.

molecule of vitellin. Vitellin in crustacean was synthesized by fat body, hemocytes, ovaries or hepatopancreas. It is evidenced that vitellogenin fragment was cleaved into smaller size of vitellin fragment by protease function. At the end of the third phase, the oocytes become bright colored by the association of vitellin with carotenoids. By the end of vitellogenesis, the eggs develop cortical granules filled with a jelly-like substance destined to form part of egg shell membrane after ovulation.

In the stage IV ovaries (Figure 1.4d), the fully mature oocytes is composed of extracellular cortical rods. These cortical specializations are precursors of jelly layer (JL) of the egg. Spawning and direct contact of the spawned eggs with sea water leads to the release of extracellular cortical rods. Then, increasing vitellin envelope and formation of corona that is composed of a flocculent matrix around the egg consisting of jelly layer occur. The biochemical composition of the shrimp cortical rods and the nature of jelly layer still scarcely understood. Precursors isolated from mature ovaries comprised of approximately 70-75% protein and 25-30 % carbohydrate. Shrimp ovarian peritrophin (SOP) was demonstrated that it is a component of the cortical rod precursor of the jelly layer in shrimp eggs. It is glycosylated and binds chitin. The color of mature ovaries is characteristic dark green color as a result of deposition of carotenoid pigments.

1.7 Vitellogenesis and oocyte maturation

In crustaceans, oocytes grow during oogenesis through the process of vitellogenesis. During vitellogenesis, vitellogenin, the precursor of the major yolk protein, vitellin, is synthesized and is taken in by the oocytes. In the oocytes, vitellogenin is processed and accumulated. Vitellin is utilized as a nutritional source during embryogenesis. Vitellin and vitellogenin have been purified in several shrimps and determined to be large lipoprotein molecules (molecular weight, 280–700 kDa).

In decapod crustaceans, vitellogenesis is a necessary prerequisite for ovaries to reach full maturation (Serrano-Pinto et al., 2003). Vitellogenesis is comprised of vitellogenin (Vg) synthesis and its accumulation in ovarian oocytes as vitellin (Tsukimura et al., 2000; Ghekiere et al., 2004, 2005). Vg, a precursor of egg yolk protein, is synthesized by both ovaries and hepatopancreas (Lui et al., 1974; Eastman-Reks and

Fingerman, 1985; Yano and Chinzei, 1987; Quackenbush, 1989; Rankin et al., 1989; Browdy et al., 1990; Fainzilber et al., 1992; Khayat et al., 1994; Chen et al., 1999; Tseng et al., 2001). In decapod crustaceans, Vg has been identified electrophoretically and immunologically in the hemolymph of vitellogenic females of various species (Fielder et al., 1971; Wolin et al., 1973; Fyffe and O'Connor, 1974; Yano, 1987; Quintio et al., 1989; Shafir et al., 1992; Jasmani et al., 2000; Vazquez-Boucard et al., 2002).

In *Marsupenaeus japonicus*, Yano et al. (1996) reported that electron dense materials showing the presence of Vg found in the irregular surface of yolk granule stage oocytes were incorporated into the micropinocytotic vesicles of the oocytes. This indicated that Vg is temporally transferred into hemolymph after its synthesis by ovarian tissue and is then incorporated into oocytes by pinocytosis.

It has long been suspected that vitellogenesis including Vg synthesis and its incorporation into oocytes in decapod crustaceans is controlled by stimulating and inhibiting antagonistic hormones. Several studies have shown that vitellogenesis is regulated by a vitellogenesis-inhibiting hormone (VIH) or gonad-inhibiting hormone (GIH) from the X organ–sinus gland complex of the eyestalk (Bomirski et al., 1981; Quackenbush and Herrnkind, 1983; Meusy et al., 1987; Rotllant et al., 1993; De Kleijn et al., 1998) (Figure 1.5). Knowledge of hormonal induction of Vg synthesis and secretion in crustaceans, however, is fragmentary. Understanding the roles of steroid hormones on vitellogenesis may lead to the development of ways to induce ovarian maturation in decapods crustaceans.

1.8 Hormonal control of shrimp and Female reproductive hormone

1.8.1 Hormonal control of shrimp

Closing the life cycle of aquaculture animal is crucial to the success and sustainability of the aquaculture industry. The increasing scarcity of high quality wild-caught broodstock for the giant tiger shrimp *P. monodon* brought attention to the need of captive broodstock. However, different sets of problems are associated with the captive broodstock. The development of oocyte in the ovary of captive females *P. monodon*

showed a higher rate of regression than that of wild shrimp, and difference in the oocyte size were observed. Biological and physiological processes (growth, reproduction, body color, and metabolism etc.) in shrimp are hormonal controlled (Figure 1.6).

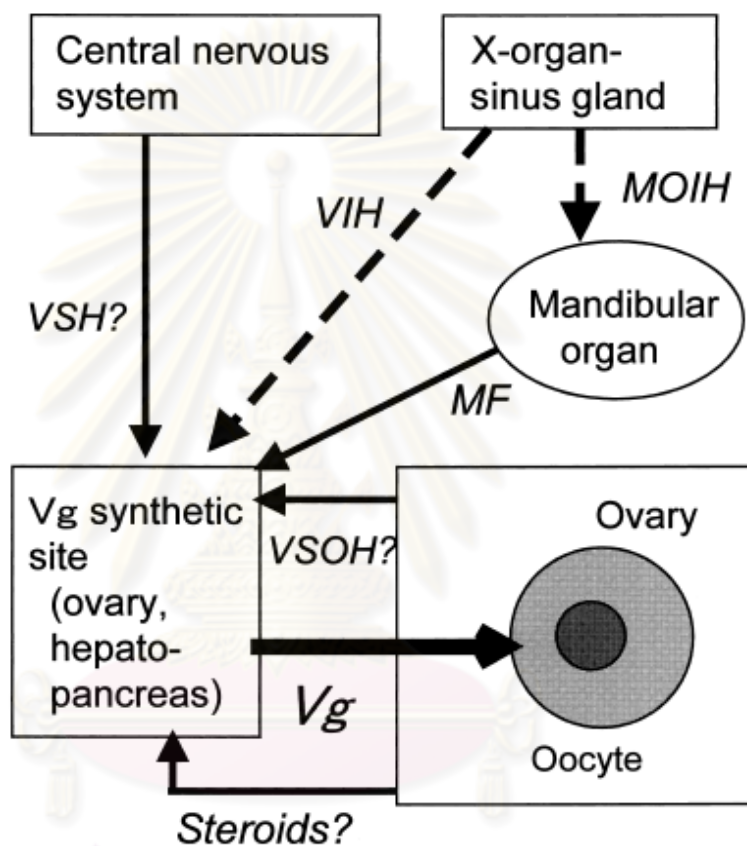


Figure 1.5 Schematic diagram of the endocrine control of vitellogenesis in shrimp, MF: methyl farnesoate, MOIH: mandibular organ inhibiting hormone, Vg: vitellogenin (Okumura et al., 2004).

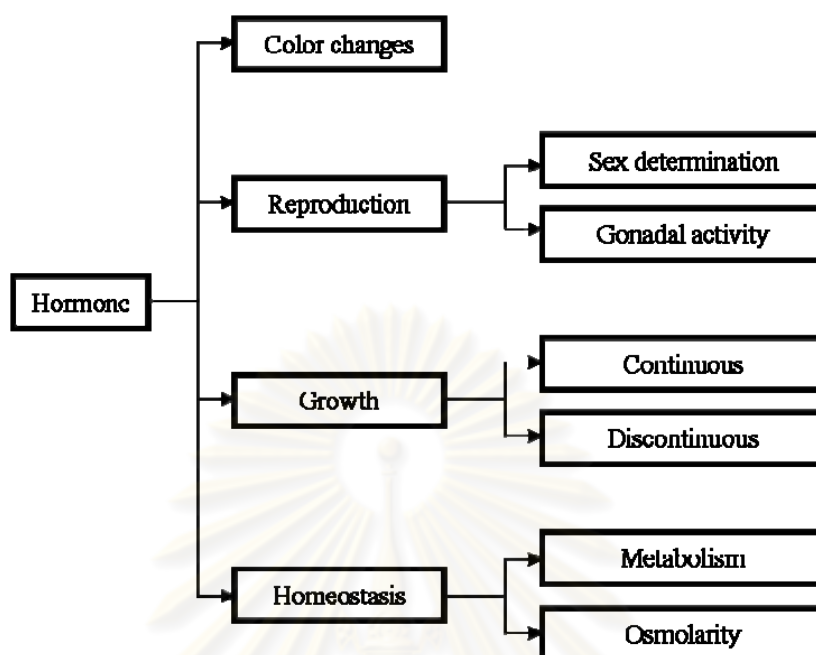


Figure 1.6 Diagram illustrating the hormonal controls of physiological processes of penaeid shrimp.

The current practice to stimulate ovarian development by eyestalk ablation is stressful to the animal, and it could lead to mortality. In order to avoid eyestalk ablation, different techniques to stimulate ovarian development such as maturation diet and hormone stimulation have been attempted. The use of these techniques to variable success reveals our lack of general understanding of oocyte development in crustacean. Therefore, the knowledge on hormonal factors influencing the ovarian and oocyte development in crustacean is necessary to develop the hormonal manipulation techniques in shrimp.

Eyestalk hormones play the important role for regulating several physiological mechanisms and unilateral eyestalk ablation is practically used for induction of ovarian development but this technique does not have the potential effects on testicular development of *P. monodon*. Therefore, the molecular mechanisms controlling testicular and ovarian maturation may be different.

1.8.2 Female reproductive hormone

Hormonal regulation is one of the several factors that control the female reproduction. The female reproductive hormone was produced from various tissues (Figure 1.7) including eyestalks, mandibular organ and Y-organ.

1.8.2.1 Eyestalk hormones

It is well-known that eyestalk ablation induces ovarian development and oviposition. This effect has been attributed to the presence of a vitellogenesis-inhibiting factor present in the MTXO-SG neurosecretory system (Figures 1.8 and 1.9). A group of neuropeptides that directly affect reproductive performances in crustacean have been identified. Many of these molecules belongs share a high degree of similarity with crustacean hyperglycemic hormone (CHH).

Gonad inhibiting hormone (GIH) is secreted from the X-organ in the eyestalk, and inhibits the synthesis of vitellogenin in the ovary. The peptides also have an impact on the males, and hence it is called gonad inhibiting hormone instead of vitellogenesis inhibiting hormone (Huberman 2000).

Treerattrakool et al (2008) cloned and characterized GIH from cDNA obtained from the eyestalk of *P. monodon* (*Pem*-GIH), measured tissue expression, and performed a knockdown experiment of *Pem*-GIH using dsRNA interference. They discovered a 79 amino acids that was closely related to type II CHH. The *Pem*-GIH gene expression was observed in the eyestalk, brain, thoracic and abdominal nerve cords of adult *P. monodon* (Treerattrakool et al. 2008). Injection of dsRNA of *Pem*-GIH can reduce transcript levels in the eyestalk and in the abdominal nerve cord both *in vitro* and *in vivo*. *Pem*-GIH-knockdown shrimp showed increase vitellogenin gene expression (Treerattrakool et al. 2008).

Peptides with gonad inhibiting properties was also cloned and characterized in whiteleg shrimp *L. vannamei* (Tsutsui et al. 2007), and lobster *Homarus americanus* (called VIH)(Ohira et al. 2006). Both GIH from *L. vannamei* and *H. americanus* have shown *in vitro* to be inhibiting vitellogenin gene expression.

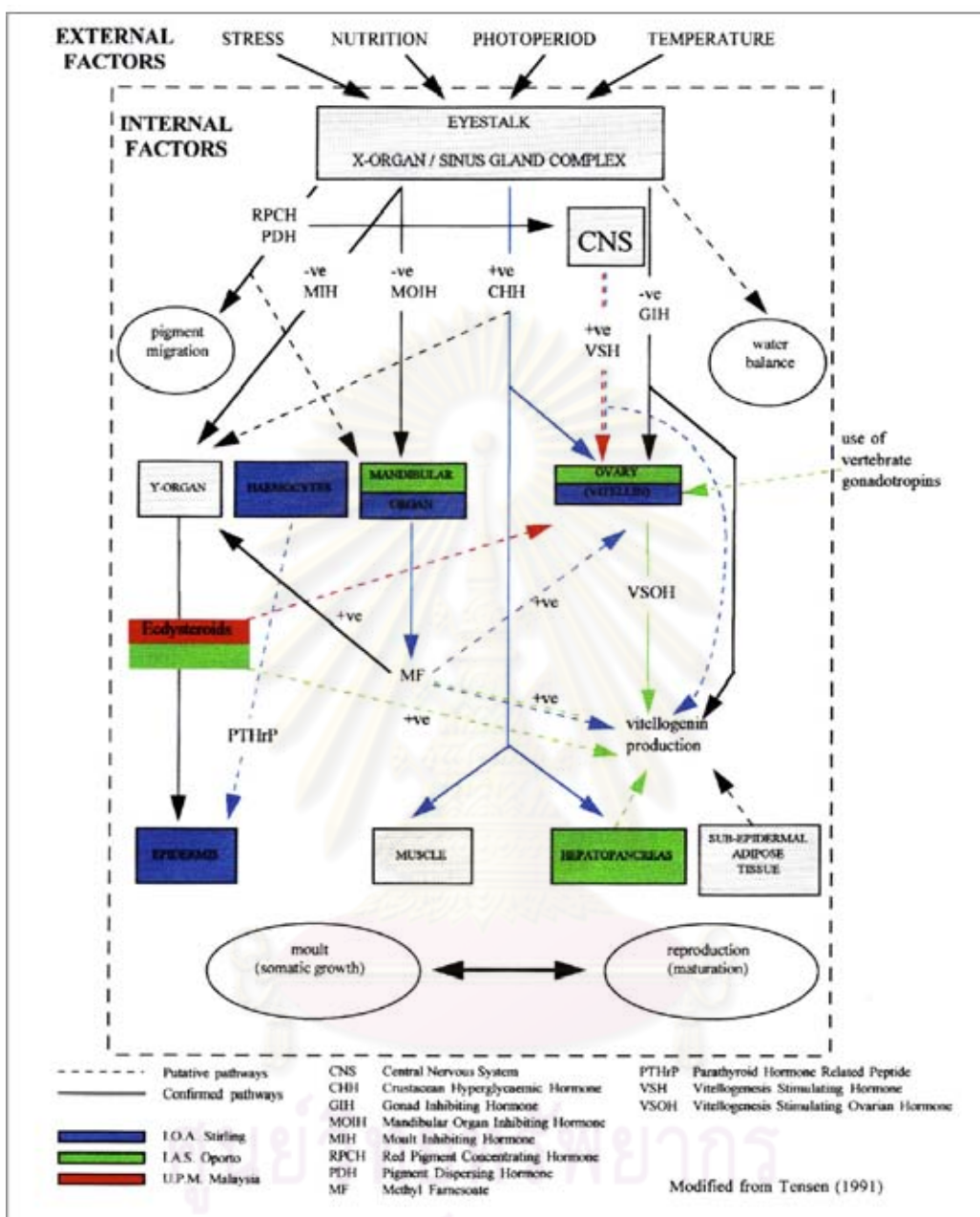


Figure 1.7 Diagram showing complexity of the neuroendocrine system controlling growth and maturation in female crustaceans. (Laufer et al., 1991).

There has been only one report in the literature of GSH. Tiu and Chan (2007) used recombinant protein and RNA interference approach to examine the gonad-stimulating property of the previously reported molt-inhibiting hormone, MeMIH-B, from *Metapenaeus ensis*. MeMIH-B can up regulate vitellogenin expression in

hepatopancreas and ovary both *in vitro* and *in vivo* (Tiu and Chan, 2007). Injection of shrimp with MeMIH-B dsRNA reduced the expression of MeMIH-B in the eyestalk and thoracic ganglion and vitellogenin expression in both the hepatopancreas and ovary was lowered as a result. The secretion of GSH from the thoracic ganglion is confirmed in red claw crayfish *Cherax quadricarinatus* (Cahansky et al. 2008).

Two other hormones that can indirectly affect ovarian maturation are molt-inhibiting hormone (MIH) and mandibular organ inhibiting hormone (MOIH). MIH is secreted from the X-organ and has an effect on the production of ecdysteroids by the Y-organ. The role of ecdysteroids on ovarian development and reproduction has to do with the balance between growth and reproduction. Ecdysteroids' main role includes the control of molting, and therefore it is inevitably linked to reproduction as well. Molt inhibiting hormone (MIH) have been identified, cloned, and characterized in many organisms such as crab *Charybdis feriatus* (Chan et al. 1998), crab *Cancer magister* (Umphrey et al. 1998), shrimp *Metapenaeus ensis* (Gu et al. 2001), and whiteleg shrimp *Litopenaeus vannamei* (Lago-Lestón et al. 2007). In a review paper, Nakatsuji et al (2009) compared MIH structures, analyzed MIH protein and transcripts level during the molting cycle, and animal responses to MIH in crustaceans.

Only MOIH from crab *Cancer pagarus* and spider crab *Libinia emarginata* has been identified and characterized (Liu et al. 1997; Wainwright et al. 1996).

1.8.2.2 Ecdysteroids

Ecdysteroids primarily serves as molting hormones in crustaceans, a similar function as in other arthropods. Their roles in reproduction have been suspected. As reproductive development in crustacean often occurred at the same period of continuing somatic growth (molting), one cannot overlook the importance of the molting cycle when considering various aspects of crustacean reproduction. The roles of ecdysteroids in reproduction are difficult to generalize as each group of species has different reproductive strategies in relation to the timing between molting and reproductive development.

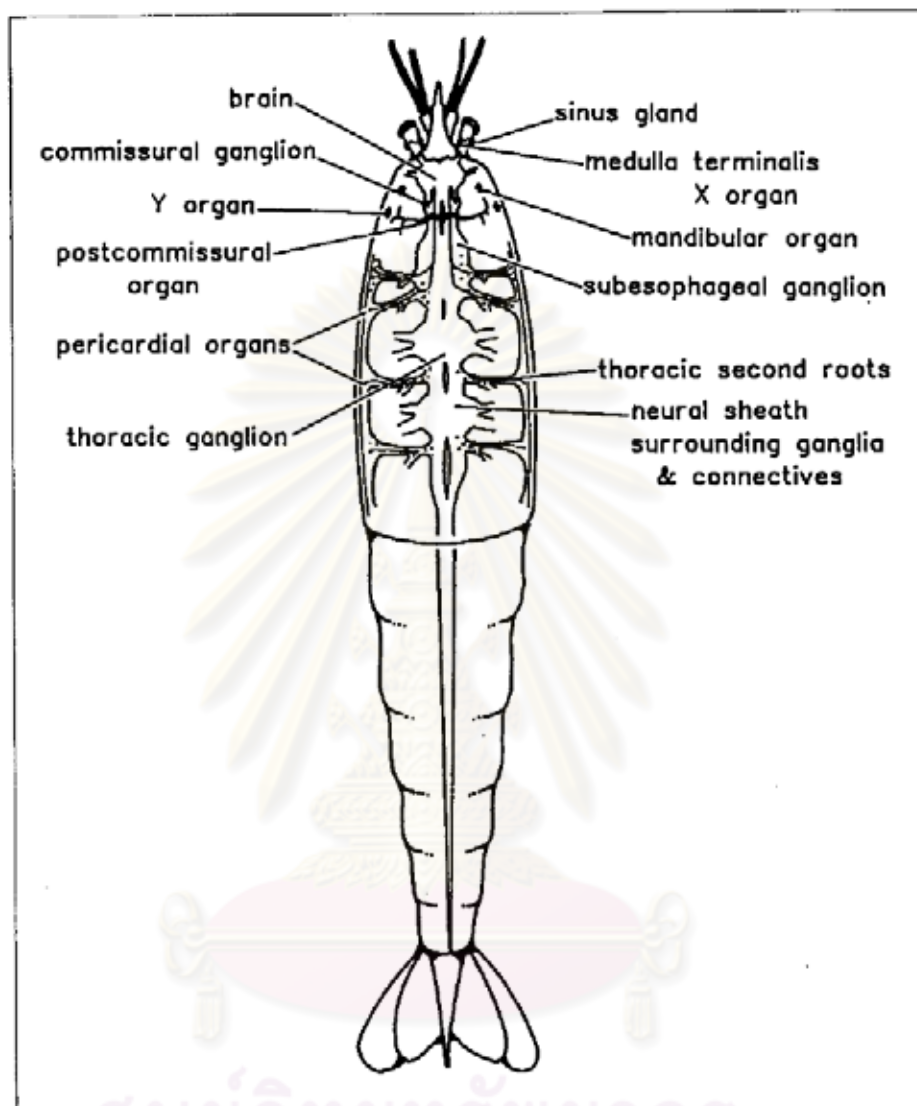


Figure 1.8 Major endocrine and neuroendocrine structures of generalized female crustacean. Included are the organs important for female reproduction, the eyestalk sinus gland x-organ, the mandibular organ, Y-organ, and thoracic ganglion (Laufer et al., 1991).

For examples, active vitellogenesis and spawning in peneaid shrimp occurs during the prolonged premolt period before ecdysis, while *Macrobrachium* spp. alternates between reproductive molt and non-reproductive molt (Subramoniam 2000). Subramoniam (2000) summarized the involvement of ecdysteroids in reproduction and embryogenesis in crustacean.

Ecdysteroids are synthesized by the Y-organs in crustacean, secreted into the hemolymph, and distributed to target tissues for conversion into active forms; 20-hydroxyecdysone (20E; also called crustecdysone, ecdysterone; Goodwin, 1978) (Subramoniam 2000). There is also evidence that ecdysteroids was also synthesized in the ovary and testis of crustaceans (Brown et al. 2009; Styrihave et al. 2008). Its production is negatively regulated by the molt-inhibiting hormone (MIH), secreted from the X-organ, and positively regulated by methyl farnesoate (MF). Important forms of ecdysteroids are 20-hydroxyecdysone (20E or 20HE) and ponasterone A (PoA) (Figure 1.11).

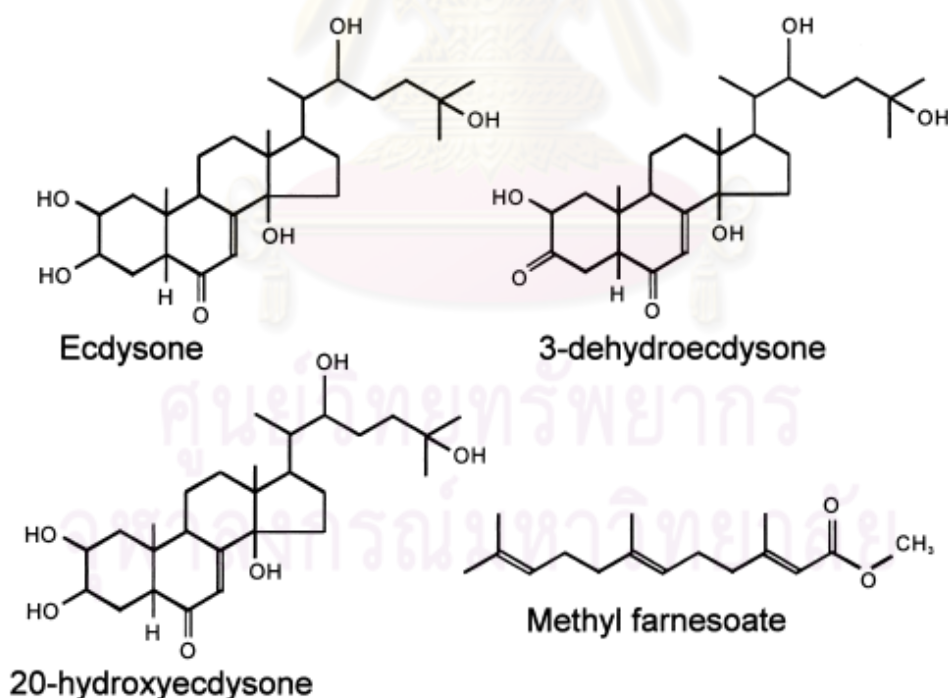


Figure 1.11 The chemical structures of ecdysteroids and methyl farnesoate (MF) (Okumura et al., 2004).

In the majority of the crustaceans, molting and hence somatic growth continue after the sexual maturity; with the result, Y-organ is active in adults also. Interestingly, the ovary in several crustacean species accumulates ecdysteroids for possible use during embryogenesis (Subramoniam et al., 1999).

In *P. monodon*, the predominant form of ecdysteroids in circulation is 20E (Kuo and Lin 1996). The peak concentration of ecdysteroids during *P. monodon* molting cycle coincides with stage D1 and D2 (proecdysis) followed by a rapid decline (Kuo and Lin 1996). Similar pattern of hemolymph ecdysteroid concentration was observed in *L. vannamei* (Chan 1995). The molting cycle was shown to override reproductive development in *P. monodon* (Quinitio et al. 1993) in that the shrimp would spawn or resorb their eggs prior to molting.

Variation in ecdysteroids concentration during oogenesis was observed in shrimp *Palaemon serratus* Pennant (Azevedo et al. 2002). Cytochrome P450 enzymes was hypothesized to be involved with ecdysteroids synthesis and lipid storage in copepod *Calanus finmarchicus* (Hansen et al. 2008). The ecdysteroids are also packaged into oocytes to be used by the embryo. 20E was shown to accumulate in the ovary of *L. vannamei*, and its presence coincided with the inhibition of total protein synthesis in the ovary during secondary vitellogenesis (Stage II or III) (Chan 1995). Injection of 20E (10 ng/g body weight; similar normal to hemolymph concentration) did not lead to ovarian maturation in *L. vannamei* (Chan 1995). Other hormones are hypothesized to interact with circulating ecdysteroids to regulate vitellogenesis and ovarian maturation (Subramoniam 2000).

Ecdysteroids concentration was shown to be related to with both vitellogenesis and molting. (Gunamalai et al 2004) monitored the concentration of 20E in the hemolymph and ovary through the molting cycle of mole crab *Emerita asiatica*, and examined the effect of 20E injection at different molting stages on the molting cycle, ovarian development, and embryonic development. They reported that ovarian 20E concentration increased with ovarian development (intermolt), peaked at the mid-vitellogenic stage (*E. asiatic* ovarian Stage IV), and started to decline as the crab went into pre-molt stage (Gunamalai et al 2004). As the concentration of 20E in the ovary

decreased, the hemolymph 20E concentration sharply increased as the crab entered the pre-molt stage before it dropped post-molt (Gunamalai et al 2004). Injection of 20E at different stages of development had different effects on hatching and molting. The timing of injection in relation to molting or ovarian developmental stages could result in shorten molting time and, in some cases, no hatching (Gunamalai et al 2004).

In *Drosophila*, the balance between the concentration of 20E and juvenile hormones (JH) seems to play a significant role in the development of the oocytes (Gruntenko and Rauschenbach 2008; Richard et al. 1998; Soller et al. 1999). More precisely, 20E acts as a negative feedback by stimulating the resorption of yolk protein back into the hemolymph unless the condition (environment, nutrition, and mating status) were suitable (Soller et al. 1999). Thus, 20E prevents the developing oocytes from progressing beyond the control point (oocyte stage in *Drosophila*) unless JH is present to modify the response of the oocyte to allow development beyond stage 9 (Soller et al. 1999). It is still unclear whether JH or 20E, alone or both, stimulates the early vitellogenesis in *Drosophila* (Richard et al. 2001; Richard et al. 1998). Gruntenko and Rauschenbach (2008) hypothesized dopamine and octopamine involvement in maintaining the balance of JH and 20E and their roles in reproduction of *Drosophila*.

1.8.2.3 Vertebrate-type steroid hormones

Vertebrate-type steroids have been found in many groups of invertebrate including crustacean (Lafont and Mathieu 2007). Steroids such as progesterone (PG), 17 α -hydroxyprogesterone (17-OHP), testosterone, and 17 β -estradiol (E2) are present in many crustacean species including kuruma prawn *M. japonicus* (Cardoso et al. 1997), giant freshwater prawn *M. rosenbergii* (Martins et al. 2007), black tiger shrimp *P. monodon* (Quinitio et al. 1994), mud crab *Scylla serrata* (Warrier et al. 2001).

Quinitio et al (1994) analyzed the profile of steroid hormones in relation to vitellogenin activity in female *P. monodon*. Progesterone and 17 β estradiol were detected in the hemolymph only in shrimp with mature ovaries, while the level was low or undetectable in the hemolymph in those with immature ovaries (Quinitio et al. 1994) .

The concentration of progesterone showed a positive correlation with vitellogenesis (Quinitio et al. 1994).

Okumura and Sakiyama (2004) compared the hemolymph concentrations of several vertebrate-type steroids in kuruma prawn during both natural and induced (by eyestalk ablation) ovarian development. They observed no correlation and concluded that vertebrate-type steroids were not involved in ovarian development of kuruma prawn (Okumura and Sakiyama 2004).

Yano and Hoshino (2006) reported that 17β -estradiol induced vitellogenesis and oocyte development in previtellogenic ovary of kuruma prawn *in vitro*. They proposed that 17β -estradiol is an ovarian vitellogenesis-stimulating hormone (OVSH) in immature decapods crustaceans.

Gunamalai et al (2006) monitored the concentration of 17β -estradiol and progesterone in the hemolymph, ovary and hepatopancreas of mole crab *Emeriata asiatica* and freshwater prawn *M. rosenbergii*. Both 17β -estradiol and progesterone peaked in all tissues during the intermolt period of the reproductive molt cycle in freshwater prawn, and the basal level of 17β estradiol was detectable in the ovary and hepatopancreas during the non-reproductive molt cycle (Gunamalai et al. 2006).

Martins et al (2007) performed similar experiment to monitor the hemolymph concentration of 17α -hydroxyprogesterone, testosterone, and 17β -estradiol in female freshwater prawn *M. rosenbergii* and correlated the results with each stage of ovarian development. They reported high concentration of 17α -hydroxyprogesterone throughout the reproductive cycle and the concentration peaked during pre-vitellogenic (*M. rosenbergii* ovarian stage 2) and late vitellogenic/ mature (*M. rosenbergii* ovarian stage 5) (Martins et al. 2007). The concentration of the glucuronide-conjugated 17β -estradiol also peaked during the previtellogenesis stage, while there was no significant variation in testosterone concentration (Martins et al. 2007).

Dietary source of vertebrate type steroids might play a role in ovarian development of penaeid shrimp. Meunpol et al (2007) extracted PG and 17α -OHP from

polychaetes *Perinereis* sp., a commonly used component in maturation diets for shrimp broodstock. They also reported that PG and 17α -OHP, both from the polychaetes extracts and synthetic, are capable of stimulating development of *P. monodon* oocytes from pre-vitellogenic stage to maturation (cortical rods) (Meunpol et al. 2007). It is possible the vertebrate steroids from polychaetes could stimulate the ovarian development in broodstock shrimp or supplement steroids produce by the shrimp.

Estrogen and androgen receptors were detected in the brain and thoracic ganglion of mud crab *Scylla paramamosain* using immunocytochemistry method (Ye et al. 2008). The presence of these receptors in the central nervous system suggested the possibility that estrogen and androgen may act as negative feedback in the endocrine system of crustacean (Ye et al. 2008).

Recently, the full-length cDNA of *progesterin membrane receptor component 1* (*Pgmrc1*) of *P. monodon* was successfully identified and characterized. *Pgmrc1* was 2015 bp in length containing an ORF of 573 bp corresponding to a polypeptide of 190 amino acids. Northern blot analysis revealed a single form of *Pgmrc1* in ovaries of *P. monodon*. Quantitative real-time PCR indicated that the expression level of *Pgmrc1* mRNA in ovaries of both intact and eyestalk-ablated broodstock was greater than that of juveniles ($P < 0.05$). *Pgmrc1* was up-regulated in mature (stage IV) ovaries of intact broodstock ($P < 0.05$). Unilateral eyestalk ablation resulted in an earlier up-regulation of *Pgmrc1* since the vitellogenic (II) ovarian stage. Moreover, the expression level of *Pgmrc1* in vitellogenic, early cortical rod and mature (II–IV) ovaries of eyestalk-ablated broodstock was greater than that of the same ovarian stages in intact broodstock ($P < 0.05$). *Pgmrc1* mRNA was clearly localized in the cytoplasm of follicular cells, previtellogenic and early vitellogenic oocytes. Immunohistochemistry revealed the positive signals of the *Pgmrc1* protein in the follicular layers and cell membrane of follicular cells and various stages of oocytes.

No report of progesterone, estrogen and androgen receptors in other crustacean species at present. The presence of both receptors in the central nervous system of crustacean indicates that vertebrate type steroids might play a role in crustacean

endocrine system. Assessing the role of vertebrate steroids in crustaceans could have many applications. The effect of dietary vertebrate steroids on ovarian maturation suggested potential uses of these steroids to stimulate reproductive development.

1.8.2.4 Prostaglandins and other eicosanoids

It has been proposed that prostaglandins play a role in ovarian maturation in crustacean. Prostaglandins are derived from fatty acids such as arachidonic acid or eicosapentaenoic acid. Prostaglandins as a group have many physiological functions in many animals. In invertebrates, prostaglandins were found in sponges, cnidarians, nematodes, platyhelminthes, mollusks, annelids, crustaceans, acari, urochordates, and insects ((Rowley et al. 2005; Stanley 2006). Their known functions in invertebrates are diverse including immunity, homeostasis, feeding, larval settlement, and reproduction (Rowley et al. 2005).

Tahara and Yano (2003) monitored the hemolymph concentration of prostaglandins during ovarian maturation in kuruma prawn *M. japonicus*. They reported the concentration of prostaglandins (PGF_{2α} and PGE₂) in the hemolymph peaked during early vitellogenic stage and declined during the later developmental stages ((Tahara and Yano 2003).

Tahara and Yano (2004) analyzed total lipids, fatty acids, and prostaglandins in the ovaries of the kuruma prawn. Total lipid concentration increased with gonadosomatic index, and arachidonic acid concentration was lower at the early stages of development (pre-vitellogenic and early vitellogenic) than at the maturation stage (Tahara and Yano 2004). Prostaglandins concentration in the ovary peaked during the pre-vitellogenic stage and decreased at the later stage (Tahara and Yano 2004). The concentration peaked in the ovary before the hemolymph.

Spaziani et al (Spaziani et al. 1993) observed an increasing trend of prostaglandins (PGF_{2α} and PGE₂) concentrations in the ovary of Florida freshwater crayfish *Procambarus paeninsulanus* during the late vitellogenic stage with the concentration peaking just prior to ovulation. They also reported a gradual increase of PGE₂ as vitellogenesis progresses (Spaziani et al. 1993). Spaziani et al (1995) also

reported that $\text{PGF}_{2\alpha}$ can induce ovarian contraction (cAMP-mediated) and suggested that $\text{PG}_{2\alpha}$ may be involved with ovulation.

The reproduction-related functions of prostaglandin in other animals appeared to occur at several stages of oocyte maturation (Rowley et al. 2005; Stanley 2006). So far the concentration profile of prostaglandins in crustacean during ovarian development suggested its importance at the end of oocyte maturation. This hypothesis still needs to be confirmed with more research. Since precursor of prostaglandins is fatty acids, dietary manipulation could have some effects on prostaglandins in crustacean.

1.9 Molecular technique used for studies in this thesis

1.9.1 PCR

The introduction of the polymerase chain reaction (PCR) by Mullis et al. (1987) has opened a new approach for molecular genetic studies. This method is a molecular biology technique for enzymatically replicating DNA without using a living organism, such as *E. coli* or yeast and is a method using specific DNA sequences by the two oligonucleotide primers, 17-30 nucleotides in length. Million copies of the target DNA sequence can be synthesized from the low amount of starting DNA template within a few hours.

The PCR reaction components are composed of DNA template, a pair of primers for the target sequence, dNTPs (dATP, dCTP, dGTP and dTTP), buffer and heat-stable DNA polymerase (usually *Taq* polymerase). The amplification reaction consists of three steps; denaturation of double stranded DNA at high temperature, annealing to allow primers to form hybrid molecules at the optimal temperature, and extension of the annealed primers by heat-stable DNA polymerase. The cycle is repeated for 30-40 times (Figure 1.12). The amplification product is determined by agarose or polyacrylamide electrophoresis.

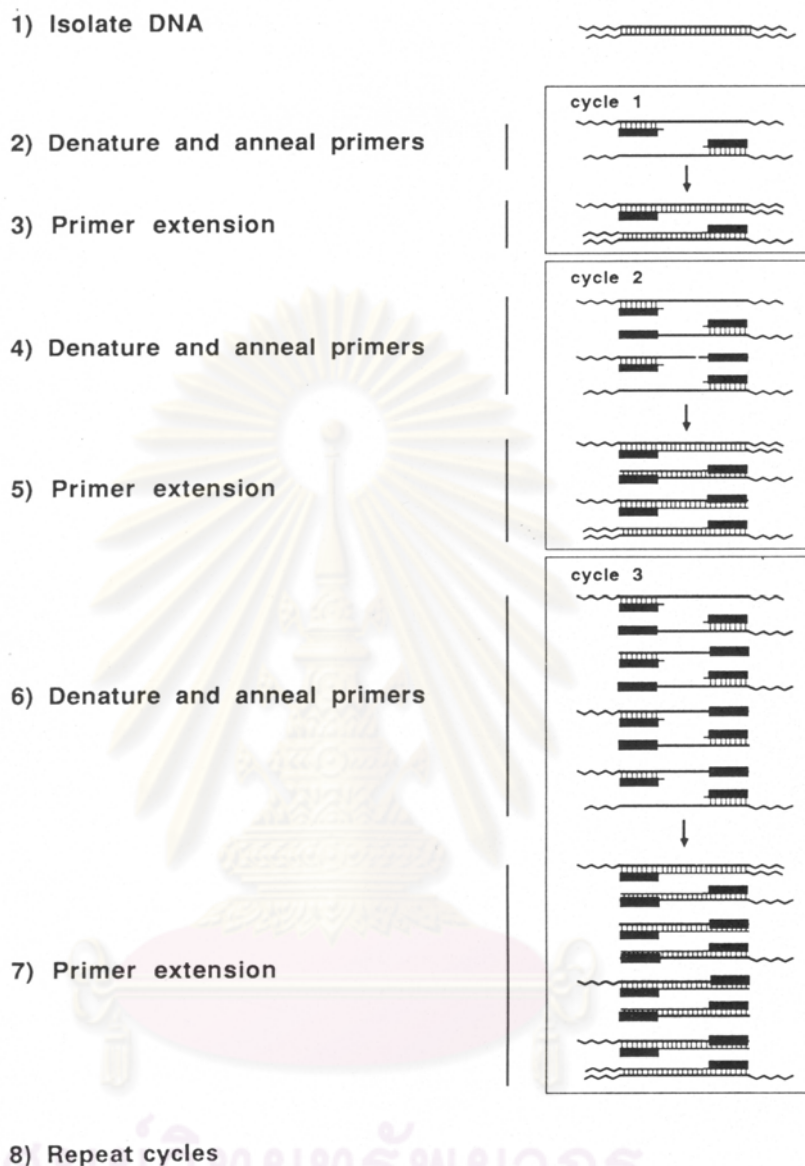


Figure 1.12 General illustration of the polymerase chain reaction (PCR) for amplifying DNA

1.9.2 Reverse Transcription-polymerase chain reaction (RT-PCR) and semiquantitative RT-PCR

RT-PCR is the method that was used to amplify, isolate or identify a known sequence transcripts. This method is a comparable method of conventional PCR but the

first strand cDNA template rather than genomic DNA was used as the template in amplification. This method contained 2 steps, in the first step first strand cDNA was synthesis using reverse transcriptase, which is made from a messenger RNA (mRNA). After that the cDNA was amplified using specific primer as same as amplified from genomic DNA (Fig. 1.13).

RT-PCR is a comparable method of conventional PCR but the first strand cDNA rather than genomic DNA used as the template in the amplification reaction. It is a basic technique for determination of gene expression in a particular RNA population. The template for RT-PCR can be the first stranded cDNA synthesized from total RNA or poly A⁺ RNA. Reverse transcription of total RNA can be performed with oligo(dT) or random primers using a reverse transcriptase. The product is then subjected to the second strand synthesis using a gene specific primer. The resulting product is used as the typical PCR.

Semiquantitative RT-PCR is a semiquantitative approach where the target genes and the internal control (e.g. a housekeeping gene) are separately or simultaneously amplified using the same template. The internal control (such as β -actin, elongation factor EF-1 α or G3PDH) is used under the assumption that those coding genes are transcribed constantly and independently from the extracellular environment stimuli and that their transcripts are reverse transcribed with the same efficiency as the product of interesting transcript.

1.9.3 Rapid Amplification of cDNA Ends-polymerase chain reaction (RACE-PCR)

RACE-PCR is an approach used for isolation of the full length of characterized cDNA. This method generates cDNA fragments by using PCR to amplify sequences between a single region in the mRNA and either the 3'- or the 5'-end of the transcript. To use RACE it is necessary to know or to deduce a single stretch of sequence within the mRNA. From this sequence, specific primers are chosen which are oriented in the 3' and 5' directions, and which usually produce overlapping cDNA fragments (Primrose. 1998).

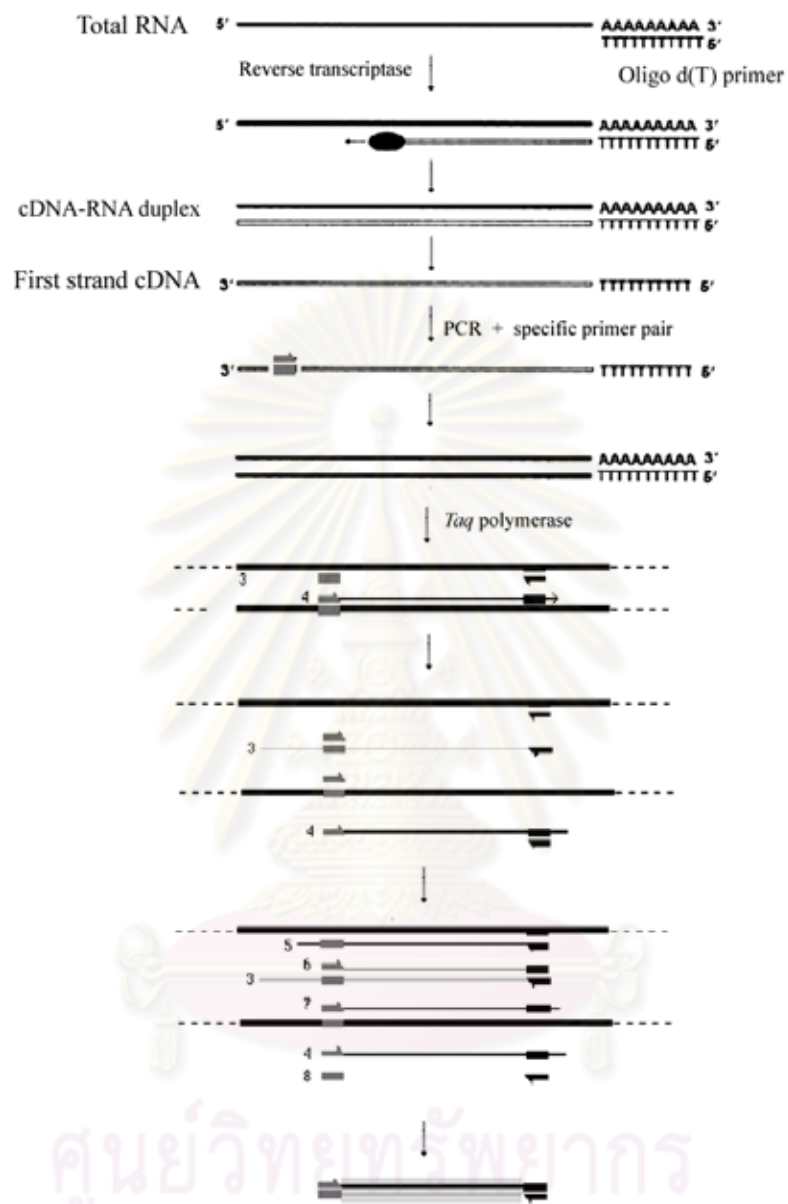


Figure 1.13 Overall concepts of the RT-PCR procedure. During first-strand cDNA synthesis an oligo d(T) primer anneals and extends from sites present within the total RNA. Second strand cDNA synthesis primed by the 18 - 25 base specific primer proceeds during a single round of DNA synthesis catalyzed by *Taq* polymerase. These DNA fragments serve as templates for PCR amplification.

Using SMART (Switching Mechanism At 5' end of RNA Transcript) technology, terminal transferase activity of Powerscript Reverse Transcriptase (RT) adds 3-5 nucleotides (predominantly dC) to the 3' end of the first strand cDNA. This activity is harnessed by the SMART oligonucleotides whose terminal stretch of dG can anneal to the dC-rich cDNA tail and serve as an extended template for reverse transcriptase. A complete cDNA copy of original mRNA is synthesized with the additional SMART sequence at the end (Fig. 1.14).

The first strand cDNA of 5' and 3' RACE is synthesized using a modified oligo (dT) primers and serve as the template for RACE-PCR reactions. Gene specific primers (GSPs) are designed from interested gene for 5'-RACE PCR (antisense primer) and 3'-RACE PCR (sense primer) and used with the universal primer (UPM) that recognize the SMART sequence. RACE products are characterized. Finally, the full length cDNA is isolated.

1.9.4 Genome walk analysis

Genome walk analysis is a method for identifying unknown genomic regions flanking a known DNA sequences. Initially, genomic DNA is separately digested with different blunt-end generating restriction endonucleases (usually, *Hae* III, *Dra* I, *Pvu* II and *Ssp* I). The digested genomic DNA in each tube was then ligated to the adaptor. The ligated product is used as the template for PCR amplification.

PCR was carried out with the primer complementary to the adaptor (AP1) and the interesting gene (gene specific primer; GSP). The resulting product is amplified with nested primers (AP2 and nested GSP). The nested PCR products were cloned and characterized (Fig. 1.15). This technique allows isolation of the promoter region of interesting genes and 3' and 5' Un-translated region (UTR) that required further characterization of SNPs at 3' and 5'UTR.

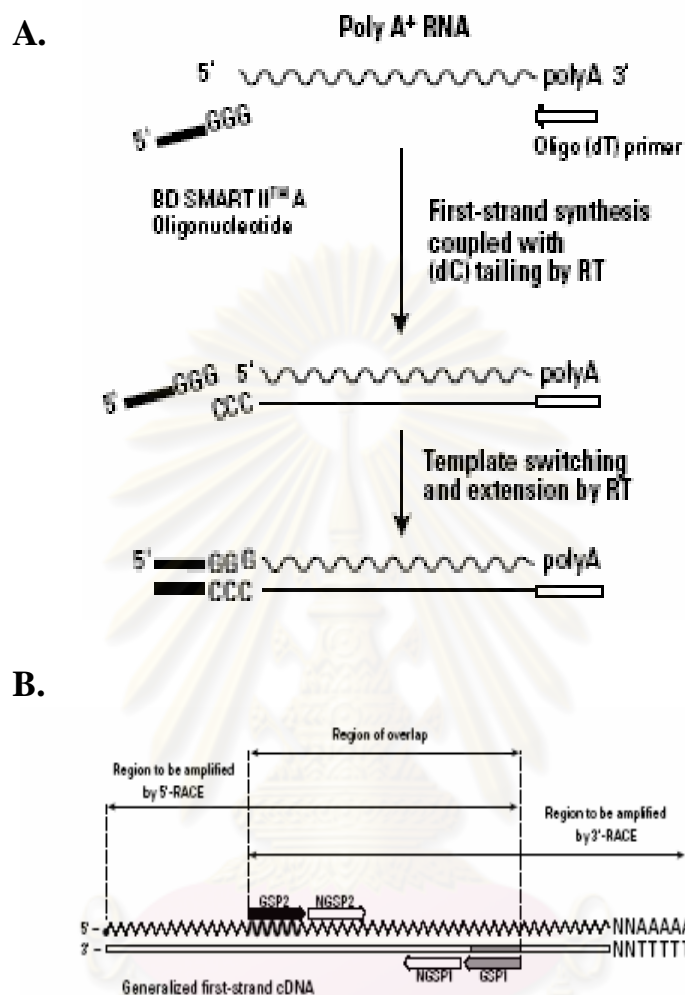


Figure 1.14 (A) Mechanism of a SMART™ technology cDNA synthesis. First-strand synthesis is primed using a modified oligo (dT) primer. After Powerscript reverse transcriptase reaches the end of the mRNA template, it adds several dC residues. The SMART II A oligonucleotide anneals to the tail of the cDNA and serves as an extended template for PowerScript RT. (B) The relationship of gene-specific primers to the cDNA template. This diagram shows a generalized first strand cDNA template.

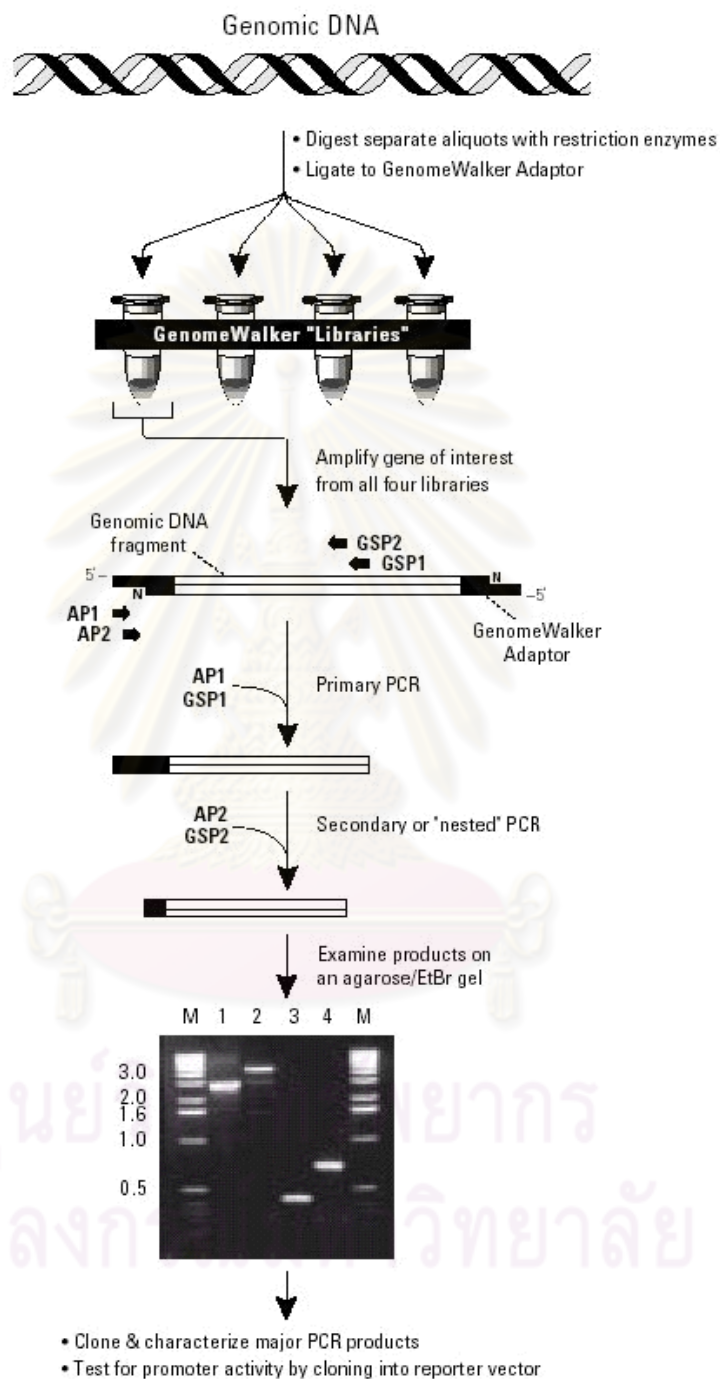


Figure 1.15 A flow chart illustrating the GenomeWalk analysis protocol.

1.9.5 DNA sequencing

DNA sequencing is the process of determining the exact order of the bases (A, T, C and G) in a piece of DNA. In essence, the DNA is used as a template to generate a set of fragments that differ in length from each other by a single base. The fragments are then separated by size, and the bases at the end are identified, recreating the original sequence of the DNA. There are two general methods for sequencing of DNA segments: the “chemical cleavage” procedure described by Maxam and Gilbert, 1977 and the “chain termination” procedure was described by Sanger, 1977. Nevertheless, the latter method is more popular because chemical cleavage procedure requires the use of several hazardous substances. DNA fragments generated from PCR can be directly sequenced or alternatively, those fragments can be cloned and sequenced. This eliminates the need to establish a genome library and searching of a particular gene in the library.

DNA sequencing is the molecular biology technique for determined sequence of a piece of DNA. This technique provides high resolution and facilitating interpretation. However, sequencing of a large number of individuals using conventional method is extremely tedious and prohibitively possible. The sequencing method has been facilitated by the direct and indirect use of DNA fragments generated through PCR. At present, automatic DNA sequencing has been introduced and commonly used (Figure 1.15). This greatly allows wider application of DNA sequencing analysis for population genetic and systematic studies.

1.9.6 Quantitative real-time PCR

Real-time polymerase chain reaction, also called “quantitative real-time polymerase chain reaction” (Q-PCR/qPCR) or “kinetic polymerase chain reaction”, is a laboratory technique based on the polymerase chain reaction, which is used to amplify and simultaneously quantify a target DNA molecule. It enables both detection and quantification (as absolute number of copies or relative amount when normalized to DNA input or additional normalizing genes) of a specific sequence in a DNA sample (Figure 1.16).

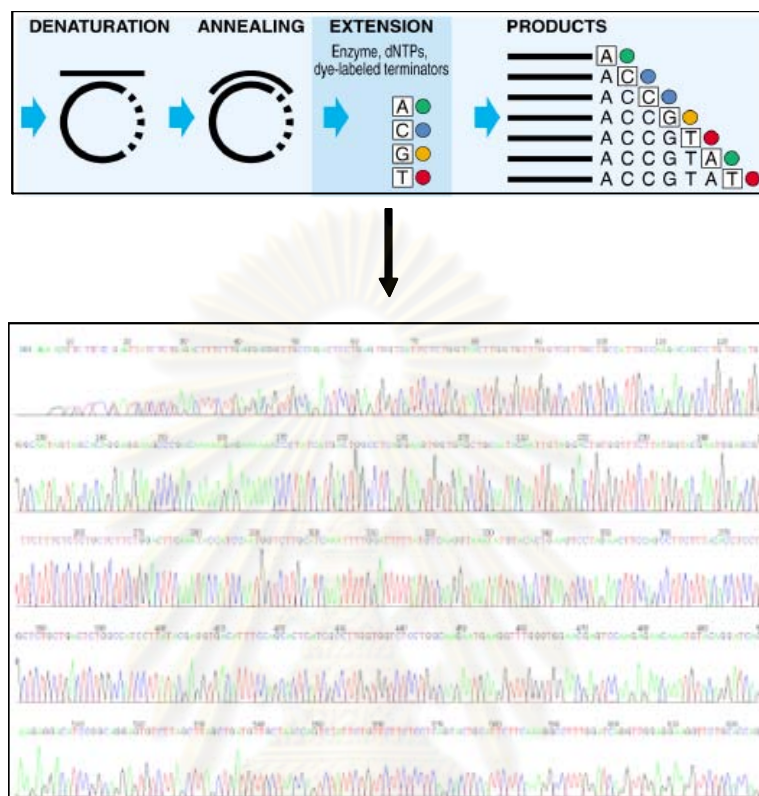


Figure 1.16 A schematic diagram illustrating principles of automated DNA sequencing.

The procedure follows the general principle of polymerase chain reaction; its key feature is that the amplified DNA is quantified as it accumulates in the reaction in real time after each amplification cycle (Figure 1.17). Two common methods of quantification are: (1) the use of fluorescent dyes that intercalate with double-stranded DNA, and (2) modified DNA oligonucleotide probes that fluoresce when hybridized with a complementary DNA (VanGuilder *et al.*, 2008)

Typically, the reaction is prepared as usual, with the addition of fluorescent dsDNA dye. The reaction is run in a thermocycler and after each cycle, the levels of fluorescence are measured with a detector; the dye only fluoresces when bound to the dsDNA (i.e., the

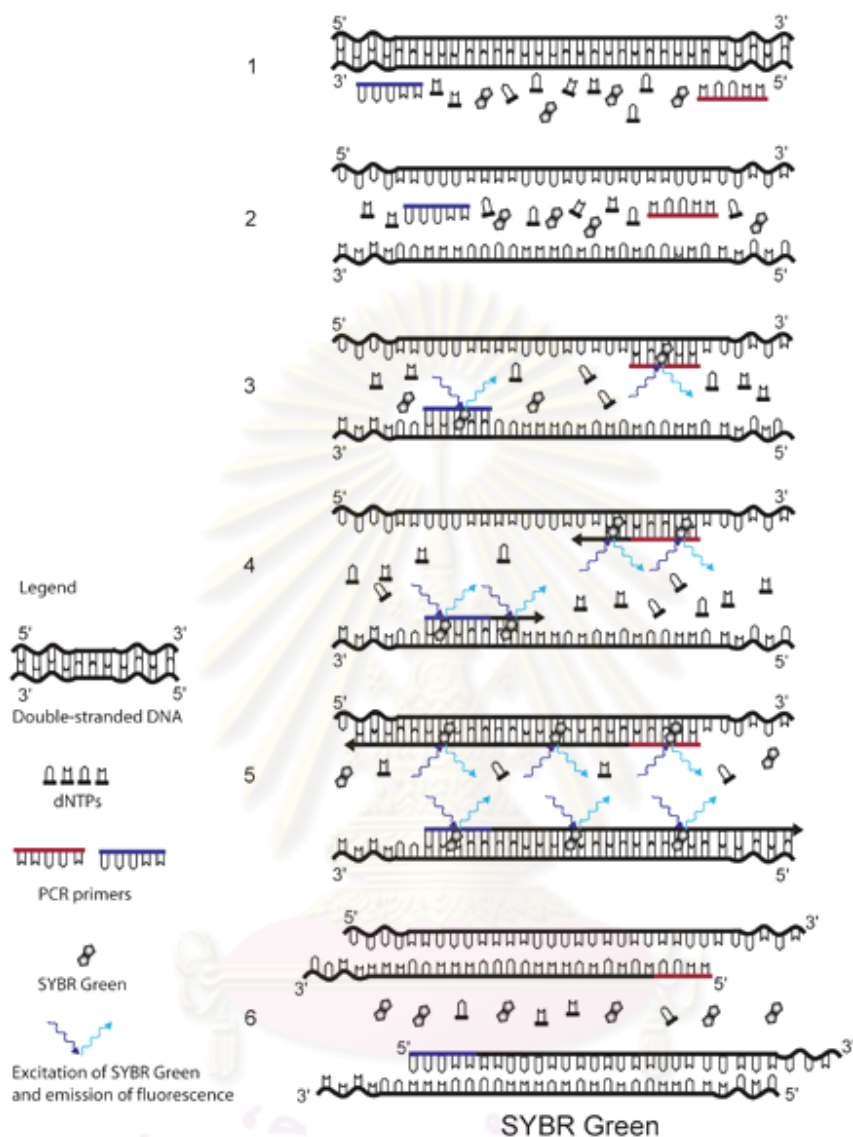


Figure 1.17 The principle of SYBR Green detection in real-time. The fluorescent dye SYBR Green is added to the PCR mixture. SYBR Green is a DNA binding dye that fluoresces strongly when bound to double-stranded DNA. At the start of the reaction, very little double stranded DNA is present, and so the fluorescent signal detected by the thermocycler is low. As the reaction proceeds and PCR product accumulates, the amount of double-stranded DNA increases and with it the fluorescence signal. The signal is only detectable during annealing and extension, since the denaturation step contains predominantly single-stranded DNA.

PCR product). With reference to a standard dilution, the dsDNA concentration in the PCR can be determined.

A DNA-binding dye binds to all double-stranded (ds) DNA in PCR, causing fluoresce of the dye. An increase in DNA product during PCR therefore leads to an increase in fluoresce intensity and is measured at each cycle, thus allowing DNA concentrations to be quantified. However, SYBR Green binds to all dsDNA PCR products, including nonspecific PCR products (such as “primer dimmers”). This can potentially interfere with or prevent accurate quantification of the intended target sequence.

1.9.7 *In situ* hybridization

In situ hybridization allows specific nucleic acid sequences to be detected in morphologically preserved chromosomes, cells or tissue sections. In combination with immunocytochemistry, *in situ* hybridization can relate microscopic topological information to gene localization at the DNA, mRNA, and protein level. The technique was originally developed by Pardue and Gall (1969). At that time radioisotopes were the only labels available for nucleic acids, and autoradiography was applied of detecting hybridized sequences. Furthermore, as molecular cloning was not possible in those days, *in situ* hybridization was restricted to those sequences that could be purified and isolated by conventional biochemical methods (e.g., mouse satellite DNA, viral DNA, ribosomal RNAs).

At present, non-radioactive labeling using the digoxigenin (DIG) system is commonly applied for *in situ* hybridization. Digoxigenin is linked to the C-5 position of uridine nucleotides via a spacer arm containing eleven carbon atoms (Figure 1.18). The DIG-labeled nucleotides may be incorporated, at a defined density, into nucleic acid probes by DNA polymerases (such as *E. coli* DNA polymerase I, T4 DNA polymerase, T7 DNA polymerase, Transcriptase, and Taq DNA Polymerase) as well as RNA Polymerase (SP6, T3, or T7 RNA Polymerase), and Terminal Transferase.

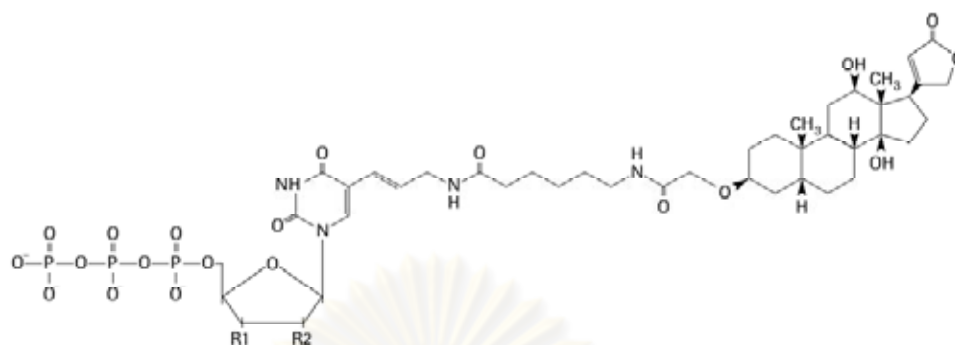


Figure 1.18 Digoxigenin-UTP/dUTP/ddUTP, alkali-stable. Digoxigenin-UTP (R1 = OH, R2 = OH) Digoxigenin-dUTP (R1 = OH, R2 = H) Digoxigenin-ddUTP (R1 = H, R2 = H)

DIG label may be carried out by random primed labeling, nick translation, PCR, 3'-end labeling/tailing, or *in vitro* transcription. Hybridized DIG-labeled probes may be detected with high affinity anti-digoxigenin (anti-DIG) antibodies that are conjugated to alkaline phosphatase, peroxidase, fluorescein, rhodamine, or colloidal gold. Alternatively, unconjugated anti-digoxigenin antibodies and conjugated secondary antibodies may be used.

Detection sensitivity depends upon the method used to visualize the anti-DIG antibody conjugate. For instance, when an anti-DIG antibody conjugated to alkaline phosphatase is visualized with colorimetric (NBT; blue tetrazolium chloride and BCIP; 5-Bromo-4chloro-3-indolyl phosphate, toluidine salt) or fluorescent (HNPP) alkaline phosphatase substrates, the sensitivity of the detection reaction is routinely 0.1 pg of the target on a Southern blot.

1.10 Effects of *O*-methyltransferase and ecdysteroids on ovarian development and/or molting of crustaceans

1.10.1 *O*-methyltransferase

O-methyltransferase (OMT) is ubiquitously present in diverse organisms and plays an important regulatory role in growth, development, reproduction and defense mechanisms in plants and animals. In animal two kinds of OMT; catechol-*O*-methyltransferase (COMT) and farnesoic acid-*O*-methyltransferase (FAMeT) were identified according to their selectivity to methyl acceptors.

1.10.1.1 Catechol-*O*-methylation (COMT)

Catechol-*O*-methyltransferase (COMT) functionally transferred of the methyl group from S-adenosine-methionine to one of the hydroxyl group of catechol compounds (Figure 1.19). Accordingly, COMT plays an important role in the catabolism and *O*-methylation of endogenous catecholamines with hormonal and neurotransmission activities such as dopamine, noradrenaline, epinephrine, catecholestroge) and their metabolites, ascorbic acid (Guldberg and Marsden. 1975, Mannisto et al. 1992., Kopin. 1985 and Filipenko et al., 2001), some indolic intermediates of melanin metabolism (Smit et al., 1990) and xenobiotic catechols and carcinogenic catechol-containing flavonoids (Zho and Liehr. 1994).

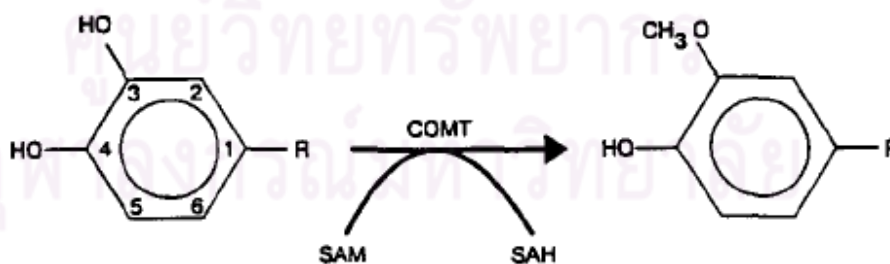


Figure 1.19 The *O*-methylation of the catechol substrate catalysed by COMT. (Lundstrom et al. 1995)

Interestingly, 17β -estradiol can be hydroxylated at 2- and 4- carbons of ring A by specific hydroxylases (estrogen-2/4-hydroxylases). The hydroxyestrogens can be *O*-methylated by COMT to form methoxyestrogens (Figure 1.20; Ball et al. 1983, Fishman 1983). In the mammalian ovaries, catecholestrogens have been demonstrated as potent autocrine/paracrine regulators of ovarian functions. They stimulate progesterone synthesis, cAMP and β -adrenergic receptors (Spicer and Hammond, 1989). Therefore, COMT should also involve the steroidogenic pathway in shrimp and may play the important role on ovarian development of *P. monodon*.

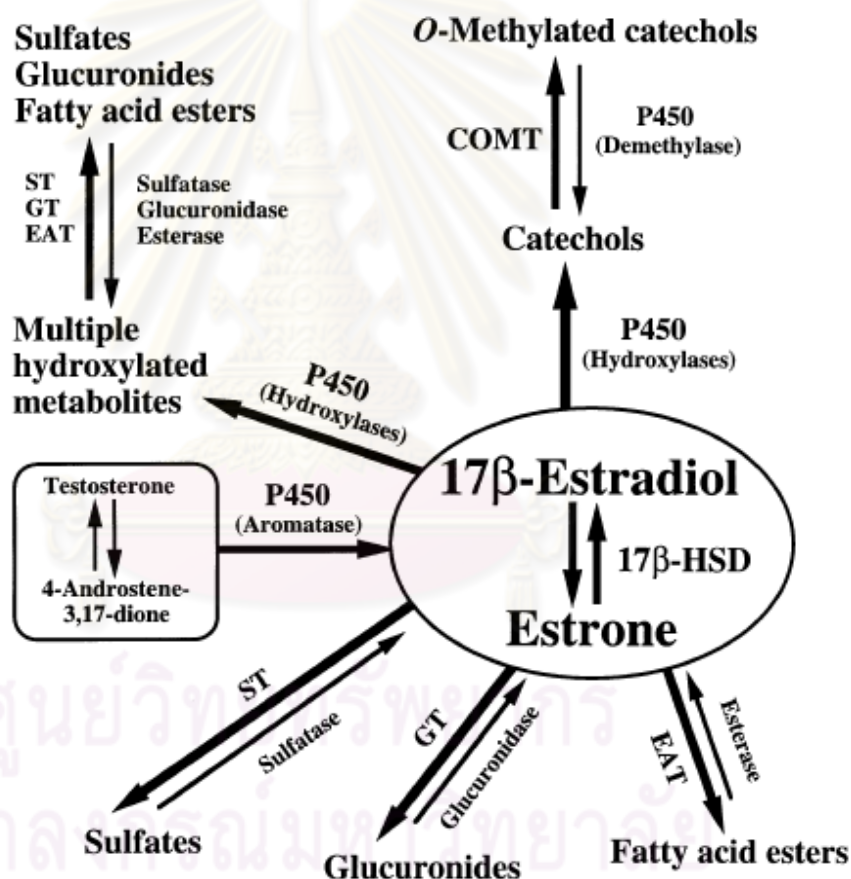


Figure 1.20 Complexities of estrogen metabolism. Abbreviations used. ST: sulfotransferase, GT: glucosyltransferase, EAT: estrogen acyltransferase, 17β -HSD: 17β hydroxysteroid dehydrogenase, COMT: catechol-*O*-methyltransferase and P450: cytochrome P450 (Zho and Conney., 1998).

COMT has an important role in the metabolism of catecholestrogens which are 2- and 4-hydroxylated products of estrogens. The competition with catecholamines for the metabolism through COMT locally in tissues (e.g. breast, ovaries and uterus) has been noticed *in vitro* (Ball et al. 1972). Catecholestrogens seem to have importance at least in early pregnancy and in the initiation of some estrogen-dependent tumors (Männistö et al. 1992b; Cavalieri et al. 1997; Weisz et al. 1998; Zhu and Conney 1998). Expression of COMT is regulated by estrogens (Xie et al. 1999). The role of COMT and catecholestrogens *in vitro* and *in vivo* has not been clarified (Männistö and Kaakkola 1999).

Li et al. (2006) isolated the full length cDNA of *O*-methyltransferase in *Fenneropenaeus chinensis* from the hemocytes of bacteria-infected shrimp by suppression subtractive hybridization (SSH) coupled with the SMART cDNA method. The phylogenetic analysis indicated that *F. chinensis OMT* was not a member of *FAMeT* but recognized as a new member of *COMT*.

More recently, the recombinant COMT protein of *F. chinensis COMT* (Fc-COMT) was expressed *in vitro*. The rFc-COMT was found in the soluble form in *E. coli* lysate. Two types of methyl products of DHBAc (VA and IVA) were detected in the enzymatic reaction mixtures with rFc-COMT by HPLC-MS. The rFc-COMT has the catalytic activity for transferring the methyl group from SAM to the 3'- or 4'-hydroxyl group of the benzyl ring of DHBAc (Li et al., 2010).

1.10.1.2 Farnesoic acid-*O*-methyltransferase (FAMeT)

Methyl farnesoate (MF) is structurally similar to the insect juvenile hormones (JH III, Figure 1.21). MF synthesized in mandibular organ (MO) from farnesoic acid (FA) by the action of farnesoic acid *O*-methyltransferase (FAMeT) in the presence of *S*-adenosyl methionine (Nagaraju, 2007). From the MO, MF is secreted into the hemolymph and distributing to the target organ. MF has an effect on several organs including the Y-organ and ovaries.

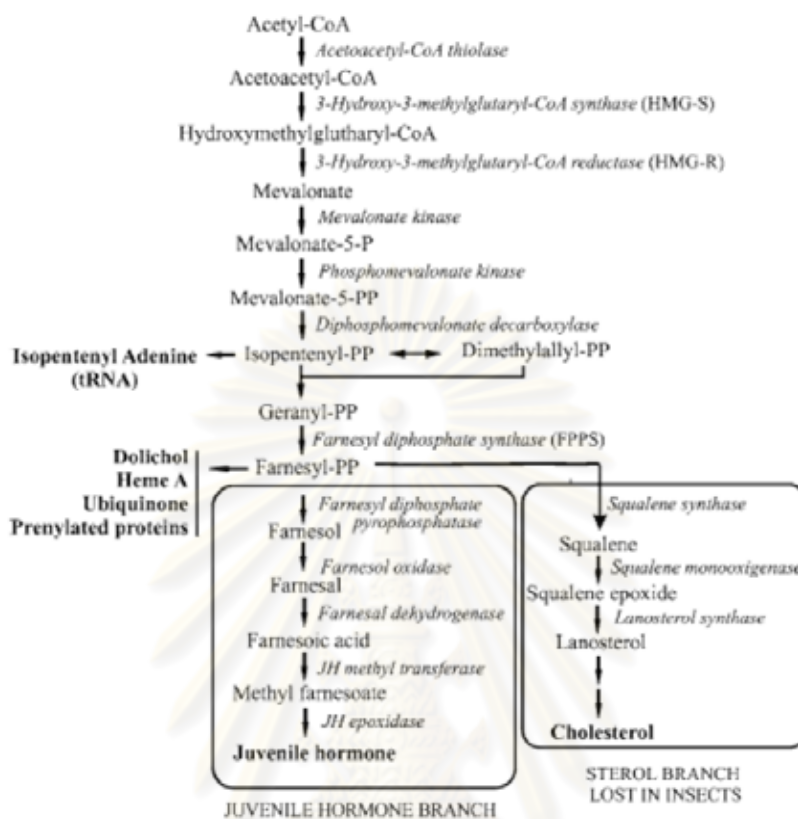


Figure 1.21 The malonate and juvenile hormone biosynthetic pathways in insects (Belles et al. 2005).

MF was first isolated from the hemolymph of the spider crab *Libinia emarginata* and is believed to regulate growth and reproduction in crustaceans (Huberman, 2000). It has been reported that MF maintain juvenile morphology and, therefore, inhibits gonadal development in juveniles but enhances reproductive maturation in adults (Laufer et al., 1987; Borst and Laufer, 1990; Laufer and Sagi, 1991; Laufer and Biggers, 2001; Nagaraju et al., 2003).

Methyl farnesoate has been shown to stimulate ovarian development during pre-vitellogenic and vitellogenic stages in several species of crustacean. Laufer et al (1998) studied the effect of orally administered MF on ovarian maturation in red swamp crayfish

Procambarus clarkii at different stages of ovarian development. Both previtellogenic (immature) and vitellogenic ovaries of the crayfish was stimulated, as measured by ovarian index, after 30 days of feeding diets with MF supplement ($1-2 \mu\text{g indiv}^{-1} \text{day}^{-1}$; Laufer et al. 1998). Similar results also obtained on a longer feeding trial, 60 days (Laufer et al. 1998).

Rodriguez et al (2002) examined oocyte development of *P. clarkii* after the injection of MF in combination with other hormones: twice a week with MF ($2.5 \mu\text{g crayfish}^{-1}$; 10^{-8} mol) alone or in combination with other hormones (JH III, 17β -hydroxyprogesterone, or 17β -estradiol; 10^{-7} mol each), and during the 3 week experiments. Results indicated that injections of MF and MF in combination with 17β -estradiol increased gonadosomatic index ($\text{GSI} > 1.0$ at the end of the trial) of crayfish during middle of the vitellogenic stage.

Nagaraju et al (2003) examined the effect of MF injection on ovarian development of adult freshwater prawn *Macrobrachium malcolmsonii*. MF at physiological concentration (2 ng mL^{-1} hemolymph; twice 7 days apart) was shown to increase ovarian index and mean oocyte diameters of *M. malcolmsonii*. After the duration of their trial (14 days), the oocytes of the MF injected shrimp had progressed from the previtellogenic stage (clear) at the beginning of the trial to the vitellogenic stage (dark brown in color) at the end of the trial, while there was little change in the control groups. The evidence of ovarian stimulation by MF injection was also documented for previtellogenic freshwater crab *Oziotelphusa senex* (Reddy et al. 2004).

Nagaraju et al. (2006) indicate that MO of the freshwater south Indian rice field crab *Oziotelphusa senex senex* secreted terpenoid hormone (methyl farnesoate, MF). The secretory rate of MF by the MO isolated during premolt and vitellogenesis was significantly greater compared to the secretory rate of MO isolated from intermolt and previtellogenesis stage crabs. Accordingly, the regulation of the crustacean molt and reproduction is complex and also involves MF, besides steroid (ecdysteroid) and peptide (sinus gland peptide) hormones.

Kalavathy et al. (1999) studied the relations between the MF levels and gonad index and body weight in *O. senex senex* Fabricius. MF stimulates testicular growth in the freshwater crab as evidenced by increased testicular weight, testicular index and testicular follicle diameter in MF-injected crabs. Therefore, MF may act as a male reproductive hormone in crustaceans.

Nagaraju et al. (2003) also found the relation to body weight, sex, molt and reproduction in this crab. The weight of the MO exhibited a positive correlation with the body weight. The weight of the MO increased with ovarian index, molting and as the crab progressed towards reproduction and the MF content of the MO increased with increase in the organ weight. The results presented strongly support a potential role of the MO in regulating both molting and reproduction in this crab species.

Jo et al (1999) noticed matured oocyte degradation in the spider crab *Libinia emarginata* after several weeks following bilateral eyestalk ablation and the increase in MF concentration in the hemolymph. Another example of MF inhibiting effect on ovarian development was observed in juvenile tadpole shrimp *Triops longicaudatus*. Tsukimura et al (2006) reported that juvenile tadpole shrimp receiving orally administered MF (regardless of delivery vector) had smaller the number of oocytes, and lower ovarian weight. However, MF has no effect on adult tadpole shrimp and MF functions as a juvenilizing agent rather than inhibitor of ovarian development (Tsukimura et al. 2006).

In *P. monodon*, FA had no effects on expression of *vitellogenin* in ovaries (GSI = 3-4%) *in vitro*. However, treatment of hepatopancreas with FA (1.3 and 13 nM) resulted in a rapid expression of the *vitellogenin* gene after 3 h. Nevertheless, higher concentration of FA (i.e. at >130 nM) inhibited to transcription of the vitellogenin encoding gene (Tiu et al., 2006). This strongly support the hypothesis that FA functions as a hormone in crustacean with the final conversion to MF occurring in the target tissues (Nagaraju 2007).

Marsden et al (2008) studied the effect of orally-administered MF on ovarian development and fecundity in *P. monodon*. They monitored ovarian development (by

visual inspection) and fecundity (number of spawns, number of eggs, hatch rate, zoea 1 survival, and mean zoea 1 output) between eyestalk-ablated *P. monodon* (Stage 0, previtellogenic) fed moist artificial diet containing in $5.5 \mu\text{g MF g}^{-1}$ diet and those shrimp fed the same diet without additional MF during a 14 day feeding trial (Marsden et al. 2008). No histological analysis of oocyte was described. The ovarian development of shrimp fed MF-supplemented feed was arrested at stage III (late vitellogenic) at a higher percentage than that of shrimp fed diet without MF supplement, and that the number of spawns per shrimp and relative fecundity were lower in shrimp fed MF-supplemented feed compared to that of shrimp fed diet without MF (Marsden et al. 2008).. Shrimp from both experimental dietary group performed worse (higher % arrested Stage III ovary) than the control group fed mussel and squid mantle (Marsden et al. 2008).

The results from several experiments such Marsden et al (2008) Jo et al (1999), and Tsukimura et al (2006) hinted at the possible drawback of MF stimulation of ovarian development. The acceleration of oocyte development by MF stimulation might lead to a developmental arrest if subsequent developmental steps were not occurring or the timing was not suitable for the animals. The difference between species, method of MF delivery, and the animal physiological state could potentially affect the results. It appears that the effect of MF on crustacean reproduction has more nuance than simply stimulation or inhibition of reproductive process. Understanding its mechanisms, its timing, and its interaction with other hormones could better clarify its roles in crustacean reproduction.

Kuballa et al. (2006) isolated multiple isoforms of putative FaMeT from six crustacean species. The portunid crabs *Portunus pelagicus* and *Scylla serrata* code for three forms. Two isoforms (short and long) were isolated from the penaeid shrimp *P. monodon* and *F. merguensis* and the scyllarid *Thenus orientalis* and parastacid *Cherax quadricarinatus*. Putative FAMEt sequences were also amplified from the genomic DNA of *P. pelagicus* and compared to the putative FAMEt transcripts expressed. Each putative FAMEt cDNA isoform was represented in the genomic DNA, indicative of a multi-gene family. Various tissues from *P. pelagicus* were individually screened for putative FAMEt expression using PCR and fragment analysis. Each tissue type expressed all three isoforms of putative FAMEt irrespective of sex or moult stage. Protein domain analysis

revealed the presence of a deduced casein kinase II phosphorylation site present only in the long isoform of putative FAMEt.

Ruddell et al. (2003) characterized a putative FAMEt in the female edible crab *Cancer pagurus*. A full length cDNA was identified from the MO of the female crab by cDNA library screening and RT-PCR. A high degree of sequence identity was found between this and other putative crustacean FAMEt. The conceptual translation and protein sequence analysis suggested that phosphorylation could occur at multiple sites in the FAMEt. This finding is consistent with the recent observation that endogenous FAMEt activity in the MO extracts can be regulated by phosphorylation *in vitro*. They demonstrated that the recombinant FAMEtase could be expressed as a LacZ-fusion protein in *Escherichia coli* and have undertaken its partial purification from inclusion bodies. In an established assay system, the rFAMEt lacked activity. Northern blotting demonstrated widespread expression of an approximately 1250-nucleotide FAMEt transcript in female *C. pagurus* tissues. Levels of FAMEtase transcripts in MO of female *C. pagurus* were found to fluctuate during vitellogenesis and embryonic development. An HPLC-based method was used to measure hemolymph MF titers ($N > 70$) and specimens were classified into “high MF” and “low MF” groups. The high MF titers, which occurred before or during early vitellogenesis, coincided with, or were preceded by the elevated levels of putative FAMEt mRNA in the MO.

Silva Gunawardene et al (2001) isolated and characterized FAMEt from the greasyback shrimp *Metapenaeus ensis* and analyzed its expression from many shrimp tissues. The highest expression of FAMEt in the central nervous system and constant expression in the ventral nerve cord of mature females during reproductive cycle. Another study on the function and localization of FAMEt in the same species showed that FAMEt localized in the neurosecretory cells of the X-organ-sinus gland complex of the eyestalk and was expressed in all molting stages (Silva Gunawardene et al. 2002).

Hui et al (2008) analyzed FAMEt expression and its functions in *L. vannamei*. Similar to that observed in *M. ensis*, LvFAMEt was widely expressed in many shrimp tissues. LvFAMEt also expressed throughout the larval stages of shrimp (whole animal

assay) with high expression during the nauplius, zoea, and mysis stage. A variation of LvFAMeT level was observed during the molt cycle in both male and female shrimp. The function of LvFAMeT on molting was examined by a gene knock down experiment using LvFAMeT dsRNA injection. The results showed that the knockdown of LvFAMeT affected the regulation of two molt-relating genes, *cathepsin* and *hemocyanin*, resulting in failure to molt and mortality (Hui et al. 2008).

The role of FAMeT in regulation of MF production and its relevance to ovarian development is yet to be examined. FAMeT wide distribution in shrimp tissues suggested that the gene's role might not be limited to only reproduction and molting-related functions, and that their effect might be extensive.

1.10.2 Broad-Complex (*Br-c*)

In *Drosophila*, the *Broad-Complex (Br-c)* is a key member of the 20-hydroxyecdysone regulatory hierarchy that coordinates changes in gene expression during metamorphosis. The family of transcription factors encoded by the *Br-c* share a common amino-terminal domain which is fused by alternative splicing to one of four pairs of C2H2 zinc-finger domains (Z1, Z2, Z3, and Z4) (Bayer et al., 1996). The common core region contains a highly conserved 120 amino acids, called the BTB or POZ domain which appears to be involved in protein-protein interaction (Bardwell & Treisman 1994, Zollman et al. 1994). The BR isoforms are critical mediators of the ecdysteroid hierarchy because they are required in the regulation of intermolt, early and late gene activities in *Drosophila* (Belyaeva et al. 1980, Karim et al. 1993).

The relation between *Br-c* and metamorphosis was reported (Fletcher and Thummel, 1995). The *Br-c* and *E74* are induced directly by ecdysone and encode families of transcription factors that regulate ecdysone primary- and secondary-response genes. Genetic analyses have revealed that mutations in the *Br-c* and *E74* are lethal during metamorphosis and that these mutations cause some similar lethal phenotypes and alterations in secondary-response gene transcription. Representative alleles from each *Br-c* and *E74* complementation group were combined and results indicated that the functions of *Br-c* and *E74* to regulate ecdysone-inducible target gene transcription

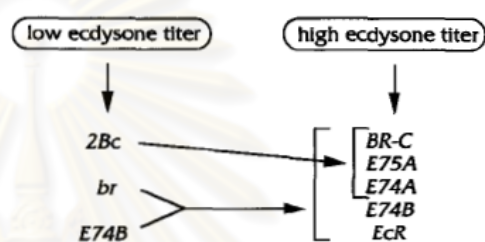
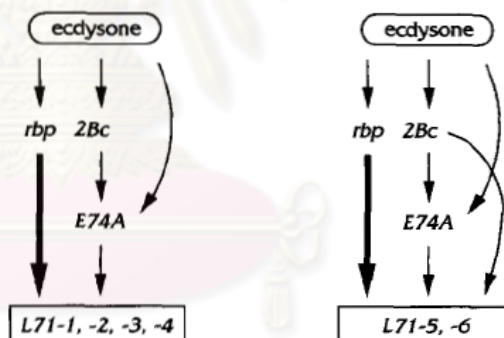
A Glue Genes**B Early Genes****C Late Genes**

Figure 1.22 Models for the regulation of glue, early, and late gene transcription by the BR-C+ and E74' functions. (A) The *rbp*⁺ and E74B⁺ functions act together to regulate glue gene transcription in mid third instar larvae. The *rbp*⁺ is required for the proper timing of glue gene induction while E74B⁺ is required for maximal levels of glue gene transcription. In the absence of both functions, glue mRNA is almost undetectable. (B) The BR-C and E74B have redundant functions in up-regulating early gene transcription in late third instar larvae. It has been shown previously that the early induction of the 2Bc' function, apparently by a low titer ecdysone pulse, is required for the maximal induction of the BR-C, E74A, and E75A early mRNAs by the high titer late larval ecdysone pulse

together (Figure 1.22). Analysis of the morphological and molecular phenotypes of the double-mutant animals reveals that *Br-c* and *E74* alleles act together to produce both novel and synergistic effects. The *Br-c* and *E74* share functions in puparium formation, pupation and early gene induction. These transcription factors may directly interact to regulate the expression of salivary gland glue and late genes. This data is supported the combinations of ecdysone primary-response genes regulate common morphogenetic pathways during insect metamorphosis (Karim et al., 1993).

In both *Drosophila* and *Manduca*, *Br-c* induction only occurs in the final larval instar. *Br-c* protein activates the pupal program and suppresses both the larval and adult programs. JH application at the onset of the adult molt causes re-expression of *Br* and the formation of a second pupal cuticle, suggesting that *Br-c* is sufficient to mediate the action of JH (Zhou and Riddiford 2002). The *Br-c* gene is expressed in a dynamic pattern during oogenesis. It is activated by ecdysteroid in follicle cells at stage 6 of oogenesis, where it is essential for the control of endoreplication and chorion gene amplification. *Br* is also involved in cell migration, as well as morphogenesis of chorionic.

RNAi knock-down of *Br-c* in the silkworm *Bombyx mori* results in the failure of animals to complete the larval–pupal transition or in later morphogenetic defects (Uhlirva et al. 2003).

Chen et al. (2004) found that the *Br-c* gene is involved in the 20E-regulatory hierarchy controlling vitellogenesis in the mosquito, *Aedes aegypti*. Unlike *E74* and *E75*, early gene expression of *Br-C* was activated in previtellogenic females during a JH-dependent period. The levels of Z1, Z2 and Z4 mRNAs were elevated in the fat body of 2-day-old females after *in vitro* exposure to JH III. However, JH III repressed 20E activation of *Br-c* in 3- to 5-day-old females, indicating a switch in hormonal commitment. The results suggested that *BR* isoforms are essential for proper activation and termination of the *Vg* gene in response to 20E.

The role of *Br-c* in embryogenesis was studied. The Z1-Z6 isoforms of *Br-c* was found in cockroach. The temporal-expression patterns indicate that *BgBR-c* isoforms are

present through out the embryogenesis of *B. germanica*, although with weak fluctuations. Silencing all *BgBr-c* isoforms in the embryo through parental RNAi elicited adiversity of phenotypes. These phenotypes suggest roles for *BgBR-C* indifferent in embryogenesis processes of *B. germanica* (Piulachs et al., 2010)..

Nishita and Takiya (2004) studied the gene encoding a *Br-C* homolog in *B. mori*. Four isoforms of *Br-c* were found in this species and expression patterns of the *Bm Br-c* isoforms during late larval to pupal development were observed in in the epidermis, fat body and silk gland. During the metamorphic transformation, the epidermis and silk gland are completely histolyzed; however, the fat body survives into the adult phase. Expression patterns of *BmBr-c* during development differed extensively between the histolyzed group and the survival group. The *BmBr-c* expression patterns in silk glands also differed between the anterior and other areas (the middle and posterior silk glands).

Clearly, elucidating the mechanism controlling the expression of the *Br-c* homolog and its function in *P. monodon* would provide insight into how ecdysone controls metamorphosis and larval ecdysis in shrimp.

CHAPTER II

MATERIALS AND METHODS

2.1 Experimental animals

Wild female *P. monodon* broodstock collected from Satun (Andaman Sea, west) was used for RACE-PCR. In addition, broodstock-sized male and female *P. monodon* were purchased from Angsila, Chonburi (Gulf of Thailand, east). Juvenile *P. monodon* male and female (approximately 20 g body weight, 4-month-old) were purchased from local farms in Chachengsao, eastern Thailand. These samples were used for RT-PCR and 20-hydroxyecdysone injection.

For quantitative RT-PCR analysis, progesterone and serotonin injection, cultured juveniles (4 months old, $N = 6$) and domesticated broodstock of *P. monodon* (18 months old, $N = 6$) were collected from the Broodstock Management Center, Burapha University (Chanthaburi, Thailand). Female broodstock were wild-caught from the Andaman Sea and acclimated under the farm conditions for 2-3 days. The post-spawning group was immediately collected after shrimp were ovulated ($N = 6$). Ovaries were dissected out from each juvenile and intact domesticated and wild broodstock and weighed. For the eyestalk ablation group, shrimp were acclimated for 7 days prior to unilateral eyestalk ablation. Ovaries of eyestalk-ablated shrimp were collected at 2-7 days after ablation. The gonadosomatic index (GSI, ovarian weight/body weight $\times 100$) of each shrimp was calculated. Ovarian developmental stages were classified by conventional histology (Qiu et al., 2005) and divided to previtellogenic (I, $N = 10$ and 4 for intact and eyestalk-ablated broodstock, respectively), vitellogenic (II, $N = 7$ and 6), early cortical rod (III, $N = 7$ and 9) and mature (IV, $N = 9$ and 11) stages, respectively.

For tissue distribution analysis, various tissues of a female juvenile and broodstock were collected, immediately placed in liquid N_2 and kept at -80°C until required. Hemolymph was collected using 10% sodium citrate as an anticoagulant and

centrifuged at 1000 g for 10 minutes. Hemocytes were then subjected to RNA extraction.

For *in situ* hybridization and immunochemistry, the latter portion was excised to small pieces and fixed with the 4% paraformaldehyde prepared in 0.1 M phosphate buffer pH 7.2, washed 3 times with 0.1 M phosphate buffer pH 7.2 and 3 times with 50% ethanol for ovaries fixed in 4% paraformaldehyde. Tissue was subsequently stored in 70% ethanol before subjected to the standard paraffin section. Ovarian developmental stages were classified by conventional histology slightly modified from Qiu *et al.* (2005)

2.2 Nucleic acid extraction

2.2.1 Genomic DNA extraction

Genomic DNA was extracted from a piece of pleopod of each shrimp using a phenol-chloroform-proteinase K method (Klinbunga *et al.*, 1999). A piece of pleopod tissue was dissected out from a frozen pleopod and placed in a prechilled microcentrifuge tube containing 500 µl of the extraction buffer (100 mM Tris-HCl, 100 mM EDTA, 250 mM NaCl; pH 8.0) and briefly homogenized with a micropestle. SDS (10%) and RNase A (10 mg/ml) solutions were added to a final concentration of 1.0 % (w/v) and 100 µg/ml, respectively. The resulting mixture was then incubated at 37°C for 1 hour. At the end of the incubation period, a proteinase K solution (10 mg/ml) was added to the final concentration of 300 µg/ml and further incubated at 55°C for 3–4 hours. An equal volume of buffer-equilibrated phenol: chloroform: isoamylalcohol (25:24:1) was added and gently mix for 10 minutes. The solution was centrifuged at 10,000 rpm for 10 minutes at room temperature. The upper aqueous phase was transferred to a newly sterile microcentrifuge tube. This extraction process was then repeated once with phenol:chloroform:isoamylalcohol (25:24:1) and once with chloroform:isoamylalcohol (24:1). The aqueous phase was transferred into a sterile microcentrifuge. One-tenth volume of 3 M sodium acetate, pH 5.2 was added. DNA was precipitated by an addition of two volume of prechilled absolute ethanol and mixed thoroughly. The mixture was incubated at -80°C for 30 minutes. The precipitated DNA was recovered by centrifugation at 12,000 rpm for 10 minutes at room temperature and washed twice with 1 ml of 70% ethanol (5 minutes and 2 – 3

minutes, respectively). After centrifugation, the supernatant was removed. The DNA pellet was air-dried and resuspended in 50 – 80 µl of TE buffer (10 mM Tris-HCl, pH 8.0 and 0.1 mM EDTA). The DNA solution was incubated at 37°C for 1 – 2 hours and kept at 4 °C until further needed.

2.2.2 RNA extraction

Total RNA was extracted from ovaries (or other tissue) of *P. monodon* using TRI Reagent®. A piece of tissue was immediately placed in a mortar containing liquid nitrogen and ground to fine powder. The tissue powder was transferred to a microcentrifuge tube containing 500 µl of TRI Reagent (50-100 mg tissue per 1 ml) and homogenized. Additional 500 µl of TRI Reagent was then added. The homogenate was left for 5 minutes, before adding 0.2 ml of chloroform. The homogenate was vortexed for 15 seconds and left at room temperature for 2-15 minutes and centrifuged at 12000g for 15 minutes at 4 °C. The mixture was separated into the lower red, phenol-chloroform phase, the interphase, and the colorless upper aqueous phase. The aqueous phase (inclusively containing RNA) was transferred to a new 1.5 ml microcentrifuge tube. Total RNA was precipitated by an addition of 0.5 ml of isopropanol and mixed thoroughly. The mixture was left at room temperature for 10-15 minutes and centrifuged at 12000g for 10 minutes at 4-25 °C. The supernatant was removed. The RNA pellet was washed with 1 ml of 75 % ethanol centrifuged at 7500g for 5 minutes. Total RNA was dissolved in appropriate volume of DEPC-treated H₂O for immediately used. Alternatively, the total RNA pellet was kept under absolute ethanol in a -80 °C freezer for long storage.

2.2.3 Preparation of DNase I-free total RNA

Fifteen micrograms of total RNA were treated with DNase I (0.5 U/1 µg of RNA, Promega) at 37°C for 30 minutes. After the incubation, the sample was gently mixed with a sample volume of phenol:chloroform:isoamylalcohol (25:24:1) for 10 minutes. The mixture was centrifuged at 12,000 g for 10 minutes at 4°C, and the upper aqueous phase was collected. The extraction process was then repeated once with chloroform:isoamylalcohol (24:1) and once with chloroform. The final aqueous phase was mixed with one-tenth final sample volume of 3 M sodium acetate (pH 5.2). After that, RNA was precipitated by adding two point five volume of -20°C-cold

absolute ethanol. The mixture was incubated at -80°C for 30 minutes, and the precipitated RNA was recovered by centrifugation at 12,000 g for 10 minutes at room temperature. The RNA pellet was then washed twice with 1 ml of -20°C cold 75% ethanol. Alternatively, the RNA pellet was kept in absolute ethanol at -80°C until required.

2.3 Measuring concentrations of nucleic acids by spectrophotometry and electrophoresis

The concentration of extracted DNA or RNA was estimated by measuring the optical density at 260 nanometre (OD_{260}). An OD_{260} of 1.0 corresponds to a concentration of 50 $\mu\text{g/ml}$ double stranded DNA, 40 $\mu\text{g/ml}$ single stranded RNA and 33 $\mu\text{g/ml}$ oligonucleotide (Sambrook et al., 2001). Therefore, the concentration of DNA/RNA samples ($\mu\text{g/ml}$) were estimated by multiplying an OD_{260} value with a dilution factor and 50, 40, 33 for DNA, RNA and oligonucleotides, respectively. The purity of DNA samples can be guided by a ratio of $\text{OD}_{260} / \text{OD}_{280}$. The ratio much lower than 1.8 indicated contamination of residual proteins or organic solvents whereas the ratio greater than this value indicate contamination of RNA in the DNA solution (Kirby, 1992).

The amount of high molecular weight DNA can be roughly estimated on the basis of the direct relationship between the amount of DNA and the level of fluorescence after ethidium bromide staining after agarose gel electrophoresis. Genomic DNA was run in a 0.8 - 1.0% agarose gel prepared in 1x TBE buffer (89 mM Tris-HCl, 89 mM boric acid and 2.0 mM EDTA, pH 8.3) at 4 V/cm. After electrophoresis, the gel was stained with ethidium bromide (0.5 $\mu\text{g/ml}$). DNA concentration was estimated from the intensity of the fluorescent band by comparing with that of undigested λDNA .

2.4 Agarose gel electrophoresis (Sambrook and Russell, 2001)

Appropriate amount of agarose was weighed out and mixed with 1x TBE buffer (89 mM Tris-HCl, 8.9 mM boric acid and 2.0 mM EDTA, pH 8.3). The gel slurry was heated until complete solubilization in the microwave. The gel solution was left at room temperature to approximately 55°C before poured into a gel mould. The comb was inserted. The gel was allowed to solidify at room temperature for

approximately 45 minutes. When needed, the gel mould was placed in the gel chamber and sufficient 1x TBE buffer was added to cover the gel for approximately 0.5 cm. The comb was carefully withdrawn. To carry out agarose gel electrophoresis, one-fourth volume of the gel-loading dye (0.25% bromphenol blue and 25% ficoll) was added to each sample, mixed and loaded into the well. A 100-bp DNA ladder or λ -Hind III was used as the standard DNA markers. Electrophoresis was carried out at 4 - 5 V/cm until the tracking dye migrated about three-quartered of the gel. After electrophoresis, the gel was stained with ethidium bromide (0.5 μ g/ml) for 5 minutes and destained to remove unbound EtBr by submerged in H₂O for 15 minutes. The DNA fragments were visualized under the UV light using a UV transilluminator.

2.5 Isolation and characterization of the full length cDNA and genomic DNA using rapid amplification of cDNA ends-polymerase chain reaction (RACE-PCR) and genome walking technique

2.5.1 RACE-PCR

2.5.1.1 Preparation of the 5' and 3' RACE-PCR template

Total RNA was extracted from ovaries of *P. monodon* using TRI Reagent. Messenger (m) RNA was purified using a QuickPrep micro mRNA Purification Kit (GE Healthcare). The RACE-Ready cDNA was synthesized using a BD SMART™ RACE cDNA Amplification Kit (BD Clontech) by combining 1.5 μ g of ovarian mRNA with 1 μ l of 5'CDS primer and 1 μ l of 10 μ M SMART II A oligonucleotide for 5'RACE-PCR and 1 μ g of ovarian mRNA with 1 μ l of 3'CDS primer A oligonucleotide for 3'RACE-PCR. The components were mixed and briefly centrifuged. The reaction was incubated at 70 °C for 2 minutes and snap-cooled on ice for 2 minutes. The reaction tube was briefly centrifuged. After that, 2 μ l of 5X First-strand buffer, 1 μ l of 20 mM DTT, 1 μ l of dNTP Mix (10 mM each) and 1 μ l of PowerScript Reverse Transcriptase were added. The reactions were mixed by gently pipetting and briefly centrifuged. The tubes were incubated at 42 °C for 1.5 hours in an air incubator. The first strand reaction products were diluted with 125 μ l of Tricine-EDTA Buffer and heated at 72 °C for 7 minutes. The first strand cDNA template was stored at -20°C.

Table 2.1 Primer sequences for the first strand cDNA synthesis and RACE-PCR

Primer	Sequence
SMART II A Oligonucleotide	5' -AAGCAGTGGTATCAACGCAGAGTACGC GGG-3'
3'-RACE CDS Primer A	5' -AAGCAGTGGTATCAACGCAGAGTAC(T) ₃₀ N-1N-3' (N=A, C, G or T; N-1=A, G or C)
5'-RACE CDS Primer	5' -(T) ₂₅ N-1N-3' (N=A, C, G or T; N-1=A, G or C)
10X Universal Primer A Mix (UPM)	Long: 5' -CTAATACGACTCACTATAGGGCAA GCAGTGGTATCAACGCAGAGT-3' (0.4 μm) Short: 5' -CTAATACGACTCACTATAGGGC-3' (2 μm)
Nested Universal Primer A (NUP)	5' -AAGCAGTGGTATCAACGCAGAGT-3' (10 μm)

2.5.1.2 Primer design

A gene-specific primer (GSPs) was designed from ESTs significantly matched *COMT* (hemocyte cDNA library; clone no. HC-H-S01-0684-LF), *Br-cZ1* (ovarian cDNA library, clone no. OV-N-S01-1207-W) and *Br-cZ4* (hemocyte cDNA library, clone no. HC-H-S01-0767-LF) and previously deposited *FAMeT* sequence (GenBank accession no. AAX24112.1) (Table 2.2).

2.5.1.3 RACE-PCR and cloning of amplification products

The same master mix for 5'- and 3'-RACE-PCR and control reactions was prepared. For each amplification reaction, 35.75 μl of deionized H₂O, 5 μl of 10X Advantage 2 PCR buffer, 1 μl of dNTP mix (10 μM each) and 1 μl of 50X Advantage 2 polymerase mix were combined. 5'-RACE-PCR and 3'-RACE-PCR were set up according to Table 2.4 and 2.5, respectively.

Table 2.2 The gene specific primer (GSP1), their sequences and T_m of *COMT*, *FAMeT* and *Br-C* gene.

Gene	Sequence	T _m
<i>3'PmCOMT</i>	F:5'-GCTCTGGTGGAGTCATCGCCTTC-3'	66
<i>5'PmFAMeT</i>	R:5'-GGCAGAGGCAGCGCCTTGGGAT CCGC -3'	70
<i>3'PmFAMeT</i>	F:5'-CTGCTCAGCAAGGAGGGAAGGGGAT -3'	70
<i>5'PmBr-cZ1</i>	R:5'-TGATCGGACCACGTGCGAACCAG-3'	68
<i>3'PmBr-cZ1</i>	F:5'-GCCACCAACCGCTCACGCATG-3'	70
<i>3'PmBr-cZ4</i>	R: 5'-TTGACCTCCTTGATCACACC- 3'	60

The reaction was carried out for 20 cycles composing of a 94 °C for 30 second, 68 °C for 30 seconds and 72 °C for 3 minutes. The primary 5' and 3' RACE-PCR products were electrophoretically analyzed.

After characterization of primary RACE product, if the discrete expected product (s) is not obtained. The primary PCR product was 50-fold diluted (1 µl of the product + 49 µl of TE) and amplified with nested GSP and NUP primer (5'-AAG CAGTGGTATCAACGCAGAGT-3'). The amplification reaction was performed using 5 µl of the diluted PCR product as a template using the same condition for the first PCR for 15 cycles.

The resulting products are size-fractionated through agarose gels. The expected fragment is eluted from the gel, cloned into pGEM-T Easy and further characterized by DNA sequencing.

Nucleotide sequences of EST and 5' and 3' RACE-PCR are assembled and blasted against data previously deposited in the GenBank using BlastN and BlastX (Altschul et al., 1990; available at <http://ncbi.nlm.nih.gov>). The protein domain of deduced amino acids of each gene is searched using SMART (<http://smart.embl-heidelberg.de/>). The pI and molecular weight of the deduced protein are estimated using Protparam (<http://www.expasy.org/tools/protparam.html>).

Table 2.3 Composition of 5' -RACE-PCR

Component	5' -RACE Sample	UPM only (Control)	GSP1 only (Control)
5' -RACE-Ready cDNA	1.25 μ l	1.25 μ l	1.25 μ l
UPM(10X)	5.0 μ l	5.0 μ l	-
5' GSP(GSP1, 10 μ M)	1.0 μ l	-	1.0 μ l
H ₂ O	-	1.0 μ l	5.0 μ l
Master Mix	42.75 μ l	42.75 μ l	42.75 μ l
Final volume	50 μ l	50 μ l	50 μ l

Table 2.4 Composition of 3' -RACE-PCR

Component	3' -RACE Sample	UPM only (Control)	GSP1 only (Control)
3' -RACE-Ready cDNA	1.25 μ l	1.25 μ l	1.25 μ l
UPM(10X)	5.0 μ l	5.0 μ l	-
3' GSP(GSP2, 10 μ M)	1.0 μ l	-	1.0 μ l
H ₂ O	-	1.0 μ l	5.0 μ l
Master Mix	42.75 μ l	42.75 μ l	42.75 μ l
Final volume	50 μ l	50 μ l	50 μ l

2.5.2 Genome walking analysis

2.5.2.1 Digestion of genomic DNA

After the full length cDNA of *PmCOMT* was obtained from RACE-PCR,. Genomic organization of this gene was further characterized using genome walking analysis.

Two and a half micrograms of genomic DNA of an individual of *P. monodon* were singly digested in a reaction volume of 100 μ l containing 40 units of a blunt end generating restriction enzyme (*Dra* I, *Eco* RV, *Pvu* II and *Ssp* I, respectively), 1X appropriate restriction enzyme buffer and deionized H₂O. The reaction was incubated at 37°C for 4 hours. Five microlitres of the digest was run on a 0.8% agarose gel to determine whether the digestion was complete.

An equal volume (95 μ l) of buffer-equilibrated phenol was added. The mixture was vortexed at the low speed for 5-10 seconds and centrifuged for 5 minutes at room temperature to separate the aqueous and organic phases. The upper layer was transferred into a fresh 1.5 ml microcentrifuge tube. An equal volume (95 μ l) of chloroform:isoamylalcohol was added, vortexed and centrifuged. The upper layer was transferred into a fresh 1.5 ml tube. One-tenth volume of 3 M NaOAc (pH 4.5) was added and mixed followed by 2.5 volume of ice cold absolute ethanol and thoroughly mixed. The mixture was kept at -80 °C for 30 minutes. The digested DNA was recovered by centrifugation at 12,000 rpm for 10 minutes at room temperature. The supernatant was discarded. The DNA pellet was briefly washed with ice-cold 70% ethanol and centrifuged at 12000 rpm for 5 minutes at room temperature. The supernatant was discarded. The pellet was air-dried. DNA was dissolved in 10 μ l of TE (10 mM Tris, pH 8.0, 0.1 mM EDTA).

2.5.2.2 Ligation of genomic DNA to GenomeWalker adaptors

The ligation reaction was set up in a 10 μ l reaction volume containing 4 μ l of digested DNA, 1.9 μ l of: 25 μ M of GenomeWalker Adaptor (GenomeWalker Adaptor Forward: 5' -GTA ATA CGA CTC ACT ATA GGG CAC GCG TGG TCG ACG GCC CGG GCA GGT-3' and GenomeWalker Adaptor Reverse: 5' -PO₄-ACC TGC CC-NH₂-3'), 1.6 μ l of 10X ligation buffer and 3 units of T4 DNA ligase. The reaction mixture was incubated at 16 °C overnight. The reaction was terminated by incubation at 70 °C for 5 minutes. The ligated product was ten fold diluted by an addition of 72 μ l of TE (10 mM Tris, pH 8.0, 0.1 mM EDTA).

2.5.2.3 PCR-based genomic DNA walking

PCR-based genomic DNA walking was carried out in a 25 μ l reaction containing 10 mM Tris-HCl, pH 8.8, 50 mM KCl, 0.1% Triton X-100, 200 μ M each of dATP, dCTP, dGTP and dTTP, 2 mM MgCl₂, 0.2 μ M each of Adaptor primer1 (AP1: 5'-GTAATACGACTCACTATAGGGC-3') and gene specific primer (*PmCOMT* GWF:5'-CGCTCTGGTGGAGTCATCG-3'), 1 μ l of each DNA library of *P. monodon* and 1.0 unit of DyNAzyme™ II DNA Polymerase (Finnzymes). The amplification reactions were carried out using the two-step cycle parameters including 7 cycles of a denaturing step at 94 °C for 25 seconds and an annealing/extension step at 70 °C for 3 minutes followed by 35 cycles of 94 °C for 25 second, annealing at 65 °C for 3 minutes and the final extension at 67 °C for an additional 7 minutes. Five microlitres of the primary PCR product was electrophoretically analyzed by a 1.2% agarose gel. A 100 bp ladder and λ -*Hind* III was included as the DNA markers.

The primary PCR product was 50 fold-diluted (1 μ l of each primary PCR and 49 μ l of deionized H₂O) and 1 μ l of this was used as the DNA template for the semi-nested PCR. The PCR components of the secondary PCR were similar as those of the primary PCR with the exception that AP1 was replaced with 0.2 μ M of AP2 primer (5'-ACTATAGGGCACGCGTGGT-3') and 0.2 μ M of GSP.

PCR was carried out composing of 5 cycles of a denaturing step at 94 °C for 25 seconds and an annealing/extension step at 70 °C for 3 minutes followed by 20 cycles of 94 °C for 25 second and 65 °C for 3 minutes. The final extension at 67 °C was carried out for an additional 7 minutes. Five microlitres of the secondary PCR product was electrophoretically analyzed by a 1.2% agarose gel. A 100 bp ladder and λ -*Hind* III was included as the DNA markers.

2.5.2.4 Overlapping PCR of genomic *PmCOMT*

For amplification of the remaining *PmCOMT* genomic sequence, two fragments were amplified using primers ORFPmCOMT-F (5'-ATGTCTTCTCTGAA AAGTTACCA -3') and 5'COMT-R (5'-ACATCGCCGCTCTACGGTGCT-3') and COMTRT-F (5'- AGCACCGTAGAGCGGCGATGTT-3') and COMTRT-R (5'-CGAAGGCGATGACTCCACCAGA-3'). The amplification profiles were PCR was performed by predenaturation at 94°C for 3 min followed by 35 cycles of a 94°C denaturation for 30 s, a 53 (ORFPmCOMT-F + 5'COMT-R) or 55°C (COMTRT-

F/R), annealing for 1 min and a 72°C extension for 2 or 1 min, respectively. The final extension was carried out at 72°C for 7 min. The PCR products were cloned and sequenced. Nucleotide sequences of these genes were assembled and compared with their cDNAs.

2.6 Cloning of PCR-amplified DNA

2.6.1 Elution of DNA from agarose gels

The DNA fragment was fractionated through agarose gels in duplication. One was run side-by-side with a 100 bp DNA markers and the other was loaded into the distal well of the gel. After electrophoresis, lanes representing the DNA standard and its proximal DNA sample were cut and stained with ethidium bromide (0.5 µg/ml) for 5 minutes. Positions of the DNA markers and the EtBr-stained fragment were used to align the position of the non-stained target DNA fragment. The DNA fragment was excised from the gel with a sterile razor blade. DNA was eluted out from the agarose gels using a QIAquick gel Extraction kit (QIAGEN) according to the protocol recommended by the manufacture. The excised gel was transferred into a microcentrifuge tube and weighed. Three gel volumes of the QG buffer were added. The mixture was incubated at 50°C for 10 minutes with briefly vortexing every 2 – 3 minutes. After the gel was completely dissolved, 1 gel volume of isopropanol was added and gently mixed. The mixture was applied to the QIAquick spin column placed on a 2 ml collection tube and centrifuged at 13,000 rpm for 1 minute at room temperature. The flow-through was discarded and 0.75 ml of the PE buffer was added. The QIAquick spin column was centrifuged at 13,000 rpm for 1 minute at room temperature. The flow-through was discarded. The column was further centrifuged at room temperature for an additional 1 minute at 13,000 rpm to remove trace amount of the washing buffer. The column was then placed in a new microcentrifuge tube and 30 µl of the EB buffer (10 mM Tris-Cl, pH 8.5) was added to the center of the QIAquick membrane. The column was incubated at room temperature for 1 minute before centrifuged at 13,000 rpm for 1 minute. The eluted sample was stored at -20°C until further required.

2.6.2 Ligation of PCR product to pGEM-T easy vector

The ligation reaction was set up in the total volume of 10 μ l containing 3 μ l of the gel-eluted PCR product, 25 ng of pGEM-T easy vector, 5 μ l of 2X rapid ligation buffer (60 mM Tris-HCl pH 7.8, 20 mM MgCl₂, 20 mM DTT, 2 mM ATP and 10 % PEG 8000) and 3 Weiss units of T4 DNA ligase. The ligation mixture was gently mixed by pipetting and incubated at 4°C overnight.

2.6.3 Preparation of competent cells

A single colony of *E. coli* JM109 was inoculated in 10 ml of LB broth (1% Bacto tryptone, 0.5% Bacto yeast extract and 0.5% NaCl) with vigorous shaking at 37°C overnight. The starting culture was inoculated into 50 ml of LB broth and continued culture at 37°C with vigorous shaking to the OD₆₀₀ of 0.5 – 0.8. The cells were chilled on ice for 10 minutes before centrifuged at 3,000 g for 10 minutes at 4°C. The pellets were resuspended in 30 ml of ice-cold MgCl₂-CaCl₂ solution (80 mM MgCl₂ and 20 mM CaCl₂) and centrifuged as above. The supernatant was discarded and the pellet was resuspended in 2 ml of ice-cold 0.1 M CaCl₂ and divided into 200 μ l aliquots. These competent cells could be used immediately or stored at –70°C for subsequent used.

2.6.4 Transformation of the ligation product to *E.coli* host cells

The competent cells were thawed on ice for 5 minutes and divided to aliquots of 100 μ l. Two microlitres of the ligation mixture was added and gently mixed by pipetting. The mixture was incubated on ice for 30 minutes. The reaction tube was then placed in a 42°C water bath for 45 seconds without shaking. The tube was then immediately snapped on ice for 2-3 minutes. One microlitre of SOC medium (2% Bacto tryptone, 0.5% Bacto yeast extract, 10 mM NaCl, 2.5 mM KCl, 10 mM MgCl₂, 10 mM MgSO₄ and 20 mM glucose) was added to the tube. The cell suspension was incubated with shaking at 37°C for 1.5 hours. At the end on the incubation period, the cultured cell suspension was centrifuged at 12,000 rpm for 20 seconds at room temperature. The pellet was gently resuspended in 100 μ l of SOC and spread on a LB agar plate containing 50 μ g/ml of ampicillin, 25 μ g/ml of IPTG and 20 μ g/ml of X-gal. The plate was left until the cell suspension was absorbed and further incubated at

37°C overnight. The recombinant clones containing inserted DNA are white whereas those without inserted DNA are blue.

2.6.5 Detection of recombinant clone by colony PCR

Colony PCR was performed in a 25 µl reaction volume containing 10 mM Tris-HCl, pH 8.8, 50 mM KCl, 0.1% Triton X-100, 200 µM each of dATP, dCTP, dGTP and dTTP, 1.5 mM MgCl₂, 0.2 µM of pUC1 (5'-TCC GGC TCG TAT GTT GTG TGG A-3') and pUC2 (5'-GTG GTG CAA GGC GAT TAA GTT GG-3') primers and 0.5 unit of DyNAzyme™ II DNA Polymerase. A recombinant colony was picked up by the micropipette tip and mixed well in the amplification reaction. The PCR profiles was predenaturing at 94°C for 3 minutes, followed by 30 cycles of 94°C for 30 seconds, 55°C for 60 seconds and 72 °C for 90 seconds. The final extension was carried out at 72°C for 7 minutes. The resulting PCR products were analyzed by agarose gel electrophoresis.

2.6.6 Isolation and digestion of recombinant plasmid DNA

A recombinant clone was inoculated into 3 ml of LB broth (1% Bacto-tryptone, 0.5% Bacto-yeast extract and 1.0 % NaCl) containing 50 µg/ml of ampicillin and incubated at 37°C with constant shaking at 250 rpm overnight. The culture was transferred into 1.5 ml microcentrifuge tube and centrifuged at 12,000 g for 1 min. The cell pellet was collected and resuspended with 250 µl of the buffer P1. The mixture was completely dispersed by vortexing. The mixture was then treated with 250 µl of the buffer P2, gently mixed and placed on ice for 10 min. Additionally, 350 µl of the buffer N3 was added and gently mixed. To separate the cell debris, the mixture was centrifuged at 12,000 g for 10 minutes. The supernatant was transferred into the QIAprep column and centrifuged at 12,000 g for 30 - 60 seconds. The flow-through was discarded. The QIAprep spin column was washed by adding 0.75 ml of the buffer PE and centrifuged for 30-60 seconds. The flow-through was discarded. The spin tube was centrifuge for an additional 1 minute to remove the residual wash buffer. The QIAprep column was placed in a new 1.5 ml microcentrifuge tube and 40 µl of the EB buffer (10 mM Tris-Cl, pH 8.5) was added to elute the extracted plasmid

DNA. The column was left at room temperature for 1 minute and centrifuge at 12,000 g for 1 minute.

The insert size of each recombinant plasmid was examined by digestion of the plasmid with *Eco* RI. The digest was carried out in a 15 µl containing 1X restriction buffer (90 mM Tris-HCl; pH 7.5, 10 mM NaCl and 50 mM MgCl₂), 1 µg of recombinant plasmid and 2-3 units of *Eco* RI and incubated at 37°C for 3 hours before analyzed by agarose gel electrophoresis.

In addition, clones showing corresponded DNA insert size were separately digested with *Hind* III and *Rsa* I to verify whether a single insert possibly contained only one type of sequence. Typically, the digestion reaction was set up in the total volume of 15 µl containing appropriate restriction enzyme buffer (buffer E; 6 mM Tris-HCl; pH 7.5, 6 mM MgCl₂, 100 mM NaCl and 1 mM DTT for *Hind* III and buffer C; 10 mM Tris-HCl; pH 7.9, 10 mM MgCl₂, 50 mM NaCl and 1 mM DTT for *Rsa* I), 5 µl of the amplified product and 2 units of either *Hind* III or *Rsa* I. The reaction mixture was at incubated at 37°C for 3-4 hours. Digestion patterns were analyzed by agarose gel electrophoresis.

2.6.7 DNA sequencing

Cloned DNA fragments from typical PCR, RT-PCR, RACE-PCR and genome walking analysis were sequenced by automated DNA sequencer using M13 forward and/or M13 reverse primer as the sequencing primer by MACROGEN (Korea).

2.7 Phylogenetic analysis

The amino acid sequence of *PmCOMT* and *PmFAMeT* was phylogenetically compared with that from other species found in GenBank. Multiple alignments were carried out with ClustalW (Thompson et al., 1994). A bootstrapped neighbor-joining tree (Saitou and Nei 1987) was constructed with the Seqboot, Prodist, Neighbor, and Consense routines in Phylip (Felsenstein 1993) and illustrated with Treeview (<http://taxonomy.zoology.gla.ac.uk/rod/treeview.html>).

2.8 RT-PCT and tissue distribution analysis of *PmCOMT*, *PmFAMeT*, *PmBr-cZ1* and *PmBr-cZ4*

2.8.1 Primer design

Forward and reverse primers of each gene were designed from nucleotide sequence obtained from ESTs library (*PmCOMT*, *PmBr-cZ1* and *PmBr-cZ4*) and partial sequence of *PmFAMeT* from *P. monodon* (*PmFAMeT*) (Table 2.5) using Primer Premier 5.0. Generally, the PCR primers is 20-24 bp in length with melting temperatures of 60-70°C and the GC content of 40-50% (Table 2.5).

2.8.2 First strand cDNA synthesis

The first strand cDNA was synthesized from 1.5 µg of DNase-treated total RNA were reverse-transcribed to the first strand cDNA using an ImPromp-IITM Reverse Transcription System Kit (Promega, U.S.A.). Total RNA was combined with 0.5 µg of oligo dT₁₂₋₁₈ and appropriate DEPC-treated H₂O in final volume of 5 µl. The reaction was incubated at 70°C for 5 minutes and immediately placed on ice for 5 minutes. Then 5X reaction buffer, MgCl₂, dNTP Mix, RNasin were added to final concentrations of 1X, 2.25 mM, 0.5 mM and 20 units, respectively. Finally, 1 µl of ImProm-IITM Reverse transcriptase was add and gently mixed by pipetting. The reaction mixture was incubated at 25°C for 5 minutes and at 42°C for 90 minutes. The reaction mixture was incubated at 70°C for 15 minutes to terminate the reverse transcriptase activity. Concentration and rough quality of the newly synthesized first strand cDNA was spectrophotometrically examined (OD₂₆₀/OD₂₈₀) and electrophoretically analyzed by 1.0% agarose gels, respectively. The first stranded cDNA was 10 fold-diluted and kept at -20°C until required.

2.8.3 RT-PCR analysis

Generally, PCR was carried out in a 25 µl reaction mixture containing 10 mM Tris-HCl, pH 8.8, 50 mM KCl, 0.1% Triton X-100, 200 µM each of dATP, dCTP, dGTP and dTTP, 2 mM MgCl₂, 0.2 µM of a primer, 200 ng of first strand cDNA of *P. monodon* and 1.0 unit of DyNAzymeTM II DNA Polymerase (Finnzymes, Finland). The PCR profiles was predenaturing at 94°C for 3 minutes, followed by 30 cycles of 94°C for 30 seconds, 55°C for 45 seconds and 72 °C for 1 minute. The final extension was carried out at 72°C for 7 minutes. The resulting PCR products were

electrophoretically analyzed through 1.0-2.0% agarose gels and visualized under a UV transilluminator after ethidium bromide staining.

2.8.4 Tissue distribution analysis by RT-PCR

Expression of each genes in various tissue of female juvenile and broodstock (eyestalk, gills, heart, hemocytes, hepatopancrease, lymphoid organ, intestine, pleopods, stomach, thoracic ganglion and ovaries) and testes of male juvenile and broodstock was analyzed by RT-PCR. *EF-1 α ₅₀₀* (F: 5'-ATGGTTGTCAACTTTGCCCC-3' and R: 5'-TTGACCTCCTTGATCACACC-3') was included as the positive control. The thermal profiles were 94°C for 3 min followed by 30 cycles of denaturation at 94°C for 30 s, annealing at 55°C for 45 s and extension at 72°C for 1 min. The final extension was carried out at 72°C for 7 min. The amplicon was electrophoretically analyzed through 1.5% agarose gels and visualized with a UV transilluminator after ethidium bromide staining (Sambrook and Russell, 2001).

2.9 Semi-quantitative Reverse Transcription-Polymerase Chain Reaction (RT-PCR)

Expression levels of *PmCOMT* and *PmFAMeT* were semiquantitatively determined. *Elongation factor 1 alpha (EF1- α)* was used as an internal control. The amplification conditions need to be optimized.

2.9.1 Primers

Primer pairs used for semiquantitative RT-PCR of *PmCOMT* and *PmFAMeT* were illustrated in Table 2.5. Primer for *EF1- α* were designed (F: 5'-ATGGTTGTCAACTTTGCCCC-3' and R: 5'-TTGACCTCCTTGATCACACC-3').

2.9.2 Total RNA extraction and the first strand synthesis

Total RNA was extracted from hemocyte, testes and ovaries of broodstock-sized and juvenile *P. monodon* using TRI Reagent as previously described.

2.9.3 Determination of PCR conditions

Amplification was performed in a 25 µl reaction volume containing 0.1 µg of the first strand cDNA template, 1X PCR buffer (10mM Tris-HCl pH 8.8, 50 mM KCl and 0.1% Triton X-100), 200 µM each of dNTP and 1 unit of Dynazyme™ DNA Polymerase (FINZYMES, Finland). PCR was carried out using the conditions described in Table 2.5.

2.9.4 Primer concentration

The optimal primer concentration for each primer pair (between 0 - 0.3 µM) was examined using the standard PCR conditions. The resulting product was electrophoretically analyzed. The primer concentration that gave specificity of the amplification product and clear results were selected for further optimization of PCR condition.

2.9.5 MgCl₂ concentration

The optimal MgCl₂ concentration of each primer pair (between 0 - 4 mM MgCl₂) was examined using the standard PCR conditions and the optimal primer concentration in 2.10.4. The concentration that gave the highest specificity was chosen.

2.9.6 Cycle number

The PCR amplifications were carried out at different cycles (e.g. 20, 25, 30 and 35 cycles) using the optimal concentration of primers MgCl₂ and analyzed by gel electrophoresis. Relationships between the number of cycles and the intensity of the PCR product were plotted. The number of cycles that still provided the PCR product in the exponential range and did not reach a plateau level of amplification was chosen.

2.9.7 Gel electrophoresis and quantitative analysis

The amplification product of genes under investigation and EF-1α were electrophoretically analyzed by the same gel. The intensity of interesting genes and that of EF-1α was quantified from glossy prints of the gels using the Quantity One programme (BioRad)

Table 2.5 The gene specific primer (GSP1), their sequences and Tm of *PmCOMT*, *PmFAMeT*, *PmBr-cZ1* and *PmBr-cZ4* gene for RT-PCR and Tissue distribution analysis

Gene	Sequence	Tm
PmCOMT-RT-F	F: 5'- TTGACATAAGTGAAGAGTTTGC -3'	60
PmCOMT-RT-R	F: 5'- GAAGGCGATGACTCCACCAG -3'	64
PmFAMeT-RT-F	F: 5'- CCACCATTCCAGAGCCTTTC -3'	62
PmFAMeT-RT-R	R: 5'- TTCCCTCCTTGCTGAGACGA - 3'	62
PmBr-cZ1-RT-F	F: 5'- ACGCTCACCTCCGCCAGTC - 3'	68
PmBr-cZ1-RT-R	R: 5'- AGTGCCACATTTGCCGCATTAT - 3'	68
PmBr-cZ4-RT-F	F: 5'- CTCAGAATTAAGGGCTTGGCAG -3'	66
PmBr-cZ4-RT-R	R: 5'- TGGAGGTGTTACCGATGGCTGC - 3'	70
EF-1α₅₀₀-F	R: 5'- ATGGTTGTCAACTTTGCCCC - 3'	60
EF-1α₅₀₀-R	R: 5'- TTGACCTCCTTGATCACACC - 3'	60

2.10 Effects of dopamine and serotonin on expression of genes in ovaries of juvenile *P. monodon*

Expression levels of *PmCOMT* and *PmFAMeT* related with dopamine and serotonin were examined using semi-quantitative RT-PCR analysis.

2.10.1 Dopamine administration

Female juvenile *P. monodon* (approximately 5 months old with the body weight of 20-25 g) were purchased from Chonburi (eastern Thailand) used in this experiments. They were acclimatized at the laboratory conditions (ambient temperature of 28-30 °C, salinity of 12 ppt) for 7 days in 150-liter fish tanks. The experimental animals were not fed approximately 24 hours before the treatment.

Shrimp were intramuscularly into the first abdominal segment injected individually with dopamine hydrochloride to obtain the doses of 10^{-6} mole/shrimp ($N = 5$ for each group). Shrimp injected with the 0.85% saline solution (at 0 hr) were included as the control. The samples were collected at 0, 3, 6, 12 and 24 hr post injection. Ovaries of each shrimp were collected and subjected to total RNA

extraction. The first strand cDNA was synthesized and used as the template for semi-quantitative RT-PCR of *PmCOMT* and *PmFAMeT*.

2.10.2 Serotonin administration

For serotonin (5-HT) injection, juvenile *P. monodon* (5-month-old) were purchased from a commercial farm in Chonburi (eastern Thailand) and acclimated for 7 days at the laboratory conditions (28–30 °C and 30 ppt seawater) in 150-liter fish tanks.

Four groups of female shrimp (approximately 35 g body weight) were injected intramuscularly into the first abdominal segment with 5-HT (50 µg/g body weight, $N=5$ for each group). Specimens were collected at 12, 24, 48 and 72 h post treatment (hpt). Shrimp injected with the 0.85% saline solution (at 0 hpi) were included as the control. Specimens were collected at 0, 3, 6, 12 and 24 hr post injection. Ovaries of each shrimp were collected and subjected to total RNA extraction. The first strand cDNA was synthesized and used as the template for semi-quantitative RT-PCR of *PmCOMT* and *PmFAMeT*.

2.10.3 Data analysis

The expression level of each gene was normalized by that of *EF-1 α* . Expression levels between different groups of *P. monodon* were statistically tested using one way analysis of variance (ANOVA) followed by Duncan's new multiple range test. Significant comparisons were considered when the *P*-value was < 0.05 .

2.11 Quantitative real-time PCR of *PmCOMT*, *PmFAMeT*, *PmBr-cZ1* and *PmBr-cZ4* in ovaries of *P. monodon*

2.11.1 Experimental animals

2.11.1.1 Intact wild and domesticated *P. monodon* used for expression analysis of various genes during ovarian development

Female juveniles of *P. monodon* ($N = 4$, average body weight 33 g, 6-month-old), domesticated broodstock: 10-month-old ($N = 6$, average body weight 46.68 ± 3.55 g and GSI < 1), 14-month-old ($N = 4$, average body weight 64.06 ± 3.20 g and GSI =

<1), and 18-month-old ($N = 8$, average body weight 77.12 ± 3.10 g and $GSI = 1-1.5$), wild intact broodstock ($N = 8$, average body weight 135.29 ± 8.20 g) and eyesstalk ablated broodstock ($N = 8$, average body weight 135.29 ± 8.20 g) were used for real-time PCR analysis.

2.11.1.2 Serotonin administration

Domesticated female *P. monodon* (18-month-old with the average body weight of 107 ± 16.24 g) were sampled from the earth ponds and acclimated in the fish tank for 96 hours. Five group of shrimp are single injected intramuscularly with serotonin ($50 \mu\text{g/g}$ of body weight) into the first abdominal segment of each shrimp and specimens are collected at 0 hr, 1, 12, 24, 48 and 72 hr post injection. Shrimp injected with the normal saline (0.85% at 0 hr) is also included as the control. Ovaries of each shrimp were sampling and immediately placed in liquid N_2 . Specimens were stored at -80°C prior to RNA extraction and first-strand cDNA synthesis.

2.11.1.3 Progesterone administration

Domesticated female *P. monodon* (18-month-old with the average body weight of 100.79 ± 17.59 g) were sampled from the earth ponds and acclimated in the fish tank for 96 hours. Five group of shrimp are single injected intramuscularly with progesterone ($0.1 \mu\text{g/g}$ of body weight) into the first abdominal segment of each shrimp and specimens are collected at 0 hr, 1, 12, 24, 48 and 72 hr post injection (hpi). Shrimp injected with the absolute ethanol was used as the vehicle control (at 12 and 72 hpi). Ovaries of each sample were sampling and immediately placed in liquid N_2 . Specimens were stored at -80°C prior to RNA extraction and first-strand cDNA synthesis.

2.11.1.4 20β -hydroxyecdysone administration

Commercially cultured female juveniles of *P. monodon* (the average body weight of 17.56 ± 3.46) were acclimated in the fish tank for 2 weeks. Five group of juvenile shrimp are single injected intramuscularly with 20β -hydroxyecdysone ($1 \mu\text{g/g}$ of body weight) into the first abdominal segment of each shrimp and specimens are collected at 0 hr, 6, 12, 24, 48, 72, 96 and 168 hr post injection. Shrimp injected with 10% ethanol was also included as a control (at 0 hr). Ovaries of each sample

were sampling and immediately placed in liquid N₂. The sample were stored at -80°C prior to RNA extraction and first-strand cDNA synthesis.

2.11.2 Primer design and construction of the standard curve

The intron/exon structure of the target gene was characterized. Several primer pairs were designed from cDNA sequence of each gene and used to PCR against genomic DNA as the template. The PCR fragment was cloned and sequenced. The forward or reverse primer covering intron/exon boundaries or alternatively, a primer pairs sandwiching the large intron was designed. Sizes of the expected PCR product size was usually less than 100-200 bp or less than 500 bp when the small amplification product could not be designed.

For construction of the standard curve of each gene, the DNA segment covering the target PCR product and *EF-1α* were amplified from primers used for quantitative real-time PCR. The amplification products were cloned and sequenced. The recombinant plasmid was extracted and used as the template for estimation of the copy number of a particular gene. A 10 fold-serial dilution corresponding to 10³-10⁸ molecules (10³-10⁸ molecules for *PmFAMeT*) was prepared. The copy of standard DNA molecules can be calculated using the following formula:

$$X \text{ g/}\mu\text{l DNA}/(\text{plasmid length in bp} \times 660) \times 6.022 \times 10^{23} = Y \text{ molecules/}\mu\text{l}$$

Standard curves representing 10³-10⁸ copies (in triplicate) of each gene and the internal control, *EF-1α₂₁₄* (F: 5'-GTCTTCCCCTTCAGGACGTC-3' and R: 5'-CTTTACAGAC ACGTTCTTCACG TTG-3') were constructed using the conditions described below. The standard curves with correlation coefficient = 0.995-1.000 or efficiency higher than 95% were accepted to be used to deduce the copy number of examined genes.

2.11.3 Quantitative real-time PCR analysis

The target transcripts and the internal control *EF-1α* of the synthesized cDNA were amplified in a reaction volume of 10 μl using 2X LightCycler® 480 SYBR Green I Master (Roche, Germany). The specific primer pairs were used at a final

Table 2.6 Nucleotide sequences and T_m of primers used for quantitative real-time PCR of *PmCOMT*, *PmFAMeT*, *PmBr-cZ1*, *PmBr-cZ4* and *EF1 α* .

Gene	Sequence	T_m
PmCOMT-qRT-F	F: 5'- AACGACTGAATGATGTA ACTCT -3'	60
PmCOMT-qRT-R	R: 5'- CTCCCAGAACGGTTTTTCCTAT -3'	62
PmFAMeT-qRT-F	F: 5'-TTCGACATCACTCATTACGGC-3'	62
PmFAMeT-qRT-R	R: 5'-GAACACTTCATACATGGGTGTGG- 3'	68
PmBr-cZ1-qRT-F	F: 5'- CGCAAAAGGCCACCAGAATCG - 3'	66
PmBr-cZ1-qRT-R	R: 5'-TCTGTGACTGTTTCATCGCTGTTG - 3'	68
PmBr-cZ4-qRT-F	F: 5'- ACGCAGGACCATCCATTCAACC - 3'	68
PmBr-cZ4-qRT-R	R: 5'- CGGACAGGCACCAGTCATTAGCT - 3'	72
EF-1α₂₁₄-F	F: 5'- GTCTTCCCCTTCAGGACGTC - 3'	64
EF-1α₂₁₄-R	R: 5'- CTTTACAGACACGTTCTTCACGTTG - 3'	72

concentration of 0.3 μ M and 50 ng of the first strand cDNA template. The thermal profile for SYBR Green real-time PCR was 95°C for 10 minutes followed by 40 cycles of 95°C for 15 seconds, 58°C for 30 seconds and at 72°C for 30 seconds. The cycles for the melting curve analysis were 95°C for 15 seconds, 65°C for 1 minute and at 98°C for continuation and cooling was 40°C for 10 seconds. The real-time RT-PCR assay was carried out in a 96 well plate and each sample was run in duplicate using a LightCycler® 480 Instrument II system (Roche). A ratio of the absolute copy number of the target gene and that of *EF-1 α* was calculated. The relative expression level (copy number of each gene /that of *EF-1 α*) between shrimp possessing different stages of ovarian development (or treatment) were statistically tested ($P < 0.05$).

2.12 *In situ* hybridization (ISH)

2.12.1 Sample preparation

Ovaries of intact and eyestalk-ablated *P. monodon* broodstock were fixed in 4% paraformaldehyde prepared in 0.1% phosphate-buffered saline (PBS, pH 7.2) overnight at 4°C. The fixed ovarian tissue was washed four times with PBS at room temperature and stored in 70% ethanol at -20°C until used. Tissue was histologically

prepared, embedded in paraffin and Conventional paraffin sections (5 μm) were carried out onto poly-L-lysine-coated slides.

2.12.2 Preparation of cRNA probes

For *PmFAMeT*, *PmBr-cZ1* and *PmBr-cZ4* the template used for synthesis of the cRNA probes were PCR-amplified. The T7 (TAATACGACTCACTAT AGGG) and SP6 sequence (ATTTAGGTGACACTATAGAA) (Table 2.7) promoter sequences were added to the 5' of forward and reverse primers, respectively. PCR was carried out in a 25 μl reaction volume containing 10 ng of recombinant plasmid containing the complete ORF of the target transcripts were used as the template. The PCR condition was initially performed by predenaturation at 94°C for 2 minutes followed by 30 cycles of denaturation at 94°C for 30 seconds, annealing at 60°C for 30 seconds and at 72°C for 1 minute. The PCR product was purified using a MinElute PCR purification Kit (Qiagen). The concentration of purified PCR product was estimated by comparing with the DNA marker after electrophoresis and also spectrometrically estimated.

Table 2.7 Nucleotide sequences and T_m of primers for synthesis of the cRNA probes of *PmCOMT*, *PmFAMeT*, *PmBr-cZ1* and *PmBr-cZ4*

Gene	Sequence	T _m
PmCOMT-ISH-F	F:5'-TAATACGACTCACTATAGGGCATAATCCCGATCCT TTGGT3'-3'	66
PmCOMT-ISH-R	F:5'ATTTAGGTGACACTATAGAATTCCTAATAGCCACTG TGCC3'-3'	60
PmFAMeT-ISH -F	F:5'-TAATACGACTCACTATAGGGACACCCCTGACATCC TGAGT-3'	60
PmFAMeT-ISH -R	R: 5'- ATTTAGGTGACACTATAGAATCCATGAAGGGATC ACTGTC3'- 3'	60
PmBr-cZ1-ISH -F	F: 5'- TAATACGACTCACTATAGGGGGAAGATTATA TCCTGCACACA - 3'	62
PmBr-cZ1-ISH -R	R: 5'- ATTTAGGTGACACTATAGAACTGTGACTGTT CATCGCTGTTG -3'	66
PmBr-cZ4-ISH -F	F: 5'-TAATACGACTCACTATAGGGTTCACAACTG GTAATGAGCAC - 3'	62
PmBr-cZ4-ISH R	R:5'-ATTTAGGTGACACTATAGAATGTAGTCGTCT GGGTCGTCA -3'	70

For *PmCOMT*, the sense and anti-sense cRNA probes were synthesized from a linearized plasmid containing the full length ORF of *PmCOMT* using primers (ORFPmCOMT-F (5'-ATGTCTTCTCTGAAAAGTTACCA-3') and ORFPmCOMT-R (5'-TTTATTATTGGGGAGGAGGG -3')). Briefly, 2.5 µg of recombinant *PmCOMT* plasmid was digested with of *Nde* I (sense, NEB) or *Nco* I (anti-sense, promega) in a 50 µl containing 1X appropriate buffer and 20 units of each restriction enzyme. The reaction was incubated at 37°C overnight. The digestion product was purified using a MinElute PCR purification Kit (Qiagen). The concentration of purified PCR product were estimated by comparing with the DNA marker after electrophoresis and also spectrophotometrically estimated.

2.12.3 Synthesis of the cRNA probes

For synthesis of the cRNA probe, 0.4 µg of the gel-eluted product (for linearized plasmid) or 1 µg of the gel-eluted PCR product was used as the template using the protocol recommended by the manufacturer (Roche). The mixture was incubated at 40°C for 2 hours for the antisense probe and 37°C for 2 hours for the sense probe. The template DNA was eliminated by treating with DNase I at 37°C for 20 minutes. The reaction was terminated by adding 2 µl of 0.2 M EDTA (pH 8.0). The synthesized probe (1 µl) was determined by electrophoresis and the remaining reaction mixture was purified using an RNeasy® MinElute® Cleanup kit (Qiagen). The cRNA probe concentration was spectrophotometrically measured and stored at -80°C until needed.

2.12.4 Dot blot analysis

The quality of cRNA probes was determined before used for *in situ* hybridization using dot blot analysis. Serial dilutions of the pre-diluted probe and control cRNA were made. The diluted probe (1 µl) was spotted on a piece of the Hybond N⁺ membrane. The spotted probe was fixed to the membrane by cross-linking with UV-light for 1 minute. The membrane was washed with the washing buffer for 1 minute and incubated in the blocking solution for 1 minute. After that, the membrane was incubated in Anti-DIG-alkaline phosphatase (1:5,000 in the blocking solution) for 3 minute, washed with the washing buffer for 1 minute and incubates in the detection buffer. The positive hybridization signals was developed using NBT/BCIP solution.

The intensities of the control and the dilution of probe were compared to estimate the concentration of the cRNA probe.

2.12.5 Hybridization and detection

Tissue sections were dewaxed with xylene and dehydrated in absolute ethanol. The sections were prehybridized with 2x SSC containing 50% deionized formamide, 1 µg/µl yeast tRNA, 1 µg/µl salmon sperm DNA, 1 µg/µl BSA and 10% (w/v) dextran sulfate at 50°C for 30 min and hybridized with either the sense or antisense probe in the prehybridization solution overnight at 50°C. After hybridization, the tissue sections were washed twice with 4x SSC for 5 min each and once with 2x SSC containing 50% (v/v) formamide for 20 min at 50°C. The sections were immersed in prewarmed RNase A buffer (0.5 M NaCl, 10 mM Tris-HCl, pH 8.0, 1 mM EDTA) at 37 °C for 30 min and treated with RNase A (10 µg/ml) at 37 °C for 30 min. Tissue sections were washed four times with the RNase A buffer (37°C, 10 min each) and 2x SSC (50°C, 15 min each). Then tissue sections was wash twice with 2x SSC for 15 min at 50°C. And high stringent washing was carried out twice in 0.2x SSC at 50°C for 20 min each. Detection of the positive hybridization signals was carried out with a DIG Wash and Block Buffer kit (Roche) (Qui and Yamano, 2005).

2.13 *In vitro* expression of recombinant protein using the bacterial expression system

2.13.1 Primer design

A pair of primer was designed to amplify the full length cDNA of each gene. The forward and reverse primers contained a *Nde* I site and a *Bam* HI site and six His encoded nucleotides, respectively (Table 2.8).

2.13.2 Construction of recombinant plasmid in cloning and expression vectors

The full length cDNA of each genes were amplified by PCR, ligated to pGEM®-T Easy vector and transformed in to *E. coli* JM109. Plasmid was extracted from a positive clone and used as the template for PCR amplification using 0.2 µM of each primer, 0.75 unit *Pfu* DNA polymerase (Promega) and 0.2 mM of each dNTP.

Table 2.8 Nucleotide sequences and T_m of primers for amplification the ORF of *PmCOMT*, *PmFAMeT*, *PmBr-cZ1* and *PmBr-cZ4*

Gene	Sequence	T _m
PmCOMT-ORF-F	F: 5'-ATGTCTTCTCTGAAAAGTTACCA -3'	62
PmCOMT-ORF-R	R:5'- TTTATTATTGGGGAGGAGGG -3'	58
PmFAMeT-ORF-F	F: 5'-TGCTCGCAAGTAACTCGGGATG-3'	68
PmFAMeT-ORF-R	R:5' -GTGAACAAAGCCACAAAGCAGGA-3'	88
PmBr-cZ1-ORF-F	F: 5' -AAAAC TGGTTCGCACGTGG -3'	58
PmBr-cZ1-ORF-R	R:5'-GGAGATCTTTATGGCAGGTTAAT -3'	64
PmBr-cZ4-ORF-F	F: 5'-GCGGCGTGGTGTGGACGCTC-3'	76
PmBr-cZ4-ORF-R	R:5'- TTTTCATCACAGGGCTTATC -3'	56

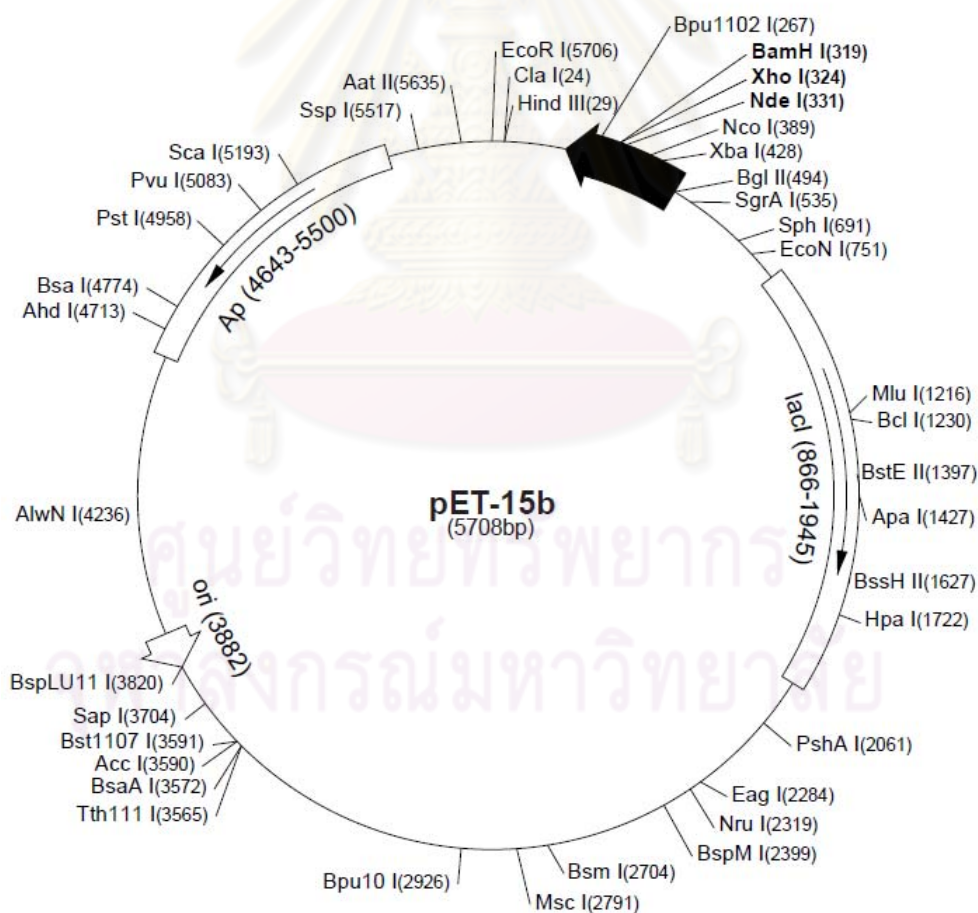


Figure 2.1 The pET-15b vector map (Novogen).

The thermal profiles were predenaturation at 95°C for 2 minutes followed by 25 cycles of denaturation at 95°C for 30 seconds, annealing at 60°C for 30 seconds and at 72°C for 4 minutes and the final extension at 72°C for 7 minutes. The amplification product was digested with *Nde* I and *Bam* RI and analyzed by agarose gel electrophoresis. The gel-eluted product was ligated into pET15b and transformed into *E. coli* JM109. The recombinant plasmid was subsequently transformed into *E. coli* BL21-CodonPlus(DE3)-RIPL.

Table 2.9 The gene specific overhang primer, their sequences and T_m of *COMT*, *FAMeT* and *Br-C* gene for *in vitro* expression.

Gene	Sequence	T _m
PmCOMT-ORF/ <i>Nde</i> I-F*	F: 5'-CCGCATATG <u>TC</u> TTCTCTGAAAAGTTACCA -3'	70
PmCOMT-ORF/ <i>Bam</i> HI-R*	R:5'-CGGGGATCCTCAATGATGATGATGATGATG TTTTTTAAAACATAGAGTCA-3'	76
PmFAMeT-ORF/ <i>Nde</i> I-F*	F:5'-CCGCATATGGGCGAGAGCTGGGCTTCCTA -3'	70
PmFAMeT-ORF/ <i>Bam</i> HI-R*	R:5'-CGGGGATCCTTAATGATGATGATGATGATG AAATTCGAACTTCCACT -3'	74
PmBr-cZ1-ORF/ <i>Xba</i> I-F	F:5'-CGGTCTAGAATGGAGGAGGGCTACCTAGCA C-3'	68
PmBr-cZ1-ORF/ <i>Bam</i> HI-R*	R:5'-CGGGGATCCTTAATGATGATGATGATGATG TTAATGTTTATAATTCCTCTTATGG-3'	76
PmBr-cZ4-ORF/ <i>Xba</i> I-F	F: 5'-CGGTCTAGAATGGAGGACGGACTACTAAGCT-3'	64
PmBr-cZ4-ORF/ <i>Nde</i> I-R*	R5'-CGGCATATGTTAATGATGATGATGATGATG TTAAGGAGTTACAGCTGTGGCT-3'	72

**Nde* I site (underlined) and an *Bam* HI site (italicized) and six His encoded nucleotides (boldfaced),

2.13.3 Expression of recombinant proteins

A bacterial colony carrying recombinant plasmid of each gene was inoculated into 3 ml of LB medium containing 50 µg/ml ampicillin and 50 µg/ml chloramphenicol at 37°C and 50 µl of the overnight culture was transferred to 50 ml of LB medium containing ampicillin and chloramphenicol and further incubated to an OD₆₀₀ of 0.4-0.6. One OD₆₀₀ milliliter was time-interval taken at 1, 2, 3, 6, 12 and 24 hr after IPTG induction (0.4 mM final concentration). The culture was centrifuged at 12000 g for 1 min, resuspended with 1x PBS and analyzed by 15% SDS-PAGE

(Laemmli, 1970). In addition, 20 ml of the IPTG induced-culture (6 hr) were centrifuged, resuspended in the lysis buffer (0.05 M Tris-HCl; pH 7.5, 0.5 M Urea, 0.05 M NaCl, 0.05 M EDTA; pH 8.0 and 1 mg/ml lysozyme) and sonicated 2-3 times at 15-30% amplitude, pulsed on for 10 seconds and pulsed off for 10 seconds in a period of 2-5 min. The protein concentration of both soluble and insoluble fractions was measured (Bradford, 1976). Overexpression of recombinant protein was analyzed by 15% SDS-PAGE. For western blot analysis, the electrophoresed proteins were transferred to a PVDF membrane (Towbin et al., 1979) and analyzed as previously described in Imjongjairak et al. (2005).

Recombinant protein was analyzed in 15% SDS-PAGE. The electrophoresed proteins were transferred onto a PVDF membrane (Hybond P; GE Healthcare) (Towbin et al., 1979) in 25 mM Tris, 192 mM glycine (pH 8.3) buffer containing 10% methanol at 100 V for 90 min. The membrane was treated in the DIG blocking solution (Roche) for 1 hr and incubated with the Anti-His antibody IgG2a (GE Healthcare; 1:5000 in the blocking solution) for 1 h at room temperature. The membrane was washed 3 times with 1× Tris Buffer Saline-Tween20 (TBST; 50 mM Tris-HCl, 0.15 M NaCl, pH 7.5, 0.1% Tween20) and incubated with goat anti mouse IgG (H+L) conjugated with alkaline phosphatase (Bio-Rad Laboratories) at 1:3000 for 1 h and washed 3 times with 1× TBST. Immunoreactive signals were visualized using NBT/BCIP (Roche) as the substrate.

2.13.4 Purification of recombinant proteins

Recombinant protein was purified using a His GraviTrap kit (GE Healthcare). Initially, 1 liter of IPTG-induced cultured overnight at 37°C was harvested by centrifugation at 5000 rpm for 15 min. The pellet was resuspended in the binding buffer (20 mM sodium phosphate, 500 mM NaCl, pH 7.4), sonicated and centrifuged at 14000 rpm for 30 min. The insoluble fraction was purified by using a His GraviTrap kit (GE Healthcare) under denaturing. The insoluble fraction was loaded into the column and washed with 10 ml of the binding buffer containing 20 mM imidazole (20 mM sodium phosphate, 500 mM NaCl, pH 7.4 and 8M urea), 5 ml of the binding buffer containing 50 mM imidazole (20 mM sodium phosphate, 500 mM NaCl, 50 mM imidazole, pH 7.4 and 8M urea) and 5 ml of the binding buffer containing 80 mM imidazole (20 mM sodium phosphate, 500 mM NaCl, 80 mM

imidazole, pH 7.4 and 8M urea), respectively. The recombinant protein was eluted with 6 ml of the elution buffer (20 mM sodium phosphate, 500 mM NaCl, 500 mM imidazole, pH 7.4 and 8M urea). Fractions from the washing and eluting steps were analyzed by SDS-PAGE and western blotting. The purified protein was stored at 4°C or -20°C for long term storage.

2.13.5 Peptide sequencing of recombinant proteins

Peptide sequencing was applied to confirm that the expressed proteins were rPmCOMT, rPmFAMeT-1 and rPmFAMeT-s by using NanoLC-MS/MS

2.13.5.1 In-gel digestion

The expected sizes (on SDS-PAGE or western blot) were excised, the gel pieces were subjected to in-gel digestion using a method developed by Proteomics Laboratory, Genome Institute, National Center for Genetic Engineering and Biotechnology (BIOTEC), National Science and Technology Development Agency (NSTDA), Thailand (Jaresitthikunchai et al., 2009). Briefly, the excised band was washed 3 times with 3% hydrogen peroxide and water, respectively. The gel plugs were dehydrated with 100% acetonitrile (ACN), reduced with 10mM DTT in 10mM ammonium bicarbonate at room temperature for 1 hour and alkylated at room temperature for 1 hour (dark) in 100 mM iodoacetamide (IAA) supplemented with 10 mM ammonium bicarbonate. After alkylation, the gel pieces were dehydrated twice with 100% ACN for 5 minutes. To perform in-gel digestion of proteins, 10 µl of trypsin solution (10 ng/µl trypsin in 50% ACN/10mM ammonium bicarbonate) was added to the gels followed by incubation at room temperature for 20 minutes, and then 20 µl of 30% ACN was added to keep the gels immersed throughout digestion. The gels were incubated at 37°C for a few hours or overnight. To extract peptide digestion products, 30 µl of 50% ACN in 0.1% formic acid (FA) was added into the gels, and then the gels were incubated at room temperature for 10 minutes in a shaker for three times. Peptides extracted were collected and pooled together in the new tube. The pool extracted peptides were dried by incubated at 40°C for 3-4 hours and kept at -80°C for further mass spectrometric analysis.

2.13.5.2 NanoLC-MS/MS

Nano-electrospray liquid chromatography ionization tandem mass spectrometry (nanoLC-MS/MS) was performed as followed. Selected protein spots were submitted to the HCTultra ETD II system™ (Bruker Daltonics). This system was controlled by the Chromeleon Chromatography Management system and comprised a two-pump Micromass/Loading Iontrap system with an autosampler. Injected samples were first trapped and desalted on an AccLaim PepMap C18 μ Precolumn Cartridge (5 μ m, 300- μ m inside diameter by 5 mm) for 3 minutes with 0.1% formic acid delivered by a loading pump at 20 μ l/minutes, after which the peptides were eluted from the pre-column and separated on a nano column, AccLaim PepMap 100 C18 (15 cm x 3 μ m) connected in-line to the mass spectrometer, at 300 nl/minutes using a 30 minutes fast gradient of 4 to 96% solvent B (80% acetonitrile in 0.1% formic acid).

2.13.5.3 Database searches

After data acquisition, MS/MS ion from nanoLC-MS/MS were identified using MASCOT (<http://www.matrixscience.com>) searched against data of the local shrimp database. In addition, data from nanoLC-MS/MS were searched against data of the National Central for Biotechnology Information (NCBI, nr). For MS/MS ion search, the peptide charge was 1+, 2+ and 3+, MS/MS ion mass tolerance was ± 1.2 Da, fragment mass tolerance ± 0.6 Da, and allowance for 1 miss cleavage. Variable modification was methionine oxidation and cysteine carbamidomethylation. Proteins with the highest score or higher significant scores were selected. The significant hit proteins were selected according to Mascot probability analysis and regarded as positive identification after additional conformation with molecular weight (MW)/isoelectric point (pI) values

2.13.6 Polyclonal antibody production and western blot analysis

Polyclonal antibody against rPmCOMT, rPmFAMeT-s and rPmFAMeT-l was immunologically produced in rabbit by Faculty of Associated Medical Sciences, Chiangmai University. Western blot analysis was carried out to examine specificity and sensitivity of the antibody.

For western blot analysis, ovarian tissues of *P. monodon* were homogenized in the sample buffer (50 mM Tris-HCl; pH 7.5, 0.15 M NaCl) supplemented with the proteinase inhibitors cocktail (EDTA free; Roche). The homogenate was centrifuged

at 12000g for 30 min at 4°C and the supernatant was collected. Protein concentrations of the tissues extract were determined by the dye binding method (Bradford, 1976). Thirty micrograms of ovarian proteins were heated at 100°C for 5 min, immediately cooled on ice and size-fractionated by 15% SDS-PAGE (Laemmli, 1970). Electrophoretically separated proteins were transferred onto a PVDF membrane (Hybond P; GE Healthcare) (Towbin et al., 1979) in the 25 mM Tris, 192 mM glycine (pH 8.3) buffer containing 10% methanol at a constant current of 350 mA for 1 h. The membrane was treated with the DIG blocking solution (Roche) for 1 hr and incubated with the primary antibody (1:300 in the blocking solution) for 1 hr at room temperature. The membrane was washed 3 times with 1x Tris Buffer Saline-Tween-20 (TBST; 50 mM Tris-HCl, 0.15 M NaCl, pH 7.5, 0.1% Tween-20) and incubated with goat anti-rabbit IgG (H+L) conjugated with alkaline phosphatase (Bio-Rad Laboratories) at 1:3000 for 1 h and washed 3 times with 1x TBST. Immunological signals were visualized using NBT/BCIP (Roche) as the substrate.

2.14 Immunohistochemistry

The paraffin sections were prepared from pieces of ovaries fixed with 4% paraformaldehyde. Deparaffinized sections were autoclaved in 0.01 sodium citrate (pH 6.0) containing 0.1% Tween-20 at 120°C for 5 minutes. Then incubated in the blocking solution I (3% H₂O₂ in methanol) for 15 minutes. After treatment in the blocking solution II (Roche) for 4 hours, section were incubated with purified anti-COMT, anti-FAMeT-s, anti-FAMeT-l, preimmunise and blocking solution (control) for 1 hour in the humid chamber. The sections were rinsed three times for 5 minutes with 1XPBS (pH 7.2) and incubate with goat anti-rabbit IgG conjugated with horse radish peroxidase for 1 hour. The section were again rinse three times for 5 minutes with 1XPBS (pH 7.2). Localization of antigen was visualized using diaminobenzidine (Wako) as the substrate. Tissue section were dehydrated and mounted for long term storage.

CHAPTER III

RESULTS

3.1 Isolation and characterization of the full length cDNA of *catechol-O-methylation (PmCOMT)*, *farnesoic acid-O-methyltransferase (PmFAMeT)* and *broad complexes (PmBr-c)* genes in *P. monodon*

3.1.1 Total RNA extraction and first strand synthesis

The quantity and quality of total RNA were estimated by spectrophotometry. The ratio of OD₂₆₀/OD₂₈₀ of extracted RNA ranged from 1.8-2.0 indicating that RNA samples were relatively pure. Agarose gel electrophoresis indicated smear total RNA with a few discrete bands implying the accepted quality of extracted total RNA (Fig. 3.1). The ovarian mRNA was purified and large amount of mRNA was obtained (typically 30-50 µg from each specimen). The purified mRNA was subjected to the synthesis of 5' and 3' RACE-PCR template.

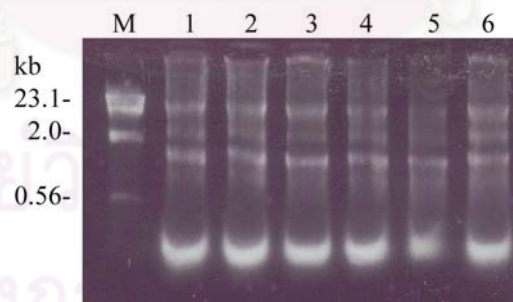


Figure 3.1 A 0.8% ethidium bromide-stained agarose gel showing the quality of total RNA from ovaries of *P. monodon* broodstock (Lanes 1 - 6). Lanes M is λ /*Hind* III marker.

3.1.2 Characterization of the full length cDNA of *PmCOMT*

The partial nucleotide sequence of *PmCOMT* was initially obtained from EST analysis of the hemocyte cDNA library. This EST significantly match *O-methyltransferase* of *F. chinensis* (E -value = $1e-110$, Fig 3.2). The primary 3' RACE-PCR of *PmCOMT* was further carried out for isolation of the full length cDNA of this gene. The positive amplification product of 900 bp in size was obtained (Fig. 3.3). The RACE-PCR fragment was cloned and sequenced for both directions (Fig. 3.4). Nucleotide sequences of 3' RACE-PCR and the original EST were assembled (Fig. 3.5A).

The full length cDNA of *PmCOMT* was 1176 bp in length containing an ORF of 666 bp corresponding to a polypeptide of 221 amino acids. The 5' and 3' UTRs of *PmCOMT* were 17 and 465 bp (excluding the poly A tail), respectively. The poly A additional signals (AATAAA) were located at 150 and 468 nucleotides upstream from the poly A tail (Fig. 3.5B). The closest similarity to *PmCOMT* was *O-methyltransferase (OMT)* of *F. chinensis* (E -value = 0.0). The calculated pI and molecular weight of the deduced *PmCOMT* protein was 5.73 and 24.1 kDa, respectively. A predicted *O-methyltransferase* domain was found at positions 18-221 (E -value = $1.7e-73$) of the deduced *PmCOMT*. Two putative glycosylation sites were found at positions 19-21 (NTS) and 205-207 (NVT). Nine predicted phosphorylation sites (positions 6, 7, 21, 76, 125, 140, 150, 154, and 185) were found in the deduced *PmCOMT* (Fig. 3.5C).

A.

```
TTGACAGGTTCTGAAGATGCTTTCTCTGAAAAAGTTACCATAATCCCGATCCTTTGGTGCAGTATTGTG
TAAATCATTTCATTGAGATTAACCGACGCGCAAAAACGACTGAATGATGTAACCTCTGCAGCACCGTAGAG
CGGCGATGTTGGGGGCACCTGAGGTTCTGCAGCTCAATGCCAACATAATGCAGGCTATCGGGGCAAAGA
AAGTACTAGACATTGGGGTGTTCACAGGCGCCAGTTCCTCTCTGCTGCTCTGGCACTGCCTCCGAATG
GCAAGGTCCACGCCCTTGACATAAGTGAAGAGTTTGCCAACATAGGAAAACCGTTCTGGGAGGAAGCTG
GAGTTATCAACAAGATAAGTCTGCACATCGCTCCAGCTGCTGAGACTCTCCAGAAGTTCATTGACGGCG
GAGAAGCTGGCACCTTCGACTATGCTTTTCATTGATGCCGACAAAGGGAATTATGAGCTGTACTATGAAC
TTTGCTCACTCTCTTGCCTCTGGTGGAGTCATCGCCTTCGACAACACACTTTGGGATGGAGCTGTGA
TTGACCCCACTGATCAAACCCCTGGCACAGTGGCTATTAGGAAAATTAACGAAAAGCTGAGAGATGACC
AGAGAATCAATATTTCTTCTTCTGAAGATTGGTGTATGGCGTACTCTATGTTTTAAAAAATGAACATTTT
TTCACCCGATAGGCACACATCTTCCGAGTAGTAAATTCCTGTTTCAGGAGAATGCTGATGAC
```

B.

O-methyltransferase [Fenneropenaeus chinensis] Length=221 Score = 402 bits (1032), Expect = $1e-110$ Identities = 199/221 (90%), Positives = 209/221 (94%), Gaps = 0/221 (0%) Frame = +3

Query	18	MSSLKSYHNPDPPLVQYCVNHSLRLTDAQKRLNDVTLQHRRRAAMLGAPEVLQLNANIMQAI	197
Sbjct	1	MSSLKSY N DPLVQYCVNHSLRLTD QKRLND TLOHRRRAAMLGAPEVLQLNANIMQAI	60
Query	198	GAKKVLIDIGVFTGASSLSAALALPPNGKVHALDISEEFANIGKPFWEEAGVINKISLHIA	377
Sbjct	61	GAKKVLIDIGVFTGASSLSAALALPPNGKV+ALDISEEF NIGKP+WEEAGV NKISLHIA	120
Query	378	PAAETLQKFIDGGEAGTFDYAFIDADKGNELYELCLTLLRSGGVIAFDNTLWDGAVID	557
Sbjct	121	PAAETLQKFID GEAGTFDYAFIDADK +Y+ YYELCL LLR GGVIAFDNTLWDGAVID	180
Query	558	PTDQTPGTVAIRKINEKLRDDQRINISFLKIGDGVTLCFKK	680
Sbjct	181	PTDQ PGT+AIRK+NEKL+DDQRINISFL+IGDG++LCFKK	221

Figure 3.2 Nucleotide sequence (A) and BlastX results (B) of an EST from hemocyte cDNA library of *P. monodon* that significantly matched *F. chinensis* OMT. The positions of sequences primers were illustrated in boldface and underlined. The putative start codon was illustrated in boldface.

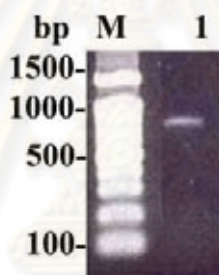


Figure 3.3 Agarose gel electrophoresis showing 3' RACE-PCR of *PmCOMT* (lanes 1). A 100 bp DNA ladder (lane M) was used as the DNA marker.

A.

GCTCTGGTGGAGTCATCGCCTTCGACAACACACTTTGGGATGGAGCTGTGATTGACCCCACTGATCAAA
 CCCCTGGCACAGTGGCTATTAGGAAAATTAACGAAAACTGAGAGATGACCAGAGAATCAATATTTCCCT
 TCCTGAAAATTGGTGACGGCGTGACTCTATGTTTTAAAAAATGAATATTTTTTCCCCCGAAAAGGACC
 CCTCCTCCCCAATAATAAATTCCTGGTTCCAGAAAAAGGTTAAGAACTTTAACAAGGATGGAACAATTG
 ACCCCCCATACCATAACCTATGAAAAGTTTTAAAACAATTGGCCGGCCTTTACCGGCCCCCTCCTGGC
 ACGGGGGGCCAAAAACATCCTCCATTGGCCCCGAATTTACCGAAAAATCTTATTTAAAACCCCTTTTAAA
 ACCAGGGGCTGTAACTGGGAATGGCTGAATATGGATTTCCCTTTCCCCCAAAGGTCCCTGGCCAGAAT
 TGATTCTAAATAAAAAATTGGCAACAACCTTTAAATGGAACTTTCCCTCCGGTCCATTGCCACTTGGCCAAA
 CTACCGCCAAATACTAACTTTTAATGGACCAAATGGAAATGGTAAAACACCCCCCCCCCTATATTA
 TCCCCGAATTTAAATCCTACGTCTCGAANAAAAAANNAAAAAANAAAAAANAAAAAANAAAAAANAAAAA
GGTCTCCGGCGTGGAG
ACCACCGGCTGGCCCATAGAGAGAGCCAATATAAACCAAT

Figure 3.4 Nucleotide sequence of the 3'UTR of *PmCOMT* generated by the primary 3' RACE-PCR. The positions of sequencing primers are illustrated in boldface and underlined.

A.

TTGACAGGTTCTCTGAAGATGCTTTCTCTGAAAAGTTACCATAATCCCGATCCTTTGGTGCAGTATTGTG
TAAATCATTTCATTGAGATTAACCGACGCGCAAAAACGACTGAATGATGTAACCTCTGCAGCACCGTAGAG
CGGCGATGTTGGGGGCACCTGAGGTTCTGCAGCTCAATGCCAACATAATGCAGGCTATCGGGGCAAAGA
AAGTACTAGACATTGGGGTGTTCACAGGCGCCAGTTCCTCTCTGCTGCTCTGGCACTGCCTCCGAATG
GCAAGGTCCACGCCCTTGACATAAGTGAAGAGTTTGCCAAACATAGGAAAACCGTTCCTGGGAGGAAGCTG
GAGTTATCAACAAGATAAGTCTGCACATCGCTCCAGCTGCTGAGACTCTCCAGAAGTTCATTGACGGCG
GAGAAGCTGGCACCTTCGACTATGCTTTTCATTGATGCCGACAAAAGGGAATTATGAGCTGTACTATGAAC
TTTGCCCTCACTCTCTTGGCTCTGGTGGAGTCATCGCTTCGACAACACACTTTGGGATGGAGCTGTGA
TTGACCCCACTGATCAAACCCCTGGCACAGTGGCTATTAGGAAAATTAACGAAAACTGAGAGATGACC
AGAGAATCAATATTTCTTCTGAAAATTTGGTGACGGCGTGACTCTATGTTTTTAAAAAATGAATATTTT
TTCCCCCGAAAAGGACCCCTCCTCCCAATAATAAATTTCTGGTTCCAGAAAAAGGTTAAGAATTTTA
ACAAGGATGGAACAATTGACCCCCCATAACCATAACCTATGAAAAGGTTTTTAAAAACAATTGGCCGGCCT
TTACCGGCCCTCCTGGCACGGGGGGCCAAAAACATCCTCCATTGGCCCCGAATTTACCGAAAAATCTT
ATTTAAACCCCTTTTAAAAACCAGGGGCTGTAACGGGAATGGCTGAATATGGATTTCTTTCCCCCA
AAGGTCCCTGGCCAGAATTGATTCTAAATAAAAAATGGCAACAACCTTTAAATGGAAGTTTCTCCGGTC
CATTGCCACTTGGCCAAACTACCGCAAATACTAATTTTAAATGGACCAATGGAATGGTAAAACCAC
CCCCCCCCCTATATTATCCCCGAATTTAAATCCTACGTCTCGAAAAAAAAAAAAAAAAAAAAAAAAAAA
AAA

B.

O-methyltransferase [Fenneropenaeus chinensis] Length=221 Score = 402 bits
(1032), Expect = 2e-110 Identities = 199/221 (90%), Positives = 209/221 (94%),
Gaps = 0/221 (0%) Frame = +3

Query	18	MSSLKSYHNPDPVQYCVNHSRLRLTDAQKRLNDVTLQHRRAMLGAPEVLQLNANIMQAI	197
		MSSLKSY N DPLVQYCVNHSRLRLTD QKRLND TLQHRRAMLGAPEVLQLNANIMQAI	
Sbjct	1	MSSLKSYDNTDPLVQYCVNHSRLRLTDVQKRLNDATLQHRRAMLGAPEVLQLNANIMQAI	60
Query	198	GAKKVLIDIGVFTGASSLSAALALPPNGKVHALDISEEFANIGKPFWEAGVINKISLHIA	377
		GAKKVLIDIGVFTGASSLSAALALPPNGKV+ALDISEEF NIGKP+WEEAGV NKISLHIA	
Sbjct	61	GAKKVLIDIGVFTGASSLSAALALPPNGKVYALDISEEFTNIGKPYWEEAGVSNKISLHIA	120
Query	378	PAAETLQKFIDGGEAGTFDYAFIDADKGNLYELCLLLRSGGVIAFDNTLWDGAVID	557
		PAAETLQKFID GEAGTFDYAFIDADK +Y+ YYELCL LLR GGVIADFNTLWDGAVID	
Sbjct	121	PAAETLQKFIDAGEAGTFDYAFIDADKESYDRYELCLILLRPGGVIAFDNTLWDGAVID	180
Query	558	PTDQTPGTVAIRKINEKLRDDQRINISFLKIGDGVTLCFKK	680
		PTDQ PGT+AIRK+NEKL+DDQRINISFL+IGDG++LCFKK	
Sbjct	181	PTDQKPGTLAIRKMNEKLRDDQRINISFLRIGDGLSLCFKK	221

C.

TTGACAGGTTCTCTGAAGATGCTTTCTCTGAAAAGTTACCATAATCCCGATCCTTTGGTGC 60
M S S L K S Y H N P D P L V Q 15
AGTATTGTGTAATCATTTCATTGAGATTAACCGACGCGCAAAAACGACTGAATGATGTAA 120
Y C V N H S L R L T D A Q K R L N D V T 35
CTCTGCAGCACCGTAGAGCGGCGATGTTGGGGGCACCTGAGGTTCTGCAGCTCAATGCCA 180
L Q H R R A A M L G A P E V L Q L N A N 55
ACATAATGCAGGCTATCGGGGCAAAGAAAGTACTAGACATTGGGGTGTTCACAGGCGCCA 240
I M Q A I G A K K V L D I G V F T G A S 75
GTTCACTCTCTGCTGCTCTGGCACTGCCTCCGAATGGCAAGTCCACGCCCTTGACATAA 300
S L S A A L A L P P N G K V H A L D I S 95
GTGAAGAGTTTGCCAAACATAGGAAAACCGTTCCTGGGAGGAAGCTGGAGTTATCAACAAGA 360
E E F A N I G K P F W E E A G V I N K I 115
TAAGTCTGCACATCGCTCCAGCTGCTGAGACTCTCCAGAAGTTCATTGACGGCGGAGAAG 420
S L H I A P A A E T L Q K F I D G G E A 135
CTGGCACCTTCGACTATGCTTTTCATTGATGCCGACAAAAGGGAATTATGAGCTGTACTATG 480
G T F D Y A F I D A D K G N Y E L Y Y E 155
AACTTTGCCTCACTCTCTTGGCTCTGGTGGAGTCATCGCTTCGACAACACACTTTGGG 540

L C L T L L R S G G V I A F D N T L W D	175
ATGGAGCTGTGATTGACCCCACTGATCAAACCCCTGGCACAGTGGCTATTAGGAAAATTA	600
G A V I D P T D Q T P G T V A I R K I N	195
ACGAAAACTGAGAGATGACCAGAGAATCAATATTTCTTCTGAAAATTGGTGACGGCG	660
E K L R D D Q R I N I S F L K I G D G V	215
TGACTCTATGTTTTAAAAAATGAATATTTTTTCCCCCGAAAAGGACCCCTCCTCCCCAA	720
T L C F K K *	221
<u>TAATAAA</u> TTTCTGGTTCCAGAAAAAGGTTAAGAAGCTTTAACAAGGATGGAACAATTGACC	780
CCCCATACCATACACCTATGAAAAGGTTTTAAAAACAATTGGCCGGCCTTTACCGGCCCT	840
CCTGGCACGGGGGGCCAAAAACATCCTCCATTGGCCCCGAATTTACCGAAAAATCTTATT	900
AAAACCCCTTTTTAAAACCGGGGCTGTAAGTGGGAATGGCTGAATATGGATTTCCCTTC	960
CCCCCAAAGGTCCTGGCCAGAATTGATTC <u>TAATAAA</u> AATTGGCAACAACCTTTAAATGG	1020
AAGTTTCTCCGGTCCATTGCCACTTGGCCAAACTACCGCCAAATACTAACTTTTTAATGG	1080
ACCAAATGGAATGGTAAAACACCCCCCCCCCTATATTATCCCCGAATTAAAATCCT	1140
ACGTCTCGAAAAAAAAAAAAAAAAAAAAAAAAAAAAA	1176

Figure 3.5 The full length cDNA of *PmCOMT* (A) and BlastX result (B) of *PmCOMT* against the previously deposited sequences in the GenBank. (C). Nucleotide sequences illustrating organization of *PmCOMT* gene. Coding nucleotides and deduced amino acids of each exon are capitalized. Start and stop codons are illustrated in boldface and underlined. The catechol-*O*-methyltransferase domain is highlighted. Polyadenylation additional signals (AATAAA) are underlined.

3.1.3 Characterization of full length cDNA of *PmFAMeT*

The partial nucleotide sequence of *PmFAMeT* in this thesis was obtained from RT-PCR using the primers designed from the partial *FAMeT* gene sequence of *P. monodon* previously deposited in the GenBank (Accession no. AAX24112). Nucleotide sequence of the amplification product significantly match *farnesoic acid O-methyltransferase* of *P. monodon* (E -value = $4e-147$, Fig 3.6).

Both 5' and 3' RACE-PCR of *PmFAMeT* were carried out (Fig. 3.7A). The discrete amplification bands of 254 and 1333 bp from the respective reactions were cloned and sequenced (Fig. 3.7B and C). Nucleotide sequences of RACE-PCR fragments and the original EST were assembled (Fig. 3.8A). Sequence similarity analysis revealed that the full length cDNA of *PmFAMeT* was already obtained and it significantly matched that of *L. vannamei* (E -value = $2e-164$)

A.

CCGCTTCAGGGACATCAAGGGCAAGACCCCTCCGGTTCCAGGTGAAGGCTGCCATGATGCCACCTTGC
 CCTGACCTCAGGGGAGGAGGAGACTGACCCATATGCTGGAGGTGTTTCATTGCGGGATGGGAAGGCGCTGC
CTCTGCCATTAGGTTCAAGAAAAGCTGATGACTTAACTAAAAGTGGACACCCCTGACATCCTGAGTGAAGA
 AGAATATCGTGAATTCTGGGTTGCCTTCGACCATGATGTTATCCGTGTTGGCAAGGGAGGCGAGTGGGA
 GCCATTGATGAGTGCCACCATTCAGAGCCTTTCGACATCACTCATTACGGCTACAGTACTGGCTGGGG

TGCTGTTGGCTGGTGGCAGTTCCATAGTGAGGTGCACTTCCAAACTGAGGACTGCCTCACGTACAACCTT
 CATTCCCTGTGTACGGGTGACACCTTTACCTTCAGTGTTCCTGTAGCAATGATGCCCATCTGGCACTCAC
 CTCTGGCCCTGAGGAGACCACCCCATGTATGAAGTGTTC**CATTGGTGGTTGGGAAAACCAGCACT**CTGC
 CATT**CGTCTCAGCAAGGAGGGAAGGGGATCTGGT**GAGGACATGATCAAGTTCGACACCCCGACGTTGT
 CTGCTGCGAAGAGGAGAGGAAAGTTCTACGTCAGCTTCAAGGACGGCCATATCAGGGTGGGATACCAGGA
 CAGTGATCCCTTC

B.

Farnesoic acid O-methyltransferase [Penaeus monodon]

Length=280

Score = 523 bits (1347), Expect = 4e-147

Identities = 245/250 (98%), Positives = 247/250 (98%), Gaps = 0/250 (0%)

Frame = +2

Query 71 MGESWASYRTDENKQYRFKDIKDKTLRFQKAAHDAHLALTSGEEETDPMLEVFIGGWEG 250
 MG+SWASY TDENKQYRF+DIK KTLRFQ KAAHDAHLALTSGEEETDPMLEVFIGGWEG
 Sbjct 1 MGDSWASYGTDENKQYRFRDIKGGKTLRFQVKAHDAHLALTSGEEETDPMLEVFIGGWEG 60

Query 251 AASAIRFKKADDLTKVDTPDILSEEEYREFWVAFDHDVIRVGKGGEWEPFMSATIPFPD 430
 AASAIRFKKADDLTKVDTPDILSEEEYREFWVAFDHDVIRVGKGGEWEPFMSATIPFPD
 Sbjct 61 AASAIRFKKADDLTKVDTPDILSEEEYREFWVAFDHDVIRVGKGGEWEPFMSATIPFPD 120

Query 431 ITHYGYSTGWGAVGWWQFHSEVHFQTEDCLTYNFIPVYGDFTFVSVACSNDAHLALTSGP 610
 ITHYGYSTGWGAVGWWQFHSEVHFQTEDCLTYNFIPVYGDFTFVSVACSNDAHLALTSGP
 Sbjct 121 ITHYGYSTGWGAVGWWQFHSEVHFQTEDCLTYNFIPVYGDFTFVSVACSNDAHLALTSGP 180

Query 611 EETTPMYEVFIGGWENQHSAIRLSKEGRGSGEDMIKVDTDPDVVCCCEERKFVVSFKDGH 790
 EETTPMYEVFIGGWENQHSAIRLSKEGRGSGEDMIKVDTDPDVVCCCEERKFVVSFKDGH
 Sbjct 181 EETTPMYEVFIGGWENQHSAIRLSKEGRGSGEDMIKVDTDPDVVCCCEERKFVVSFKDGH 240

Query 791 RVGYQSDPF 820
 RVGYQSDPF
 Sbjct 241 RVGYQSDPF 250

Score = 132 bits (331), Expect = 3e-29

Identities = 69/136 (50%), Positives = 86/136 (63%), Gaps = 6/136 (4%)

Frame = +2

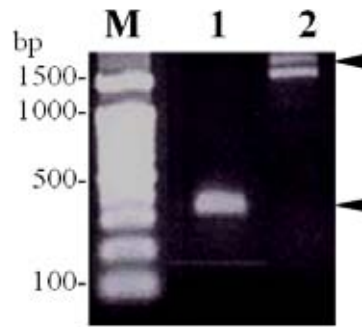
Query 92 YRTDENKQYRFKDIKDKTLRFQKAAHDAHLALTSGEEETDPMLEVFIGGWEGAASAIRF 271
 ++T++ Y F + T F ++DAHLALTSG EET PM EVFIGWE SAIR
 Sbjct 144 FQTEDCLTYNFIPVYGDFTFVSVACSNDAHLALTSGPEETTPMYEVFIGGWENQHSAIRL 203

Query 272 KK-----ADDLTKVDTPDILSEEEYREFWVAFDHDVIRVGKGGEWEPFMSATIPFPDIT 436
 K +D+ KVDPD++ EE R+F+V+F IRVG +PFM T PEP+ IT
 Sbjct 204 SKEGRGSGEDMIKVDTDPDVVCCCEERKFVVSFKDGHIRVGYQDS-DPFMEWTDPEPWKIT 262

Query 437 HYGYSTGWGAVGWWQF 484
 H GY TGWGA G W+F
 Sbjct 263 HIGYCTGWGATGKWKF 278

Figure 3.6 (A) Partial nucleotide sequence of *FAMeT* amplified from the first strand cDNA template from ovaries of *P. monodon*. The positions of sequencing primers were illustrated in boldface and underlined. (B). BlastX results of nucleotide sequence of an EST exhibiting significant similarity with *FAMeT* of *F. chinensis*.

A.



B.

GAATGCTTGGGTGCTGCCGGTGTGCTGTGTCTGGATTGTGCTCTGCTCGCAAGTAACTCGGGATGGGCG
 AGAGCTGGGCTTCTACCGTACAGATGAGAACAAGCAGTACCGCTTCAAGGACATCAAGGACAAGACCC
 TCCGGTTCCAGGGGAAGGCTGCCCATGATGCCACCTTGCCCTGACCTCAGGAGAAGAG**GAGACTGACC**
CTATGCTGGAGGTGTTCA

C.

CGTCTCAGCAAGGAGTGAAGGGGATCTGGCGAGGACATGATCAAGGTCGACACCCCCGACGTTGTTTTC
 TGCGAAGAGGAGAGGAAGTTTTACGTCAGCTTCAAGGACGGCCATATCAGGGTGGGATACCAGGACAGT
 GATCCCTTCATGGAGTGGACTGACCCCTGAGCCATGGAAGATCACCCACATTGGTTACTGCACAGGCTGG
 GGAGCAACTGGAAGTGAAGTTCGAATTTAAGTCTGCTTTGTGGCTTTGTTTACGGAATGCACCAA
 CCACTAATTTTTTTTTCTTTTCTTTTATTTGATTTTCTCATGGGACAAATGGTTTTACATGTTTTTG
 GAGTATCTTTTTCTCATGATGATGTTTTTTTTCAGTGAGGCAACATCAGTTTTGCATTTATTAACCTT
 CAAAAGTAATATTAATTTTAAAAGTGCAAAGTGCATAGATTAATAAGGGCTACCAGAAGTATGCTCTTT
 ATTTTTGCAAGCAGACATTGAGTTTATGATGTTATGTAACAAGGTTATTCAGAGTAATAGTGAATGAA
 AAAATGTATCATGACGATTCATTCAAATTTATTAACATTTAAACAAATAAAAGGAATTTTTACAGAAAAA
 AAAAAAAAAAAAAAAAAA

Figure 3.7 (A). 5'- and 3'RACE-PCR of *PmFAMeT* (lanes 1 and 2). A 100 bp DNA ladder (lanes m) was used as the DNA marker. Nucleotide sequence of 5'UTR (B) and 3' UTR (C) of *PmFAMeT* generated by the secondary 5' RACE PCR and the primary 3' RACE-PCR, respectively. The positions of sequencing primers are illustrated in boldface and underlined.

A.

GAATGCTTGGGTGCTGCCGGTGTGCTGTGTCTGGATTGTGCTCTGCTCGCAAGTAACTCGGGATGGGCG
 AGAGCTGGGCTTCTACCGTACAGATGAGAACAAGCAGTACCGCTTCAAGGACATCAAGGACAAGACCC
 TCCGGTTCCAGGGGAAGGCTGCCCATGATGCCACCTTGCCCTGACCTCAGGAGAAGAG**GAGACTGACC**
CTATGCTGGAGGTGTTCAATTGGCGGATGGGAAGGCGCTGCCTCTGCCATTAGGTTCAAGAAAGCTGATG
 ACTTAACTAAAGTGGACACCCCTGACATCCTGAGTGAAGAAGAATATCGTGAATTCGGGTTGCCCTTCG
 ACCATGATGTTATCCGTGTTGGCAAGGGAGGCGAGTGGGAGCCATTCATGAGTGCCACCATTCCAGAGC
 CTTTCGACATCACTCATTACGGCTACAGTACTGGCTGGGGTGTGTTGGCTGGTGGCAGTTCATAGTG
 AGGTGCACTTCCAAACTGAGGACTGCCTCACGTACAACCTTCATTCCTGTGTACGGTGACACCTTTACCT
 TCAGTGTTCCTGTAGCAATGATGCCCATCTGGCACTCACCTCTGGCCCTGAGGAGACCACCCCATGT
 ATGAAGTGTTCATTGGTGGTTGGGAAAACCAGCACTCTGCCATT**CGTCTCAGCAAGGAGGGAAGGGGAT**
 CTGGCGAGGACATGATCAAGGTCGACACCCCCGACGTTGTTTGTGCGAAGAGGAGAGGAAGTTTTTACG
 TCAGCTTCAAGGACGGCCATATCAGGGTGGGATACCAGGACAGTGATCCCTTCATGGAGTGGACTGACC
 CTGAGCCATGGAAGATCACCCACATTGGTTACTGCACAGGCTGGGGAGCAACTGGAAGTGAAGTTCG
 AATTTTAAAGTCTGCTTTGTGGCTTTGTTTACGGAATGCACCAACCACTAATTTTTTTTTCTTTCTTT

TTTATTGTATTTTCTCATGGGACAAATGGTTTTACATGTTTTGGAGTATCTTTTTCCATCATGATGTAT
 GTTTTTTCAGGTGAGGCAACATCAGTTTTGCATTTATTAACCTTCAAAAAGTAATATTAATTTTTAAAAGT
 GCAAAGTGCATAGATTAATAAGGGCTACCAGAAGTATGCTCTTTATTTTTGCAAGCAGACATTGAGTTT
 ATGATGTTATTGTAACAAGGTTATTCAGAGTAATAGTGAATGAAAAAATGTATCATGACGATTCATTCA
 AATTATTAACATTAACAATAAAAAGGAATTTTACAGAAAAAAAAAAAAAAAAAAAAAAAAAAAA

B.

farnesoic acid O-methyltransferase [Litopenaeus vannamei]
 Length=280

Score = 584 bits (1505), Expect = 1e-164
 Identities = 264/280 (94%), Positives = 274/280 (97%), Gaps = 0/280 (0%)
 Frame = +3

Query	63	MGESWASYRTDENKQYRFKDIKDKTLRFQ GKAAHDAHLALTSGEEETDPMLEVF IGGWEG	242
Sbjct	1	MG+SWASY TDENKQYRF+DIK KTLRFQ KAAHDAH+ALTSGEEETDPMLEVF IGGWEG	60
Query	243	AASAIRFKKADDLTKVDTPDILSEEEYREFWVAFDHDVIRVGKGGEWEPFMSATIPEPFD	422
Sbjct	61	AASAIRFKKADDL KVDTPDILSEEEYREFW+AFDHDV+RVGKG EWEPFMSATIPEPFD	120
Query	423	ITHYGYSTGWGAVGWQFHSEVHFQTE DCLTYNFIPVYGDTF F SVACSNDAHLALTS GP	602
Sbjct	121	ITHYGYSTGWGA GWQFHSE+HFQTE DCLTYNFIPVYGDTF+F SVACSNDAHLALTS GP	180
Query	603	EETTPMYEVFIGGWENQHSAIRLSKEGRGSGEDMIKVDTPDVVCC ^{EE} ERK FYVSFKDGHI	782
Sbjct	181	EETSPMYEVFIGGWENQHSAIRLSKEGRGSGEDMIKVDTPDVVCC ^{EE} ERK FYVSFKDGHI	240
Query	783	RVGYQSDPFMEWTDPEPWK ITHIGYCTGWGATGKWKFEF	902
Sbjct	241	RVGYQSDPFMEWTDPEPWK ITHIGYCTGWGA+GKWKFEF	280

Figure 3.8 The full length cDNA of *PmFAMeT* combined from 5'RACE-PCR, 3'RACE-PCR and an original EST (A). The positions of sequencing primers are illustrated in boldface and underlined. (B). Results from BlastX indicating significant similarity between *P. monodon FAMeT* and that of *L. vannamei*.

Kuballa et al. (2006) reported the existent of multiple isoforms of putative *FaMeT* from six crustacean species including *P. monodon*. Accordingly, a pair of primers covering the region that exhibited sequence polymorphism was designed. The amplification product was cloned and sequences (Fig. 3.9) and two different sequences with the presence or absence of a 15 bp indel (AGGGAAGGGGATCTG) were found (Fig. 3.10). This resulted in the identification of two different isoforms of *PmFAMeT*.

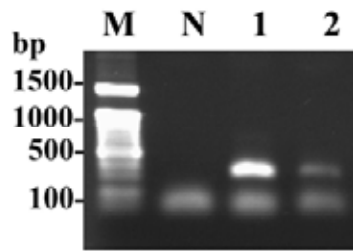


Figure 3.9 RT-PCR of *PmFAMeT* (lanes 1 and 2). Lanes M and N are a 100 bp DNA ladder and the negative control (without the cDNA template), respectively.

A.

```
CCACCATTCCAGAGCCTTTCGACATCACTCATTACGGCTACAGTACTGGCTGGGGTGCTGTTGGCTGGT
GGCAGTTCCATAGTGAGGTACGCTTCCAAACTGAGGACTGCCTCACGTACAACCTTCATTCCTGTGTACG
GTGACACCTTTACCTTCAGTGTTCCTGTAGCAATGATGCCCATCTGGCACTCACCTCTGGCCCTGAGG
AGACCACACCCATGTATGAAGTGTTCATTGGTGGTTGGGAAAACCAGCACTCTGCCATTCGTCTCAGCA
AGGAGGGAAGGGATCTGGCGAGGACATGATCAAGGTCGACACCCCGACGTTGTTTGTCTGCGAAGAGG
```

B.

```
CCACCATTCCAGAGCCTTTCGACATCACTCATTACGGCTACAGTACTGGCTGGGGTGCTGTTGGCTGGT
GGCAGCTCCATAGTGAGGTGCACTTCCAAACTGAGGACTGCCTCACGTACAACCTTCATTCCTGTGTACG
GTGACACCTTTACCTTCAGTGTTCCTGTAGCAATGATGCCCATCTGGCACTCACCTCTGGCCCTGAGG
AGACCACACCCATGTATGAAGTGTTCATTGGTGGTTGGGAAAACCAGCACTCTGCCGTTTCGTCTCAGCA
AGGGCGAGGACATGATCAAGGTCGACACCCCGACGTTGTTTGTCTGCGAAGAGG
```

C.

```
PmFAMeT-1 CCACCATTCCAGAGCCTTTCGACATCACTCATTACGGCTACAGTACTGGCTGGGGTGCTG
PmFAMeT-s CCACCATTCCAGAGCCTTTCGACATCACTCATTACGGCTACAGTACTGGCTGGGGTGCTG
*****

PmFAMeT-1 TTGGCTGGTGGCAGTTCATAGTGAGGTACGCTTCCAAACTGAGGACTGCCTCACGTACA
PmFAMeT-s TTGGCTGGTGGCAGCTCCATAGTGAGGTGCACTTCCAAACTGAGGACTGCCTCACGTACA
*****

PmFAMeT-1 ACTTCATTCCTGTGTACGGTGACACCTTACCTTCAGTGTTCCTGTAGCAATGATGCC
PmFAMeT-s ACTTCATTCCTGTGTACGGTGACACCTTACCTTCAGTGTTCCTGTAGCAATGATGCC
*****

PmFAMeT-1 ATCTGGCACTCACCTCTGGCCCTGAGGAGACCACACCCATGTATGAAGTGTTCATTGGTG
PmFAMeT-s ATCTGGCACTCACCTCTGGCCCTGAGGAGACCACACCCATGTATGAAGTGTTCATTGGTG
*****

PmFAMeT-1 GTTGGGAAAACCAGCACTCTGCCATTTCGTCTCAGCAAGGAGGGGATCTGGCGAGG
PmFAMeT-s GTTGGGAAAACCAGCACTCTGCCGTTTCGTCTCAGCAAGG-----GCGAGG
*****

PmFAMeT-1 ACATGATCAAGGTCGACACCCCGACGTTGTTTGTCTGCGAAGAGG
PmFAMeT-s ACATGATCAAGGTCGACACCCCGACGTTGTTTGTCTGCGAAGAGG
*****
```

Figure 3.10 Nucleotide sequences of *PmFAMeT-1* (A) and *PmFAMeT-s* (B) obtained by sequencing of the RT-PCR product using primers flanking the expected indel. (C) Pairwise alignment indicating an indel of 15 nucleotide corresponding to a presence/absence of a pentapeptide in different isoforms of *PmFAMeT*.

The full length cDNA of *PmFAMeT* combined from 5' and 3' RACE PCR and EST sequences were found and they were 1296 and 1311 bp in length for the short (*PmFAMeT-s*) and the long form (*PmFAMeT-l*), respectively (Fig. 3.11). These transcripts were composed of an open reading frame (ORF) of 828 and 843 bp corresponding to the deduced proteins of 275 and 280 amino acids with the identical 5' and 3'UTR of 69 and 315 bp (excluding the poly A tail), respectively. A pentapeptide (EGRGS) was found in *PmFAMeT-l* but not in *PmFAMeT-s*. The calculated pI and molecular weight of the deduced PmFAMeT-l and PmFAMeT-s protein was 4.69 and 32.1 kDa and 4.67 and 31.6, respectively. The deduced PmFAMeT-l and PmFAMeT-s proteins contained 2 crustacean FAMeT domains at positions 8 and 138 (*E*-value = 2.33e-32) and 144 and 278 (*E*-value = 2.33e-32) and 8 and 138 (*E*-value = 2.33e-32) and 144 and 273 (*E*-value = 2.33e-32), respectively (Fig. 3.12). *PmFAMeT* is significantly matched *FAMeT* of *L. vannamei* (*E*-value = 2e-157, GenBank accession no. AAX24111).

A.

ATGGGCGAGAGCTGGGCTTCCTACCGTACAGATGAGAACAAGCAGTACCGCTTCAAGGACATCAAGGAC
AAGACCCTCCGGTTCCAGGGGAAGGCTGCCCATGATGCCACCTTGCCCTGACCTCAGGAGAAGAGGAG
ACTGACCCTATGCTGGAGGTGTTTCATTGGCGGATGGGAAGGCGCTGCCTCTGCCATTAGGTTCAAGAAA
GCTGATGACTTAACTAAAGTGGACACCCCTGACATCCTGAGTGAAGAAGAATATCGTGAATTCTGGGTT
GCCTTCGACCATGATGTTATCCGTGTTGGCAAGGGAGGCGAGTGGGAGCCATTCATGAGTGCCACCATT
CCAGAGCCTTTTCGACATCACTCATTACGGCTACAGTACTGGCTGGGGTGCTGTTGGCTGGTGCCAGTTC
CATAGTGAGGTGCACTTCCAAACTGAGGACTGCCTCACGTACAACCTTCATTCCTGTGTACGGTGACACC
TTTACCTTCAGTGTTCCTGTAGCAATGATGCCATCTGGCACTCACCTCTGGCCCTGAGGAGACCACA
CCCATGTATGAAGTGTTCATTGGTGGTTGGGAAAACCAGCACTCTGCCATTCGTCTCAGCAAGGAGGGA
AGGGGATCTGGCGAGGACATGATCAAGGTCGACACCCCGACGTTGTTTGCTGCGAAGAGGAGAGGAAG
TTTTACGTCAGCTTCAAGGACGGCCATATCAGGGTGGGATACCAGGACAGTGATCCCTTCATGGAGTGG
ACTGACCCTGAGCCATGGAAGATCACCCACATTGGTTACTGCACAGGCTGGGGAGCAACTGGAAAGTGG
AAGTTCGAATTT**TAA**

B.

ATGGGCGAGAGCTGGGCTTCCTACCGTACAGATGAGAACAAGCAGTACCGCTTCAAGGACATCAAGGAC
AAGACCCTCCGGTTCCAGGGGAAGGCTGCCCATGATGCCACCTTGCCCTGACCTCAGGAGAAGAGGAG
ACTGACCCTATGCTGGAGGTGTTTCATTGGCGGATGGGAAGGCGCTGCCTCTGCCATTAGGTTCAAGAAA
GCTGATGACTTAACTAAAGTGGACACCCCTGACATCCTGAGTGAAGAAGAATATCGTGAATTCTGGGTT
GCCTTCGACCATGATGTTATCCGTGTTGGCAAGGGAGGCGAGTGGGAGCCATTCATGAGTGCCACCATT
CCAGAGCCTTTTCGACATCACTCATTACGGCTACAGTACTGGCTGGGGTGCTGTTGGCTGGTGCCAGTTC
CATAGTGAGGTGCACTTCCAAACTGAGGACTGCCTCACGTACAACCTTCATTCCTGTGTACGGTGACACC
TTTACCTTCAGTGTTCCTGTAGCAATGATGCCATCTGGCACTCACCTCTGGCCCTGAGGAGACCACA
CCCATGTATGAAGTGTTCATTGGTGGTTGGGAAAACCAGCACTCTGCCATTCGTCTCAGCAAGGGCGAG
GACATGATCAAGGTCGACACCCCGACGTTGTTTGCTGCGAAGAGGAGAGGAAGTTTTACGTCAGCTTC
AAGGACGGCCATATCAGGGTGGGATACCAGGACAGTGATCCCTTCATGGAGTGGACTGACCCTGAGCCA
TGGAAGATCACCCACATTGGTTACTGCACAGGCTGGGGAGCAACTGGAAAGTGGAAAGTTCGAATTT**TAA**

Figure 3.11 The full length ORF of *PmFAMeT-l* (A), *PmFAMeT-s* (B).

A.

```

GAATGCTTGGGTGCTGCCGGTGTGCTGTGTCTGGATTGTGCTCTGCTCGCAAGTAACTCG 60
GGATGGGGCGAGAGCTGGGCTTCCTACCGTACAGATGAGAACCAAGCAGTACCGCTTCAAGG 120
  M G E S W A S Y R T D E N K Q Y R F K 19
ACATCAAGGACAAGACCCTCCGGTTCAGGGGAAGGCTGCCCATGATGCCACCTTGCCC 180
D I K D K T L R F Q G K A A H D A H L A 39
TGACCTCAGGAGAAGAGGAGACTGACCCTATGCTGGAGGTGTTTCATTGGCGGATGGGAAG 240
L T S G E E E T D P M L E V F I G G W E 59
GCGCTGCCTCTGCCATTAGGTTCAAGAAAGCTGATGACTTAACTAAAGTGGACACCCCTG 300
G A A S A I R F K K A D D L T K V D T P 79
ACATCCTGAGTGAAGAAGAATATCGTGAATTCTGGGTTGCCTTCGACCATGATGTTATCC 360
D I L S E E E Y R E F W V A F D H D V I 99
GTGTTGGCAAGGGAGGCGAGTGGGAGCCATTCATGAGTGCCACCATTCCAGAGCCTTTCG 420
R V G K G G E W E P F M S A T I P E P F 119
ACATCACTCATTACGGCTACAGTACTGGCTGGGGTGCTGTTGGCTGGTGGCAGTTCATA 480
D I T H Y G Y S T G W G A V G W W Q F H 139
GTGAGGTGCACCTTCCAAACTGAGGACTGCCTCACGTACAACCTTCATTCCTGTGTACGGTG 540
S E V H F Q T E D C L T Y N F I P V Y G 159
ACACCTTTACCTTCAGTGTTCCTGTAGCAATGATGCCCATCTGGCACTCACCTCTGGCC 600
D T F T F S V A C S N D A H L A L T S G 179
CTGAGGAGACCACACCCATGTATGAAGTGTTCATTGGTGGTGGGAAAACCAGCACTCTG 660
P E E T T P M Y E V F I G G W E N Q H S 199
CCATTTCGTCTCAGCAAGGAGGGAAGGGGATCTGGCGAGGACATGATCAAGGTCGACACCC 720
A I R L S K E G R G S G E D M I K V D T 219
CCGACGTTGTTTTCGCAAGAGGAGGAGAAAGTTTACGTACAGCTTCAAGGACGGCCATA 780
P D V V C C E E E R K F Y V S F K D G H 239
TCAGGGTGGGATAACCAGGACAGTATCCCTTCATGGAGTGGACTGACCCTGAGCCATGGA 840
I R V G Y Q D S D P F M E W T D P E P W 259
AGATCACCCACATTGGTTACTGCACAGGCTGGGGAGCAACTGGAAAAGTGGAAAGTTCGAAT 900
K I T H I G Y C T G W G A T G K W K F E 279
TTTTAAGTCTCTGCTTTGTGGCTTTGTTTCACGGAATGCACCAACCACCTAATTTTTTTTTTCTT 960
F * 280
TTCTTTTTTATTGTATTTTCTCATGGGACAAATGGTTTTTACATGTTTTTGGAGTATCTTT 1020
TTCCTCATGATGTATGTTTTTTCAGGTGAGGCAACATCAGTTTTTGCATTTATTAACCTTC 1080
AAAAGTAATATTAATTTTTAAAAGTGCAAAGTGCATAGATTAATAAGGGCTACCAGAAGTA 1140
TGCTCTTTATTTTTGCAAGCAGACATTGAGTTTATGATGTTATTGTAACAAGGTTATTCA 1200
GAGTAATAGTGAATGAAAAAATGTATCATGACGATTCATTCAAATTATTAACATTAAC 1260
AAATAAAAGGAATTTTACAGAAAAAAAAAAAAAAAAAAAAAAAAAAAAA 1310

```

B.

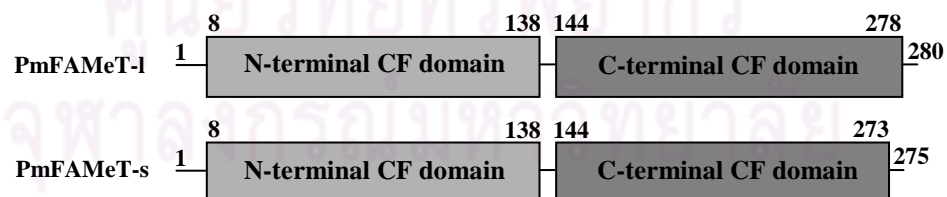


Figure 3.12 The full length cDNA and deduced amino acid sequences of *PmFAMeT-l* and *PmFAMeT-s* (A) which are different according to a pentapeptide (EGRGS, underlined). The start and stop codons are boldfaced and underlined. The poly A additional signal (AATAAA) is boldfaced, italicized and underlined. Crustacean FAMEt domains (positions 8 - 138 and 144 - 278) in the deduced FAMEt are highlighted. The diagram representing PmFAMeT is also illustrated (B).

Further analysis of the protein sequence, with NetPhos 2.0 (<http://www.cbs.dtu.dk/services/NetPhos/>), for potential posttranslational modifications shows multiple high scoring (score > 0.8) sites for possible phosphorylation at 6 threonine, 3 tyrosine and 6 or 5 serine side chains within the deduced PmFAMeT-1 and PmFAMeT-s proteins, respectively.

3.1.4 Characterization of the full length cDNA of *PmBr-c* genes

3.1.4.1 *PmBr-cZ1*

The partial nucleotide sequence of *PmBr-cZ1* was initially obtained from EST analysis of the ovarian cDNA library. This EST significantly match *Broad complex core protein isoform 6* of *A. mellifera* (*E*-value = 1e-110, Fig 3.13).

A.

```
AAGCAGTGGTATCAACGCAGAGTACGCGGGGACAGAAAACGGGTACCTCGATCACCACAGAAAACCTGGT
TCGCACGTGGTCCGATCATTTTTGAAGAGAAGGTGGTTCTGCAGACAGCATGGAGGAGGGCTACCTAGC
ACTGCGATGGAACAACCACAACACCATCTTACCAAGATCCTCACCTCCTTAGGGAGCAGGAGGCTTA
TGTGGATGTTTTCTTAGCTTGTGCGGGAAGATTATATCCTGCACACAAATTTGTACTTTCTACATGTAG
TGAGTATTTCAAGGAAATGTTTTCCAAGAACCATGTAAGCATCCCATTGTTTTTCATGAAGGATGTCTC
AATAAGGACATGGAGGCCTTGCTGGACTTCATGTACAAGGGTGAGGTCCATGTACCACAAAGCGAGTT
GGGTTTCATTGCTGCGTACAGCTGAAGGGCTTCAGGTAAGGCTTGCTGTACCTGATGACTCTCCTCG
TGGTTCTCTACCACCCCTATTGTGCCTTCTGCCTCGTCCGTCACCTCCGCCAGTCTTAT
GGCTCCAATGCATATGCGGGGTAACGCAAAAAGGCCACCAGAATCGGGTAAAAAGGATGACCCTCCAAA
GTTGACTTTACGTCTGACCTTGGACCCCGGCCACCAACCGCTCACGCATGAGGAACAGACCATCAGG
CATGCCAGAACTGAAGAGAATTAAGAGAGAGGAACATAGTGCGGCAAAATGTGGGCACTATTGAGCCTGG
AGAGGTTCCAGGATCTCCAAGTCCAACACCAAGTAGTCACAACAGCGATGAACAGTCACAGAACCTTGC
CCATAAGATCAAGACCGAAAGATCAGAATACTCTAAAGAAGAAGCAGAAGACCTGGATGAGGATGAAGG
GGTGGCAGGAGAAGTAATGTCTGGGGAAGAAGAGCAGGAACAAGAACCAGAAGGGAAGAAGGGAAGA
GGAAGAAGAAGAGGAAGGAGCATTAGGGGAAGGGGAAGGCCTCTCCACGGTGTCTCTCAGATGTTGA
GGATGGCTATGAACAATCTAACTCTTCCCTTCCCAATCTGACATATCCACAACGGAAGTCTACAGGT
TGATTTGAGTGAGGACGGGACACAGTTTCATAATCGGTCCCTGGTGGCTTTGGAGATATGATGTCAAGAAC
TTCGTCACTAGCAGGAGATGATGAGAGAAAATGGTGACAAAAGAGCAGAAGAAGCCATTTGTTTGTCTCT
CTGTGGGCAGTCATTTACACGTCGTGACAACCTTGCCAACCATATCAAGACCCACACCGGTGACCGTCC
GTTTATGTGCCAGTACTGCCACAAGTGCTTCTCAAGGAAGGACTACTTGAAGCAGCATGAACGCATCCA
CACTGGAGAGAAGCCCTACCCCTGTGACATCTGTGGTTCGTGCATTTACCAGGAAA
```

B.

REDICTED: similar to Broad-complex core-protein isoform 6 [*Apis mellifera*]
Length=454

Score = 136 bits (342), Expect = 4e-30

Identities = 81/206 (39%), Positives = 114/206 (55%), Gaps = 14/206 (6%)

Frame = +3

```
Query 165 DSMEEGYLALRWNNHNTIFTKILTLRLREQEAYVDVSLACAGRLYPAHKFVLSSTCEYFKE 344
DS ++ LRWNN T LR+ E +VDV+LAC GR AHK VLS CS YFKE
Sbjct 3 DSQQQ--FCLRWNNFQANITSQFEALRDEDFVDVTLACDGRRLQAHKVLSLACSYPYFKE 60

Query 345 MFSKNPCKHPIVFMKDVSTKDMEALLDFMYKGEVHVPOSELGSLLRTAEGQLVKGLAVPD 524
+F NPCKHPI+FM+DV + +++LL+FMV GEV++ Q+EL + LRTAE LQ++GL
Sbjct 61 LFKTNPCKHPIIFMRDVEFEHLQSLLEFMYAGEVNIQAELPTFLRTAESLQIRGLT--- 117

Query 525 DSPRGSSTTPIVpsassvprspppsLMAPMHMRGKRKRPPESA-----KKDPPKLT 680
```

```

          DS          +++ S   L++P   + K PP S+          K+ D P+++
Sbjct  118  DSQNNQHNNKHLKTNNIHASNGRGLISPNLEEEERSKTPPTSSPPPLKRLCKRSDSPQIS  177

Query  681  LRPDLGPPATNRSRMRNRPSGMPELK  758
          P   A   R RP  P+++
Sbjct  178  -SPVPA AACASGTPRTRPLIEPQVQ  202

Score = 41.2 bits (95), Expect = 0.17
Identities = 25/86 (29%), Positives = 39/86 (45%), Gaps = 9/86 (10%)
Frame = +3

Query  1191  GPGGFGDMSRST--SLAGDDERNGDKEQK-----KPFVCPGCGQSFTRRDNLNLANHIK  1343
          G GG G +   S AG+ E N +++          P CP+C + ++  NL H++
Sbjct  269  GGGGGGSLEGGMPGPPSHAGNTELNQEQQADLRKLHSLDPRPCPVCNRMYSNLSNLRQHMR  328

Query  1344  THTGDRPFMCQYCHKCFSRKDYLKQH  1421
          + C C+K F K YLK+H
Sbjct  329  LIHNPQSVTCPLCNKPFKTKLYLKRH  354

```

Figure 3.13 Nucleotide sequence (A) and BlastX result (B) of an EST showing significant similarity with *BrC-ZI* of *Apis mellifera*. The positions of sequences primers were illustrated in boldface and underlined.

The 5' and 2 fragments of 3' RACE-PCR of this gene homologue was further carried out. The positive amplification product of 158 and 1800 (fragment 1) and 1437 (fragment 2) bp in size were obtained, respectively (Fig. 3.14). The RACE-PCR fragments were cloned and sequenced for both directions (Fig. 3.15). Nucleotide sequences of RACE-PCR fragments and the original EST were assembled.

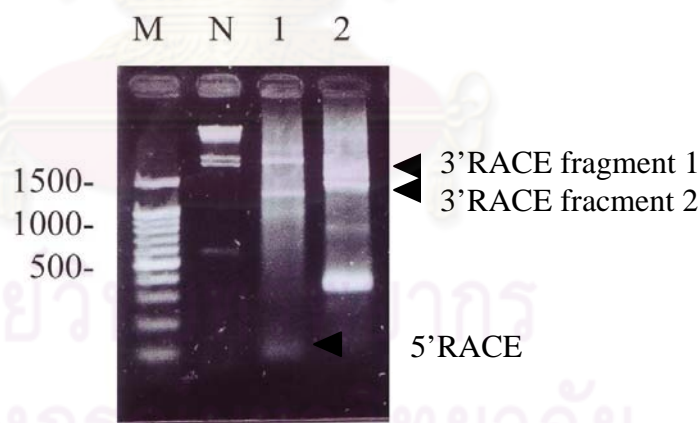


Figure 3.14 Agarose gel electrophoresis showing 5'-and 3' RACE-PCR of *PmBr-cZI* (lanes 1 and 2, respectively). Lane N = the negative control (without cDNA template). A 100 bp DNA ladder (lanes M) was used as the DNA marker.

A.

GCCACCAACCGCTCACGCATGAGGAAACAGACCATCAGGCATGCCAGAACTGAAGAGA
 ATTAAGAGAGAGGAACATAGTGCGGCAAATGTGGGCACTATTGAGCCTGGAGAGGTT
 CCAGGATCTCCAAGTCCAACACCAAGTAGTCACAACAGCGATGAACAGTCACAGAAC
 CTTGCCCATAAAGATCAAGACCGAAAGATCAGAATACTCTAAAGAAGAAGCAGAAGAC
 CTGGATGAGGATGAAGGGGTGGCAGGAGAAGTAATGTCTGGGGAAGAAGAGCAGGAA
 CAAGAACCAGAAGAGGAAGAAGAGGAAGAGGAAGAAGAAGAGGAAGGAGCATTAGGG
 GAAGGGGAAGGCCTCTCCACGGTGTCTCTCAGATGTTGAGGATGGCTATGAACAA
 TCTAACTCTTCCCTTCCCAATTCTGACATATCCACAACGGAAGTCTACAGGTTGAT
 TTGAGTGAGGACGGGACACAGTTCATAATCGGTCTGGTGGCTTTGGAGATATGATG
 TCAAGAACTTCGTCACTAGCAGGAGATGATGAGAGAAATGGTGACAAAGAGCAGAAG
 AAGCCATTTGTTTGTCTCTCTGTGGGCAGTCATTTACACGTCTGTGACAACCTTGCC
 AACCATATCAAGACCCACACCGGTGACCGTCCGTTTATGTGCCAGTACTGCCACAAG
 TGCTTCTCAAGGAAGGACTACTTGAAGCAGCATGAACGCATCCACACTGGAGAGAAG
 CCCTACCCCTGTGACATCTGTGGTCTGTGCATTTACCAGGAAAGGAGGATTGACAGAC
 CACATGCGCTGTCATTTGACTTCCGAGCCTTTTCTGTGAAACATGTGGCAAGAGC
 TTCAAGCAAAAATGTGGTTTTCGCTTCCATAAGAGGAATTATAAACAT**TAAC**CTGCC
 ATAAAGATCTCCAACACTTAATTCAGTTCATTTATGAGGCGGATATGGATAGCC
 TGTCTCTCAGTTAGTTGGATGTGGTCCCTTTAAAAATATGCCAGATAAAGGGCTAAT
 TTATGCCCTGTACTAAGTTAAGTCGTGCCATTTCTTTATGTTGAGCACCTAATTT
 CTGTGTTCAGATAGTCAATTTTACCCTGAGCTTTGTCTATGGCCCTGGCCAGATGTA
 TATTTTGGGTATATGATTATGGTTAGTGAAATATCACAACCTTGTATATTGCTGCTCA
 CATAAGGAACTTGTGTAATTTGATTTATGTTTTGACTTCAACAGGCTTAATGTA
 TGGCAAGGTTTTTGCAAAATGAAATGACTTTTTAAATGTTAGACTAATCTCAGGTA
 AGCTGTATTAATAACAGTGCTTACCTTGGTGGAGTCATTACCTAAAATTATGCAATC
 ATAATATCAGTTTTAAAATATACTTTATATCTTACTACTTTTGATATTTCTTCAT
 CTTTTATATATATATATAATGTTTTAAAAATTCAAATTTATGACATATTGCAGACC
 TCCTAACTTGGTCGTATGTTTCTTGTGTATTTATGACTCGCACAGAAAGAATTTGT
 ATGACACCTTTTTTTTTTCATGTTTGATACTCTCTCATCTGTAACCTACACTTTAGG
 TGCTCTTTGTGGTATGTTGCACTCCTTGAGTGCTGTTTTCTTCTGCCTTTTATAAGT
 TAAGATTAGATGCACCAGTATTTATTTAATTATGAAAATAACCTTTTGTAAAAATAA
 AAAAAACAATAAGATTATGTTATAAATAATATATAATTAAGAAATAAAGAAATATG
 ACACCTAAAAAAAAAAAAAAAAAAAAAAAAAAAA

B

GCCACCAACCGCTCACGCATGAGGAAACAGACCACCAGGCATGCCAGAACTGAAGAGA
 ATTAAGAGAGAGGAACGTAATGCGGCAAATGTGGGCACTATTGAGCCTGGAGAGGTT
 CCAGGATCTCCAAGTCCAACACCAAGTAGTCACAACAGCGATGAACAGTCACAGAAC
 CTTGCCCATAAAGATCAAGACCGAAAGATCAGAATACTCTAAAGAAGAAGCAGAAGAC
 CTGGATGAGGATGAAGGGGTGGCAGGAGAAGTAATGTCTGGGGAAGAAGAGCAGGAA
 CAAGAACCAGAAGAGGAAGAAGAGGAAGAGGAAGAAGAAGAAGAGGAAGGAGCATT
 GGGGAAGGGGAAGGCCTCTCCACGGTGTCTCTCAGATGTTGAGGATGGCTATGAA
 CAATCTAACTCTTCCCTTCCCAATTCTGACATATCCACAACGGAAGTCTACAGGTT
 GATTTGAGTGAGGACGGGACACAGTTCATAATCGGTCTGGTGGCTTTGGAGATATG
 ATGTCAAGAACTTCGTCACTAGCAGGAGATGATGAGAGAAATGGTGACAAAGAGCAG
 AAGAAGCCATTTGTTTGTCTCTCTGTGGGCAGTCATTTACACGTCTGTGACAACCTT
 GCCAACCATATCAAGACCCACACCGGTGACCGTCCGTTTATGTGCCAGTACTGCCAC
 AAGTGCTTCTCAAGGAAGGACTACTTGAAGCAGCATGAACGCATCCACACTGGAGAG
 AAGCCCTATCCCTGTGACATCTGTGGTCTGTGCATTTACCAGGAAAGAAGGATTGACA

GACCACATGCGCTGTCATTCTGACTTCCGAGCCTTTTCCTGTGAAACATGTGGCAAG
 AGCTTCAAGCAAAAATGTGGTCCGCGCTTCCATAAGAGGAATTATAAACATTAACCT
 GCCATAAAGATCTCCAACACTTAATTCACTGTTCCATTTATGAGGCGGATATGGATA
 GCCTGTCTCTCAGTTAGTTGGATGTGGTCCCTTTAAAAATATGCCAGATAAAGGGCT
 AATTTATGCCCTGTACTAAGTTAAGTCGTGCCATTTCCCTTTATGTTGAGCACCTAA
 TTTCTGTGTTTTCAGATAGTCAATTTTACCCTGAGCTTTGTCTATGGCCCTGGCCAGAT
 GTATATTTTGGGTATATGATTATGGTTAGTGAAATATCACAACCTTGTATATTGCTGC
 TCACATAACAGGGAACCTTGTGTAAATTTGATTTATGTTTTGACTTCAACAGGCTTAAT
 GTATGGCAAAGGTTTTGCAAAATGGAAATTGACTTTTAAATGTTAGATTAATCTCAG
 GTAAGCTGTATTAATAACAGTGCTTACCTTGGTGGAGTCATTACCTAAAATTTATGCA
 ATCATAATATCAGTTTTTAAATATACTTTTATATTCTTACTTAAAAAAAAAAAAAAAA
 AAAAAAAAAA

C

AAGCAGTGGTATCAACGCAGAGTACGCGGGACAGAAAACGGGTACCTCGATCACCA
CAGAAAACGGTTCGCACGTGGTCCGATCATTTTTGAAGAGAAGGTGGTTCTGCAGA
CAGC**ATGG**AGGAGGGCTACCTAGCACTGCGATGGAACAACCACA

Figure 3.15 Nucleotide sequence of 3'UTR, fragment 1 (A), fragment 2 (B) and 5'UTR (C) of *PmBr-cZl* generated by the secondary RACE-PCR. Nucleotide sequencing was carried out. The positions of sequencing primers are illustrated in boldface and underlined.

Two different forms of the full length cDNA of *PmBR-cZl* (the log and short form; *PmBR-cZl-s* and *PmBR-cZl-l*) were found. The *PmBR-cZl-s* and *PmBR-cZl-l* were 2422 and 2060 bp in length containing ORFs of 1440 and 1443 bp corresponding to the polypeptides of 480 and 481 amino acids, respectively (Figs. 16 and 17). The calculated pI and molecular weight of the deduced *PmBR-cZl-s* and *PmBR-cZl-l* protein were 5.46 and 53.88 kDa and 5.54 and 53.64, respectively. Both deduced proteins contained BTB domains at positions 31 and 126 (E -value = 4.14e-22) and 4 ZnF C2H2 domains.

GACAGAAAACGGGTACCTCGATCACCAAGAAAACGGGTACCTCGATCACCA	60
TTGAAGAGAAGGTGGTTCTGCAGACAGCAT ATGG AGGAGGGCTACCTAGCACTGCGATGGAA	120
M E E G Y L A L R W N	11
CAACCACAACACCATCTTCACCAAGATCCTCACCCCTCCTTAGGGAGCAGGAGGCTTATGT	180
N H N T I F T K I L T L L R E Q E A Y V	31
GGATGTTTTCTTAGCTTGTGCGGGAAGATTATATCCTGCACACAAATTTGTACTTTCTAC	240
D V S L A C A G R L Y P A H K F V L S T	51
ATGTAGTGAGTATTTCAAGGAAATGTTTTCCAAGAACCATGTAAGCATCCCATTGTTTT	300
C S E Y F K E M F S K N P C K H P I V F	71
CATGAAGGATGTCCTCAACTAAGGACATGGAGGCCTTGCTGGACTTCATGTACAAGGGTGA	360
M K D V S T K D M E A L L D F M Y K G E	91
GGTCCATGTACCACAAAGCGAGTTGGGTTTCATTGCTGCGTACAGCTGAAGGGCTTCAGGT	420
V H V P Q S E L G S L L R T A E G L Q V	111
AAAAGGCCTTGCTGTACCTGATGACTCTCCTCGTGGTTCTCTACCACCCCTATTGTGCC	480

```

K G L A V P D D S P R G S S T T P I V P 131
TTCTGCCTCGTCCGTCACCTCCGCCAGTCTTATGGCTCCAATGCATATGCG 540
S A S S V P R S P P P S L M A P M H M R 151
GGGTAAACGCAAAAGGCCACCAGAATCGGCTAAAAAGGATGACCCTCCAAAGTTGACTTT 600
G K R K R P P E S A K K D D P P K L T L 171
ACGTCTGACCTTGGACCCCCGGCCACCAACCGCTCACGCATGAGGAACAGACCATCAGG 660
R P D L G P P A T N R S R M R N R P S G 191
CATGCCAGAACTGAAGAGAATTAAGAGAGAGGAACATAGTGCGGCAAATGTGGGCACTAT 720
M P E L K R I K R E E H S A A N V G T I 211
TGACCTGGAGAGGTTCCAGGATCTCCAAGTCCAACACCAAGTAGTCACAACAGCGATGA 780
E P G E V P G S P S P T P S S H N S D E 231
ACAGTCACAGAACCTTGGCCATAAGATCAAGACCCGAAAGATCAGAATACTCTAAAGAAGA 840
Q S Q N L A H K I K T E R S E Y S K E E 251
AGCAGAAGACCTGGATGAGGATGAAGGGGTGGCAGGAGAAGTAATGTCTGGGGAAGAAGA 900
A E D L D E D E G V A G E V M S G E E E 271
GCAGGAACAAGAACCAGAAGAGGAAGAAGAGGAAGAAGAGGAAGAAGGAGCATT 960
Q E Q E P E E E E E E E E E E E G A L 291
AGGGGAAGGGGAAGGCCTCTCCACGGTGTCTCTCAGATGTTGAGGATGGCTATGAACA 1020
G E G E G L S H G V L S D V E D G Y E Q 311
ATCTAACTCTTCCCTTCCCAATTCTGACATATCCACAACGGAAGTCTACAGGTTGATTT 1080
S N S S L P N S D I S T T E L L Q V D L 331
GAGTGAGGACGGGACACAGTTTCATAATCGGTCCCTGGTGGCTTTGGAGATATGATGTCAAG 1140
S E D G T Q F I I G P G G F G D M M S R 351
AACTTCGTCACTAGCAGGAGATGATGAGAGAAAATGGTGACAAAAGAGCAGAAGAAGCCATT 1200
T S S L A G D D E R N G D K E Q K K P F 371
TGTTTGTCTCTCTGTGGCAGTCATTTACACGTCGTGACAACCTTGCCAACCATATCAA 1260
V C P L C G Q S F T R R D N L A N H I K 391
GACCACACCGGTGACCGTCCGTTTATGTGCCAGTACTGCCACAAGTGCTTCTCAAGGAA 1320
T H T G D R P F M T C Q Y C H K C F S R K 411
GGACTACTTGAAGCAGCATGAACGCATCCACACTGGAGAGAAGCCCTACCCCTGTGACAT 1380
D Y L K Q H E R I H T G E K P Y P C D I 431
CTGTGGTGTGTCATTTTACCAGGAAAAGGAGGATTGACAGACCACATGCGCTGTCAATCTGA 1440
C G R A F T R K G G L T D H M R C H S D 451
CTTCCGAGCCTTTTTCTGTGAAACATGTGGCAAGAGCTTCAAGCAAAAATGTGGTTTTGCG 1500
F R A F S C E T C G K S F K Q K C G L R 471
CTTCCATAAGAGGAATTATAACATTAACTGCCATAAAGATCTCCAACACTTAATTCAC 1560
F H K R N Y K H * 480
TGTTCCATTTATGAGGCGGATATGGATAGCCTGTCTCTCAGTTAGTTGGATGTGGTCCCT 1620
TTAAAAATATGCCAGATAAAGGGCTAATTTATGCCCTGTACTAAGTTAAGTCGTGCCAT 1680
TTCTTTTATGTTGAGCACCTAATTTCTGTGTTTCAGATAGTCAATTTTACCCTGAGCTTTG 1740
TCTATGGCCCTGGCCAGATGTATATTTTGGGTATATGATTATGGTTAGTGAAATATCACA 1800
ACTTGTATATTGCTGCTCACATACAGGGAACCTTGTGTAAAATTTGATTTATGTTTTGACTT 1860
CAACAGGCTTAATGTATGGCAAAGGTTTTGCAAAAATGGAAAATGACTTTTAAATGTTAGA 1920
CTAATCTCAGGTAAGCTGTATTAATAACAGTGCTTACCTTGGTGGAGTCATTACCTAAAA 1980
TTATGCAATCATAATATCAGTTTTTAAAAATATACTTTATATTTCTTACTACTTTTGTATTT 2040
TCTTCATCTTTTATATATATATATAATAATGTTTAAAAATCAAATTTATGACATATTGCA 2100
GACCTCCTAAACTTGGTCGTATGTTTCTTGTGTATTTATGACTCGCACAGAAAAGAAATTTG 2160
TATGACACCTTTTTTTTTTTCATGTTTGATACTCTCTCTCATCTGTAACCTACACTTTAGGTG 2220
CTCTTTGTGGTATGTTGCACTCCTTGAGTGCTGTTTTCTTCTGCTTTTATAAGTTAAGA 2280
TTAGATGCACCAGTATTTATTTAATTATGAAAATAACCTTTTGTAAAAAATAAAAAAAAAAC 2340
AATAAGATTATGTTATAAATAATATATAATTAAGAAAATAAAGAAATATGACACCTAAAAA 2400
AAAAAAAAAAAAAAAAAAAAAAAAA 2422

```

Figure 3.16 The full length cDNA and deduced amino acid sequences of the short form of *P. monodon Br-cZl* (*PmBr-cZl-s*). The start and stop codons are illustrated in boldface. The poly A additional signal site is underlined. The BTB domain is highlighted.

Figure 3.17 The full length cDNA and deduced amino acid sequences of the long form of *P. monodon Br-cZ1* (*PmBr-cZ1-l*). The start and stop codons are illustrated in boldface. The poly A additional signal site is underlined. The BTB domain is highlighted.

Further analysis of the protein sequence, with NetPhos 2.0 (<http://www.cbs.dtu.dk/services/NetPhos/>) shows multiple high scoring (score > 0.8) sites for possible phosphorylation at 6 threonine, 3 tyrosine and 29 or 28 serine side chains within the respective deduced proteins.

Unlike *PmFAMeT*, the indel within the coding region was not observed in different isoforms of the *PmBr-cZ1* gene but sequence polymorphism was found suggesting allelic variation of this gene (Fig. 3.18).

```

Br C Z1-1      MEEGYLALRWNNHNTIFTKILTLREQEAYVDVSLACAGRLYP AHKFVLSTCSEYFKEMF
Br C Z1-s      MEEGYLALRWNNHNTIFTKILTLREQEAYVDVSLACAGRLYP AHKFVLSTCSEYFKEMF
*****
Br C Z1-1      SKNPCKHPIVFMKDVSTKDMEALLDFMYKGEVHVPQSELGSLLR TAEGLQVKGLAVPDDS
Br C Z1-s      SKNPCKHPIVFMKDVSTKDMEALLDFMYKGEVHVPQSELGSLLR TAEGLQVKGLAVPDDS
*****
Br C Z1-1      PRGSSTTPIVPSASSVPRSPPPSLMAPMHMRGKRKRPPESA KDDPPKLTLRPDLGPPAT
Br C Z1-s      PRGSSTTPIVPSASSVPRSPPPSLMAPMHMRGKRKRPPESA KDDPPKLTLRPDLGPPAT
*****
Br C Z1-1      NRSRMRNRPPGMPELKR IKREERNAANVTIEPGEVPGSP SPTPSSHNSDEQSQNLAHKI
Br C Z1-s      NRSRMRNRPPGMPELKR IKREEHSAANVTIEPGEVPGSP SPTPSSHNSDEQSQNLAHKI
*****
Br C Z1-1      KTERSEYSKEEAEDLDEDEGVAGEVMSGEEEQEQEP EEEEEEEEEEEEGALGEGEGLSH
Br C Z1-s      KTERSEYSKEEAEDLDEDEGVAGEVMSGEEEQEQEP EEEEEEEEEEEEGALGEGEGLSH
*****
Br C Z1-1      GVLSDVEDGYEQSNSSLPNSDISTELLQVDLSE DGTQFIIIGPGGFGDMM SRTSSLAGDD
Br C Z1-s      GVLSDVEDGYEQSNSSLPNSDISTELLQVDLSE DGTQFIIIGPGGFGDMM SRTSSLAGDD
*****
Br C Z1-1      ERNGDKEQKPFVCP LCGQSFTRRDNLNHIKTH TGD RPFMCQYCHKCF SRKDYLKQHER
Br C Z1-s      ERNGDKEQKPFVCP LCGQSFTRRDNLNHIKTH TGD RPFMCQYCHKCF SRKDYLKQHER
*****
Br C Z1-1      IHTGEKPYPCDI CGRAFTRK EGLTDHMRCHSD FRAFSCETCGK SFKQKCGR FHKRNYKH
Br C Z1-s      IHTGEKPYPCDI CGRAFTRK EGLTDHMRCHSD FRAFSCETCGK SFKQKCGR FHKRNYKH
*****

```

Figure 3.18 Pairwise alignment showing sequence polymorphism between the short and long form of *PmBr-cZ1*.

3.1.4.2 *PmBr-cZ4* genes

The partial sequences of *PmBr-cZ4* were initially obtained from EST analysis of the hemocyte cDNA library of *P. monodon*. It significantly matched *PmBr-cZ4* (*Lola-like protein*) of *Drosophila hydei* (E -value = $1e-26$; Fig 3.19).

A.

GGCGGCGTGGTGATGGACGCTCATTAATGTGTCATAATGGAGGACGGACTACTAAGCTTGAAGTGGAAAC
 AACCACAAAACACATTCTTTGAAATCCTCAGGGTATTAAGAGAAAAGGCAAATTATACAGATGCCACT
 ATTGCAGTGGATGGAAAGTTTTATCCAGTTCACAAACTGGTAATGAGCACATGCAGTGAATTTTTAGT
 GAAATTTTTGAAAAAACACCATGCAAATCACCAGTGATAGTGCTAAAAGATGTGCGCAGTCAGGACATG
 GAAGCGCTGTTGGACTATATGTACTTAGGTGAAGTTAACGTAAACCAAATGACTTAGCCTCGTTATTG
 AAGACAGCCGAATGCCTCAGAATTAAGGGCTTGGCA**GTACCTGATGAAGACACTACAAAGGTAAGGAAA**
 GCACCTCCGGATGATAGACAAGAAAGTCCGCCACCAAGAGAAAGACGAAATGAAGACAACCCCTTCCTCA
 GCACCTAGGCCAGTTTTCCCATCAGTCAATGCACCCTCTAAAACCACGACGCCATCGGTAACACCTCCA
 GTCCAGTCTGCATCGTTGCCCGGGTCCAGTCTCAGGATGGGATTCAGGACTCCTCATTAGATGTCCCG
 CCCATGGTGAAGGTAGAAATGCAAGAAGCTGACGACCCAGACGACTACAGAAAGGACAACAGTTATGAA
 GGTGGATCAGTCAACGAAGGCGACATGGGATCAGACTTTGGCGCGGAATTATCTAAAGCGGAACA

B.

Lola-like protein [Drosophila hydei]
 Length=1010

Score = 123 bits (308), Expect = 1e-26
 Identities = 56/137 (40%), Positives = 85/137 (62%), Gaps = 0/137 (0%)
 Frame = +1

Query	40	<u>EDGLLSLKWNNHKTTFEILRVLREKANYTDATIAVDGKFPVHKLVMSTCSEYFSEIFE</u>	219
		+D L+WNNH++T + L E D T+A +GKF HK+V+S CS YF+ + +	
Sbjct	3	DDQQFCLRWNNHQSTLISVFDTLLENETLVDCTLAAEGKFLKAHKVVLSACSPYFATLLQ	62
Query	220	<u>KTPCKSPVIVLKDVRSDMEALLDYMVLGEVNVNQNDLASLLKTAECLRIKGLAVPDEDT</u>	399
		+ K P+ +LKDV+ Q++ A++DYMY GEVN++Q+ L +LLK AE L+IKGL+ T	
Sbjct	63	EQYDKHPIFILKDVKYQELRAMMDYMYRGEVNISQDQLTALLKAAESLQIKGLSDNRSGT	122
Query	400	<u>TKVRKAPPDDRQESPPP</u>	450
		A +Q++P P	
Sbjct	123	GPAAAAAQQQQAPKP	139

Figure 3.19 Nucleotide sequence (A) and the BlastX result (B) of an EST significantly similar to *Br-cZA* of *Drosophila hydei*. The positions of sequences primers were illustrated in boldface and underlined.

For isolation of the full length cDNA, 3' RACE-PCR of *PmBr-cZA* was carried out and discrete amplification bands were obtained from RACE-PCR of this gene. Two fragments were found in the agarose gel. The correct fragment (long fragment) was chosen, cloned and sequenced (Fig. 3.20). The positive amplification product of approximately 1247 bp was obtained (Fig. 3.21). The amplification fragment was cloned and sequenced. Nucleotide sequences of 3'RACE-PCR fragments and the original EST were assembled.

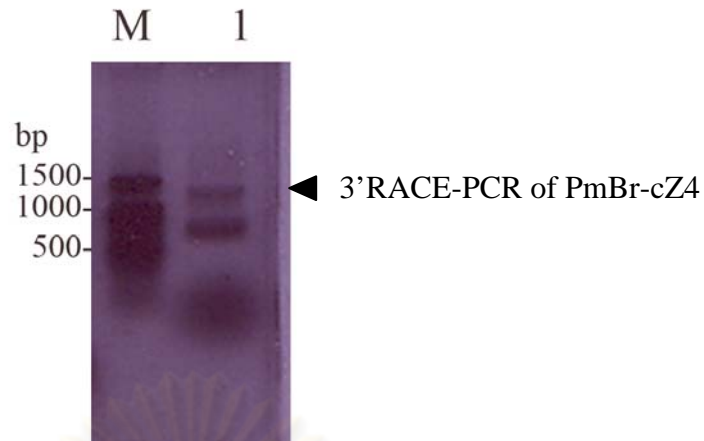


Figure 3.20 Agarose gel electrophoresis showing 3' RACE-PCR of *PmBr-cZ4* (lanes 1 and 2, respectively). Lane N = the negative control (without cDNA template). A 100 bp DNA ladder (lanes M) was used as the DNA marker.

TGACGACCCAGACGACTACAGAAAGGACAACAGTTATGAAGGTGGATCAGTCAACGA
 AGGCGAAATGGGATCAGACTTTGGCGCGGAATTATCTAAAGCGGAACACGACCCTGA
 CAGTTACGGCAGTGGATCATAACGAGGACCATCCATTCAACCTGGGGGTGACCTCCC
 TTGGGATGAGGGAGATTCAAGCAGTTTTCCACAAGAAGGCTTCTCAGGGGACTTACC
 AGCAGGCCAGCAACCTCAAGGGGACTGGGATCATGTTTCGTCCAGCTGCCCTCATTCC
 TGTGGTGGAGATACGCCAACCTGTTGCTGCAAGCACACCCACAAGCATCGCTCAGCT
 AATGACTGGTGCCTGTCCGAAGACTGCTGCTATAACCTATGGGCCAGCTAGTGGGGC
 CTTCACTCCCTACACGGCCTCAACCTCCCCAAGGGGCAGTACCCAGACTTGGCCCA
 GGTGGCACCTGCCGACAAGCAGTCTTTTATGTGCCCCGTGTGTGGGAAACAGTTTGG
 GCAGCCCTACAACCTCCGCCGCATCTGACCACCCACACGGGAGAGAGACCTTACCG
 TTGCCCCACTGTAATTATGCCGCCTCTCAGAATGTCCACCTGGAGAAGCACATCCG
 ACGCATACTTGAACAATGGCCAGAATGAAACACCCACTGGGCCAGCGGTCACTTG
 GGCCCCTGCAGCCACAGCTGTAACTCCT**TAA**TAAATTCTCATATCTGCACATCATGA
 TAAGCCCTGTGATGAAAAAGTGATAAAATACATATATCAATATTTTCGTTATTACTC
 AGATGGTCAGTGTTTTTTCTATCATATTTAGAGTTGTCTATGAATATTCAGAACAGA
 ATACAATTTATAGTAAAACCTTCCTTTTATATCATATCTATTTTCATATACTACTTTTT
 ATATACAATGATGCAGTATACAGAGGCCTTTGATTATTTTCTAAAAAGTATTTTGGT
 ATAAGGATAGTGAAAGTTATTTTACAAACATTATTCACCCAACAGTCGGGTGGTCAT
 CCGAGAGATTAGTTCAAATGGCGACAAAGCCAAGAACTATAATTATATCCGAGAGTC
 TTCTTTAGGATACTAGCTCTTACACATGAAAACCATAGCAAAGCACTTACATGAATA
 CATTTTATAAGAGGGCAATATCTCTTTTTTTTTTCATAGGTATCTTACAGTATTTGCA
 GAGTTGTGAAAATACAACCAGAAAAAAAAAAAAAAAAAAAAAAAAAAAAAAAAAAAAA

Figure 3.21 Nucleotide sequence of 3'UTR of *PmBr-cZ4* generated by the secondary 3' RACE-PCR. The positions of sequencing primers are illustrated in boldface and underlined.

The full length cDNA of *PmBr-cZ4* was successfully characterized. The full length cDNA of *PmBr-cZ4* is 1896 bp long composing of an ORF of 1332 bp encoding a polypeptide of 443 amino acids (Fig. 3.22). The predict protein was a theoretical *pI* and *Mw* of *PmBr-cZ4* were 5.16 and 47.87 kDa, respectively. The predicted *PmBr-cZ4* protein composted of one BTB domain at positions 31 and 126 (*E*-value = 4.02e-20) and two ZnF C2H2 domains. Sequence alignment between the BTB domain of *PmBr-cZ1* and *PmBr-cZ4* suggested that this functional domain is conserved across the protein family (Fig. 3.23).

A.

```

GGCGGCGTGATGGACGCTCATTAATGTGTCATAATGGAGGACGGACTACTAAGCTTG      60
      M E D G L L S L      8
AAGTGGAAACAACCACAAAACCACATTCCTTTGAAATCCTCAGGGTATTAAGAGAAAAGGCA 120
  K W N N H K T T F F E I L R V L R E K A      28
AATTATACAGATGCCACTATTGCAGTGGATGGAAAGTTTTATCCAGTTCACAACTGGTA 180
  N Y T D A T I A V D G K F Y P V H K L V      48
ATGAGCACATGCAGTGAGTATTTTAGTGAAATTTTTGAAAAAACACCATGCAAATCACCA 240
  M S T C S E Y F S E I F E K T P C K S P      68
GTGATAGTGCTAAAAGATGTGCGCAGTCAGGACATGGAAGCGCTGTTGGACTATATGTAC 300
  V I V L K D V R S Q D M E A L L D Y M Y      88
TTAGGTGAAGTTAACGTAAACCAAAATGACTTAGCCTCGTTATTGAAGACAGCCGAATGC 360
  L G E V N V N Q N D L A S L L K T A E C      108
CTCAGAATTAAGGGCTTGGCAGTACCTGATGAAGACACTACAAAGGTAAGGAAAGCACCT 420
  L R I K G L A V P D E D T T K V R K A P      128
CCGGATGATAGACAAGAAAAGTCCGCCACCAAGAGAAAGACGAAATGAAGACAACCCCTTCC 480
  P D D R Q E S P P P K R R R N E D N P S      148
TCAGACCTAGGCCAGTTTCCCATCAGTCAATGCACCCCTCTAAAACCACGACGCCATCG 540
  S A P R P V S P S V N A P S K T T T P S      168
GTAACACTCCAGTCCAGTCTGCATCGTTGCCCGTCCAGTCTCAGGATGGATTCAG 600
  V T P P V Q S A S L P G S Q S Q D G I Q      188
GACTCCTCATTAGATGTCCC GCCCATGGTGAAGGTAGAAATGCAAGAAGCTGACGACCCA 660
  D S S L D V P P M V K V E M Q E A D D P      208
GACGACTACAGAAAAGACAACAGTTATGAAGGTGGATCAGTCAACGAAGGCGAAATGGGA 720
  D D Y R K D N S Y E G G S V N E G E M G      228
TCAGACTTTGGCGGGAATTATCTAAAGCGGAACACGACCCCTGACAGTTACGGCAGTGGA 780
  S D F G A E L S K A E H D P D S Y G S G      248
TCATACGCAGGACCATCCATTCAACCTGGGGGTGACCTCCCTTGGGATGAGGGAGATTCA 840
  S Y A G P S I Q P G G D L P W D E G D S      268
AGCAGTTTTCCACAAGAAGGCTTCTCAGGGGACTTACCAGCAGGCCAGCAACCTCAAGGG 900
  S S F P Q E G F S G D L P A G Q Q P Q G      288
GACTGGGATCATGTTTCGTCCAGCTGCCCTCATTCCTGTGGTGGAGATACGCCAACCTGTT 960
  D W D H V R P A A L I P V V E I R Q P V      308
GCTGCAAGCACACCCACAAGCATCGCTCAGCTAATGACTGGTGCCTGTCCGAAGACTGCT 1020
  A A S T P T S I A Q L M T G A C P K T A      328
GCTATACCTATGGGCCAGCTAGTGGGGCTTCACTCCCTACACGGCCTCAACCTCCCCA 1080
  A I P M G P A S G A F T P Y T A S T S P      348
AGGGGCAGTACCCAGACTTGGCCAGGTGGCACCTGCCGACAAGCAGTCTTTTATGTGC 1140
  R G S T P D L A Q V A P A D K Q S F M C      368
CCCGTGTGTGGGAAACAGTTTGGGCAGCCCTACAACCTCCGCCGCATCTGACCACCCAC 1200
  P V C G K Q F G Q P Y N L R R H L T T H      388
ACGGGAGAGAGACCTTACCGTTGCCCCACTGTAATTATGCCGCCTCTCAGAATGTCCAC 1260
  T G E R P Y R C P H C N Y A A S Q N V H      408
CTGGAGAAGCACATCCGACGCATACACTTGAACAATGGCCAGAATGAAACACCCACTGGG 1320

```

```

L E K H I R R I H L N N G Q N E T P T G 428
CCAGCGGTCACCTGGGCCCCCTGCAGCCACAGCTGTAACCTCTTAATAAATTCATATCT 1380
P A V T W A P A A T A V T P * 443
GCACATCATGATAAGCCCTGTGATGAAAAAAGTGATAAAAATACATATATCAATATTTTCGT 1440
TATTACTCAGATGGTCAGTGTTTTTTCTATCATATTTAGAGTTGTCTATGAATATTCAGA 1500
ACAGAATACAATTTATAGTAAAACTTCCTTTTATATCATATCTATTTTCATATACTACTTT 1560
TTATATAACAATGATGCAGTATACAGAGGCCCTTTGATTATTTTCTAAAAAGTATTTTGGTA 1620
TAAGGATAGTGAAAGTTATTTTACAAACATTATTCACCCAACAGTCGGGTGGTCATCCGA 1680
GAGATTAGTTCAAATGGCGACAAAGCCAAGAACTATAATTATATCCGAGAGTCTTCTTTA 1740
GGATACTAGCTCTTACACATGAAAACCATAGCAAAGCACTTACATGAATACATTTTATAA 1800
GAGGGCAATATCTCTTTTTTTTTCATAGGTATCTTACAGTATTTGCAGAGTTGTGAAAAT 1860
ACAACCAGAAAAAATTTTTTTTTTTCATAGGTATCTTACAGTATTTGCAGAGTTGTGAAAAT 1896

```

Figure 3.22 The full length cDNA and deduced amino acid sequences of *PmBr-cZ4*. The start and stop codons are illustrated in boldface and underlined. The poly A additional signal site are underlined. The BTB domain is highlighted.

```

Br-CZ11      VDVSLACAGRLYP AHKFVLSTCSEYFKEMFSKNPCKHP IVFMKDVSTKDMEALLDFMYKG
Br-CZ1s     VDVSLACAGRLYP AHKFVLSTCSEYFKEMFSKNPCKHP IVFMKDVSTKDMEALLDFMYKG
Br-CZ4      TDAIIVDVGK FYPVHKLVMSTCSEYFSEIFEKTPCKSPVIVLKD VRSQDMEALLDYMYLG
           . * . : *   * : * * . * : * : * * * * * * . * : * . * * * * * : : * * * * * : * * * * * * * *
Br-CZ11      EVHVPQSELG SLLR TAEGLQVKG LAVPDDSPRGSST
Br-CZ1s     EVHVPQSELG SLLR TAEGLQVKG LAVPDDSPRGSST
Br-CZ4      EVNVNQNDL ASLLK TAECLRIKGLAVPDEDTTKVRK
           * * : * . * : * . * * * * * * * * : * * * * * * : . . .

```

Figure 3.23 Sequence alignments of the BTB domain of *PmBr-cZ1-s*, *PmBr-cZ1-l* and *PmBr-cZ4*.

Further analysis of the protein sequence, with NetPhos 2.0 (<http://www.cbs.dtu.dk/services/NetPhos/>), for potential posttranslational modifications shows multiple high scoring (score > 0.8) sites for possible phosphorylation at 7 threonine, 4 tyrosine and 18 serine side chains within the deduced *PmBr-cZ4* proteins, respectively.

3.2 Characterization of the genomic organization *PmCOMT* by using Genome Walking Technique

Genomic organization of *PmCOMT* has not been reported in any crustacean. Genome walking was carried out and the resulting fragment of approximately 200 bp obtained from the *Dra*-I mini-library was cloned and sequenced (Fig. 3.24). In addition, nucleotide sequences of the amplification product from overlapping PCR was also characterized (Fig. 3.25).

The genomic sequence of *PmCOMT* deduced from nucleotide sequences of the genome walking and overlapping amplification clones spanned 1470 bp in length and contained 3 exons (194, 111 and 361 bp) and 2 introns (143 and 147 bp). The GC content of exons (46-54%) was greater than that of introns (33%), reflecting a greater thermal stability of the coding regions than that of the noncoding regions.

A



B

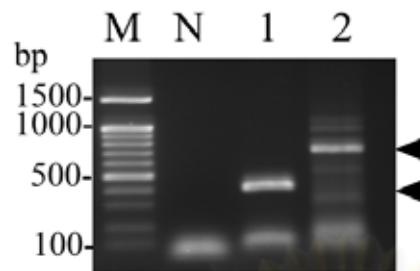
```

ACTATAGGGCACGCGTGGTCGACGGCCCGGGCAGGTAAAACATAGAGTCACGCCGTCACCAATTTTCAG
GAAGGAAATATTGATTCTCTGGTCATCTCTCAGTTTTTCGTTAATTTTCCTAATAGCCACTGTGCCAGG
GGTTTGATCAGTGGGGTCAATCACAGCTCCATCCCAAAGTGTGTTGTCGAAAGCGATGACTCCACCAGA
GCG

```

Figure 3.24 (A) Agarose gel electrophoresis showing the amplification products of the 5'UTR of *PmCOMT* generated by the secondary 5' genome walking analysis against the template from *Alu* I, *Dra* I, *Hae* III *Stu* I, and *Rsa* I mini-libraries (lanes 1-4). Lanes M and N is a 100 bp DNA ladder marker and the negative control (without genomic DNA template), respectively. (B) The amplification product obtained from *Dra* I mini-library template was cloned and sequenced. The positions of sequencing primers are illustrated in boldface and underlined.

A.



B.

AGCACCGTAGAGCGGCGATGTTGGGGGCACCTGAGGTTCTGCAGCTCAATGCCAACATAATGCAGGCTA
 TCGGGGCAAAGAAAGTGAGTTTAGTCATATGATGGTATTTAAAGACCAACTGGATATATGTGCTTGTTT
 TAGAATATGGCGTTCTATGCATTTTTAAGCATTTTGCTATTTCCCTCACAGTCATGTATTGAGGGTTGTT
 CTGTATGATTATTTAACAGGTACTAGACATTTGGGGTGTTCCACAGGCGCCAGTTCACACTCTCTGCTGCTCT
 GGCACTGCCTCCGAATGGCAAGGTCTACGCCCTTGACATAAGTGAAGAGTCTGCCAACATAGGTATTAA
 GACTATCAGAGCAGATCAGATGAATTATGCACATATTCATGTATAGATAAATGAAATAGATAGTGACTCA
 AAATGTCTCATAGGTACCTGTGGTACTATGAACATAACATGTTGACATTCCTAAGGAAACGAGTATTCC
 AGGCAAACCGTTCTGGGAGGAAGCTGGAGTTATCAACAAGATAAGTCTGCACATCGCTCCAGCTGCTGA
 GACTCTCCAGAAGTTCATTGACGGCGGAGAAGCTGGCACCTTCGACTATGCTTTTCATTGATGCCGACAA
 AGGGAATTATGAGCTGTACTATGAACTTTGCCTCACTCTCTTGCGCT**CTGGTGGAGTCATCGCCTTCG**

Figure 3.25 The PCR product of *PmCOMT* (lanes 1 and 2 using cDNA and genomic DNA as template, respectively). Lane N = the negative control (without cDNA template). A 100 bp DNA ladder (lanes M) was used as the DNA marker. (A) and nucleotide sequence (B) of *PmCOMT* using genomic DNA as the template. The positions of sequencing primers are illustrated in boldface and underlined.

The exon-intron boundaries of *PmCOMT* did not follow the GT/AG rule. Both introns interrupt the ORFs within the same codons (type 1 intron) (Fig. 3.26). Schematic diagram illustrating the genomic organization of *PmCOMT* is shown by Fig. 3.27.

TTGACAGGTTCTCTGAAG ATG TCTTCTCTGAAAAGTTACCATAATCCCGATCCTTTGGTGC	60
M S S L K S Y H N P D P L V Q	15
AGTATTGTGTAAATCATTTCATTGAGATTAACCGACGCGCAAAAACGACTGAATGATGTAA	120
Y C V N H S L R L T D A Q K R L N D V T	35
CTCTGCAGCACCGTAGAGCGGCGATGTTGGGGGCACCTGAGGTTCTGCAGCTCAATGCCA	180
L Q H R R A A M L G A P E V L Q L N A N	55
ACATGATGCAGGCTATCGGGGCAAAGAAAAGTGAGTTT AGT CATATGATGGTATTTAAAGA	240
M M Q A I G A K K V	65
CCA ACT GAATGTATGTGCTT GTTTT AGAATATGGCGTTCTATGCATTTTTAAGCATTTTTG	300
CAATTTCTCACAGTCATGTATTGAGGGT GTTCTGT ATGATTATTTAACAGGTACTAGA	360
L D	67
CATTGGGGTGTTCACAGGCGCCAGTTC ACTCTCTGCTGCTCTGGCACTGCCTCCGAATGG	420
I G V F T G A S S L S A A L A L P P N G	87
CAAGGTCCACGCCCTTGACATAAGTGAAGAGTTTGC CAACATAGGTATTAAGACTATCAG	480
K V H A L D I S E E F A N I G	102
AGCAGATCAGATGAATTATGCACATATTCATGTATAGATAATGAAATAGATAGTGACTCA	540
AAATGTCTCATAGGTACCTGTGGTACTATGAACATAACATGTTAACATTCCTAAGGAAAC	600
GAGTATTCCAGGAAAACCGTTCTGGGAGGAAGCTGGAGTTATCAACAAGATAAGTCTGCA	660
K P F W E E A G V I N K I S L H	118
CATCGCTCCAGCTGCTGAGACTCTCCAGAAGTTCATTGACGCGGAGAAGCTGGCACCTT	720
I A P A A E T L Q K F I D G G E A G T F	138
CGACTATGCTTTTCATTGATGCCGACAAAAGGGAATTATGAGCTGTACTATGAACTTTGCCT	780
D Y A F I D A D K G N Y E L Y Y E L C L	158
CACTCTCTTGGCGCTCTGGTGGAGTCATCGCCTTCGACAAACACACTTTGGGATGGAGCTGT	840
T L L R S G G V I A F D N T L W D G A V	178
GATTGACCCCACTGATCAAACCCCTGGCACAGTGGCTATTAGGAAAATTAACGAAAAC	900
I D P T D Q T P G T V A I R K I N E K L	198
GAGADATGACAGAGAATCAATATTTCTTCTGAAAATGGTGACGGCGTGCTGCTATG	960
R D D Q R I N I S F L K I G D G V T L C	218
TTTTAAAAA ATGA ATATTTTTTCCCCCGAAAAGGACCCCTCCTCCCAATAATAAAATTC	1020
F K K *	221
CTGGTTCCAGAAAAAGGTTAAGAACTTTAACAAGGATGGAACAATTGACCCCCCATACCA	1080
TACACCTATGAAAAGGTTTTAAAAACAATTGGCCGGCCTTTACCGGCCCTCCTGGCACGG	1140
GGGGCCAAAAACATCCTCCATTGGCCCCGAATTTACCGAAAAATCTTATTTAAAACCCCTT	1200
TTAAAACCAGGGCCTGTA ACTGGGAATGGCTGAATATGGATTTCTTTCCCCCAAAGG	1260
TCCCTGGCCAGAATTGATTCTAAATAAAAATTTGGCAACA ACTTTAAATGGAAGTTTCTC	1320
CGGTCCATTGGCACTTTGGCCAAACTACCGCAAATACTAACTTTTAATGGACCAAATGGA	1380
AATGGTAAAACACCCCCCCCCCTATATTTATCCCGAATTA AAATCCTACGTCTCGAA	1440
AAAAAAAAAAAAAAAAAAAAAAAAAAAA	1470

Fig 3.26 Nucleotide sequences illustrating organization of *PmCOMT* genes. Coding nucleotides and deduced amino acids of each exon are capitalized. Introns are italicized and illustrated with lower letters. Start and stop codons are illustrated in boldface and underlined. The catechol-*O*-methyltransferase domain is highlighted. Polyadenylation signals (AATAAA) are underlined.

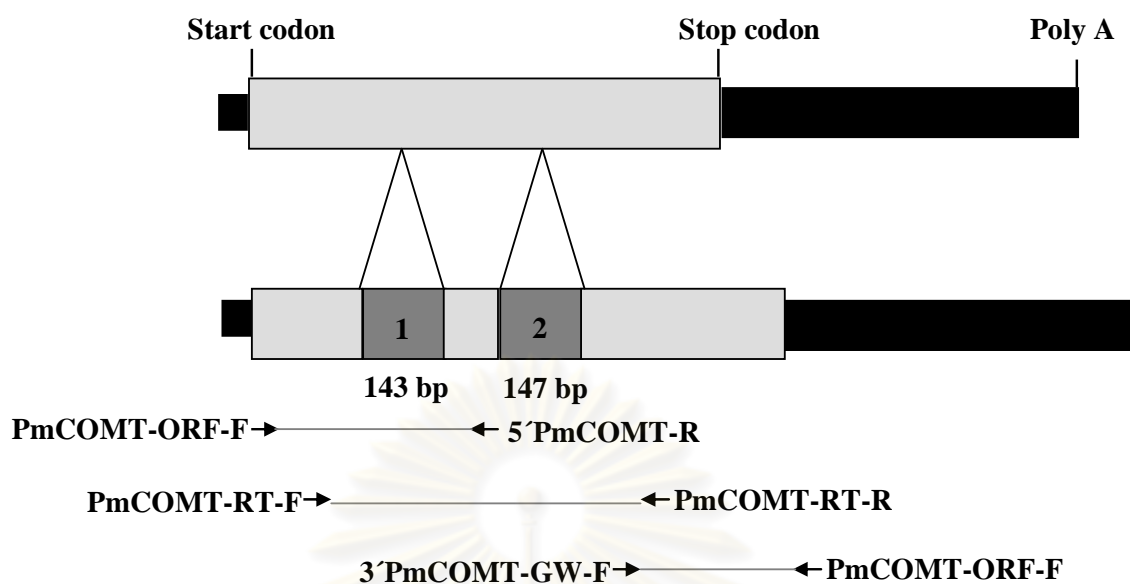


Fig. 3.27 Schematic diagrams of *PmCOMT* cDNA and gene. The complete *PmCOMT* cDNA were obtained by RACE-PCR. Genomic DNA fragments of *PmCOMT* were obtained from both genome walking analysis and overlapping PCR amplification. Noncoding regions are represented by solid bars. Introns (with numbers) are gray-shaded. Primers used for amplification of genomic *PmCOMT* and corresponding clones are illustrated.

3.3 Phylogenetic analysis

3.3.1 Phylogenetic analysis of *PmCOMT*

Phylogenetic relationships between *PmFAMeT* and *PmCOMT* and their orthologues were examined. A neighbor-joining tree clearly indicated that *COMT* and *FAMeT* from various species were allocated to be different groups of OMT. Both *PmFAMeT-l* and *PmFAMeT-s* are closely related to *FAMeT* of other decapod crustaceans and are regarded as members of crustacean *FAMeT* rather than *COMT* (Fig 3.28).

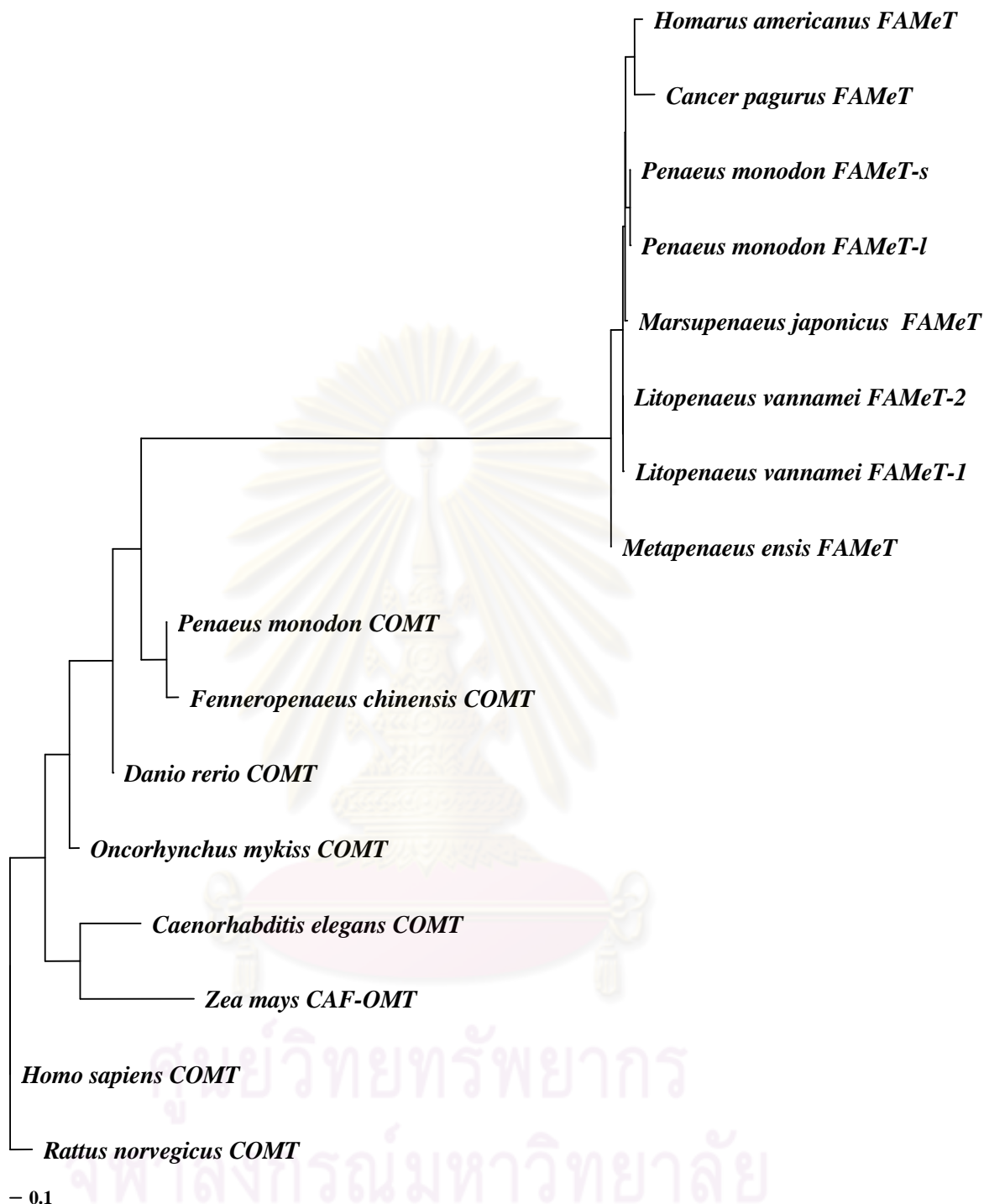


Figure 3.28 A neighbor-joining tree illustrating phylogenetic relationships of catechol-O-methyltransferase (COMT) and farnesoic-O-methyltransferase (FAMEt) of various taxa.

3.4. Determination of expression profile and tissue distribution of *PmCOMT*, *PmFAMeT*, *PmBr-cZ1* and *PmBr-cZ4* genes in *P. monodon* by RT-PCR

3.4.1 Determination of expression profile of *PmCOMT*, *PmFAMeT*, *PmBr-cZ1* and *PmBr-cZ4* genes in *P. monodon* by RT-PCR

Total RNA were extracts from ovaries or testes of 4-month-old juveniles and wild broodstock of male and female *P. monodon* ($N = 4$ for each group). DNase I-treated total RNA of each specimen was reverse-transcribed. RT-PCR was carried out.

The end-point PCR revealed greater expression levels of *PmCOMT* (Figs. 3.29-3.30 and Table 3.1) and *PmBr-cZ4* (Figs. 3.35-3.36 and Table 3.4) genes in ovaries ($N = 4$) than testes in both juvenile and broodstock of *P. monodon* ($P < 0.05$). Interestingly, the expression levels in ovaries of juvenile were greater than that in ovaries of broodstock ($P < 0.05$).

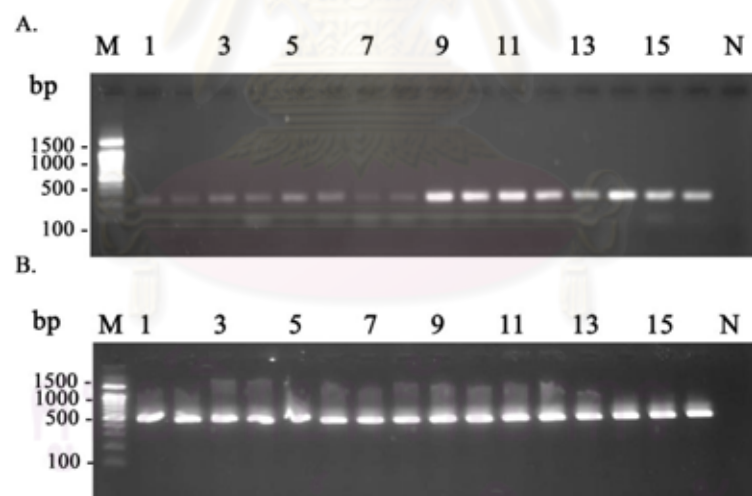
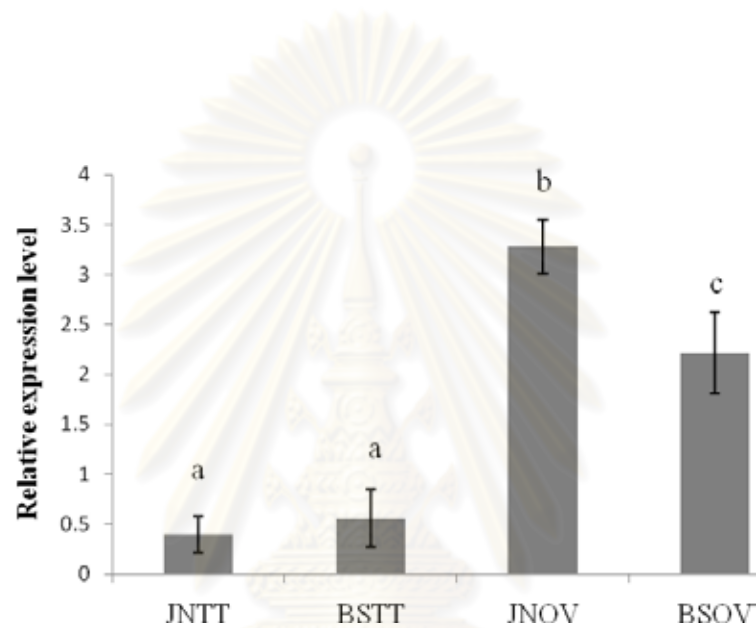


Figure 3.29 Agarose gel electrophoresis showing RT-PCR of *PmCOMT* using the first strand cDNA from ovaries of cultured juveniles (lanes 1-4, A) and wild broodstock (lanes 5-8, A) and testes of cultured juveniles (lanes 9-12, A) and wild broodstock (lanes 13-16, A) *P. monodon*. *EF-1α* was successfully amplified from the same template (B). Lanes M and N are a 100 bp DNA marker and the negative control (without cDNA template), respectively.

Table 3.1 Relative expression level of *PmCOMT* in ovaries and testes of *P. monodon*

Stage	Relative expression level
JNTT ($N = 4$)	0.3974 ± 0.1821^a
BSTT ($N = 4$)	0.5595 ± 0.2841^a
JNOV ($N = 4$)	3.2787 ± 0.2695^b
BSOV ($N = 4$)	1.6116 ± 0.4066^c

**Figure 3.30** Histograms showing the relative expression profiles of *PmCOMT* in testes of cultured juveniles (JNTT) and wild broodstock (BSTT) and ovaries of cultured juveniles (JNOV) and wild broodstock (BSOV) of *P. monodon*.

In contrast, the expression of *PmFAMeT* was not significantly different between ovaries and testes in both juvenile and broodstock ($P > 0.05$) (Figs 3.31-3.32 and Table 3.2).

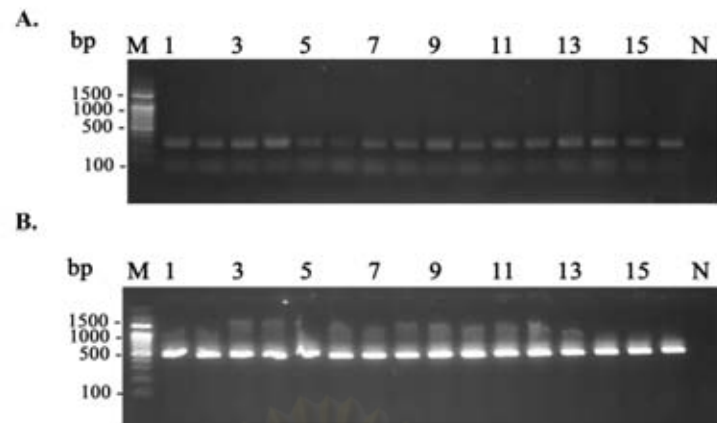


Figure 3.31 Agarose gel electrophoresis showing RT-PCR of *PmFAMeT* using the first strand cDNA from ovaries of cultured juveniles (lanes 1-4, A) and wild broodstock (lanes 5-8, A) and testes of cultured juveniles (lanes 9-12, A) and wild *P. monodon* broodstock (lanes 13-16, A). *EF-1α* was successfully amplified from the same template (lanes 1-16, B). Lanes M and N are a 100 bp DNA marker and the negative control (without cDNA template), respectively.

Table 3.2 Relative expression level of *PmFAMeT* ovaries and testes of *P. monodon*

Stage	Relative expression level
JNTT ($N = 4$)	0.2644 ± 0.0421^a
BSTT ($N = 4$)	0.2609 ± 0.0544^a
JNOV ($N = 4$)	0.2521 ± 0.0967^a
BSOV ($N = 4$)	0.2448 ± 0.0904^a

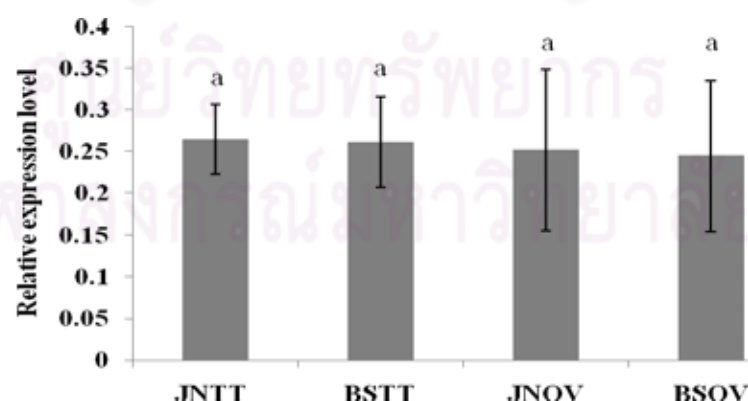


Figure 3.32 Histograms showing the relative expression profiles of *PmFAMeT* in testes of cultured juveniles (JNTT) and wild broodstock (BSTT) and ovaries of cultured juveniles (JNOV) and wild broodstock (BSOV) of *P. monodon*.

The expression profiles of *PmBr-cZ1* and *PmBr-cZ4* in ovaries of juvenile and broodstock were greater than those in testes of both stages of *P. monodon* ($P < 0.05$; Figs. 3.33-3.36 and Tables 3.3 and 3.4).

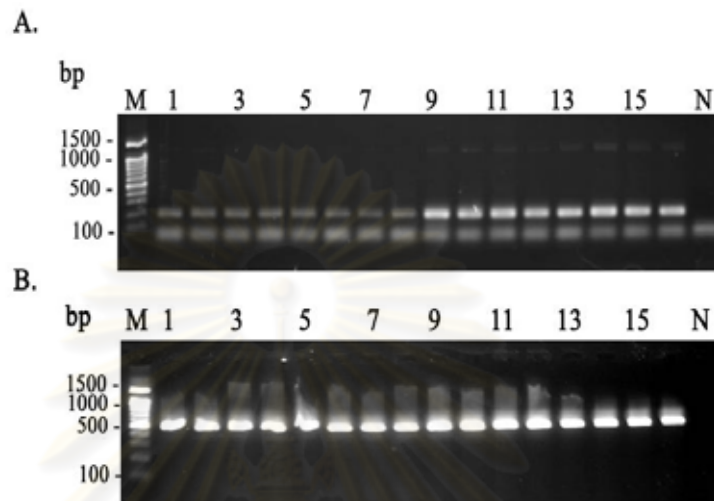


Figure 3.33 Agarose gel electrophoresis showing RT-PCR of *PmBR-cZ1* using the first strand cDNA from ovaries of cultured juveniles (lanes 1-4, A) and wild broodstock (lanes 5 - 8, A) and testes of cultured juveniles (lanes 9-12, A) and wild broodstock (lanes 13-16, A) of *P. monodon*. *EF-1α* was successfully amplified from the same template (lanes 1-16, B). Lanes M and N are a 100 bp DNA marker and the negative control (without cDNA template), respectively.

Table 3.3 Relative expression level of *PmBr-cZ1* ovaries and testes of *P. monodon*

Stage	Relative expression level
JNTT($N = 4$)	0.2876 ± 0.0711^a
BSTT($N = 4$)	0.2609 ± 0.0505^a
JNOV($N = 4$)	1.2458 ± 0.1067^b
BSOV($N = 4$)	1.0984 ± 0.1748^b

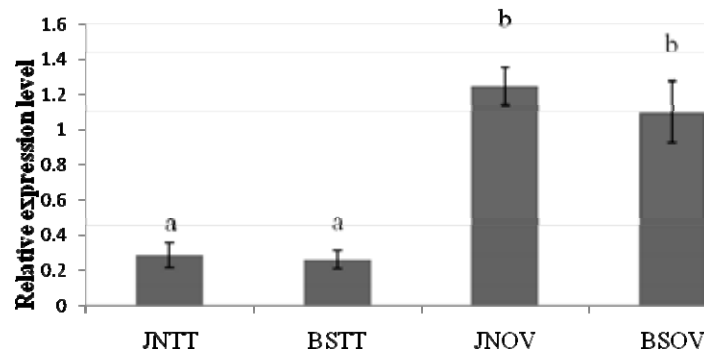


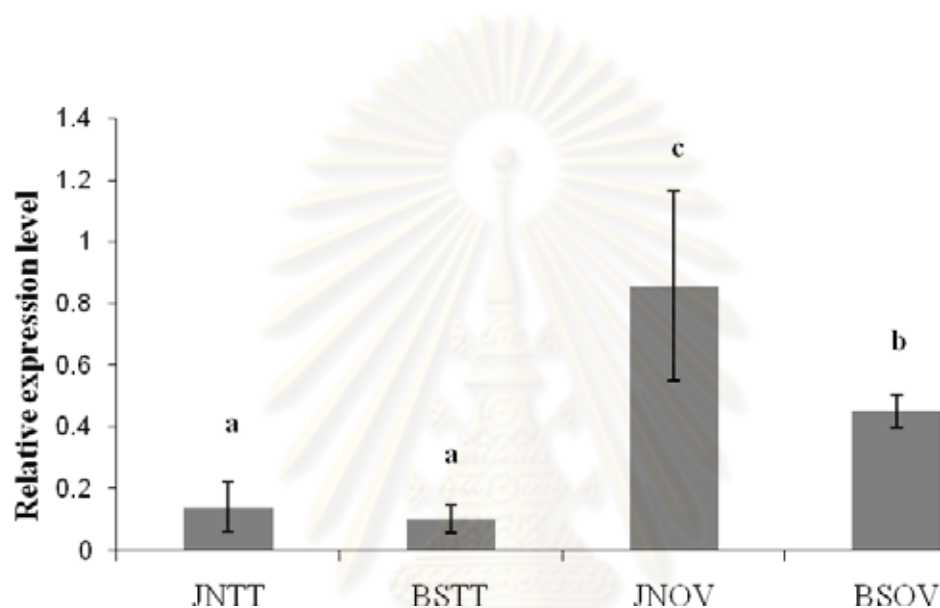
Figure 3.34 Histograms showing the relative expression profiles of *PmBr-cZl* in testes of cultured juveniles (JNTT) and wild broodstock (BSTT) and ovaries of cultured juveniles (JNOV) and wild broodstock (BSOV) of *P. monodon*.



Figure 3.35 Agarose gel electrophoresis showing RT-PCR of *PmBR-cZA* using the first strand cDNA from testes of cultured juveniles (lanes 1 - 4, A) and wild broodstock (lanes 5 - 8, A) and ovaries cultured juveniles (lanes 9 - 12, A) and wild broodstock (lanes 13 - 16, A) of *P. monodon*. *EF-1α* was successfully amplified from the same template (lanes 1-16, B). Lanes M and N are a 100 bp DNA marker and the negative control (without cDNA template), respectively.

Table 3.4 Relative expression level of *PmBr-cZ4* in ovaries and testes of *P. monodon*

Stage	Relative expression level
JNTT(<i>N</i> = 4)	0.1404 ± 0.0795 ^a
BSTT(<i>N</i> = 4)	0.1012 ± 0.0445 ^a
JNOV(<i>N</i> = 4)	0.8544 ± 0.3060 ^c
BSOV(<i>N</i> = 4)	0.4509 ± 0.0536 ^b

**Figure 3.36** Histograms showing the relative expression profiles of *PmBr-cZ4* in testes of cultured juveniles (JNTT) and wild broodstock (BSTT) and ovaries of cultured juveniles (JNOV) and wild broodstock (BSOV) of *P. monodon*.

3.4.2 Tissue distribution analysis of *PmCOMT*, *PmFAMeT*, *PmBr-cZ1* and *PmBr-cZ4* genes in *P. monodon* examined by RT-PCR

The expression of *PmCOMT*, *PmFAMeT*, *PmBr-cZ1* and *PmBr-cZ4* in ovaries and testes of 6-month-old juveniles, domesticated male and female broodstock, various tissues (heart, hemocytes, lymphoid organs, intestine, gill, pleopods, thoracic ganglion, stomach, eyestalk, hepatopancreas, ovaries and testes) of female juvenile and broodstock and testes of male juvenile and broodstock were examined using RT-PCR analysis.

3.4.2.1 *PmCOMT*

PmCOMT was constitutively expressed in all examined tissues and abundantly expressed in ovaries and intestine of female broodstock and testes of a male broodstock. Lower expression levels of *PmCOMT* were observed in, for example, hepatopancreas, stomach, thoracic ganglion, eyestalk, pleopods and epicuticle of female broodstock (Fig. 3.37).

In juveniles, *PmCOMT* was constitutively expressed in all examined tissues. It was abundantly expressed in hemocytes, hepatopancreas, stomach and thoracic ganglion of a female juvenile and testes of a male juvenile. Lower expression levels of *PmCOMT* were observed in other tissues for example, gill, heart, intestine, lymphoid organs, eyestalk and pleopods of a female juvenile (Fig. 3.38).



Figure 3.37 1.5% ethidium bromide-stained agarose gels showing results from tissue distribution analysis of *PmCOMT* (A) using the first strand cDNA of various tissues of females: HE = heart, HC = hemocytes, LO = lymphoid organs, IT = intestine, GL = gill, PL = pleopods, TG = thoracic ganglion, ST = stomach, ES = eyestalk, HP = hepatopancreas, OJ = juvenile ovaries, OJ = broodstock ovaries and males: TJ = juvenile testes, TB = broodstock testes, of *P. monodon* corresponding to lanes 1-15, respectively. *EF-1α* was successfully amplified from the same template (lanes 1-15, B). Lanes M and N are a 100 bp DNA marker and the negative control (without cDNA template), respectively.

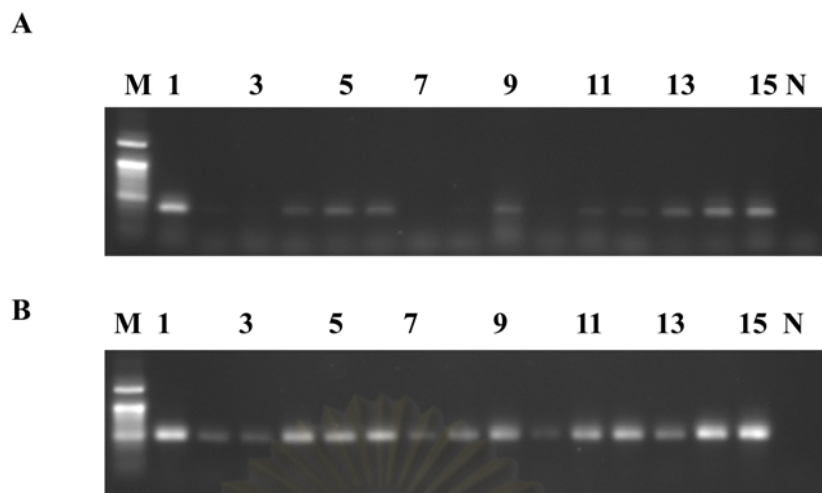


Figure 3.38 1.5% ethidium bromide-stained agarose gels showing results from tissue distribution analysis of *PmCOMT* (A) using the first strand cDNA of various tissues of female juvenile (HC = hemocytes, GL = gill, HE = heart, OJ = juvenile ovaries, HP = hepatopancreas, ST = stomach, IT = intestine, LO = lymphoid organs, TG = thoracic ganglion, ES = eyestalk, PL = pleopods) and male juvenile (TJ = juvenile testes), female broodstock (OB = broodstock ovaries) and male broodstock (TB = broodstock testes) of *P. monodon* corresponding to lanes 1-15 (A). *EF-1α* was successfully amplified from the same template (lanes 1-15, B). Lanes M and N are a 100 bp DNA marker and the negative control (without cDNA template), respectively.

3.4.2.2 *PmFAMeT*

PmFAMeT was constitutively expressed in all examined tissues of broodstock. Slightly lower expression patterns of *PmFAMeT* were observed in stomach and hemocyte of a female broodstock and testes of a male broodstock (Fig. 3.39).

In juvenile, *PmFAMeT* was expressed in all examined tissues. It was abundantly expressed in hemocytes and thoracic ganglion of a female juvenile. Lower expression levels of *PmFAMeT* were observed in other tissues for example, gill, heart, intestine, lymphoid organs and pleopods of a female broodstock and testes of male juvenile (Fig. 3.40).

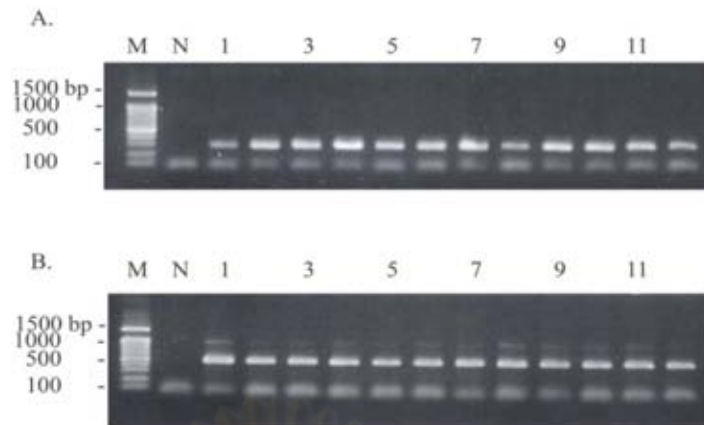


Figure 3.39 Tissue expression analysis of *PmFAMeT* (A) and *EF-1 α* (B) in various tissues of female (HE; hemocytes, gills, GL; heart, HC; ovaries, OV; lymphoid organs, LO; intestine, IT; hepatopancreas, HP; stomach, ST; thoracic ganglion, TG; eyestalk, ES, pleopods, PL; lanes 1-11) and testes (testes, TT; lane 12) of male *P. monodon* broodstock. *EF-1 α* was successfully amplified from the same template. Lanes M are a 100 bp DNA marker.



Figure 3.40 1.5% ethidium bromide-stained agarose gels showing results from tissue distribution analysis of *PmFAMeT* using the first strand cDNA of various tissues of a female juvenile (HC = hemocytes, GL = gill, HE = heart, OJ = juvenile ovaries, HP = hepatopancreas, ST = stomach, IT = intestine, LO = lymphoid organs, TG = thoracic ganglion, ES = eyestalk, PL = pleopods, male juvenile (TJ = juvenile testes), male broodstock (TB = broodsotck testes) and female broodstock (OB = broodsotck ovaries; lanes 1-15) of *P. monodon*. *EF-1 α* was successfully amplified from the same template (B). Lanes M and N are a 100 bp DNA marker and the negative control (without cDNA template), respectively.

3.4.2.3 *PmBr-cZ1*

PmBr-cZ1 was abundantly expressed in ovaries of *P. monodon* broodstock. Lower expression was observed in heart, lymphoid organs, intestine, hepatopancreas, stomach, thoracic and testes of both juvenile and broodstock (Fig. 3.41). It was abundantly expressed in hemocyte of a female juvenile. A lower expression was found in ovaries but not in other tissues of a juvenile shrimp (Fig. 3.42).

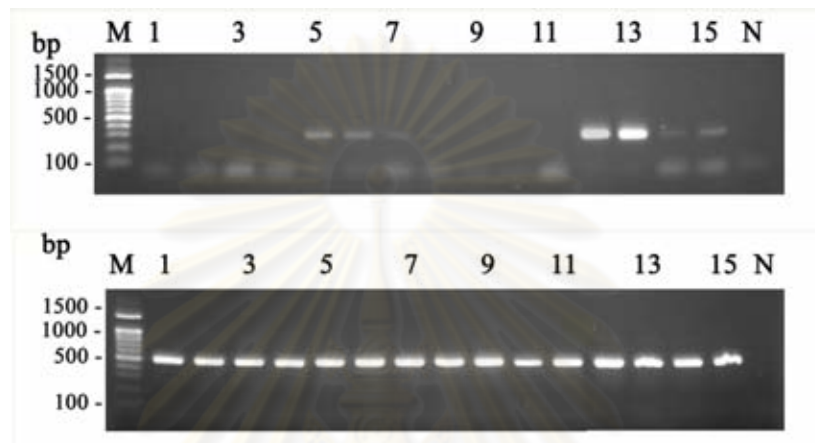


Figure 3.41 Tissue distribution analysis of *PmBr-cZ1* using the first strand cDNA of hemocytes, gills, heart, lymphoid organs, intestine, hepatopancreas, stomach, thoracic ganglia, Eyestalk, pleopods, epidermis, ovaries of juvenile, ovaries of broodstock, testes of juvenile and testes of broodstock (lanes 1 - 15) and *EF-1α* (B). Lanes M and N are a 100 bp DNA marker and the negative control (without cDNA template), respectively.

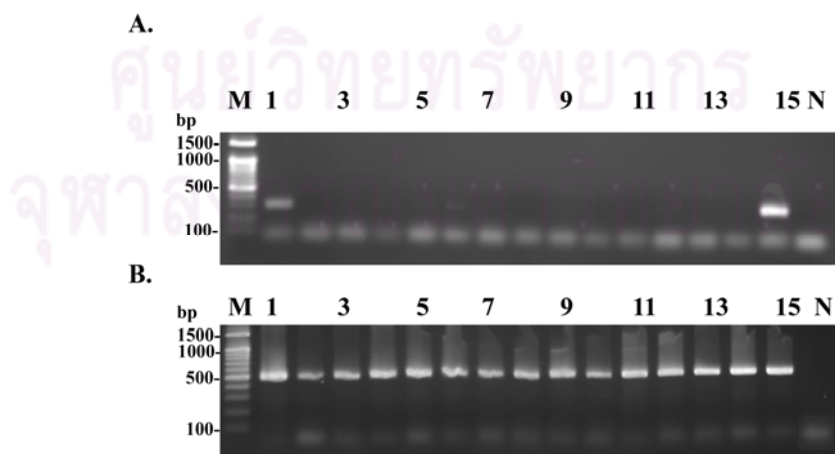


Figure 3.42 1.5% ethidium bromide-stained agarose gels showing results from tissue distribution analysis of *PmBr-cZ1* (A) using the first strand cDNA of various tissues

of female juvenile (HC = hemocytes, GL = gill, HE = heart, OJ = juvenile ovaries, HP = hepatopancreas, ST = stomach, IT = intestine, LO = lymphoid organs, TG = thoracic ganglion, ES = eyestalk, PL = pleopods, male juvenile (TJ = juvenile testes), male broodstock (TB = broodstock testes) and female broodstock (OB = broodstock ovaries) of *P. monodon*. *EF-1 α* was successfully amplified from the same template (B). Lanes M and N are a 100 bp DNA marker and the negative control (without cDNA template), respectively.

3.4.2.4 *PmBr-cZ4*

PmBr-cZ4 was abundantly expressed in ovaries of broodstock of *P. monodon* with a lower express pattern in hemocytes, gills, heart, lymphoid organs, intestine, stomach, thoracic ganglion, pleopods, antennal gland and testes of broodstock. This transcript was not expressed in hepatopancreas and eyestalk of a shrimp broodstock (Fig. 3.43). *PmBr-cZ4* was only expressed in hemocyte and ovaries of a female juvenile (Fig. 3.44)

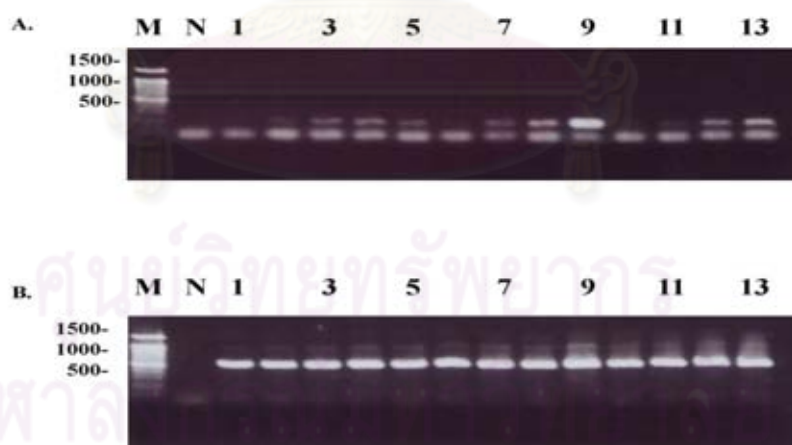


Figure 3.43 Tissue distribution analysis of *PmBr-cZ4* (A) using the first strand cDNA of hemocytes, gills, heart, lymphoid organs, intestine, hepatopancreas, stomach, thoracic ganglion, ovaries of broodstock, eyestalk, pleopods, antennal gland and testes of broodstock (lanes 1-13) and *EF-1 α* (B). Lanes M and N are a 100 bp DNA marker and the negative control (without cDNA template), respectively.



Figure 3.44 1.5% ethidium bromide-stained agarose gels showing results from tissue distribution analysis of *PmBr-cZ4(A)* using the first strand cDNA of various tissues of female juvenile (HC = hemocytes, GL = gill, HE = heart, OJ = juvenile ovaries, HP = hepatopancreas, ST = stomach, IT = intestine, LO = lymphoid organs, TG = thoracic ganglion, ES = eyestalk, PL = pleopods), male juvenile (TJ = juvenile testes), male broodstock (TB = broodstock testes) and female broodstock (OB = broodstock ovaries) of *P. monodon*. *EF-1α* was successfully amplified from the same template (B). Lanes M and N are a 100 bp DNA marker and the negative control (without cDNA template), respectively.

3.4.3 Expression levels of *PmCOMT* and *PmFAMeT* during ovarian development of wild *P. monodon* examined by semi-quantitative RT-PCR

3.4.3.1 Optimization of PCR conditions for semi-quantitative RT-PCR

Semi-quantitative RT-PCR was carried out to determine whether the expression levels of *PmCOMT*, and *PmFAMeT* were significantly different during ovarian development of *P. monodon*. In addition, this technique was also applied to evaluate the effects of dopamine (at 10^{-6} M/shrimp) and serotonin (50 ug/g body weight) administration.

To carry out semi-quantitative RT-PCR, several parameters of the amplification and PCR components required further optimization. As a result, primer and $MgCl_2$ concentrations and the number of amplification cycles were carefully

optimized. *EF-1 α* was used as the internal control. The chosen parameter for each factor was that generating the highest specificity with the relatively intense product.

The standard RT-PCR was carried out by using 100 ng of the first strand cDNA template from ovaries of juvenile *P. monodon* (approximately 15-20 g body weight) at the annealing temperature of 55 °C, 1 U of Dynazyme DNA polymerase and 0.2 μ M of each primer and various MgCl₂ concentrations for 28 cycles. After the most suitable MgCl₂ concentration was chosen. RT-PCR was carried out using an optimized MgCl₂ concentration for further optimization of primer concentration. Finally, selected primer and MgCl₂ concentrations were included for optimization of the suitable number of the amplification cycles. The number of cycles that still provided the PCR product in the exponential stage and did not reach a plateau level of amplification was chosen. The most suitable condition for amplification of *PmCOMT*, *PmFAMeT* and *EF-1 α* were showed in Table 3.5.

3.4.3.2 Differential expression of *PmCOMT* and *PmFAMeT* during ovarian development of wild *P. Monodon*

Total RNA were extracted from different stages of ovaries of wild intact and eyestalk-ablated females of *P. monodon*. After reverse transcription, RT-PCR was carried out.

Table 3.5 Optimized MgCl₂ and primer concentrations, number of amplification cycles and thermal profiles for semi-quantitative RT-PCR of *EF1- α* , *PmCOMT* and *PmFAMeT* in ovaries of *P. monodon*

Gene	MgCl ₂ (mM)	Primer con. (μ M)	No. of cycles	PCR condition
1. <i>EF-1α</i>	1.5	0.15	23	94°C for 3 min followed by optimized cycles of 94°C for 30 sec, 55°C for 45 sec and 72°C for 45 sec and 72°C for 7 min
2. <i>PmCOMT</i>	1.5	0.15	28	As described in 1.
3. <i>PmFAMeT</i>	1.5	0.15	30	As described in 1.

Results showed that the expression levels of *PmCOMT* and *PmFAMeT* were significantly increased at stages II and stages III and IV ovaries of intact broodstock, respectively ($P < 0.05$) (Fig. 3.45 and Table 3.6). In contrast, levels of both transcripts were comparable throughout the ovarian developmental stages (stages I-IV) in eyestalk ablated female broodstock ($P > 0.05$) (Figs. 3.46-3.47 and Table 3.7).

3.4.3.3 The expression profiles of *PmCOMT* and *PmFAMeT* in ovaries of *P. monodon* following dopamine and serotonin administration

Semi-quantitative RT-PCR was then applied for determining effects of neurotransmitters (serotonin and dopamine) on expression levels of *PmCOMT* and *PmFAMeT* in ovaries of juvenile *P. monodon*.

3.4.3.3.1 Dopamine administration

Results from semi-quantitative RT-PCR indicated that dopamine (10^{-6} M/shrimp) resulted in significant lower expression of *PmCOMT* in ovaries of juvenile shrimp at 24 hour post injection (hpi, $P < 0.05$; Fig. 3.48 and Table 3.7) but significant higher expression of *PmFAMeT* in ovaries of juvenile shrimp was observed at 12 and 24 hpi ($P < 0.05$) (Fig. 3.48 and Table 3.8).

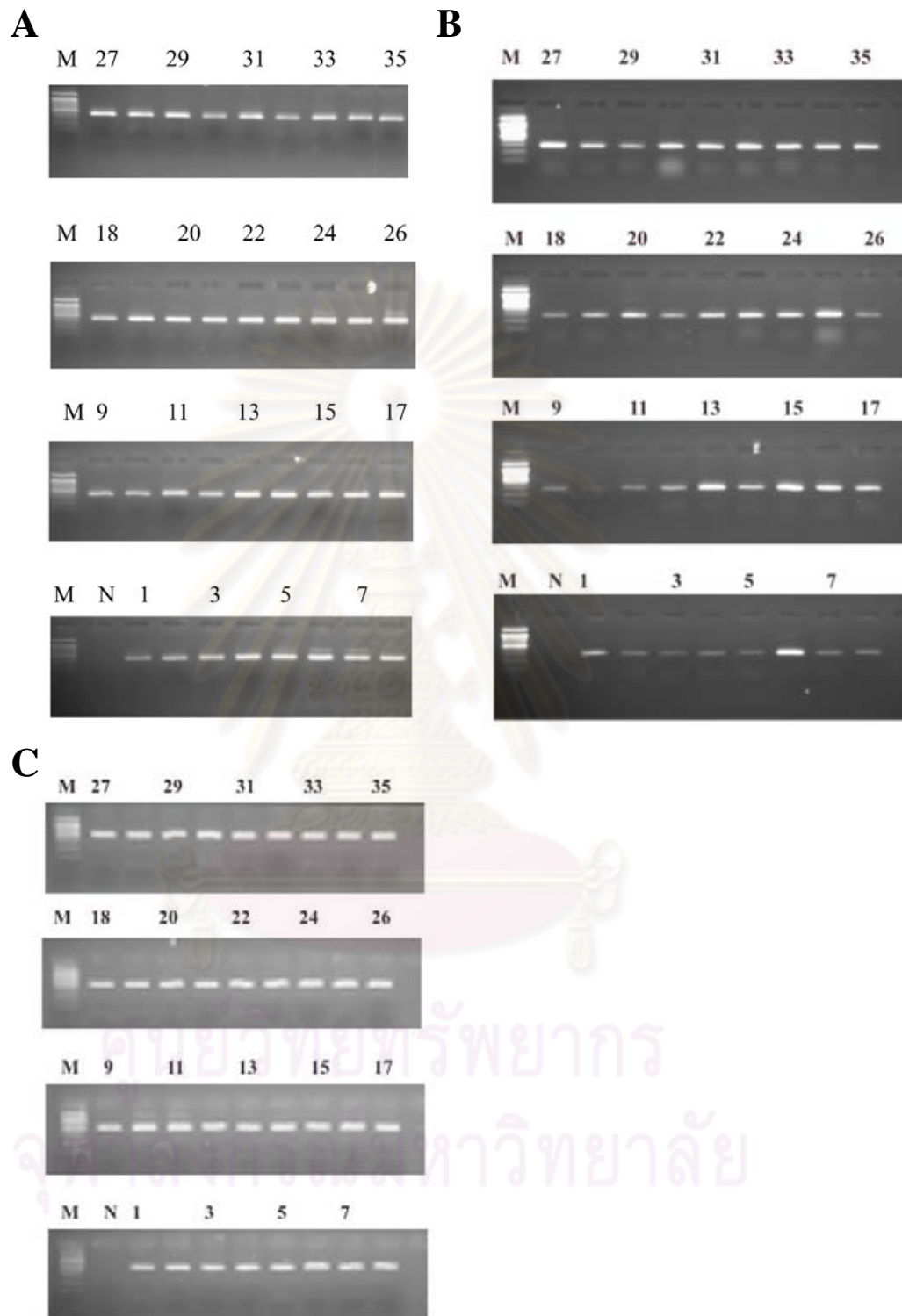


Figure 3.45 Semi-quantitative RT-PCR of *PmCOMT* (A) and *PmFAMeT* (B) and *EF-1 α* (C) in different stages of ovaries of intact *P. monodon*.

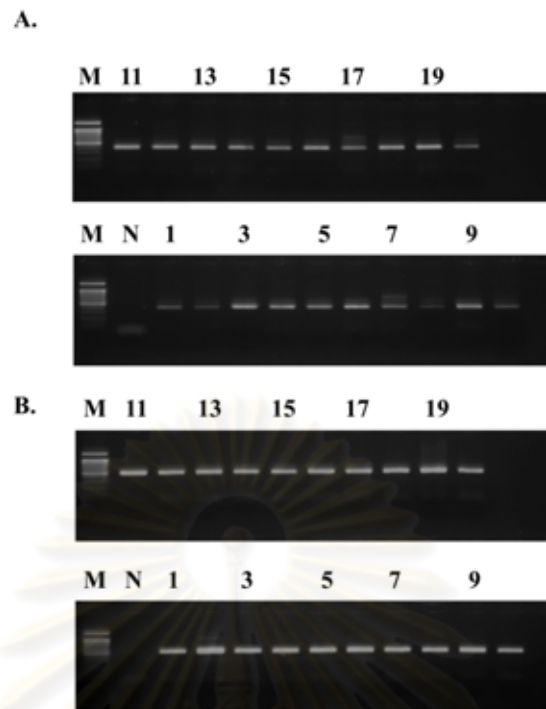


Figure 3.46 Semi-quantitative RT-PCR of *PmCOMT* (A) and *PmEF-1α* (B) in at different ovarian stages of eyestalk-ablated *P. monodon*

Table 3.6 Time course relative expression levels of *PmCOMT* and *PmFAMeT* in different ovarian stages of intact *P. monodon*

Stage	Relative expression level	
	<i>PmFAMeT</i>	<i>PmCOMT</i>
I Previtellogenetic ovaries ($N = 8$)	0.7534 ± 0.0855^a	1.3187 ± 0.0958^a
II Vitellogenetic ovaries ($N = 5$)	0.7421 ± 0.1580^a	1.1948 ± 0.0970^b
III Early cortical rod ($N = 9$)	0.8825 ± 0.0731^b	1.4069 ± 0.1830^a
IV Mature ($N = 13$)	0.9299 ± 0.0745^b	1.3712 ± 0.1248^a

Table 3.7 Time course relative expression levels of *PmCOMT* and *PmFAMeT* in different ovarian stages of eyestalk-ablated *P. monodon*

Stage	Relative expression level	
	<i>PmFAMeT</i>	<i>PmCOMT</i>
I Previtellogenetic ovaries ($N = 8$)	0.7170 ± 0.0970^a	0.7025 ± 0.1626^a
II Vitellogenetic ovaries ($N = 5$)	0.8880 ± 0.1212^a	0.7624 ± 0.0589^a
III Early cortical rod ($N = 9$)	0.7535 ± 0.1212^a	0.7501 ± 0.0972^a
IV mature ($N = 13$)	0.8541 ± 0.1772^a	0.7658 ± 0.1024^a

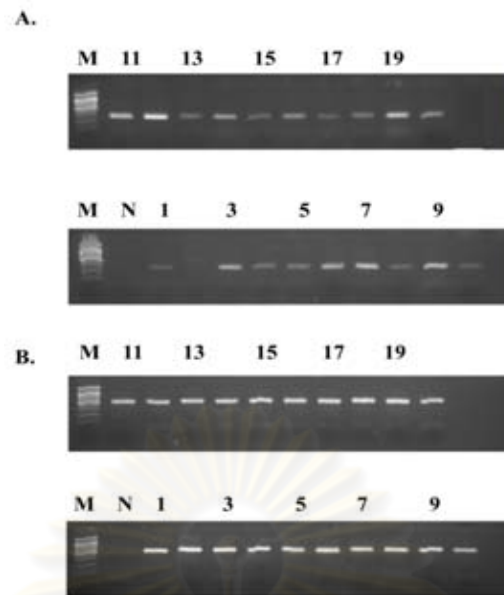


Figure 3.47 Semi-quantitative RT-PCR of *PmFAMeT* (A) and *PmEF-1α* (B) in different ovarian stages of eyestalk-broodstock *P. monodon*.

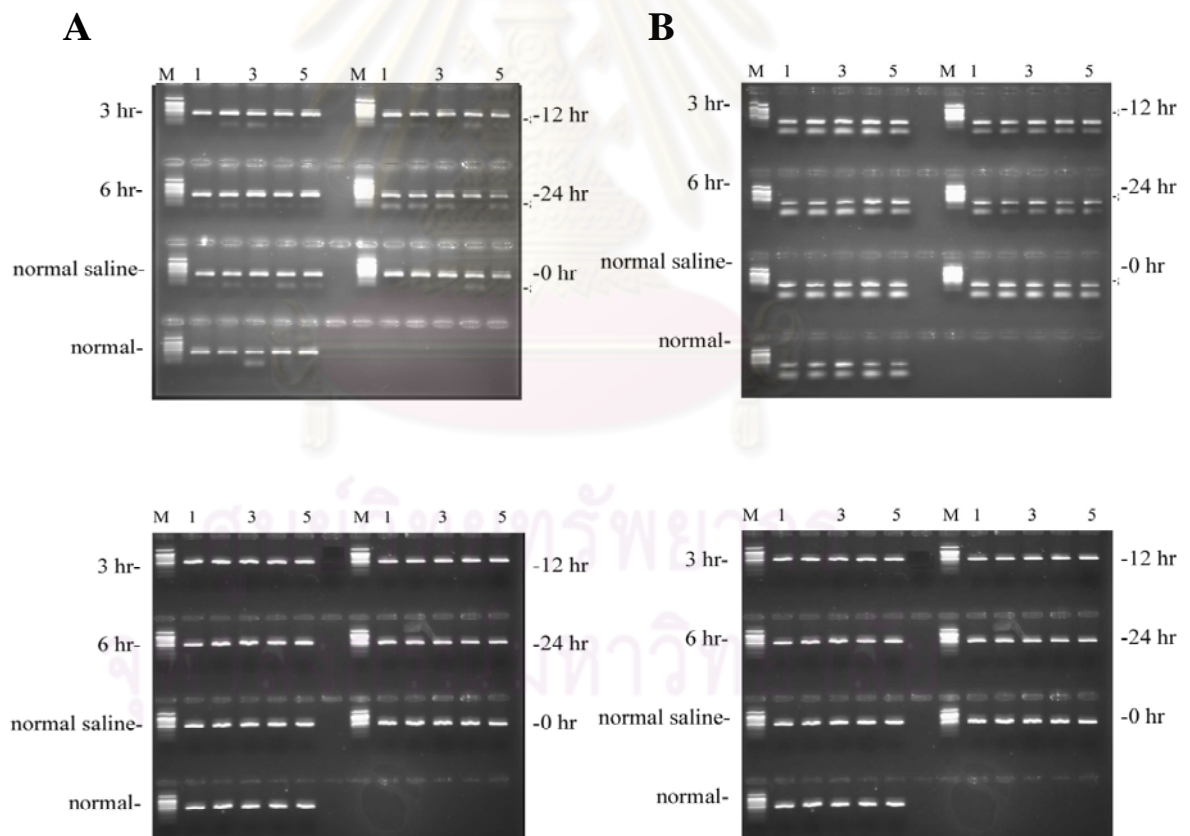


Figure 3.48 Semi-quantitative RT-PCR of *PmCOMT* (A) and *PmFAMeT* (B) of juvenile *P. monodon* treated with dopamine at 10^{-6} mole/shrimp. *EF1-α* was successfully amplified from the same template (bottom, A and B)

Table 3.8 Time course relative expression levels of *PmCOMT* and *PmFAMeT* in ovaries of *P. monodon* treated with dopamine at 10^{-6} M/shrimp

Gene	Relative expression level						
	Normal	Vehicle control	0 hpt	3 hpt	6 hpt	12 hpt	24 hpt
<i>PmCOMT</i>	0.31 ± 0.06^{ab}	0.36 ± 0.06^{abc}	0.38 ± 0.04^c	0.38 ± 0.04^c	0.37 ± 0.04^{bc}	0.39 ± 0.04^c	0.30 ± 0.04^a
<i>PmFAMeT</i>	0.54 ± 0.20^a	0.88 ± 0.13^{cd}	0.71 ± 0.13^{abc}	0.66 ± 0.17^{ab}	0.53 ± 0.14^a	0.96 ± 0.10^d	0.75 ± 0.10^{bc}

3.4.3.3.2 Serotonin administration

Results indicated that the expression of *PmFAMeT* in ovaries of juvenile *P. monodon* upon serotonin administration (50 µg/g body weight) was significantly down-regulated at 48 and 72 hpi ($P < 0.005$) (Fig. 3.49 and Table 3.9). In contrast, serotonin had no significant effects on expression of *PmCOMT* in ovaries of juvenile *P. monodon* ($P > 0.005$, Fig. 3.50 and Table 3.9).

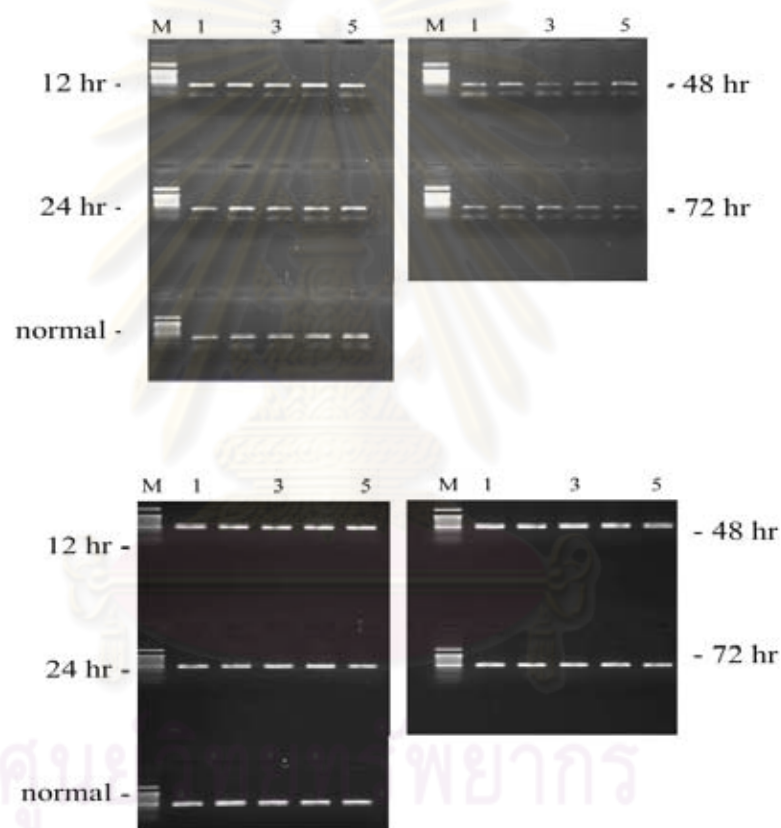


Figure 3.49 Semi-quantitative RT-PCR of *PmCOMT* (top) in ovaries of juvenile *P. monodon* treated with serotonin (50 µg/g body weight). *EF1-α* (bottom) was successfully amplified from the same template.

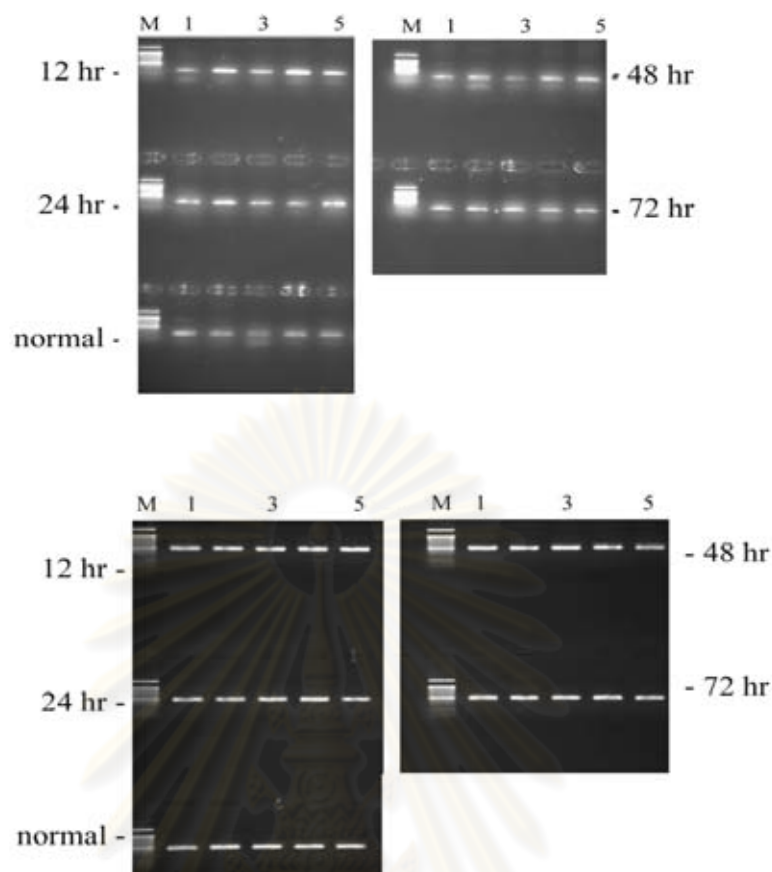


Figure 3.50 Semi-quantitative RT-PCR of *PmCOMT* (top) in ovaries of juvenile *P. monodon* treated with serotonin (50 ug/g body weight). *EF1-α* (bottom) was successfully amplified from the same template.

Table 3.9 Time-course relative expression levels of *PmCOMT* and *PmFAMeT* in ovaries of *P. monodon* juveniles treated serotonin (50 ug/g body weight)

Gene	Average of intensity of band				
	Normal saline (N=5)	12 hpt (N=5)	24 hpt (N=5)	48 hpt (N=5)	72 hpt (N=5)
<i>PmCOMT</i>	1.00 ± 0.18 ^a	0.90 ± 0.10 ^a	0.90 ± 0.07 ^a	0.83 ± 0.16 ^a	0.83 ± 0.13 ^a
<i>PmFAMeT</i>	0.17 ± 0.03 ^a	0.21 ± 0.02 ^a	0.21 ± 0.03 ^a	0.09 ± 0.05 ^b	0.09 ± 0.02 ^b

3.5 Quantitative real-time PCR analysis of *PmCOMT*, *PmFAMeT*, *PmBr-cZ1* and *PmBr-cZ4* genes in ovaries of *P. monodon*

The expression levels of *PmCOMT*, *PmFAMeT*, *PmBr-cZ1* and *PmBr-cZ4* genes in ovaries of *P. monodon* were examined by quantitative real-time PCR analysis.

The standard curve of each target gene and the control (*EF-1 α*) was constructed from the 10-fold dilutions covering 10^3 - 10^8 copy numbers of all genes except *PmFAMeT* where 10^2 - 10^8 copy numbers was used. The amplification efficiency of the target genes and the internal control are shown by Fig. 3.51

Quantitative real-time PCR was carried out in duplicate using 100 ng of the first strand cDNA template for the target genes and 1 ng of the first strand cDNA template for *EF-1 α* .

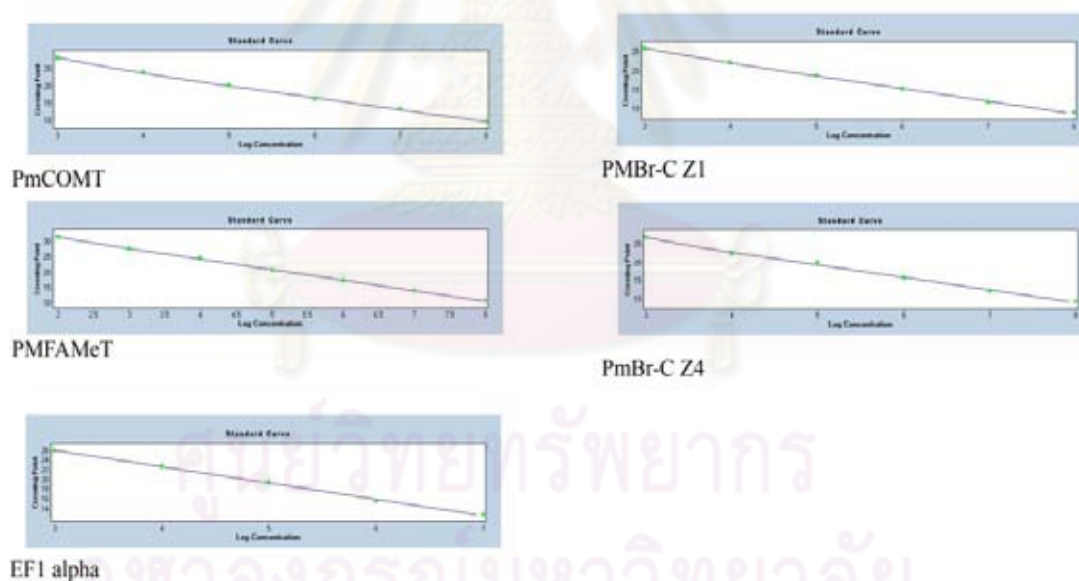
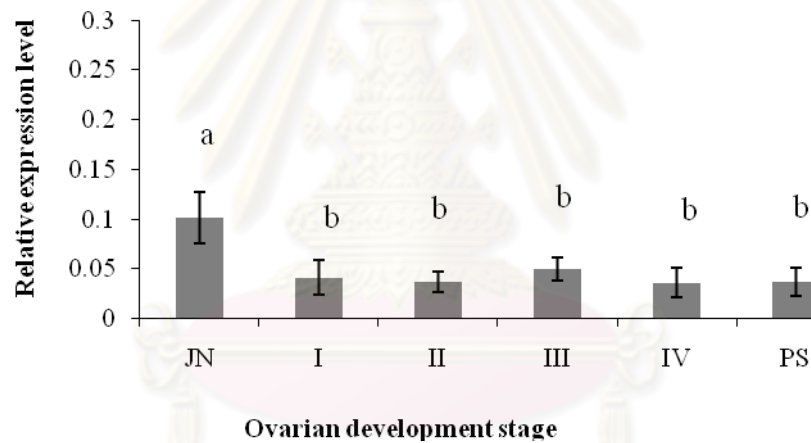


Figure 3.51 Standard curves of *PmCOMT* (Error: 0.0285, efficiency = 1.951 and the equation $Y = -3.445 \cdot \log(X) + 38.62$), *PmFAMeT* (Error:0.0208, efficiency = 1.975 and the equation $Y = -3.384 \cdot \log(X) + 37.93$), *PmBr-cZ1*(Error:0.0251, efficiency = 2.005 and the equation $Y = -3.309 \cdot \log(X) + 35.89$), *PmBr-cZ4* (Error:0.0385, efficiency = 1.953 and the equation $Y = -3.440 \cdot \log(X) + 37.10$),*EF1- α* (Error:0.0285, efficiency = 1.994 and the equation $Y = -3.335 \cdot \log(X) + 35.87$).

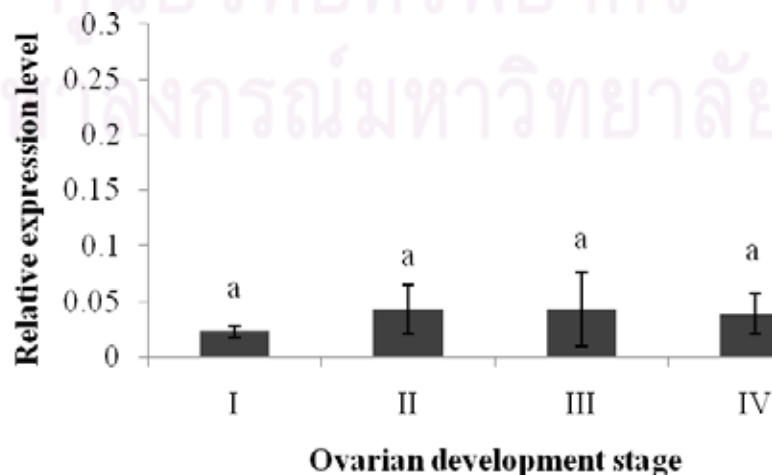
3.5.1 Expression profiles of *PmCOMT* during ovarian development of *P. monodon*

Quantitative real-time PCR revealed that the expression level of *PmCOMT* in ovaries of juveniles (4 months old) was greater than that of intact broodstock ($P < 0.05$). Interestingly, *PmCOMT* was comparably expressed during ovarian development in intact broodstock ($P > 0.05$). The expression level of *PmCOMT* in ovaries of eyestalk-ablated broodstock was not significantly different ($P > 0.05$). At these stages, the *PmCOMT* mRNA was not significantly different from that in ovaries of juveniles ($P > 0.05$) but greater than that in ovaries of intact broodstock ($P > 0.05$) (Fig. 3.52 and Table 3.10).

A



B



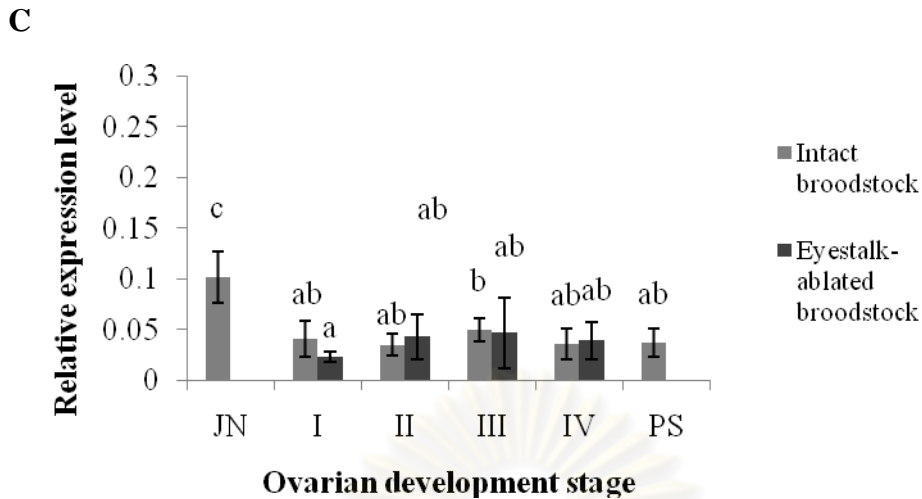


Figure 3.52 Histograms showing the relative expression profiles of *PmCOMT* in ovaries of cultured 4-month-old juveniles (JN, A) and different stages of ovarian development (stages I, previtellogenic; II, vitellogenic; III, early cortical rod; and IV, mature ovaries) of intact (A) and unilateral eyestalk-ablated (B) and intact post-spawning broodstock (PS; A). Data of intact and eyestalk-ablated broodstock were also analyzed together (C). Each bar corresponds to a particular ovarian stage. The same letters indicate that the expression levels were not significantly different ($P > 0.05$).

In domesticated broodstock, *PmCOMT* in ovaries of cultured 6-month-old juvenile and domesticated 14-month-old and 18-month-old broodstock were comparable ($P > 0.05$) (Fig. 3.53).

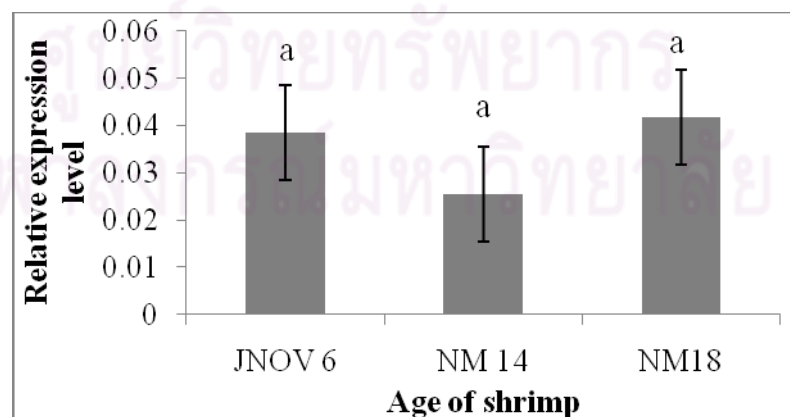


Figure 3.53 Histograms showing the relative expression profiles of *PmCOMT* in ovaries of domesticated juveniles (6 months old) and broodstock (14, and 18 months

old) *P. monodon*. Each bar corresponds to a particular ovarian stage. The same letters indicate that the expression levels were not significantly different ($P > 0.05$).

Table 3.10 Relative expression levels of *PmCOMT* in different ovarian stages of wild (A) and domesticated (B) *P. monodon*. females

A

Ovarian stage	Relative expression level			
	Intact shrimp	<i>N</i>	Eyestalk ablated shrimp	<i>N</i>
Juvenile	0.101483±0.025784 ^c	6	-	-
Stage I (GSI<1.5)	0.041000±0.017623 ^{ab}	10	0.022850±0.004649 ^a	4
Stage II (GSI 2-<4)	0.034825±0.010918 ^{ab}	8	0.042929±0.021993 ^{ab}	7
Stage III (GSI 4- <6)	0.049457±0.011968 ^b	7	0.046614±0.035120 ^{ab}	7
Stage IV (GS I>6)	0.035933±0.015196 ^{ab}	9	0.038838±0.017976 ^{ab}	8
Post-spawning	0.036917±0.013846 ^{ab}	6	-	-

B

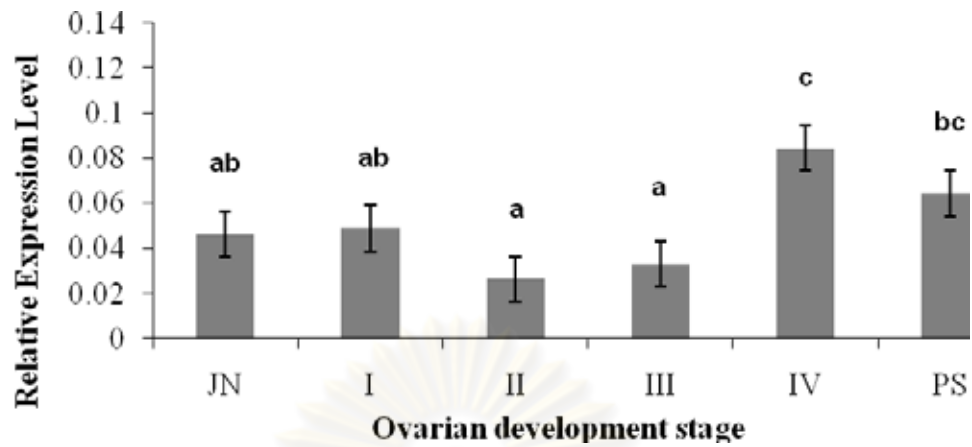
Group	Relative expression level
6 months old (<i>N</i> = 4)	0.0385±0.0085 ^a
14 months old (<i>N</i> = 4)	0.0254±0.0032 ^a
18 months old (<i>N</i> = 3)	0.0417±0.0158 ^a

3.5.2 Expression profiles of *PmFAMeT* during ovarian development of *P. monodon*

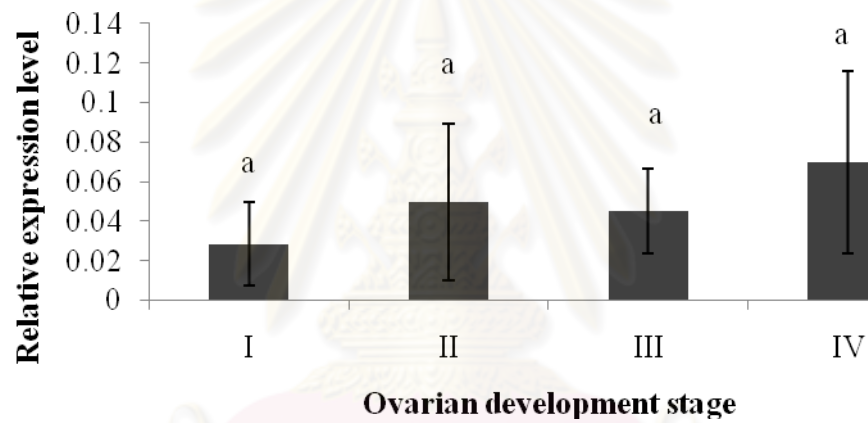
The *PmFAMeT* mRNA in ovaries of 4-month-old juveniles was comparable with that in stage I, II and III ovaries of intact broodstock. *PmFAMeT* was significantly up-regulated at stage IV (mature) ovaries in intact wild broodstock ($P < 0.05$) and returned to the basal level after spawning.

In eyestalk-ablated broodstock, its expression level seemed to be increased in stages II (vitellogenic), III (early cortical rod) and IV (mature ovaries) greater than that in stage I (previtellogenic) ovaries ($P > 0.05$). Results clearly indicated that eyestalk ablation did not have direct effects on expression of this gene (Fig. 3.54).

A



B.



C.

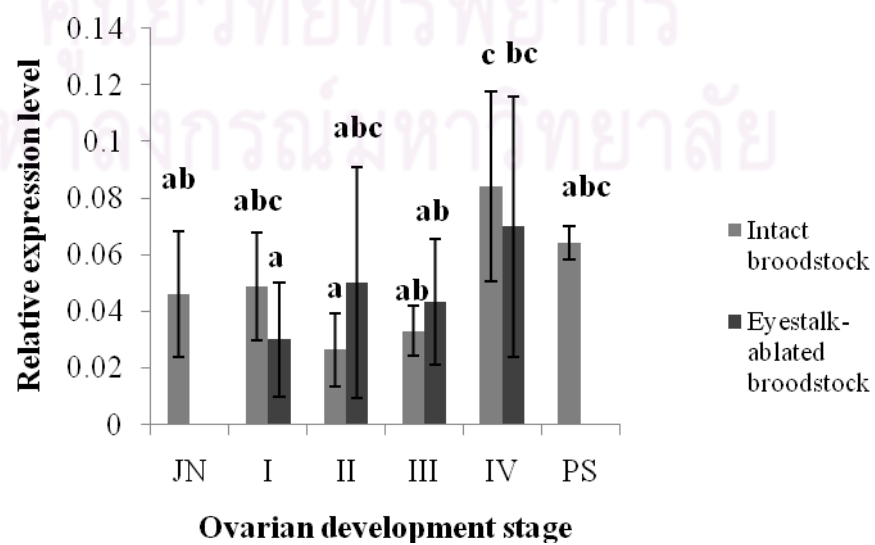


Figure 3.54 Histograms showing the relative expression profiles of *PmFAMeT* in ovaries of cultured 4-month-old juveniles (JN, A) and different stages of ovarian development (stages I, previtellogenic; II, vitellogenic; III, early cortical rod; and IV, mature ovaries) of intact (A) and unilateral eyestalk-ablated (B) and intact post-spawning broodstock (PS; A). Data of intact and eyestalk-ablated broodstock were also analyzed together (C). Each bar corresponds to a particular ovarian stage. The same letters indicate that the expression levels were not significantly different ($P > 0.05$).

The expression levels of *PmFAMeT* in ovaries of cultured 6-month-old juvenile and domesticated 14-month-old was greater than that of 18-month-old broodstock ($P > 0.05$). Although *PmFAMeT* in ovaries of 6-month-old juveniles was gradually decreased in domesticated broodstock (14 and 18 months old), results were not statistically significant when compared with 14-month-old shrimp owing to large standard deviation ($P > 0.05$) (Fig. 3.55).

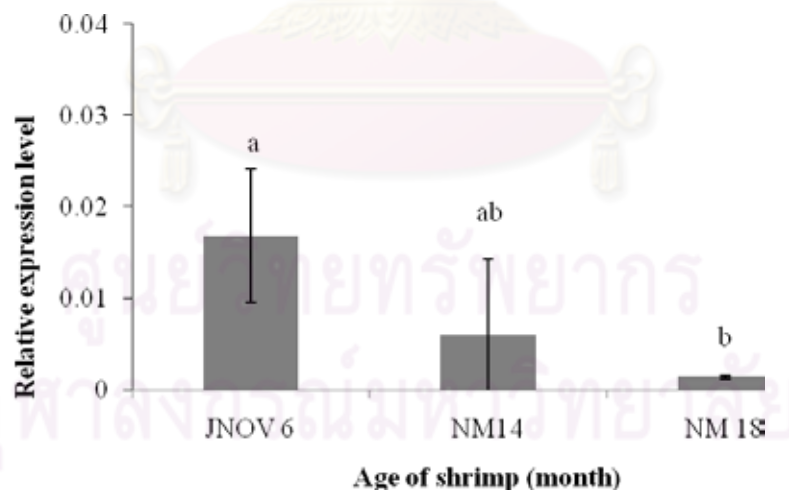


Figure 3.55 Histograms showing the relative expression profiles of *PmFAMeT* in ovaries of domesticated juveniles (6 months old) and broodstock (14, and 18 months old) *P. monodon*. Each bar corresponds to a particular ovarian stage. The same letters indicate that the expression levels were not significantly different ($P > 0.05$).

Table 3.11 Relative expression levels of *PmFAMeT* in different ovarian stages of wild (A) and domesticated (B) *P. monodon* females

A

Ovarian Stage	Relative expression level			
	Intact shrimp	<i>N</i>	Eyestalk ablated shrimp	<i>N</i>
Juvenile	0.046168±0.022243 ^{ab}	5	-	-
Stage I (GSI<1.5)	0.046657±0.019139 ^{abc}	7	0.030000±0.020000 ^c	4
Stage II (GSI 2-<4)	0.026416±0.013025 ^a	6	0.050000±0.040825 ^{abc}	7
Stage III (GSI 4- <6)	0.033000±0.008819 ^{ab}	6	0.043333±0.022361 ^{ab}	9
Stage IV (GS I>6)	0.084242±0.033545 ^a	7	0.070000±0.045947 ^{bc}	10
Post-spawning	0.064200±0.006082 ^{abc}	5	-	-

B

Group	Relative expression level
6 months old (<i>N</i> = 3)	0,0168±0.0073 ^a
14 months old (<i>N</i> = 3)	0.0059±0.0083 ^{ab}
18 months old (<i>N</i> = 3)	0.0013±0.0001 ^b

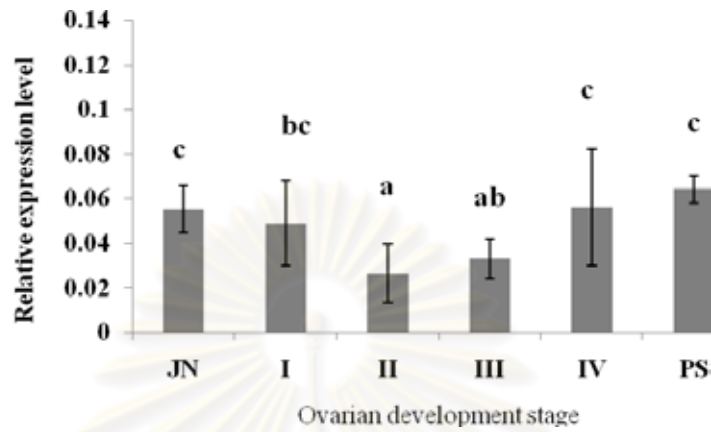
3.5.3 Expression profiles of *PmBr-cZl* during ovarian development of *P. monodon*

Quantitative real-time PCR revealed that the expression levels of *PmBr-cZl* in ovaries of juveniles and stage I ovaries of broodstock was comparable. *PmBr-cZl* was significantly down-regulated at stage II and III ovaries in intact wild broodstock ($P < 0.05$) and returned to the basal level at stage IV ovaries and after spawning.

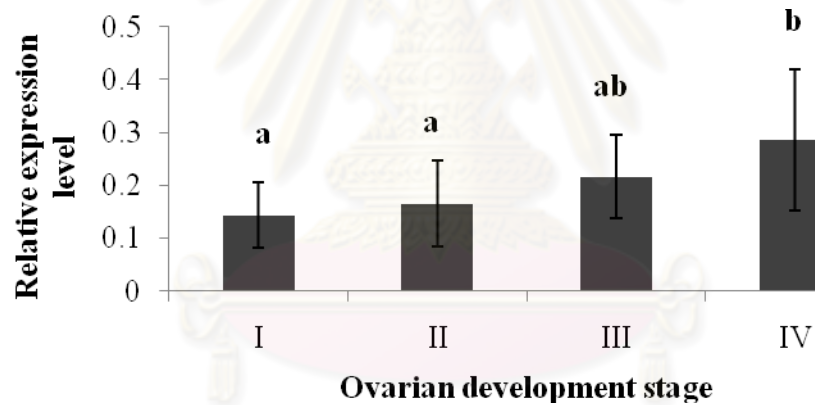
In eyestalk-ablated broodstock, its expression level in stages IV (mature ovaries) was significantly greater than that in stage I (previtellogenic) ovaries and II (vitellogenic) ($P > 0.05$). Eyestalk ablation clearly promoted the expression of *PmFAMeT* during vitellogenesis and final maturation of ovaries compared to intact broodstock (Fig. 3.56). Nevertheless, eyestalk ablation potentially reduced the expression level of for *PmBr-cZl* approximately 3.5-7 times. Therefore, the

expression profiles of *PmBr-cZI* can be used as the biomarker to indicate degrees of ovarian maturation of *P. monodon*.

A



B.



C.

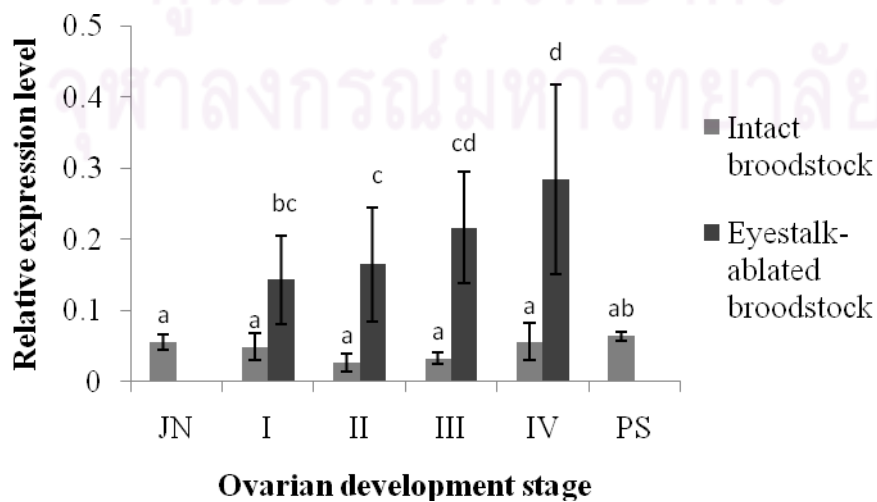


Figure 3.56 Histograms showing the relative expression profiles of *PmBr-cZl* in ovaries of cultured 4-month-old juveniles (JN, A) and different stages of ovarian development (stages I, previtellogenic; II, vitellogenic; III, early cortical rod; and IV, mature ovaries) of intact (A) and unilateral eyestalk-ablated (B) and intact post-spawning broodstock (PS; A). Data of intact and eyestalk-ablated broodstock were also analyzed together (C). Each bar corresponds to a particular ovarian stage. The same letters indicate that the expression levels were not significantly different ($P > 0.05$).

PmBr-c Zl in ovaries of cultured 6-month-old juvenile and domesticated, 14-month-old and 18-month-old broodstock were not significantly different ($P > 0.05$). The expression levels of *PmBr-cZl* in ovaries of domesticated 14-month-old broodstock seem to be increased compared to other ages of domesticated stocks but results were not statistically significant owing to large standard deviation ($P > 0.05$) (Fig. 3.57).

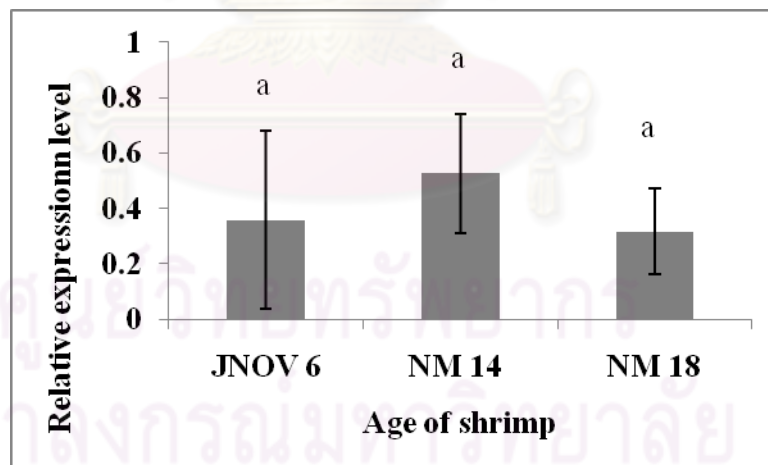


Figure 3.57 Histograms showing the relative expression profiles of *PmBr-cZl* in ovaries of domesticated juveniles (6 months old) and broodstock (14, and 18 months old) *P. monodon*. Each bar corresponds to a particular ovarian stage. The same letters indicate that the expression levels were not significantly different ($P > 0.05$).

Table 3.12 Relative expression levels of *PmBr c Z1* in different ovarian stages of wild (A) and domesticated (B) *P. monodon* females

A

Ovarian Stage	Relative expression level			
	Intact shrimp	N	Eyestalk-ablated shrimp	N
Juvenile	0.055250±0.01047 ^a	4	-	-
Stage I (GSI<1.5)	0.048857±0.01913 ^a	7	0.143257±0.06200 ^{bc}	4
Stage II (GSI 2-<4)	0.026417±0.01302 ^a	6	0.164939±0.80753 ^c	7
Stage III (GSI 4- <6)	0.033000±0.00819 ^a	6	0.216274±0.07822 ^c	10
Stage IV (GS I>6)	0.056057±0.02627 ^a	7	0.285269±0.13323 ^d	10
Post-spawning	0.064200±0.00608 ^{ab}	5	-	-

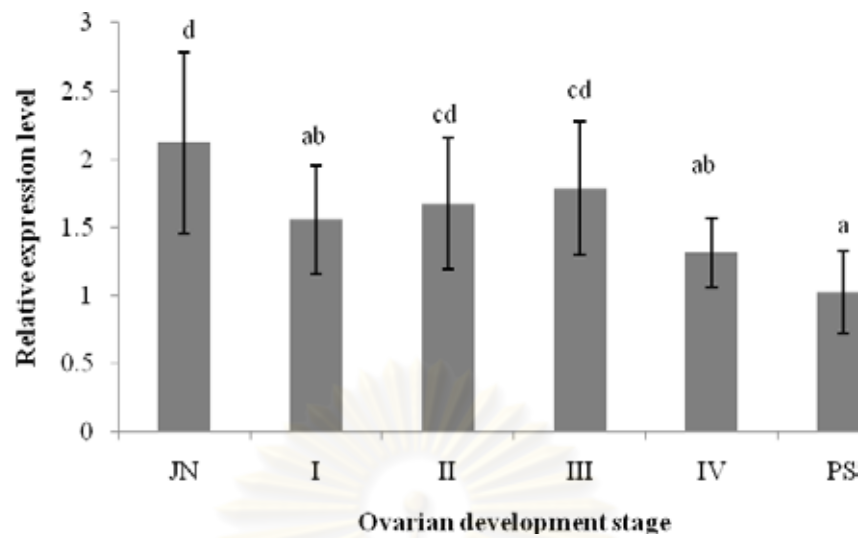
B

Group	Relative expression level
6 months old (N = 5)	0.3587 ±0.3226 ^a
14 months old (N = 14)	0.5258±0.2145 ^a
18 months old (N = 4)	0.3169±0.1560 ^a

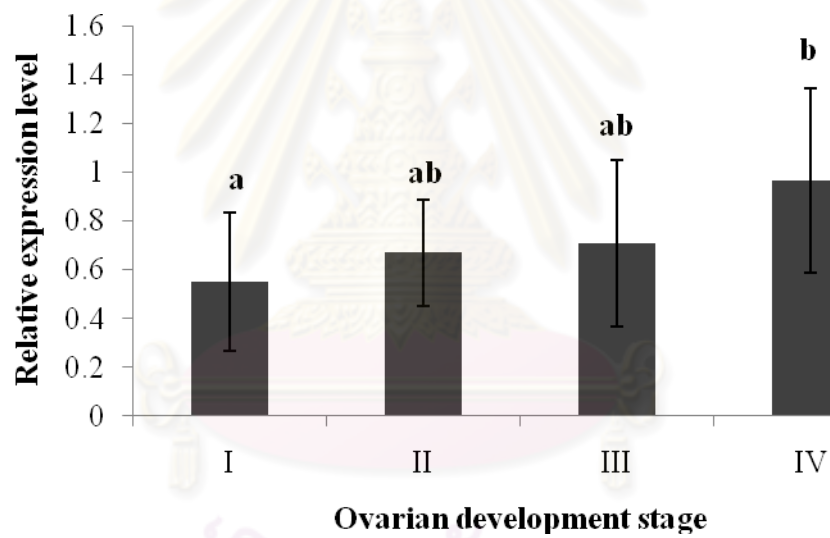
3.5.4 Expression profiles of *PmBr-cZ4* during ovarian development of *P. monodon*

The level of *PmBr-cZ4* mRNA was significantly decreased during ovarian development of intact wild *P. monodon* ($P > 0.05$). In eyestalk-ablated broodstock, its expression level in stages IV ovaries was significantly greater than that in other stage of ovaries ($P < 0.05$) (Fig. 3.58).

A



B.



C.

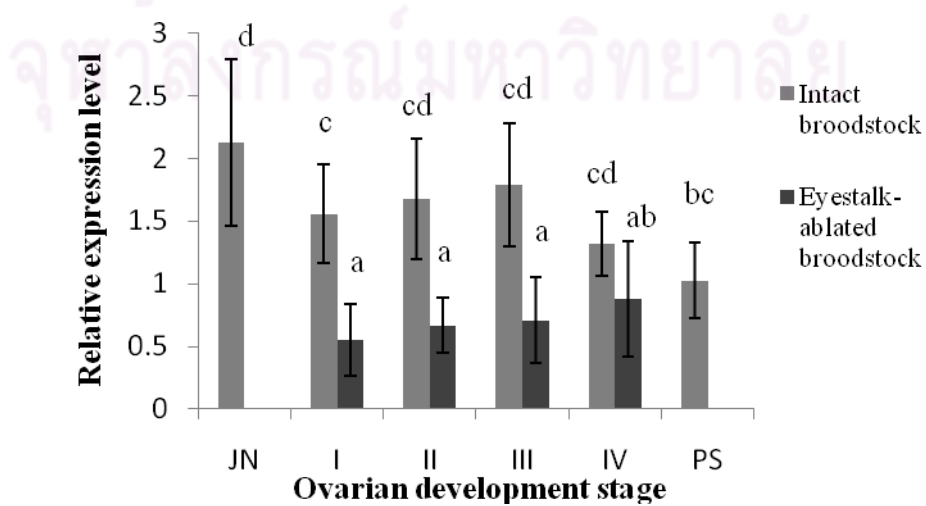


Figure 3.58 Histograms showing the relative expression profiles of *PmBr-cZ4* in ovaries of cultured 4-month-old juveniles (JN, A) and different stages of ovarian development (stages I, previtellogenic; II, vitellogenic; III, early cortical rod; and IV, mature ovaries) of intact (A) and unilateral eyestalk-ablated (B) and intact post-spawning broodstock (PS; A). Data of intact and eyestalk-ablated broodstock were also analyzed together (C). Each bar corresponds to a particular ovarian stage. The same letters indicate that the expression levels were not significantly different ($P > 0.05$).

Quantitative real-time PCR revealed that the expression levels of *PmBr-cZ4* in ovaries was reduced in 18-month-old broodstock compared to domesticated 6-month-old juveniles and 18-month-old broodstock ($P > 0.05$; Fig. 3.59). This indicated that 18-month-old shrimp should possess greater degrees of ovarian maturation than 14-month-old broodstock.

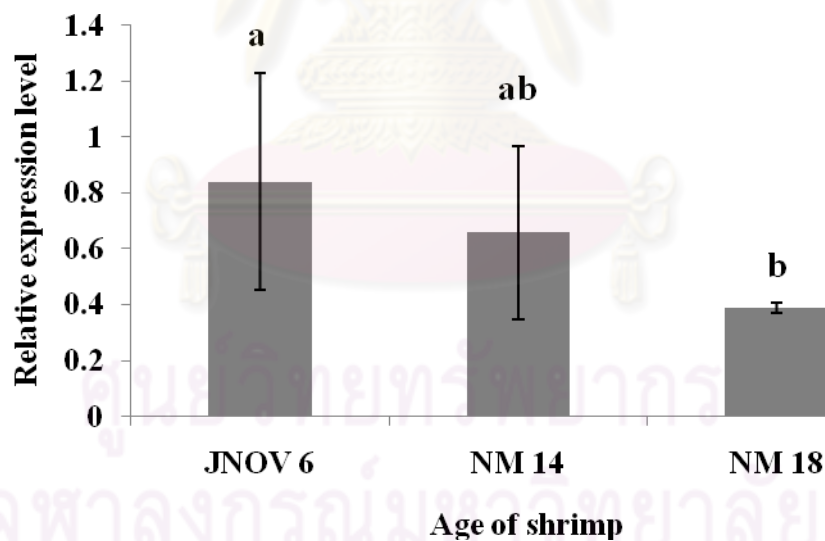


Figure 3.59 Histograms showing the relative expression profiles of *PmBr-cZ4* in ovaries of domesticated juveniles (6 months old) and broodstock (14, and 18 months old) *P. monodon*. Each bar corresponds to a particular ovarian stage. The same letters indicate that the expression levels were not significantly different ($P > 0.05$).

Table 3.13 Relative expression levels of *PmBr-cZ4* in different ovarian stages of wild (A) and domesticated (B) *P. monodon* females

A

Ovarian Stage	Relative Expression Level			
	Intact shrimp	<i>N</i>	Eyestalk-ablated shrimp	<i>N</i>
Juvenile	2.12200±0.66292 ^d	8	-	-
Stage I (GSI<1.5)	1.55550±0.39587 ^c	5	0.55250±0.28335 ^a	4
Stage II (GSI 2-<4)	1.67400±0.47914 ^c	5	0.66857±0.219502 ^a	7
Stage III (GSI 4- <6)	1.78440±0.49191 ^c	9	0.70700±0.34098 ^a	10
Stage IV (GS I > 6)	1.31580±0.25519 ^{bc}	5	0.87636±0.46007 ^{ab}	10
Post-spawning	1.02400±0.30369 ^{ab}	5	-	-

B

Group	Relative expression level
6 months old (<i>N</i> = 5)	0.8402±0.3886 ^a
14 months old (<i>N</i> = 17)	0.6580±0.3093 ^{ab}
18 months old (<i>N</i> = 4)	0.3883±0.0170 ^b

3.6 Effects of 5-HT, progesterone and 20 β -hydroxyecdysone administration on transcription of reproduction-related genes in ovaries of *P. monodon*

PmCOMT, *PmFAMeT*, *PmBr-cZ1* and *PmBr-cZ4* are involved in ovarian development and/or molting of shrimp. To verify the regulatory effects of neurotransmitters, steroid hormones and ecdysteroids on expression of these genes, various groups of domesticated shrimp samples were treated with 5-HT, progesterone or 20 β -hydroxyecdysone (20E).

3.6.1 Effects of 5-HT administration on transcription of *PmCOMT*, *PmFAMeT*, *PmBr-cZ1* and *PmBr-cZ4* in ovaries of domesticated 18-month-old broodstock

The effects of 5-HT on expression of *PmCOMT*, *PmFAMeT*, *PmBr-cZ1* and *PmBr-cZ4* in ovaries of 18-month-old *P. monodon* were examined. For *O-methyltransferase* genes, the injection of 5-HT did not promote the expression level of *PmCOMT* in ovaries of domesticated *P. monodon* broodstock (Fig. 3.60). In contrast, 5-HT administration resulted in increasing of ovarian *PmFAMeT* expression for approximately 50-fold at 1 hpt ($P < 0.05$; Fig. 3. 61).

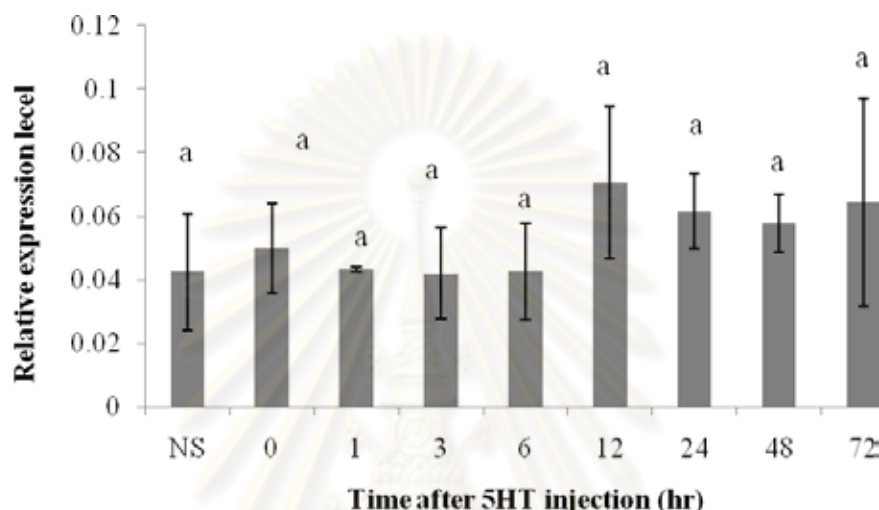


Figure 3.60 Time-course relative expression levels of *PmCOMT* in ovaries of 18 months old after serotonin injection (50 $\mu\text{g/g}$ body weight) at 1, 2, 3, 6, 12, 24, 48 and 72 hours post injection (hpt; $N = 4$ for each stage). Shrimp injected with 0.85% saline solution at 0 hpi were included as the vehicle control.

Table 3.14 Time course relative expression levels of *PmCOMT* in ovaries of juvenile *P. monodon* treated with serotonin (50 $\mu\text{g/g}$ body weight)

Group (N=3)	Relative expression level
NS (control)	0.042±0.018 ^a
0 hpi (control)	0.049±0.014 ^a
1 hpi	0.043±0.001 ^b
3 hpi	0.042±0.014 ^a
6 hpi	0.042±0.015 ^a
12 hpi	0.070±0.024 ^a
24 hpi	0.061±0.011 ^a
48 hpi	0.058±0.009 ^a
72 hpi	0.064±0.032 ^a

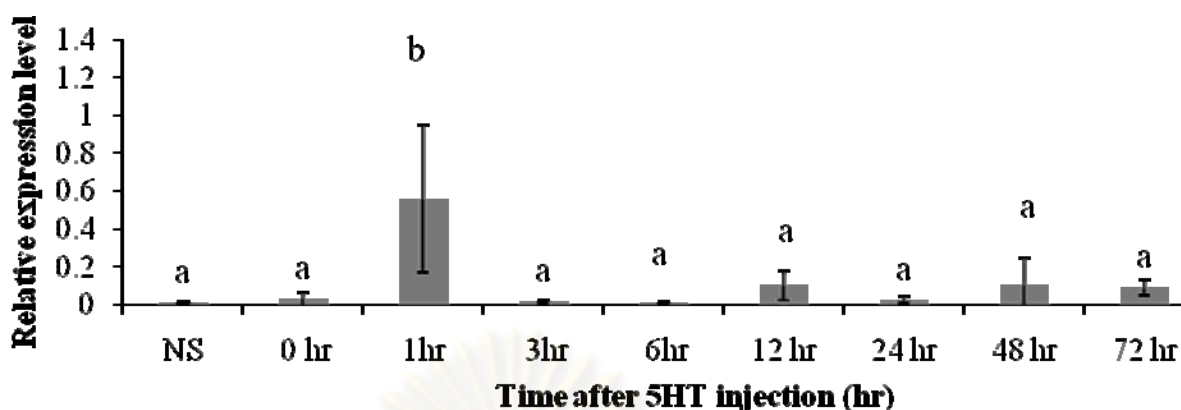


Figure 3.61 Time-course relative expression levels of *PmFAMeT* in ovaries of 18 months old after serotonin injection (50 $\mu\text{g/g}$ body weight) at 1, 2, 3, 6, 12, 24, 48 and 72 hpt ($N = 4$ for each stage). Shrimp injected with absolute ethanol and 0.85% saline solution at 0 hpi were included as the vehicle control.

Table 3.15 Time course relative expression levels of *PmFAMeT* in ovaries of 18-month-old *P. monodon* treated with serotonin (50 $\mu\text{g/g}$ body weight)

Group ($N=3$)	Relative expression level
NS (control)	0.009 \pm 0.004 ^a
0 hpi (control)	0.065 \pm 0.063 ^a
1 hpi	1.356 \pm 0.936 ^b
3 hpi	0.035 \pm 0.009 ^a
6 hpi	0.032 \pm 0.009 ^a
12 hpi	0.176 \pm 0.030 ^a
24 hpi	0.032 \pm 0.006 ^a
48 hpi	0.396 \pm 0.583 ^a
72 hpi	0.194 \pm 0.028 ^a

For ecdysteroid responsive genes, exogenous administration of 5-HT did not affect the expression of *PmBr-cZ1* (Fig. 3.62) but promote the expression level of *PmBr-cZ4* at 12 hpt ($P < 0.05$) (Fig. 3.63).

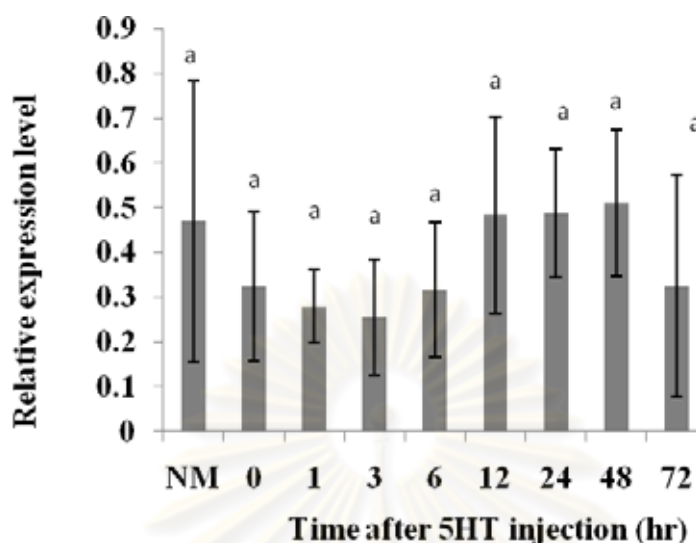


Figure 3.62 Time-course relative expression levels of *PmBr-cZI* in ovaries of 18 months old after serotonin injection (50 µg/g body weight) at 1, 2, 3, 6, 12, 24, 48 and 72 hpt ($N = 4$ for each stage). Shrimp injected with absolute ethanol and 0.85% saline solution at 0 hpi were included as the vehicle control.

Table 3.16 Time course relative expression levels of *Br-cZI* in ovaries of juvenile *P. monodon* treated with serotonin (50 µg/g body weight)

Group ($N=3$)	Relative expression level
NS (control)	0.4688±0.3136 ^a
0 hpi (control) *	0.3234±0.1669 ^a
1 hpi	0.2792±0.0830 ^a
3 hpi	0.2546±0.1299 ^a
6 hpi*	0.3165±0.1515 ^a
12 hpi*	0.4835±0.2192 ^a
24 hpi*	0.4873±0.1438 ^a
48 hpi **	0.5105±0.1626 ^a
72 hpi	0.3250±0.2477 ^a

* $N = 4$; ** $N = 5$

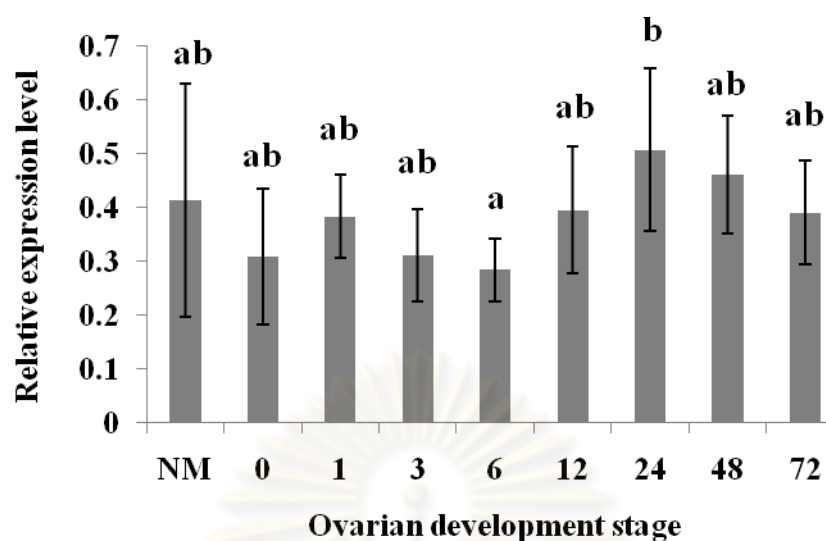


Figure 3.63 Time-course relative expression levels of *PmBr-cZ4* in ovaries of 18 months old after serotonin injection (50 $\mu\text{g/g}$ body weight) at 1, 2, 3, 6, 12, 24, 48 and 72 hpt ($N = 4$ for each stage). Shrimp injected with absolute ethanol and 0.85% saline solution at 0 hpi were included as the vehicle control.

Table 3.17 Time course relative expression levels of *Br c Z4* in ovaries of juvenile *P. monodon* treated with serotonin (50 $\mu\text{g/g}$ body weight)

Group ($N=3$)	Relative expression level
NS (control)	0.4141 \pm 0.2166 ^{ab}
0 hpi (control)*	0.3093 \pm 0.1269 ^{ab}
1 hpi	0.3838 \pm 0.0773 ^{ab}
3 hpi	0.3119 \pm 0.0860 ^{ab}
6 hpi*	0.2840 \pm 0.0574 ^a
12 hpi*	0.3951 \pm 0.1181 ^{ab}
24 hpi*	0.5070 \pm 0.1512 ^b
48 hpi**	0.4613 \pm 0.1085 ^{ab}
72 hpi	0.3910 \pm 0.0966 ^{ab}

* $N = 4$; ** $N = 5$

3.6.2 Effects of progesterone administration on transcription of *PmCOMT*, *PmFAMeT*, *PmBr-cZ1* and *PmBr-cZ4* in ovaries of domesticated 18- and 14-month-old broodstock

3.6.2.1 18-month-old shrimp

The effects of progesterone administration on expression of *PmCOMT* and *PmFAMeT* in ovaries of domesticated broodstock of *P. monodon* were examined at 12, 24 and 72 after administration. Expression of these genes in ovaries of shrimp injected with 40% ethanol were dissected out at 0 hpi and used as the control group. The result showed that the expression levels of *PmCOMT* (Fig. 3.64) and *PmFAMeT* (Fig. 3.65) in ovaries of domesticated 18-month-old broodstock were not significantly affected by progesterone injection ($P > 0.05$).

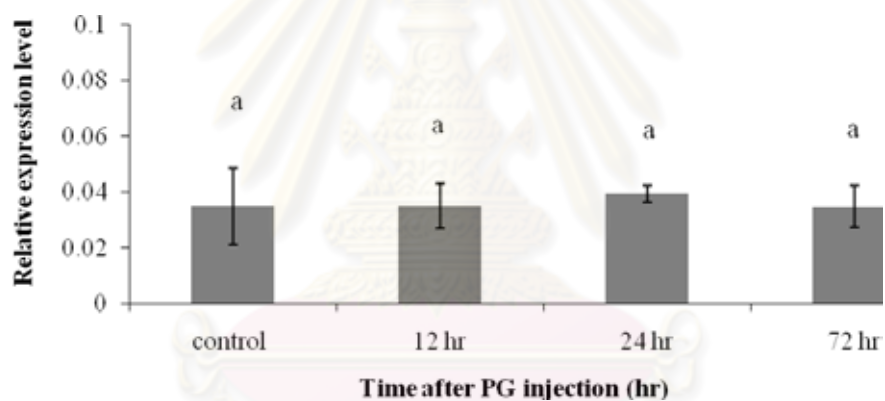


Figure 3.64 Time-course relative expression levels of *PmCOMT* in ovaries of 18 months old at 12, 24 and 48 hpi of progesterone (1 $\mu\text{g/g}$ body weight; $N = 4$ for each stage). Shrimp injected with absolute ethanol and 0.85% saline solution at 0 hpi were included as the vehicle control and the positive control, respectively.

Table 3.18 Time course relative expression levels of *PmCOMT* in ovaries of 18 months old *P. monodon* treated with progesterone (0.1 $\mu\text{g/g}$ body weight)

Group ($N=3$)	Relative expression level
0 hpi (control)	0.034 \pm 0.014 ^a
12 hpi	0.034 \pm 0.007 ^a
24 hpi	0.040 \pm 0.002 ^a
48 hpi	0.034 \pm 0.007 ^a

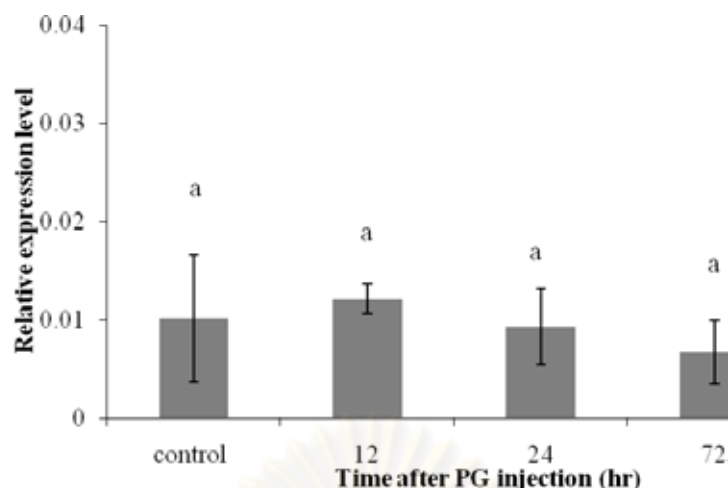


Figure 3.65 Time-course relative expression levels of *PmFAMeT* in ovaries of 18 months old at 12, 24 and 48 hpi of progesterone (1 $\mu\text{g/g}$ body weight; $N = 4$ for each stage). Shrimp injected with absolute ethanol and 0.85% saline solution at 0 hpi were included as the vehicle control and the positive control, respectively.

Table 3.19 Time course relative expression levels of *PmFAMeT* in ovaries of 18 months old *P. monodon* treated with progesterone (0.1 $\mu\text{g/g}$ body weight)

Group ($N=3$)	Relative expression level
0 hpi (control)	0.024 \pm 0.019 ^a
12 hpi	0.037 \pm 0.005 ^a
24 hpi	0.030 \pm 0.021 ^a
72 hpi	0.020 \pm 0.008 ^a

3.6.2.2 14-month-old domesticated broodstock

The effects of progesterone administration on expression of *PmCOMT*, *PmFAMeT*, *PmBr-cZ1* and *PmBr-cZ4* in ovaries of domesticated 14-month-old broodstock were examined at 12, 24 and 72 after administration. Expression of these genes in ovaries of shrimp infected with 10% ethanol were dissected out at 12 hpi and used as the vehicle control.

Results from quantitative real-time PCR revealed that progesterone did not affect the expression level of *PmCOMT* in ovaries of 14-month-old shrimp (Fig. 3.66). Although a trend of inducing effects of progesterone on the expression of *PmFAMeT* was observed at 72 hpi, results were not statistically significant due to a large standard deviation within each treatment group (Fig. 3.67).

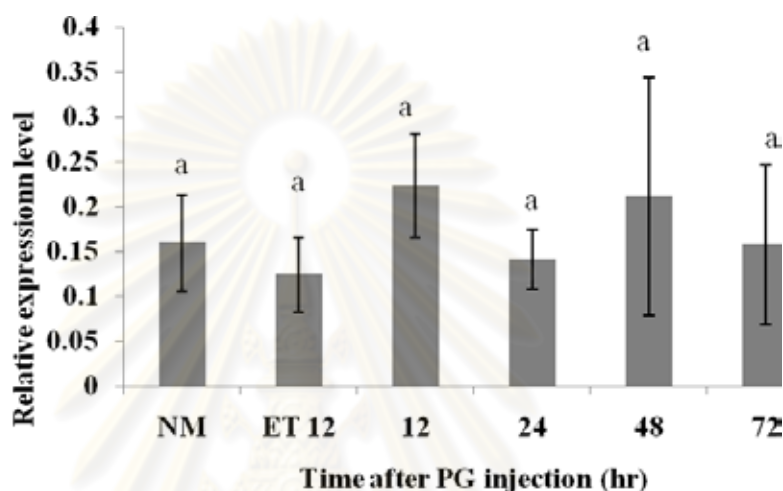


Figure 3.66 Time-course relative expression levels of *PmCOMT* in ovaries of 14 months old at 12, 24, 48 and 72 hpi of progesterone (0.1 $\mu\text{g/g}$ body weight; $N = 4$ for each stage). Shrimp injected with absolute ethanol and 0.85% saline solution at 0 hpi were included as the vehicle control and the positive control, respectively.

Table 3.20 Time course relative expression levels of *PmCOMT* in ovaries of 14 months old *P. monodon* treated with progesterone (0.1 $\mu\text{g/g}$ body weight)

Group	Relative expression level
Normal (control; $N = 5$)	0.1596 \pm 0.0538 ^a
10% ethanol at 12 hpi (control; $N = 5$)	0.1240 \pm 0.0415 ^a
12 hpi ($N = 5$)	0.2233 \pm 0.0581 ^a
24 hpi ($N = 5$)	0.1412 \pm 0.0337 ^a
48 hpi ($N = 5$)	0.2117 \pm 0.1328 ^a
72 hpi ($N=3$)	0.1576 \pm 0.0892 ^a

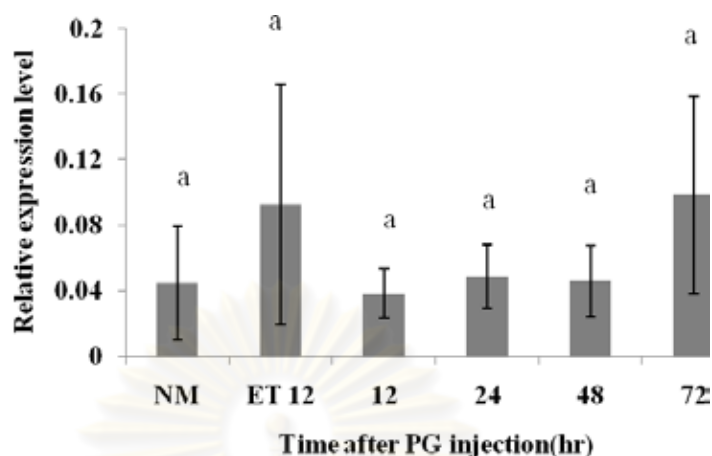


Figure 3.67 Time-course relative expression levels of *PmFAMeT* in ovaries of 14 months old at 12, 24, 48 and 72 hpi of progesterone ($0.1 \mu\text{g/g}$ body weight; $N = 4$ for each stage). Shrimp injected with absolute ethanol and 0.85% saline solution at 0 hpi were included as the vehicle control and the positive control, respectively.

Table 3.21 Time course relative expression levels of *PmFAMeT* in ovaries of 14 months old *P. monodon* treated with progesterone ($0.1 \mu\text{g/g}$ body weight)

Group	Relative expression level
Normal ($N = 4$)	0.0447 ± 0.0348^a
10% Ethanol at 12 hpi (control, $N = 6$)	0.0925 ± 0.0731^a
12 hpi ($N = 5$)	0.0383 ± 0.0150^a
24 hpi ($N = 5$)	0.0489 ± 0.0192^a
48 hpi ($N = 5$)	0.0457 ± 0.0219^a
72 hpi ($N = 4$)	0.0983 ± 0.0600^a

Like *PmCOMT* and *PmFAMeT*, the expression level of *PmBr-cZl* was not affected by exogenous progesterone administration ($P > 0.05$) (Fig. 3.68). Nevertheless, *PmBr-cZ4* was up-regulated at 48 and 72 hpi after progesterone administration ($P > 0.05$) (Fig. 3.69).

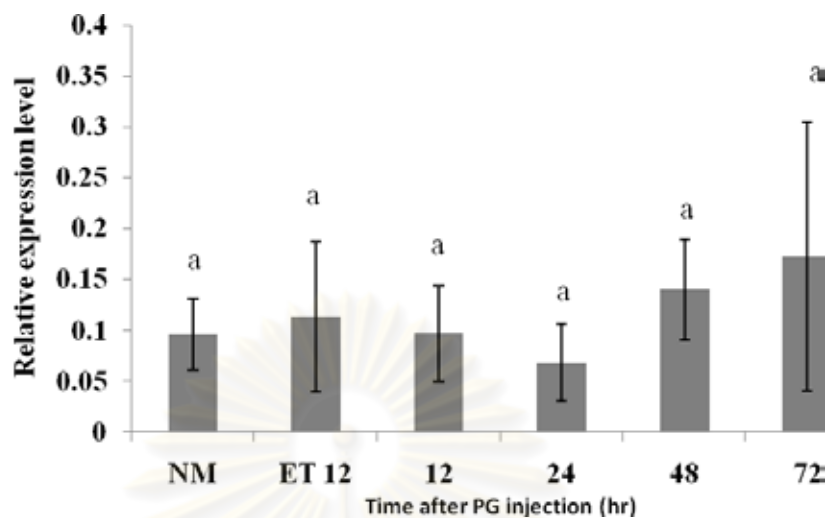


Figure 3.68 Time-course relative expression levels of *PmBr-cZ1* in ovaries of 14 months old at 12, 24, 48 and 72 hpi of progesterone (0.1 $\mu\text{g/g}$ body weight; $N = 4$ for each stage). Shrimp injected with absolute ethanol and 0.85% saline solution at 0 hpi were included as the vehicle control and the positive control, respectively.

Table 3.22 Time course relative expression levels of *PmBr-cZ1* in ovaries of 14 months old *P. monodon* treated with progesterone (0.1 $\mu\text{g/g}$ body weight)

Group	Relative expression level
Normal ($N = 3$)	0.0961±0.0356 ^a
10% Ethanol at 12 hpi (control, $N = 6$)	0.1133±0.0738 ^a
12 hpi ($N = 5$)	0.0969±0.0470 ^a
24 hpi ($N = 5$)	0.0681±0.0384 ^a
48 hpi ($N = 5$)	0.1398±0.0493 ^a
72 hpi ($N = 4$)	0.1726±0.1326 ^a

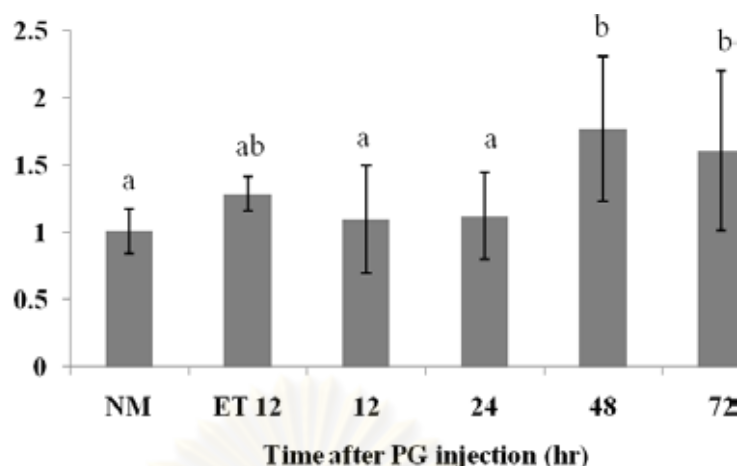


Figure 3.69 Time-course relative expression levels of *PmBr-cZ4* in ovaries of 14 months old at 12, 24, 48 and 72 hpi of progesterone (0.1 $\mu\text{g/g}$ body weight; $N = 4$ for each stage). Shrimp injected with absolute ethanol and 0.85% saline solution at 0 hpi were included as the vehicle control and the positive control, respectively.

Table 3.23 Time course relative expression levels of *PmBr-cZ4* in ovaries of 14 months old *P. monodon* treated with progesterone (0.1 $\mu\text{g/g}$ body weight)

Group	Relative expression level
Normal ($N = 4$)	1.0125 ± 0.1678^a
10% Ethanol at 12 hpi (control, $N = 5$)	1.2879 ± 0.1267^{ab}
12 hpi ($N = 5$)	1.0971 ± 0.4010^a
24 hpi ($N = 5$)	1.1241 ± 0.3217^a
48 hpi ($N = 5$)	1.7720 ± 0.5343^b
72 hpi ($N = 3$)	1.6049 ± 0.5940^b

3.6.3 Effects of 20-hydroxyecdysone (20E) administration on transcription of *PmCOMT*, *PmFAMeT*, *PmBr-cZ1* and *PmBr-cZ4* in ovaries of commercially cultured *P. monodon* juveniles

The effects of 20E administration on expression of *PmCOMT*, *PmFAMeT*, *PmBr-cZ1* and *PmBr-cZ4* in ovaries of juvenile *P. monodon* females were examined at 6, 12, 24, 48, 72, 96 and 168 after administration.

The expression of *PmCOMT* in ovaries of juvenile *P. monodon* was significantly decreased following 20E administration ($P > 0.05$). However, the results should be interpreted with caution as the expression of *PmCOMT* was also significantly in the vehicle control group (Fig. 3.70).

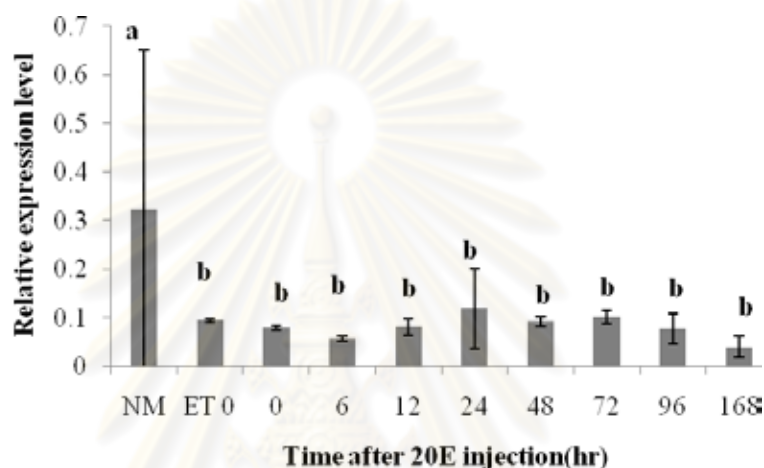


Figure 3.70 Time-course relative expression levels of *PmCOMT* in ovaries of 4 months-old at 6, 12, 24, 48, 72, 96 and 168 hpi of 20E (1 µg/g body weight; $N = 3$ for each treatment). Shrimp injected with 10% absolute ethanol and 20E (1 µg/g body weight) at 0 hpi were included as the vehicle control and the positive control, respectively.

Table 3.24 Time course relative expression levels of *PmCOMT* in ovaries of 4 months- old *P. monodon* treated with 20E(1µg/g body weight)

Group ($N=3$)	Relative expression level
NM (normal shrimp)	0.3216 ± 0.3293^a
10% EtOH (control)	0.0940 ± 0.0025^b
0 hpi (control)	0.0792 ± 0.0035^b
6 hpi	0.0563 ± 0.0040^b
12 hpi	0.0808 ± 0.0163^b
24 hpi	0.1192 ± 0.0823^b
48 hpi	0.0920 ± 0.0105^b
72 hpi	0.1021 ± 0.0128^b
96 hpi	0.0768 ± 0.0317^b
168 hpi	0.0393 ± 0.0217^b

In contrast, the expression level of *PmFAMeT* in ovaries of cultured juveniles was obviously affected after administration with 20E for 6 hpt ($P < 0.05$). The induced effects remained for 24 hours ($P < 0.05$) before reduced to the basal level since 48 hpi ($P > 0.05$) (Fig. 3.71).

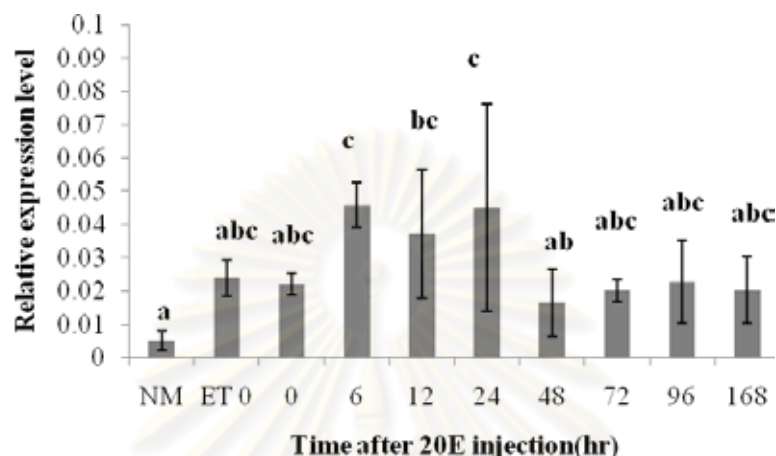


Figure 3.71 Time-course relative expression levels of *PmFAMeT* in ovaries of 4 months-old at 6, 12, 24, 48, 72, 96 and 168 hpi of 20E (1 $\mu\text{g/g}$ body weight; $N = 3$ for each treatment). Shrimp injected with 10% absolute ethanol and 20E (1 $\mu\text{g/g}$ body weight) at 0 hpi were included as the vehicle control and the positive control, respectively.

Table 3.25 Time course relative expression levels of *PmFAMeT* in ovaries of 4 months- old *P. monodon* treated with 20E (1 $\mu\text{g/g}$ body weight)

Group ($N=3$)	Relative expression level
NM (normal shrimp)	0.0040 \pm 0.0028 ^a
10% EtOH (control)	0.0239 \pm 0.0054 ^{abc}
0 hpi (control)	0.0219 \pm 0.0032 ^{abc}
6 hpi	0.0457 \pm 0.0067 ^c
12 hpi	0.0371 \pm 0.0194 ^{bc}
24 hpi	0.0449 \pm 0.0312 ^c
48 hpi	0.0165 \pm 0.0101 ^{ab}
72 hpi	0.0200 \pm 0.0032 ^{abc}
96 hpi	0.0226 \pm 0.0124 ^{abc}
168 hpi	0.0201 \pm 0.0100 ^{abc}

Interestingly, late response effects of 20E on expression of *PmBr-cZ1* (Fig. 3.72) and *PmBr-cZ4* (Fig. 3.73) were observed at 168 hpi. Notably, juvenile shrimp treated with 20E showed immediate response to exogenous 20E administration

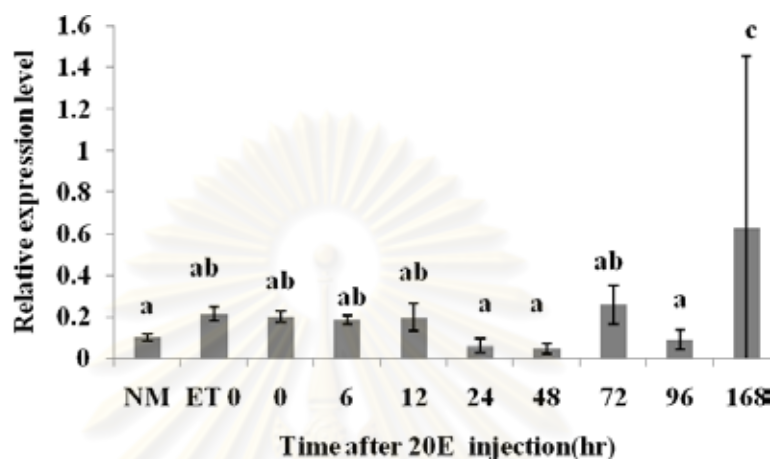


Figure 3.72 Time-course relative expression levels of *PmBr-cZ1* in ovaries of 4 months-old at 6, 12, 24, 48, 72, 96 and 168 hpi of 20E (1 µg/g body weight; $N = 3$ for each treatment). Shrimp injected with 10% absolute ethanol and 20E (1 µg/g body weight) at 0 hpi were included as the vehicle control and the positive control, respectively.

Table 3.26 Time course relative expression levels of *PmBr-cZ1* in ovaries of 4 months old *P. monodon* treated with 20E (1µg/g body weight)

Group ($N=3$)	Relative expression level
NM (Intact shrimp)	0.0992 ± 0.0147^a
10%EtOH (Control)	0.2133 ± 0.0317^{ab}
0 hpi (Control)	0.1983 ± 0.0265^{ab}
6 hpi	0.1843 ± 0.0223^{ab}
12 hpi	0.1966 ± 0.0656^{ab}
24 hpi	0.0610 ± 0.0321^a
48 hpi	0.0467 ± 0.0245^a
72 hpi	0.2590 ± 0.0955^{ab}
96 hpi	0.0888 ± 0.0469^a
168 hpi	0.6232 ± 0.8340^c

reflected by molting within 48 hours following the treatment in most individuals of all treatment. Accordingly, differential expression of both *PmBr-cZ1* and *PmBr-cZ4* should have reflected long duration effects of the ecdysteroid on expression of these genes.

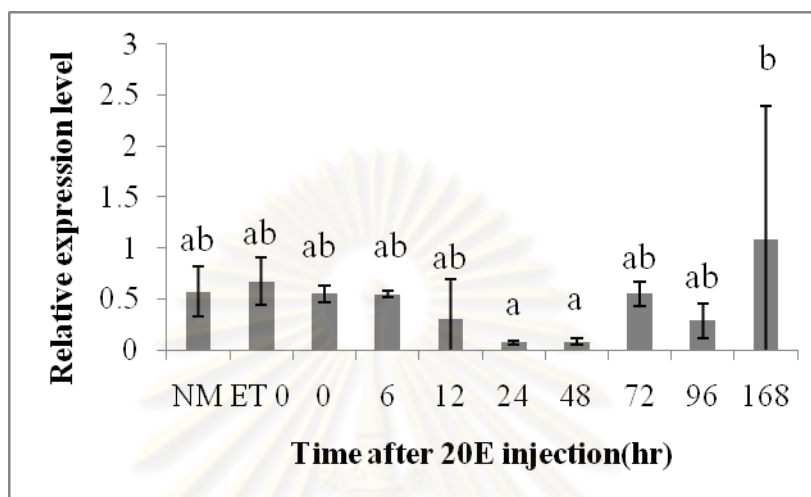


Figure 3.73 Time-course relative expression levels of *PmBr-cZ4* in ovaries of 4 months-old at 6, 12, 24, 48, 72, 96 and 168 hpi of 20E (1 μ g/g body weight; $N = 3$ for each treatment). Shrimp injected with 10% absolute ethanol and 20E (1 μ g/g body weight) at 0 hpi were included as the vehicle control and the positive control, respectively.

Table 3.27 Time course relative expression levels of *PmBr-cZ4* in ovaries of 4 months-old *P. monodon* treated with 20E (1 μ g/g body weight)

Group ($N=3$)	Relative expression level
NM (normal shrimp)	0.5690 ± 0.2452^{ab}
10% EtOH (control)	0.6733 ± 0.2356^{ab}
0 hpi (control)	0.5496 ± 0.0784^{ab}
6 hpi	0.5453 ± 0.0289^{ab}
12 hpi	0.3023 ± 0.3947^{ab}
24 hpi	0.0718 ± 0.0145^a
48 hpi	0.0793 ± 0.0303^a
72 hpi	0.5493 ± 0.1252^{ab}
96 hpi	0.2886 ± 0.1711^{ab}
168 hpi	1.0900 ± 1.3084^b

3.7 Localization of all genes in ovaries of *P. monodon* broodstock

3.7.1. Quantification of the cRNA probe

The sense and antisense cRNA probes were synthesized from the recombinant insert (700 bp) for *PmCOMT* (Fig. 3.73) or the PCR product for those of *PmFAMeT* (Fig. 3.74), *PmBr-cZ1* (Fig. 3.75) and *PmBr-cZ4* (Fig. 3.76). The amount of cRNA probes was roughly estimated by dot blot analysis. The control RNA was used as the positive control and gave the positive signal between 10 pg to 10ng.

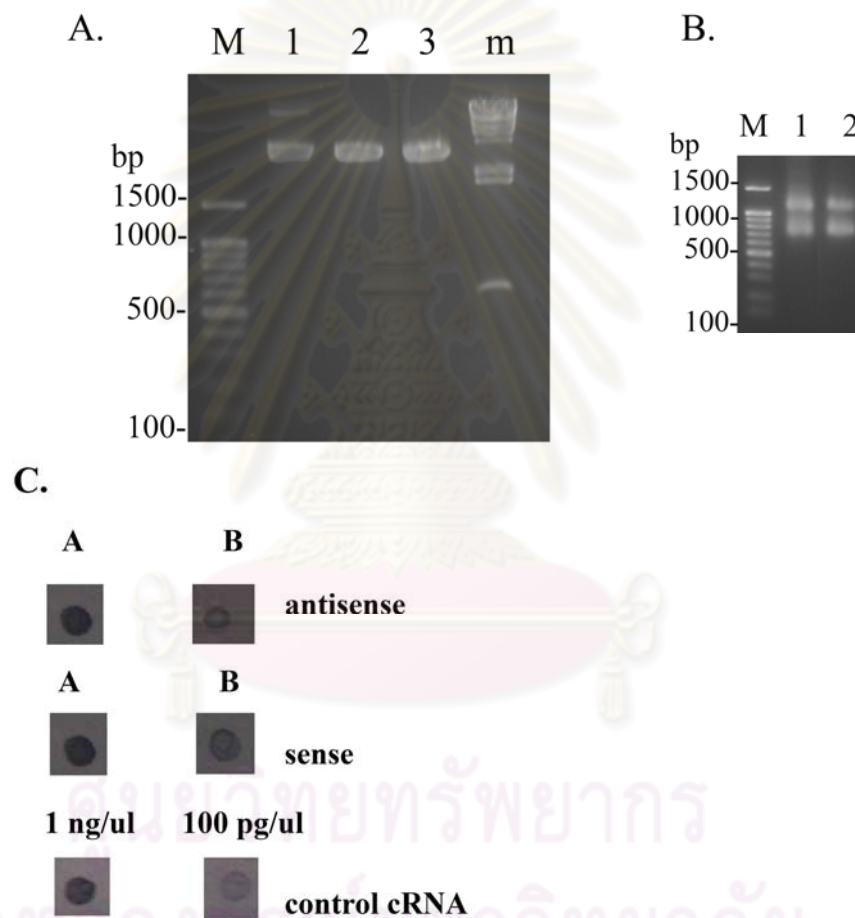


Figure 3.73 (A) The digested plasmid used as the template for synthesis of the cRNA probe of *PmCOMT* (lane 1-3, A). (B) The antisense (lane 1, B) and sense (lane 2, B) were synthesized from the gel-eluted digested plasmid template. A 100 bp ladder (lanes 1, A and B) and λ -*Hind* III was used as the DNA marker. (C) Dot blot hybridization for estimation of the concentration of the antisense, and sense *PmCOMT* and the control RNA probes.

The antisense and sense probes of these genes gave the positive signal at approximately 1 ng/ μ l. However, the sense cRNA probe of *PmFAMeT* which was lower than 1 ng/ μ l (Fig. 3.74C) and the antisense and sense probes of *PmCOMT* more than 1 ng/ μ l (Fig. 3.73C). An appropriate amount of the cRNA probe of each transcript was applied for examination of transcriptional localization using *in situ* hybridization.

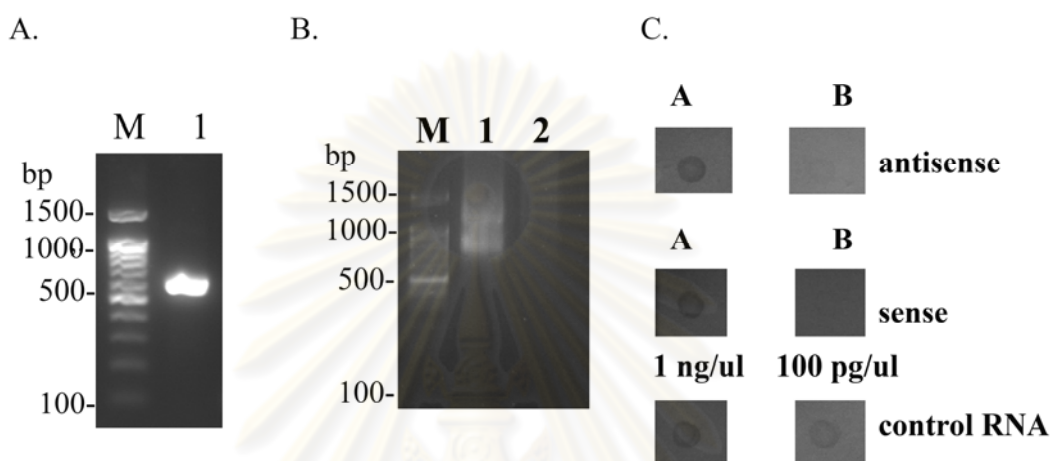


Figure 3.74 (A) The amplification product for synthesis of the cRNA probe of *PmFAMeT* (lane 1, A). (B) The antisense (lane 1, B) and sense (lane 2, B) were synthesized from the gel-eluted PCR template. A 100 bp ladder (lanes 1, A and B) was used as the DNA marker. (C) Dot blot hybridization for estimation of the concentration of the antisense, sense *PmFAMeT* and the control RNA probes.

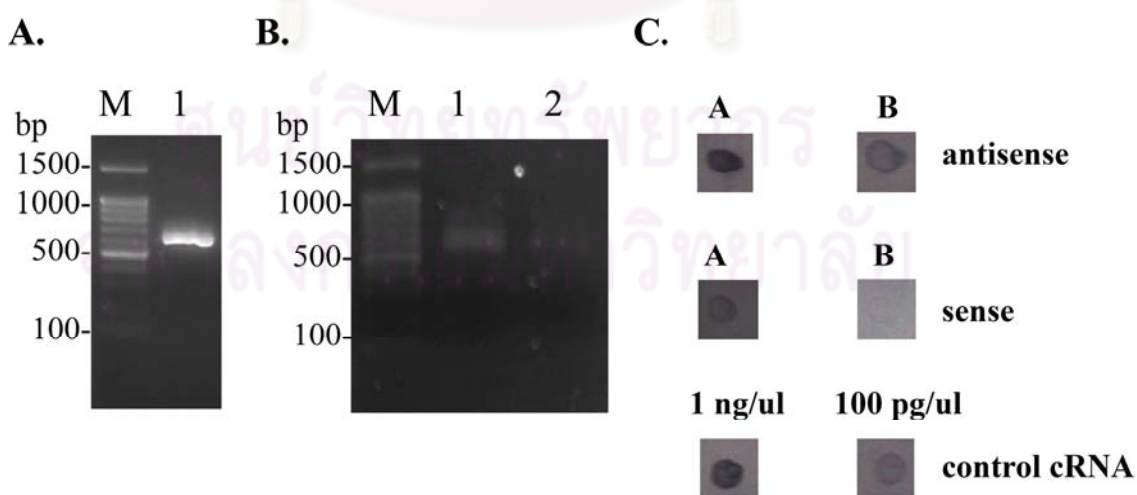


Figure 3.75 (A) The amplification product used as the template for synthesis of the cRNA probe of *PmBr-cZl* (lane 1, A). (B) The antisense (lane 1, B) and sense (lane 2, B) were synthesized from the gel-eluted PCR template. A 100 bp ladder (lanes 1, A and B) was used

as the DNA marker. (C) Dot blot hybridization for estimation of the concentration of the antisense, sense *PmBr-cZ1* and the control RNA probes.

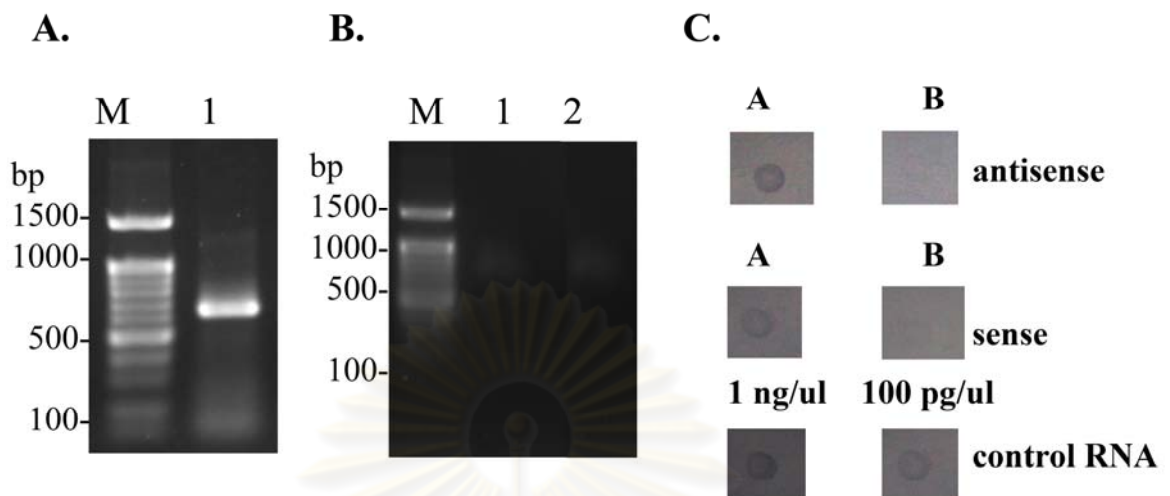


Figure. 3.76 (A) The amplification product used as the template for synthesis of the cRNA probe of *PmBr-cZ4* (lane 1, A). (B) The antisense (lane 1, B) and sense (lane 2, B) were synthesized from the gel-eluted PCR template. A 100 bp ladder (lanes 1, A and B) was used as the DNA marker. (C) Dot blot hybridization for estimation of the concentration of the antisense and sense *PmBr-cZ4* and the control RNA probes.

3.7.2 *In situ* hybridization (ISH)

The cellular localization of *PmCOMT*, *PmFAMeT*, *PmBr-cZ1* and *PmBr-cZ4* transcripts in ovaries of *P. monodon* broodstock was determined by *in situ* hybridization. No signal was observed with the sense probe for all transcripts (Figs 3.77-3.84). The positive signal was observed when the tissue sections were hybridized with the antisense probe of *PmCOMT*, *PmFAMeT*, *PmBr-cZ1* and *PmBr-cZ4*. Only the antisense *PmCOMT* probe gave the positive signal in cytoplasm of oogonia, previtellogenic oocytes and follicular cells. The remaining transcripts gave the clear signals in the cytoplasm of oogonia and previtellogenic oocytes in different stages of ovaries in both intact and eyestalk-ablated broodstock (Figs. 3.77-3.84, Table 3.28)

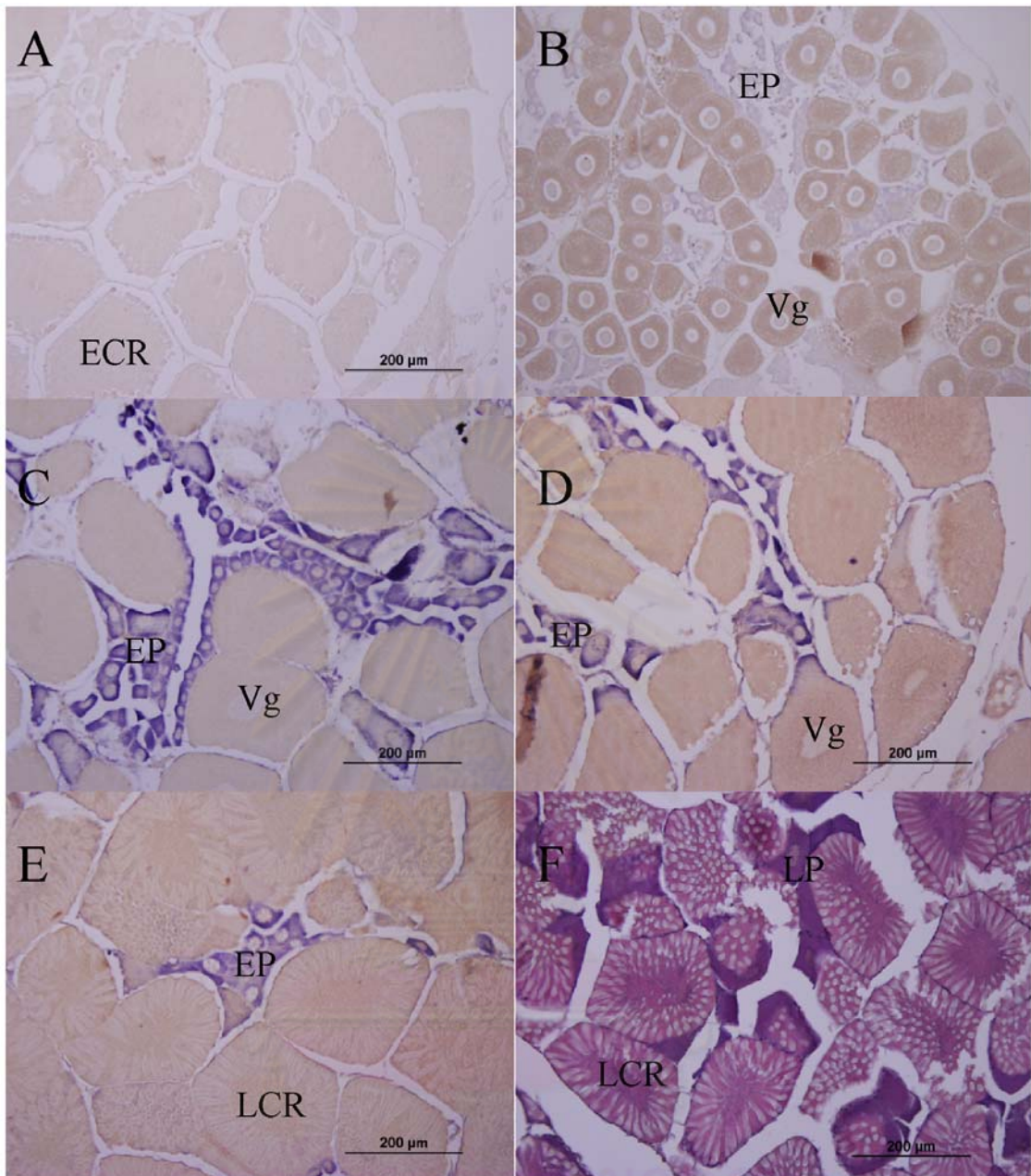


Figure 3.77 Localization of *PmCOMT* transcript during ovarian development of intact *P. monodon* broodstock visualized by *in situ* hybridization using the antisense(B-E), sense (A) cRNA probes. The conventional hematoxylin/eosin staining was carried out for identification of oocyte stages (F). EP = early previtellogenic oocytes; ECR = early cortical rod oocytes; LCR=late cortical rod oocytes; Vg = vitellogenic oocyte

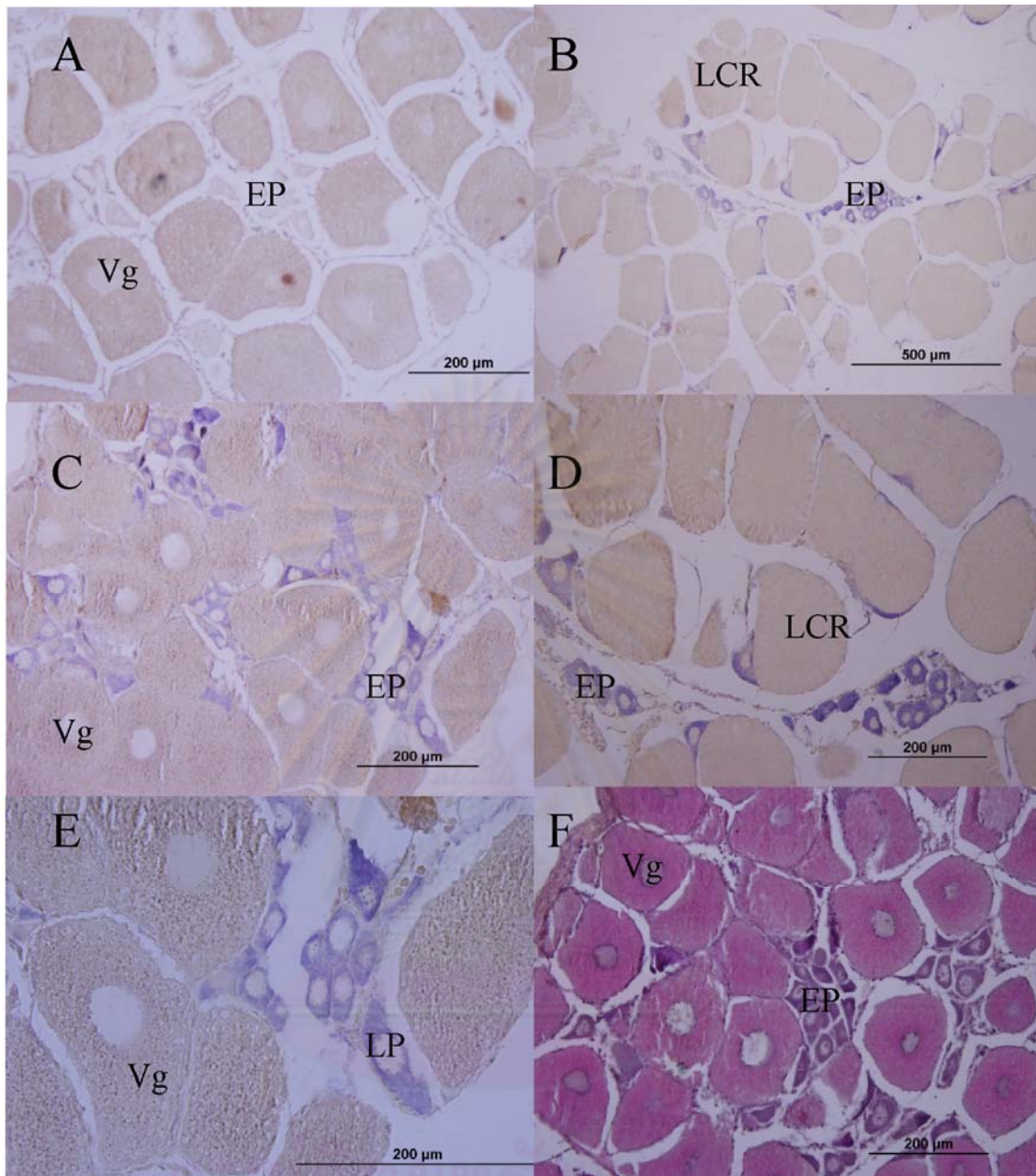


Figure 3.78 Localization of *PmCOMT* transcript during ovarian development of eyestalk-ablated *P. monodon* broodstock visualized by *in situ* hybridization using the antisense (B-E), sense (A) cRNA probes. The conventional hematoxylin/eosin staining was carried out for identification of oocyte stages (F). EP = early previtellogenic oocytes; ECR = early cortical rod oocytes; LCR=late cortical rod oocytes; Vg = vitellogenic oocyte

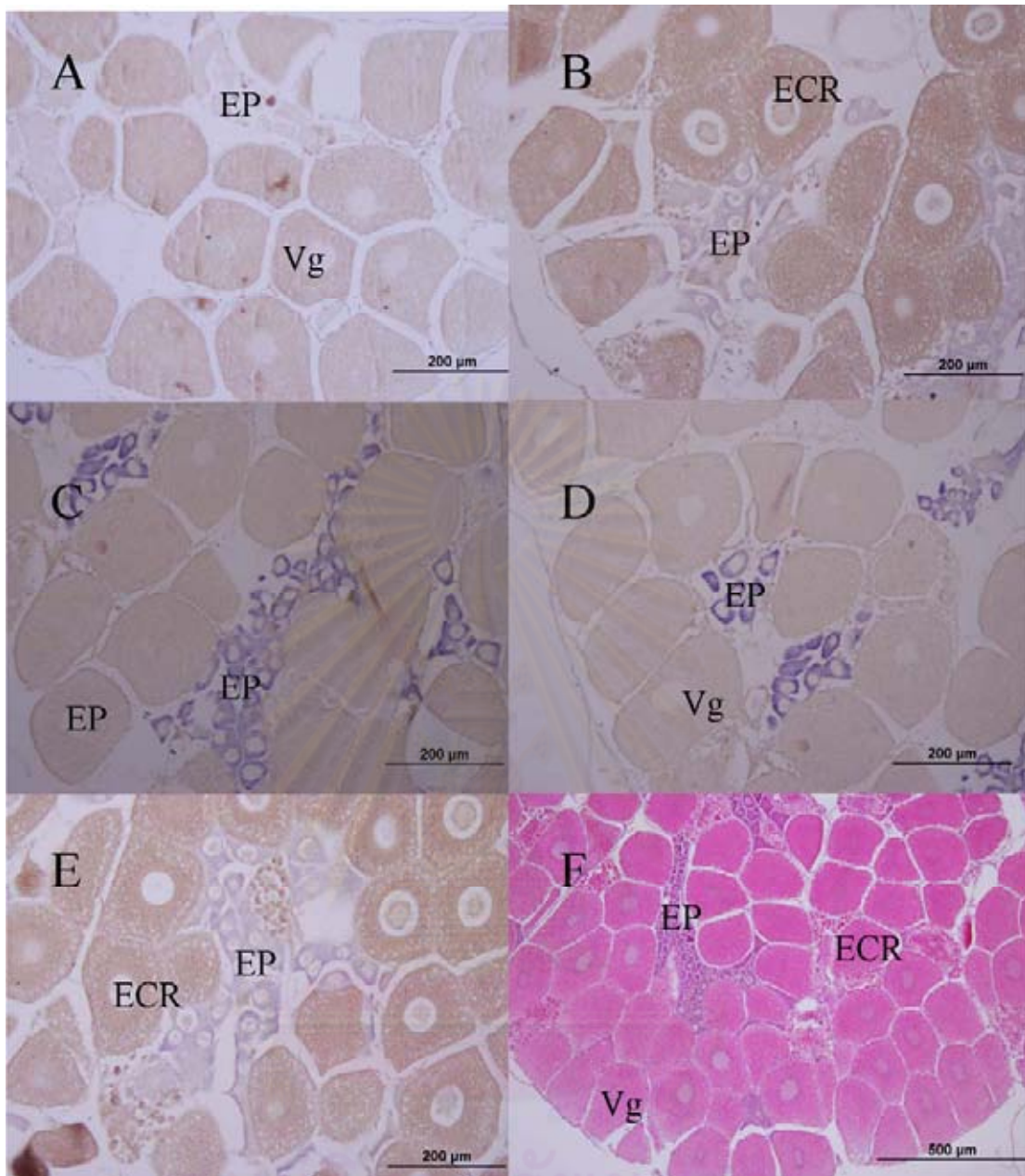


Figure 3.79 Localization of *PmFAMeT* transcript during ovarian development of intact *P. monodon* broodstock visualized by *in situ* hybridization using the antisense (B-E), sense (A) cRNA probes. The conventional hematoxylin/eosin staining was carried out for identification of oocyte stages (F). EP = early previtellogenic oocytes; ECR = early cortical rod oocytes; LCR = late cortical rod oocytes; Vg = vitellogenic oocyte

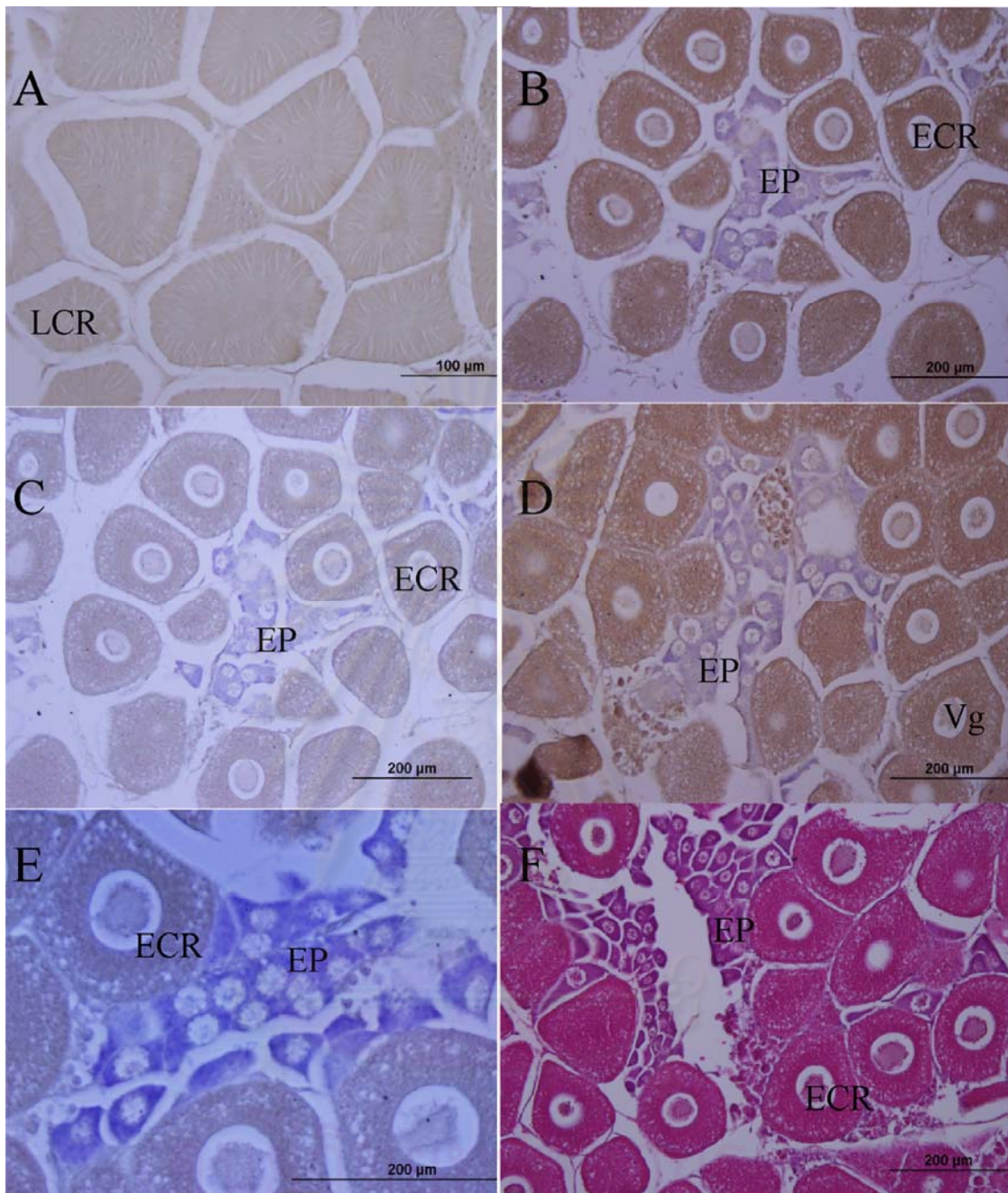


Figure 3.80 Localization of *PmFAMeT* transcript during ovarian development of eyestalk-ablated *P. monodon* broodstock visualized by *in situ* hybridization using the antisense (B-E), sense (A) cRNA probes. The conventional hematoxylin/eosin staining was carried out for identification of oocyte stages (F). EP = early previtellogenic oocytes; ECR = early cortical rod oocytes; LCR=late cortical rod oocytes; Vg = vitellogenic oocyte

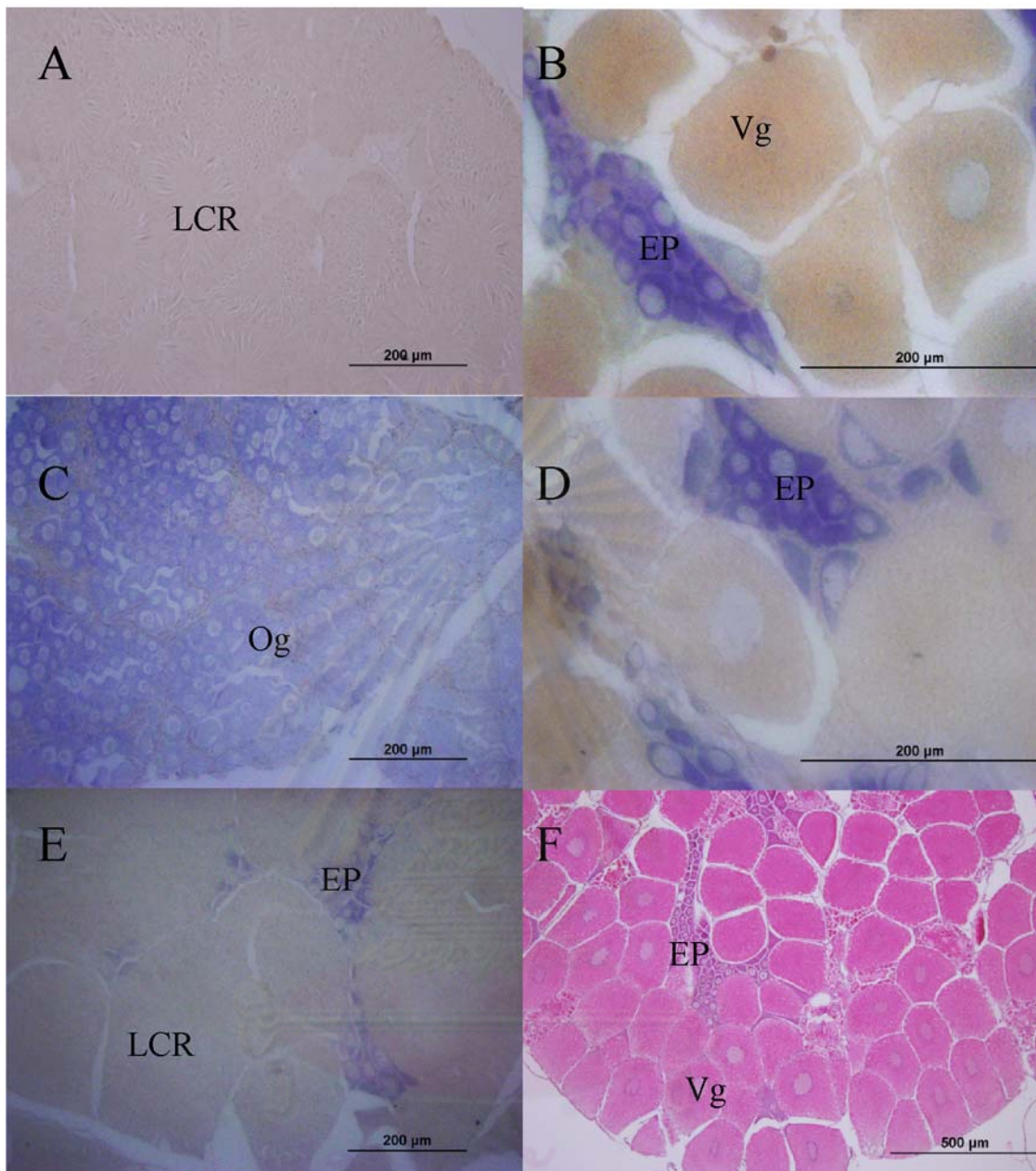


Figure 3.81 Localization of *PmBr-cZl* transcript during ovarian development of intact *P. monodon* broodstock visualized by *in situ* hybridization using the antisense(B-E), sense (A) cRNA probes. The conventional hematoxylin/eosin staining was carried out for identification of oocyte stages (F). EP = early previtellogenic oocytes; ECR = early cortical rod oocytes; LCR=late cortical rod oocytes; Vg = vitellogenic oocyte

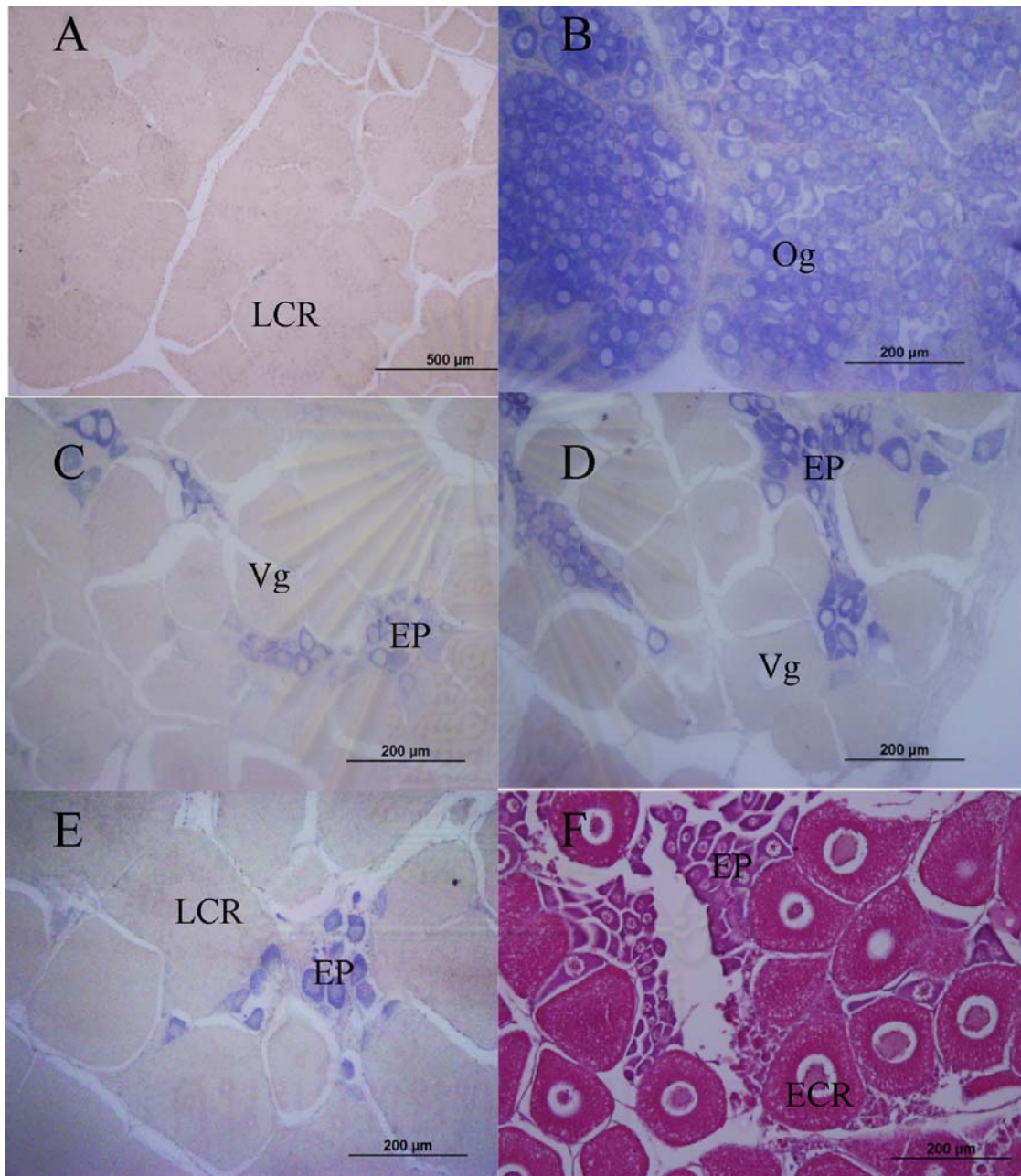


Figure 3.82 Localization of *PmBr-cZl* transcript during ovarian development of eyestalk-ablated *P. monodon* broodstock visualized by *in situ* hybridization using the antisense(B-EC), sense (A) cRNA probes. The conventional hematoxylin/eosin staining was carried out for identification of oocyte stages (F). EP = early previtellogenic oocytes; ECR = early cortical rod oocytes; LCR=late cortical rod oocytes; Vg = vitellogenic oocyte

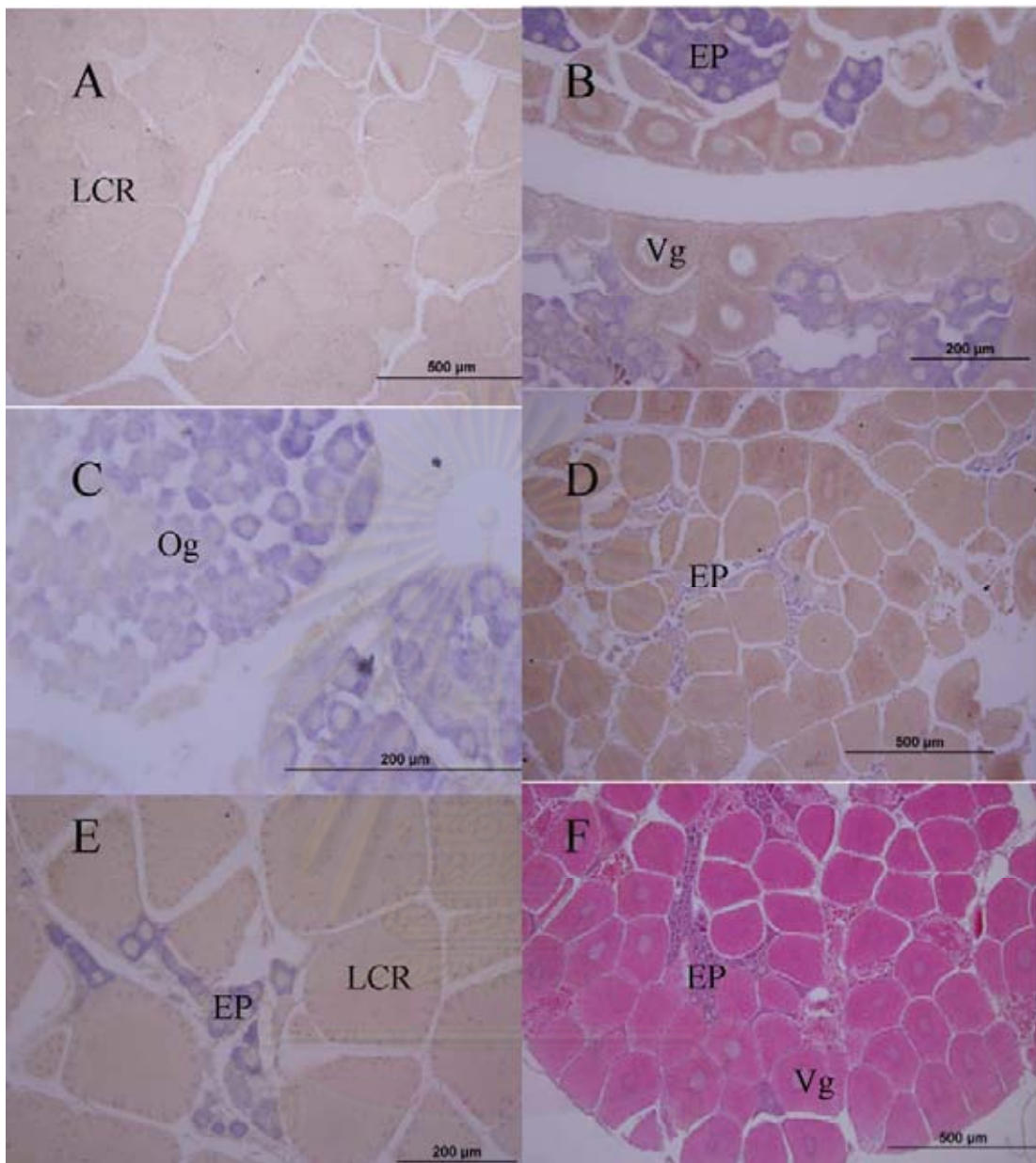


Figure 3.83 Localization of *PmBr-cZA* transcript during ovarian development of intact *P. monodon* broodstock visualized by *in situ* hybridization using the antisense(B-E), sense (A) cRNA probes. The conventional hematoxylin/eosin staining was carried out for identification of oocyte stages (F). EP = early previtellogenic oocytes; ECR = early cortical rod oocytes; LCR=late cortical rod oocytes; Vg = vitellogenic oocyte

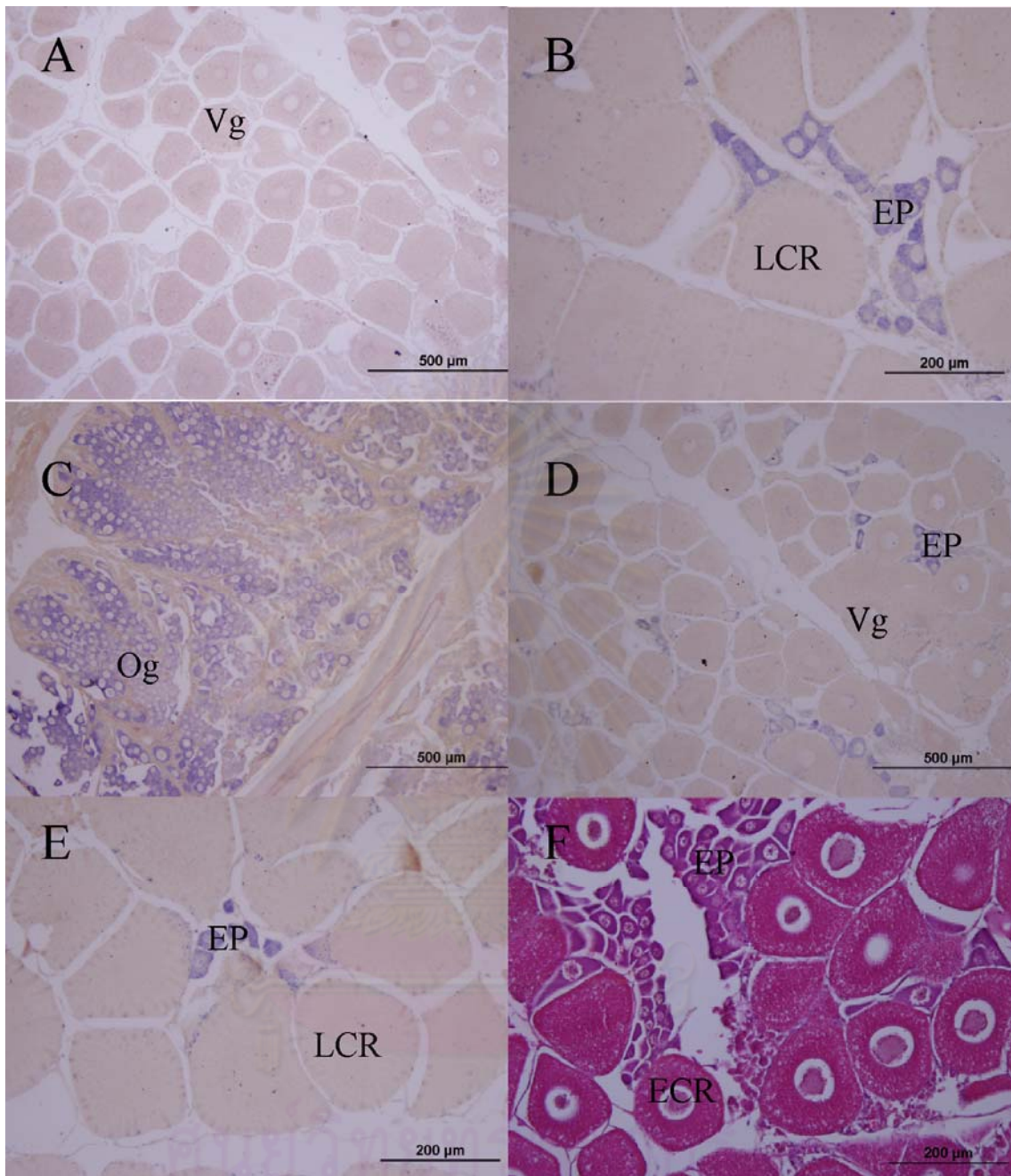


Figure 3.84 Localization of *PmBr-cZ4* transcript during ovarian development of ey *P. monodon* eyestalk-ablated broodstock visualized by *in situ* hybridization using the antisense(B-E), sense (A) cRNA probes. The conventional hematoxylin/eosin staining was carried out for identification of oocyte stages (F). EP = early previtellogenic oocytes; ECR = early cortical rod oocytes.

Table 3.28 A summary for localization of *PmCOMT*, *PmFAMeT*, *PmBr-cZ1* and *PmBr-cZ4* transcripts in ovaries of intact and eyestalk-ablated *P. monodon* broodstock determined by *in situ* hybridization.

Sample	Positions of signals			
	<i>PmCOMT</i>	<i>PmFAMeT</i>	<i>PmBr-cZ1</i>	<i>PmBr-cZ4</i>
Intact shrimp	Oogonia and previltellogenic	Previltellogenic oocytes	Oogonia and previltellogenic oocytes	Oogonia and previltellogenic oocytes
Eyestalk ablated shrimp	Oogonia, previltellogenic follicular cell surrounding stage III and IV oocytes	Oogonia and previltellogenic oocytes	Previltellogenic oocytes	Oogonia and previltellogenic oocytes

3.8 *In vitro* expression of recombinant *PmCOMT*, *PmFAMeT*, *PmBr-C Z1* and *PmBr-C Z4* using the bacterial expression system

3.8.1 Construction of recombinant plasmids in cloning and expression vector

Three recombinant plasmids carrying the full length cDNA (5'UTR + ORF + 3'UTR) of *PmCOMT*, *PmFAMeT-1* and *PmFAMeT-2* were successfully constructed for *in vitro* expression of the corresponding recombinant protein. A recombinant clone of each construct was sequenced for both directions to identify any misincorporation of nucleotides during the PCR amplification (Figs. 3.85-3.86). BlastX analysis indicated that the target genes were successfully cloned and no stop codon was misplaced to the ORF of each recombinant clone (Figs 3.87-3.89).



Figure 3.85 Agarose gel electrophoresis showing RT-PCR for amplification of the full length ORF of *PmCOMT* using the first strand cDNA of ovaries (lane 1) and hemocyte (lane 2) as the template (A) and the ORF of *PmCOMT* overhang with *Nde* I and *Bam* HI-6His tag using the first strand cDNA of ovaries as the template (lane 1, B). A 100 bp DNA ladder (lanes 1, A and B) was used as the DNA marker.

A.

```

ATGTCTTCTCTGAAAAGTTACCATAATCCCGATCCTTTGGTGCAGTATTGTGTAAATCATTTCATT
GAGATTAACCGACGCGCAAAAACGACTGAATGATGTAACCTCTGCAGCACCGTAGAGCGGCGATGT
TGGGGGCACCTGAGGTTCTGCAGTTCAATGCCAACATAATGCAGGCTATCGGGGCAAAGAAAAGTA
CTAGACATTGGGGTGTTCACAGGCGCCAGTTCACTCTCTGCTGCTCTGGCACTGCCTCCGAATGG
CAAGGTCCACGCCCTTGACATAAGTGAAGAGTTTGCCAACATAGGCAAACCGTTCTGGGAGGAAG
CTGGAGTTATCAACAAGATAAGTCTGCACATCGCTCCAGCTGCTGAGACTCTCCAGAAGTTCATT
GACGGCGGAGAAGGTGGCACCTTCGACTATGCTTTCATTGATGCCGACAAGGGGAATTATGAGCT
GTACTATGAACTTTGCCTCACTCTCTTGCGCTCTGGTGGAGTCATCGCTTTCGACAACACACTTT
GGGATGGAGCTGTGATTGACCCCACTGATCAAACCCCTGGCACAGTGGCTATTAGGAAAATTAAC

```

GAAAACTGAGAGATGACCAGAGAATCAATATTTCTTCCTGAAAATTGGTGATGGCGTGACTCT
 ATGTTTTAAAAAATGA

B.

O-methyltransferase [Fenneropenaeus chinensis]Length=221

Score = 355 bits (912), Expect = 8e-97
 Identities = 197/221 (89%), Positives = 207/221 (93%), Gaps = 0/221 (0%)
 Frame = +1

Query	1	MSSLKSYHNPDPVLVQYCVNHSRLRLTDAQKRLNDVTLQHRRAAMLGAPEVLQFNANIMQAI	180
Sbjct	1	MSSLKSY N DPLVQYCVNHSRLRLTD QKRLND TLQHRRAAMLGAPEVLQ NANIMQAI	60
Query	181	GAKKVLVDIGVFTGasslsaalalPPNGKVHALDISEEFANIGKPFWEEAGVINKISLHIA	360
Sbjct	61	GAKKVLVDIGVFTGASSLSAALALPPNGKV+ALDISEEF NIGKP+WEEAGV NKISLHIA	120
Query	361	PAAETLQKFIDGGEGGTFDYAFIDADKGNyelyyelcltllrSGGVIAFDNTLWDGAVID	540
Sbjct	121	PAAETLQKFIDAGEAGTFDYAFIDADKESYDRYYELCLILLRPGGVIAFDNTLWDGAVID	180
Query	541	PTDQTPGTVAIRKINEKLRDDQRINISFLKIGDGVTLCFKK	663
		PTDQ PGT+AIRK+NEKL+DDQRINISFL+IGDG++LCFKK	
Sbjct	181	PTDQKPGTLAIRKMNEKLRDDQRINISFLRIGDGLSLCFKK	221

Figure 3.86 (A) Nucleotide sequence of the amplified full length *PmCOMT* generated by the start-to-stop codon primers. (B) BlastX analysis of nucleotide sequence of *PmCOMT*. Primer sequences are underlined.

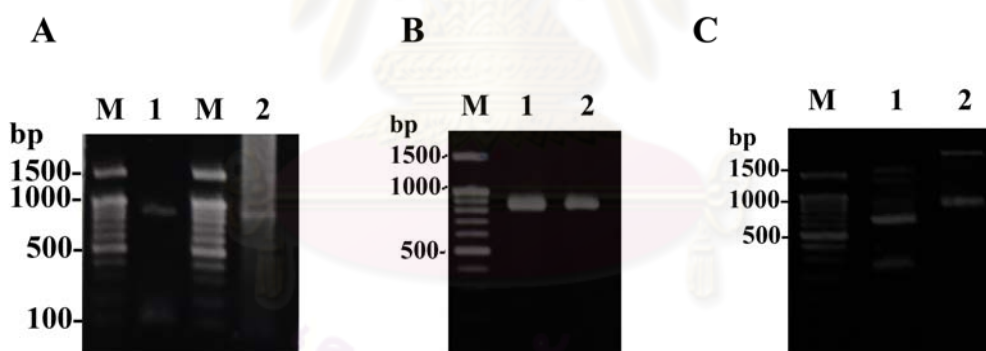


Figure 3.87 Agarose gel electrophoresis showing RT-PCR for amplification of the full length of *PmFAMeT-l* (lane 1, A) and *PmFAMeT-s* (lane 2, A), *PmFAMeT-l* (lane 1, B) and *PmFAMeT-s* (lane 2, B) overhang with *Nde I* and *Bam HI-6XHis* using the first strand cDNA from ovaries as a template. The overhang products of *PmFAMeT-l* and *PmFAMeT-s* were digested with the corresponding restriction enzymes (lanes 1 and 2, C). Lanes M = a 100 bp DNA marker.

A

TGCTCGCAAGTAACTCGGGATGGGCGATAGCTGGGCTCCCTACGGTGCCGATGAGAACAAGCAGTACCGCT
 TCAGGGACATCAAGGGCAAGACCCTCCGGTTCAGGTGAAGGCTGCCCATGATGCCACCTTGCCCTGACC
 TCAGGGGAGGAGACTGACCCTATGCTGGAGGTGTTTCATTGGCGGATGGGAAGGCGCTGCCCTCTGCCAT
 TAGGTTCAAGAAAGCTGATGACTTAACTAAAGTGGACACCCCTGACATCCTGAGTGAAGAAGAATATCGTG

AATTCTGGGTTGCCTTCGACCATGATGTTATCCGTGTTGGCAAGGGAGGCGAGTGGGAGCCATTCATGAGT
 GCCACCATTCAGAGCCTTTTCGACATCACTCATTACGGCTACAGTACTGGCTGGGGTGCTGTTGGCTGGTG
 GCAGTTCCATAGTGAGGTACACTTCCAAACTGAGGACTGCCTCACGTACAACCTTCATTCCTGTGTACGGTG
 ACACCTTTACCTTCAGTGTTCCTGTAGCAATGATGCCCATCTGGCACTCACCTCTGGCCCTGAGGAGACC
 ACACCCATGTATGAAGTGTTTCATTGGTGGTTGGGAAAACCAGCACTCTGCCATTCTGCTCAGCAAGGAGGG
 AAGGGGATCTGGCGAGGACATGATCAAGGTCGACACCCCCGACGTTGTCTGCTGCGAAGAGGAGAGGAAGT
 TCTACGTCAGCTTCAAGGACGGCCATATCANGGTGGGATAACCAGGACAGTGATCCCTTCATGGAGTGGACT
 GACCTGAGCCATGGAAGATCACCCACATTGGTTACTGCACAGGCTGGGGAGCAACTGGAAAAGTGGAAAGT
 CGAATTTTAAGTCTGCTTTGTGGCTTTGTTTAC

B

farnesoic acid O-methyltransferase [Penaeus monodon]

Length=280

Score = 602 bits (1551), Expect = 2e-170

Identities = 277/280 (98%), Positives = 277/280 (98%), Gaps = 0/280 (0%)

Frame = +2

Query	20	MGDSWAPYGADENKQYRFRDIKGTILRFQVKAHAHDAHLALTSGEEETDPMLEVFIGGWEG	199
		MGDSWA YG DENKQYRFRDIKGTILRFQVKAHAHDAHLALTSGEEETDPMLEVFIGGWEG	
Sbjct	1	MGDSWASYGTDENKQYRFRDIKGTILRFQVKAHAHDAHLALTSGEEETDPMLEVFIGGWEG	60
Query	200	AASAIRFKKADDLTKVDTPDILSEEEYREFWVAFDHDVIRVGKGGWEPEFMSATIPPEFD	379
		AASAIRFKKADDLTKVDTPDILSEEEYREFWVAFDHDVIRVGKGGWEPEFMSATIPPEFD	
Sbjct	61	AASAIRFKKADDLTKVDTPDILSEEEYREFWVAFDHDVIRVGKGGWEPEFMSATIPPEFD	120
Query	380	ITHYGYSTGWGAVGWWQFHSEVHFQTEDCLTYNFIPVYGDFTFVSVACSND AHLALTSGP	559
		ITHYGYSTGWGAVGWWQFHSEVHFQTEDCLTYNFIPVYGDFTFVSVACSND AHLALTSGP	
Sbjct	121	ITHYGYSTGWGAVGWWQFHSEVHFQTEDCLTYNFIPVYGDFTFVSVACSND AHLALTSGP	180
Query	560	EETTPMYEVFIGGWENQHSAIRLSKEGRSGEDMIKVDTPDVVCC EERKFYVSFKD GHI	739
		EETTPMYEVFIGGWENQHSAIRLSKEGRSGEDMIKVDTPDVVCC EERKFYVSFKD GHI	
Sbjct	181	EETTPMYEVFIGGWENQHSAIRLSKEGRSGEDMIKVDTPDVVCC EERKFYVSFKD GHI	240
Query	740	XVGYQSDPFMEWTDPEPWKITHIGYCTGWGATGKWKFEF 859	
		VG YQSDPFMEWTDPEPWKITHIGYCTGWGATGKWKFEF	
Sbjct	241	RVGYQSDPFMEWTDPEPWKITHIGYCTGWGATGKWKFEF 280	

Figure 3.88 Nucleotide sequence of the full length of recombinant *PmFAMeT-1* (A) and its similarity analysis using BlastX (B). Primer sequences are underlined.

A.

TGCTCGCAAGTAACTCGGGATGGGCGATAGCTGGGCTTCCTTCGGTACCGATGAGAACAAGCAGTACCGCT
 TCAGGGACATCAAGGGCAAGACCCTCCGGTTCAGGTGAAGGCTGCCCATGATGCCACCTTGCCCTGACC
 TCAGGGGAAGAGGAGACTGACCCTATGCTGGAGGTGTTTCATTGGCGGATGGGAAGGCGCTGCCTCTGCCAT
 TAGGTTCAAGAAAAGCTGATGACTTAACTAAAGTGGACACCCCTGACATCCTGAGTGAAGAAGATATCGTG
 AATTCTGGGTTGCCTTCGACCATGATGTTATCCGTGTTGGCAAGGGAGGCGAGTGGGAGCCATTCATGAGT
 GCCACCATTCAGAGCCTTTTCGACATCACTCATTACGGCTACAGTACTGGCTGGGGTGCTGTTGGTGGTG
 GCAGTTCCATAGTGAGGTACACTTCCAAACTGAGGACTGCCTCACGTACAACCTTCATTCCTGTGTACGGTG
 ACACCTTTACCTTCAGTGTTCCTGTAGCAATGATGCCCATCTGGCACTCACCTCTGGCCCTGAGGAGACC
 ACACCCATGTATGAAGTGTTTCATTGGTGGTTGGGAAAACCAGCACTCTGCCATTCTGCTCAGCAAGGGCGA
 GGACATGATCAAGGTCGACACCCCCGACGTTGTCTGCTGCGAAGAGGAGAGGAAGTTCACGTCAGCTTCA
 AGGACGGCCATATCAGGGTGGGATAACCAGGACAGTGATCCCTTCATGGAGTGGACTGACCCTGAGCCATGG
 AAGATCACCCACATTGGTTACTGCACAGGCTGGGGAGCAACTGGAAAGTGGAAAGTTCGAATTTTAAGTCTCT
GCTTTGTGGCTTTGTTTAC

B

farnesoic acid O-methyltransferase [Penaeus monodon]

Length=280


```

Score = 590 bits (1521), Expect = 7e-167
Identities = 274/280 (97%), Positives = 275/280 (98%), Gaps = 5/280 (1%)
Frame = +2

Query 20  MGDSWASFGTDENKQYRFRDIK GKTLRFQV KAAHDAHLALTSGEEETDPMLEVF IGGWEG 199
Sbjct 1    MGDSWAS+GTDENKQYRFRDIK GKTLRFQV KAAHDAHLALTSGEEETDPMLEVF IGGWEG 60

Query 200 AASAIRFKKADDLTKV DTPDILSEEEYREFWVAFDHDVIRV GKGGEWEPFMSATIPEPFD 379
Sbjct 61  AASAIRFKKADDLTKV DTPDILSEEEYREFWVAFDHDVIRV GKGGEWEPFMSATIPEPFD 120

Query 380  ITHYGYSTGWGAVGWWQFHSEVHFQTEDCLTYNFI PVYGDFTFFSVACSNDAHLALTSGP 559
Sbjct 121 ITHYGYSTGWGAVGWWQFHSEVHFQTEDCLTYNFI PVYGDFTFFSVACSNDAHLALTSGP 180

Query 560  EETTPMYEVFIGGWENQHSAIRLSK-----GEDMIKVDTPDVVCC EERKFYVSFKD GHI 724
Sbjct 181  EETTPMYEVFIGGWENQHSAIRLSK      GEDMIKVDTPDVVCC EERKFYVSFKD GHI 240

Query 725  RVGYQSDPFMEWTDPEPWKITHIGYCTGWGATGKWKFEF 844
Sbjct 241  RVGYQSDPFMEWTDPEPWKITHIGYCTGWGATGKWKFEF 280

```

Figure 3.89 Nucleotide sequence of the full length of recombinant *PmFAMeT-s* (A) and its similarity analysis using BlastX (B). Primer sequences are underlined.

The forward primer containing the *Nde* I restriction site and the reverse primer containing the *Bam* HI restriction site and a 6XHis tag of each gene were designed. The cDNA representing each of the complete ORFs of *PmCOMT*, *PmFAMeT* and *PmFAMeT-s* using the recombinant plasmid of each gene as the template. The amplified full length cDNA was cloned into pGEM-T easy vector, transformed into *E. coli* JM109 and sequenced to confirm the orientation and nucleotide sequence of recombinant clone (Fig. 3.90). The amplification product was digested with *Nde* I and *Bam* HI, eluted from the gel and ligated into pET15 expression vector. The recombinant clone was transformed into *E. coli* JM109 and subsequently into *E. coli* BL21(DE3) codon+ RIPL (Figs. 3.90-3.92)

For the amplified full length ORF of *PmFAMeT-l* and *PmFAMeT-s*, colony PCR was carried out and the amplification products were digested with *Xho* II (which recognized the 15 bp insertion in *PmFAMeT-l*) to classify the short and long forms of the insert. The selected clones were sequenced to confirm the orientation of the recombinant clones.

A.

ATATCCGATCTTTGGTGCAGTATTGTGTAATCATTTCATTGAGATTAACCGACGCGCAAAAACGAC
TCAATGATGTAACCTCTGCAGCACCGTAGAGCGGCGATGTTGGCCGACCTGAGGTTCTGCAGTTC
AATGCCAACATAATGCAGGCTATCGGGGCAAAGAAAAGTACTAGACATTGGGGTGTTCACAGGCGC
CAGTTCACTCTCTGCTGCTCTGGCACTGCCTCCGAATGGCAAGGTCCACGCCCTTGACATAAGTG
AAGAGTTTGCACATAGGCAAACCGTTCTGGGAGGAAGCTGGAGTTATCAACAAGATAAGTCTG
CACATCGCTCCAGCTGCTGAGACTCTCCAGAAGTTCATTGACGCGGAGAAGGTGGCACCTTCGA
CTATGCTTTTCATTGATGCCGACAAGGGGAATTATGAGCTGTACTATGAACTTTGCCTCACTCTCT
TGCGCTCTGGTGGAGTCATCGCTTTGACAACACACTTTGGGATGGAGCTGTGATTGACCCCACT
GATCAAACCCCTGGCACAGTGGCTATTAGGAAAATTAACGAAAAACTGAGAGATGACCAGAGAAT
CAATATTTCTTCTGAAAATTGGTGATGGCGTGACTCTATGTTTTAAAAAACATCATCATCATC
ATCATTGAGGATCC

B.

O-methyltransferase [Fenneropenaeus chinensis]

Length=221

Score = 321 bits (823), Expect = 4e-86

Identities = 180/203 (88%), Positives = 190/203 (93%), Gaps = 0/203 (0%)

Frame = +2

Query	29	NHSLRLTDAQRLNDVTLQHRRRAAMLAAPEVLQFNANIMQAIGAKKVLIDIGVFTG	208
		NHSLRLTD QKRLND TLQHRRRAAML APEVLQ NANIMQAIGAKKVLIDIGVFTG	
Sbjct	19	NHSLRLTDVQKRLNDATLQHRRRAAMLGAPEVLQLNANIMQAIGAKKVLIDIGVFTG	78
Query	209	aalalPPNGKVHALDISEEFANIGKPFWEEAGVINKISLHIAPAAETLQKFIDGGEGGTF	388
		AALALPPNGKV+ALDISEEF NIGKP+WEEAGV NKISLHIAPAAETLQKFID GE GTF	
Sbjct	79	AALALPPNGKVYALDISEEFTNIGKPYWEEAGVSNKISLHIAPAAETLQKFIDAGEAGTF	138
Query	389	DYAFIDADKGNyellyelcltllrSGGVIAFDNTLWDGAVIDPTDQTPGTVAIRKINEKL	568
		DYAFIDADK +Y+ YYELCL LLR GGVIAFDNTLWDGAVIDPTDQ PGT+AIRK+NEKL	
Sbjct	139	DYAFIDADKESYDRYYELCLILLRPGGVIAFDNTLWDGAVIDPTDQKPGTLAIRKMNEKL	198
Query	569	RDDQRINISFLKIGDGVTLCFKK 637	
		+DDQRINISFL+IGDG++LCFKK	
Sbjct	199	KDDQRINISFLRIGDGLSLCFKK 221	

Figure 3.90 Nucleotide sequence of the amplified ORF of *PmCOMT* overhang with *Nde* I- *Bam* HI-6XHis sequenced with the *PmCOMT*-ORF/*Nde* I-F primer (A) and compared with sequences in the GenBank database using BlastX results of nucleotide sequence of the ORF of *PmCOMT* overhang with *Nde* I- *Bam* HI-6His tag (B). Primer sequences are underlined.

A.

GGACGGGCATAAAGAGTACGCTTCGGGACATCAAGGGCAAGACCCCTCCGGTTCAGGTGAAGCCCCCTCAT
GATGCCACCTTGCCCTGACCTCAGGGGAGGAGGACCCCTGACCCATGCTGGAGGTGTTTCATTGGCGGATG
GGAAGGCGCTGCTCTGCCATTAGGTTCAAGAAAGCTGATGACTTAACTAAAGTGGACACCCCTGACATCC
TGAGTGAAGAAGAATATCGTGAATTCTGGGTTGCCTTCGACCATGATGTTATCCGTGTTGGCAAGGGGAGGC
GAGTGGGAGCCATTTCATGAGTGCCACCATCCAGAGCCTTTCGACATCACTCATTACGGCTACAGTACTGG
CTGGGGTGTGTTGGCTGGTGGCAGTTCATAGTGGAGTTACACTTCCAAACTGAGGACTGCCTCACGTACA
ACTTCATTCTGTGTACGGTGACACCTTTACCTTCAGTGTTGCCTGTAGCAATGATGCCATCTGGCACTC
ACCTCTGGCCCTGAGGAGACCACCCATGTATGAAGTGTTCATTGGTGGTTGGGAAAACCAGCACTCTGC
CATTCGTCTCAGCAAGGAGGGAAGGGGATCTGGCGAGGACATGATCAAGGTCGACACCCCGACGTTGTCT

GCTGCGAAGAGGAGAGGAAGTTCTACGTCAGCTTCAAGGACGGCCATATCAGGGTGGGATACCAGGACAGT
 GATCCCTTCATGGAGTGGACTGACCCTGAGCCATGGAAGATCACCCACATTGGTTACTGCACAGGCTGGGG
 AGCAAAC TGGAAGTGGAAAGTTCGAATTCATCATCATCATCATTAAGGATCC

B.

farnesoic acid O-methyltransferase [Penaeus monodon]
 Length=280

Score = 558 bits (1437), Expect = 4e-157
 Identities = 257/262 (98%), Positives = 258/262 (98%), Gaps = 0/262 (0%)
 Frame = +3

Query	24	RDIKGKTLRFQVKAPHDAHLALTSGEEDPDPMLEVFIGGWEGAASAIRFKKADDLTKVDT	203
		RDIKGKTLRFQVKA HDAHLALTSGEE+ DPMLEVFIGGWEGAASAIRFKKADDLTKVDT	
Sbjct	19	RDIKGKTLRFQVKAHDAHLALTSGEEETDPMLEVFIGGWEGAASAIRFKKADDLTKVDT	78
Query	204	PDILSEEEYREFWVAFDHDVIRVGKGGWEWPFMSATIEPFDITHYGYSTGWGAVGWQF	383
		PDILSEEEYREFWVAFDHDVIRVGKGGWEWPFMSATIEPFDITHYGYSTGWGAVGWQF	
Sbjct	79	PDILSEEEYREFWVAFDHDVIRVGKGGWEWPFMSATIEPFDITHYGYSTGWGAVGWQF	138
Query	384	HSEVHFQTEDCLTYNFIPVYGDFTF SVACSNDAHLALTSGPEETTPMYEVFIGGWENQH	563
		HSEVHFQTEDCLTYNFIPVYGDFTF SVACSNDAHLALTSGPEETTPMYEVFIGGWENQH	
Sbjct	139	HSEVHFQTEDCLTYNFIPVYGDFTF SVACSNDAHLALTSGPEETTPMYEVFIGGWENQH	198
Query	564	SAIRLSKEGRSGEDMIKVDTPDVVCC EE ERKFYVSFKDGHIRVGYQSDPFMEWTDPEP	743
		SAIRLSKEGRSGEDMIKVDTPDVVCC EE ERKFYVSFKDGHIRVGYQSDPFMEWTDPEP	
Sbjct	199	SAIRLSKEGRSGEDMIKVDTPDVVCC EE ERKFYVSFKDGHIRVGYQSDPFMEWTDPEP	258
Query	744	WKITHIGYCTG W GANWKKWKF 809	
		WKITHIGYCTG W GA WKKWKF	
Sbjct	259	WKITHIGYCTG W GATGKWKWKF 280	

Score = 132 bits (331), Expect = 6e-29
 Identities = 70/136 (51%), Positives = 87/136 (63%), Gaps = 6/136 (4%)
 Frame = +3

Query	399	FQTEDCLTYNFIPVYGDFTF SVACSNDAHLALTSGPEETTPMYEVFIGGWENQHSAIRL	578
		+ T++ Y F + G T F V ++DAHLALTSG EET PM EVFIGWE SAIR	
Sbjct	8	YGTDENKQYRFRDIKGKTLRFQVKAHDAHLALTSGEEETDPMLEVFIGGWEGAASAIRF	67
Query	579	SKEGRSGEDMIKVDTPDVVCC EE ERKFYVSFKDGHIRVGY-QSDPFMEWTDPEPWKIT	755
		K +D+ KVDTPD++ EE R+F+V+F IRVG + +PFM T PEP+ IT	
Sbjct	68	KK-----ADDLTKVDTPDILSEEEYREFWVAFDHDVIRVGKGGWEWPFMSATIEPFDIT	122
Query	756	HIGYCTG W GANWKKWKF 803	
		H GY TGWGA W+F	
Sbjct	123	HGYSTGWGAVGWQF 138	

Figure 3.91 Nucleotide sequence of the complete ORF of *PmFAMeT-1* overhang with *Nde* I- *Bam* HI-6XHis (A) and its similarity analysis using BlastX (B). Primer sequences are underlined.

A.

GGAAGCCTGAGAATTCNTCTGAATATTTTGGTTAACTTTAAGAAGGAGATATACCATGGGCAGCAGCCATC
 ATCATCATCATCACAGCAGCGGCCTGGTGCCGCGCGGCAGCCATATGGGCGAGAGCTGGGCTTCCTTCGGT
 ACCGATGAGAACAAGCAGTACCGCTTCAGGGACATCAAGGGCAAGACCCCTCCGGTTCCAGGTGAAGGCTGC
 CCATGATGCCACCTTGCCCTGACCTCAGGGGAAGAGGAGACTGACCCTATGCTGGAGGTTCATTGGCG
 GATGGGAAGGCGCTGCTCTGCCATTAGGTTCAAGAAAGCTGATGACTTAACTAAAGTGGACACCCCTGAC

ATCCTGAGTGAAGAAGAATATCGTGAATTCTGGGTTGCCCTTCGACCATGATGTTATCCGTGTTGGCAAGGG
 AGGCGAGTGGGAGCCATTCATGAGTGCCACCATTCCAGAGCCTTTCGACATCACTCATTACGGCTACAGTA
 CTGGCTGGGGTGCTGTTGGTTGGTGGCAGTTCATAGTGAGGTACACTTCCAAACTGAGGACTGCCTCAGC
 TACAACTTCATTCCTGTGTACGGTGACACCTTTACCTTCAGTGTTCCTGTAGCAATGATGCCCATCTGGC
 ACTCACCTCTGGCCCTGAGGAGACCACCCATGTATGAAGTGTTCATTGGTGGTTGGGAAAACCAGCACT
 CTGCCATTCGTCTCAGCAAGGGCGAGGACATGATCAAGGTCGACACCCCGACGTTGTCTGTGCGAAGAG
 GAGAGGAAGTTCTACGTCAGCTTCAAGGACGGCCATATCAGGTTGGGATACCAGGACAGTGATCCCTTCAT
 GGAG

B.

farnesoic acid O-methyltransferase [Penaeus monodon]

Length=280

Score = 518 bits (1333), Expect = 3e-145
 Identities = 244/252 (96%), Positives = 247/252 (98%), Gaps = 5/252 (1%)
 Frame = +2

Query 119 MGESWASFGTDENKQYRFRDIKGTLRFQVKA^{AA}HAHLALTSGEEETDPMLEVF^{IG}GWEG 298
 MG+SWAS+GTDENKQYRFRDIKGTLRFQVKA^{AA}HAHLALTSGEEETDPMLEVF^{IG}GWEG
 Sbjct 1 MGDSWASYGTDENKQYRFRDIKGTLRFQVKA^{AA}HAHLALTSGEEETDPMLEVF^{IG}GWEG 60

Query 299 AASAIRFKKADDLTKVDTPDILSEEEYREFWVAFDHDVIRVGKGGEWEPFMSATIP^{EP}FD 478
 AASAIRFKKADDLTKVDTPDILSEEEYREFWVAFDHDVIRVGKGGEWEPFMSAT^{IP}EPFD
 Sbjct 61 AASAIRFKKADDLTKVDTPDILSEEEYREFWVAFDHDVIRVGKGGEWEPFMSATIP^{EP}FD 120

Query 479 ITHYGYSTGWGAVGWWQFHSEVHFQTEDCLTYNFIPVYGDFTFSVACSNDAHLALTS^{GP} 658
 ITHYGYSTGWGAVGWWQFHSEVHFQTEDCLTYNFIPVYGDFTF^{SV}ACSNDAHLALTS^{GP}
 Sbjct 121 ITHYGYSTGWGAVGWWQFHSEVHFQTEDCLTYNFIPVYGDFTFSVACSNDAHLALTS^{GP} 180

Query 659 EETTPMYEVFIGGWENQHSAIRLSK-----GEDMIKVDTPDVVCEEERKFYVSFKD^{GHI} 823
 EETTPMYEVFIGGWENQHS^{AIRLSK} GEDMIKVDTPDVVCEEERKFYVSFKD^{GHI}
 Sbjct 181 EETTPMYEVFIGGWENQHSAIRLSK^{EGRGSGEDMIKVDTPDVVCEEERKFYVSFKD}GHI 240

Query 824 RLGYQSDPFME 859
 R+GYQSDPFME
 Sbjct 241 RVGYQSDPFME 252

Score = 137 bits (345), Expect = 1e-30
 Identities = 72/136 (52%), Positives = 87/136 (63%), Gaps = 6/136 (4%)
 Frame = +2

Query 140 FGTDENKQYRFRDIKGTLRFQVKA^{AA}HAHLALTSGEEETDPMLEVF^{IG}WEGAASAIR^F 319
 F T++ Y F + G T F V ++DAHLALTSG EET PM EVFIGGWE SAIR
 Sbjct 144 FQTEDCLTYNFIPVYGDFTFSVACSNDAHLALTS^{GPEETTPMYEVFIGGWENQHS}AIRL 203

Query 320 KK-----ADDLTKVDTPDILSEEEYREFWVAFDHDVIRVGKGGEWEPFMSATIP^{EP}FDIT 484
 K +D+ KVDTPD++ EE R+F+V+F IRVG +PFM T PEP+ IT
 Sbjct 204 SKEGRGSGEDMIKVDTPDVVCEEERKFYVSFKDGHIRVGYQDS-DPFMEWTDPEP^{WKIT} 262

Query 485 HGYSTGWGAVGWWQF 532
 H GY TGWGA G W+F
 Sbjct 263 HIGYCTGWGATGKWKF 278

Figure 3.92 Nucleotide sequence of the complete ORF of *PmFAMeT-s* overhang with *Nde* I- *Bam* HI-6XHis (A) and its similarity analysis using BlastX (B). Primer sequences are underlined.

3.8.2 Optimization of conditions for an *in vitro* expression of rPmCOMT, rPmFAMeT-1, and rPmFAMeT-s protein

Expression of 3 recombinant clones of PmCOMT, PmFAMeT-1 and PmFAMeT-s cultured at 37°C and induced with 0.4 mM IPTG for 1 and 6 hours were examined. No obvious difference on the expression level was observed when the recombinant clones of a particular protein was induced with IPTG for different period of time (Figs.3.93-3.95).

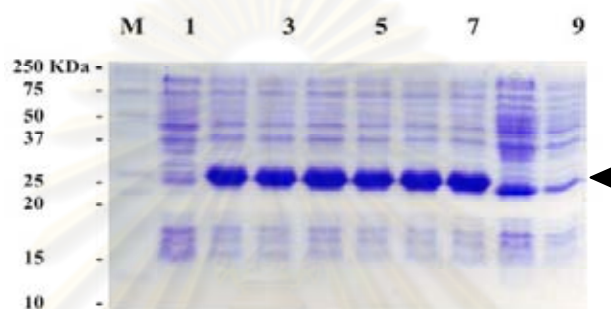


Figure 3.93 SDS-PAGE showing *in vitro* expression of rPmCOMT from the recombinant clones at 3 and 6 hours after induction with 0.4 mM IPTG (lanes 2-3, 4-5 and 6-7), respectively. A pET15b vector in *E. coli* BL21-CodonPlus (DE3)-RIPL (lane 8) and *E. coli* BL21-CodonPlus (DE3)-RIPL (lane 9) were included as the control. Lane M = the protein standard marker.

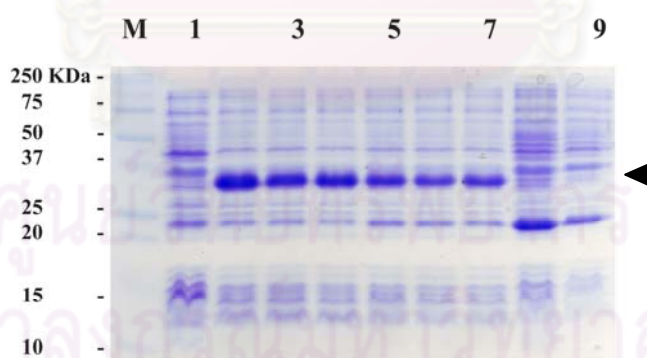


Figure 3.94 SDS-PAGE showing *in vitro* expression of rPmFAMeT-1 from the recombinant clones at 3 and 6 hours after induction with 0.4 mM IPTG (lanes 2-3, 4-5 and 6-7), respectively. A pET15b vector in *E. coli* BL21-CodonPlus (DE3)-RIPL (lane 8) and *E. coli* BL21-CodonPlus (DE3)-RIPL (lane 9) were included as the control. Lane M = the protein standard marker.

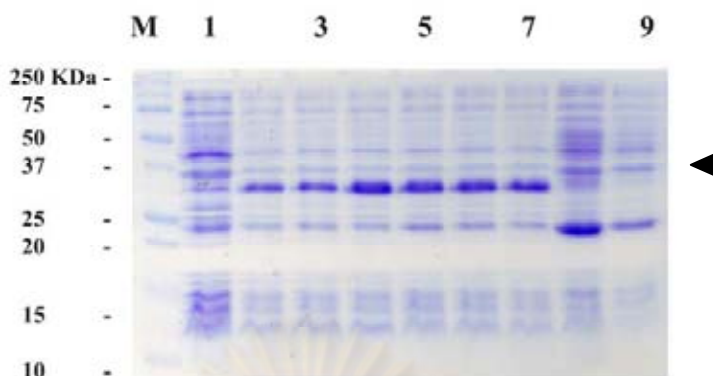


Figure 3.95 SDS-PAGE showing *in vitro* expression of rPmFAMeT-s from the recombinant clones at 3 and 6 hours after induction with 0.4 mM IPTG (lanes 2-3, 4-5 and 6-7), respectively. A pET15b vector in *E. coli* BL21-CodonPlus (DE3)-RIPL (lane 8) and *E. coli* BL21-CodonPlus (DE3)-RIPL (lane 9) were included as the control. Lane M = the protein standard marker.

Only one recombinant clone of each recombinant protein was selected and cultured at 37°C. The optimal concentration of IPTG (0.4, 0.6, 0.8 and 1.0 mM) for the production of each recombinant protein after IPTG induction for 3 and 6 hours was examined (Figs 3.96-3.98). No different effect of IPTG concentration on expression of rPmCOMT, rPmFAMeT-1 and rPmFAMeT-s was observed. Therefore, the IPTG concentration at 0.4 mM was used to induce the overexpression of these recombinant clones.

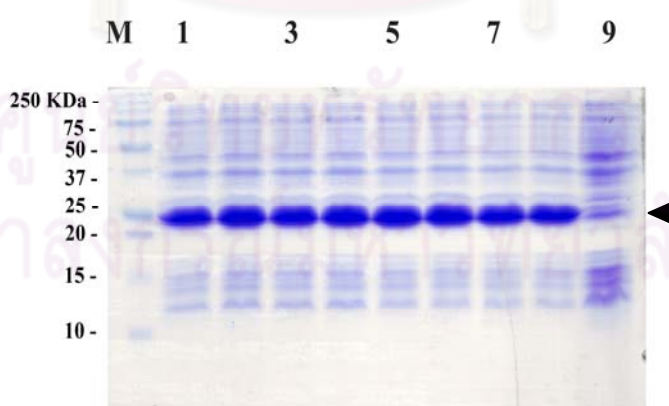


Figure 3.96 SDS-PAGE showing *in vitro* expression of rPmCOMT after induced by 0.4, 0.6, 0.8 and 1 mM IPTG for 3 (lanes 1-4) and 6 hr (lane 5-8), respectively. A pET15b vector in *E. coli* BL21-CodonPlus (DE3)-RIPL (lane 9) was included as the control.

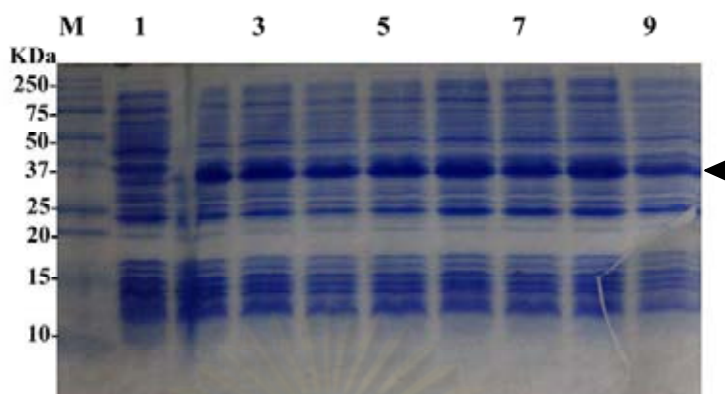


Figure 3.97 SDS-PAGE showing *in vitro* expression of rPmFAMeT-1 after induced by 0.4, 0.6, 0.8 and 1 mM IPTG for 3 (lanes 1-4) and 6 hr (lane 5-8), respectively. A pET15b vector in *E. coli* BL21-CodonPlus (DE3)-RIPL (lane 9) was included as the control.

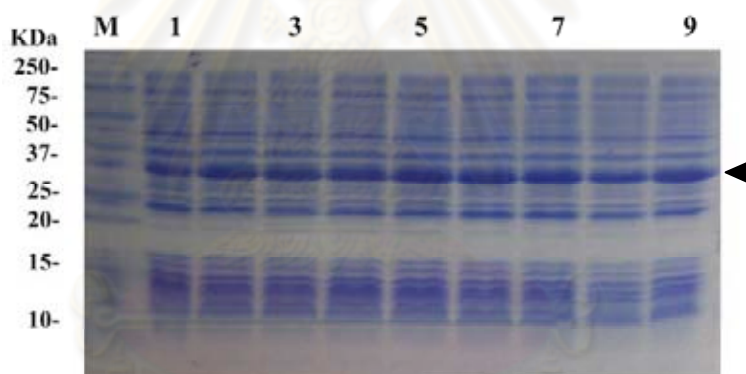
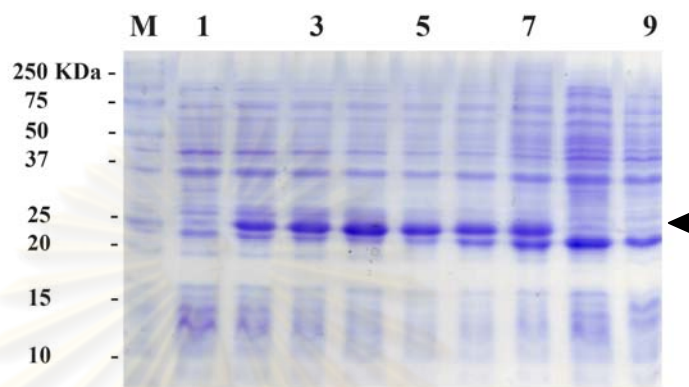


Figure 3.98 SDS-PAGE showing *in vitro* expression of rPmFAMeT-s after induced by 0.4, 0.6, 0.8 and 1 mM IPTG for 3 (lanes 1-4) and 6 hr (lane 5-8), respectively. A pET15b vector in *E. coli* BL21-CodonPlus (DE3)-RIPL (lane 9) was included as the control.

Afterwards, the expression of rPmCOMT, rPmFAMeT-1 and rPmFAMeT-s cultured at 37°C and induced with 0.4 mM IPTG for 0, 1, 2, 6, 12 and 24 hours was examined. These proteins seems to be stably expressed during the induction period therefore, the induction period of 3 hours was used for cell localization of these recombinant proteins (Figs. 3.99-3.101).

A.

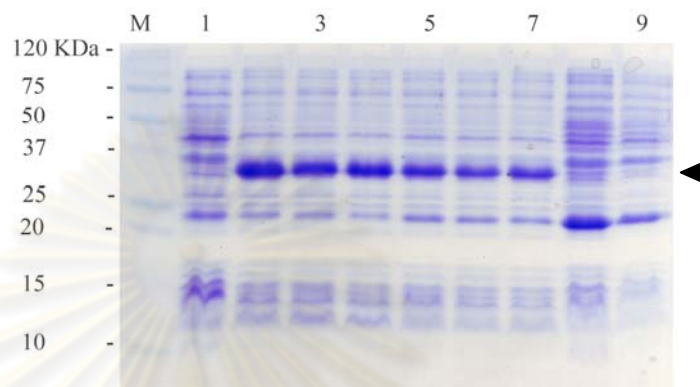


B.



Figure 3.99 SDS-PAGE (A) and Western blot analysis (B) showing *in vitro* expression of rPmCOMT at 0, 1, 2, 6, 12 and 24 hours after induction with 0.4 mM IPTG (lanes 1-7), respectively. A pET15b vector in *E. coli* BL21-CodonPlus (DE3)-RIPL (lane 8) and *E. coli* BL21-CodonPlus (DE3)-RIPL (lane 9) were included as the control.

A.



B.



Figure 3.100 SDS-PAGE (A) and Western blot analysis (B) showing *in vitro* expression of rPmFAMeT-1 at 0, 1, 2, 6, 12 and 24 hours after induction with 0.4 mM IPTG (lanes 1-7), respectively. A pET15b vector in *E. coli* BL21-CodonPlus (DE3)-RIPL (lane 8) and *E. coli* BL21-CodonPlus (DE3)-RIPL (lane 9) were included as the control.

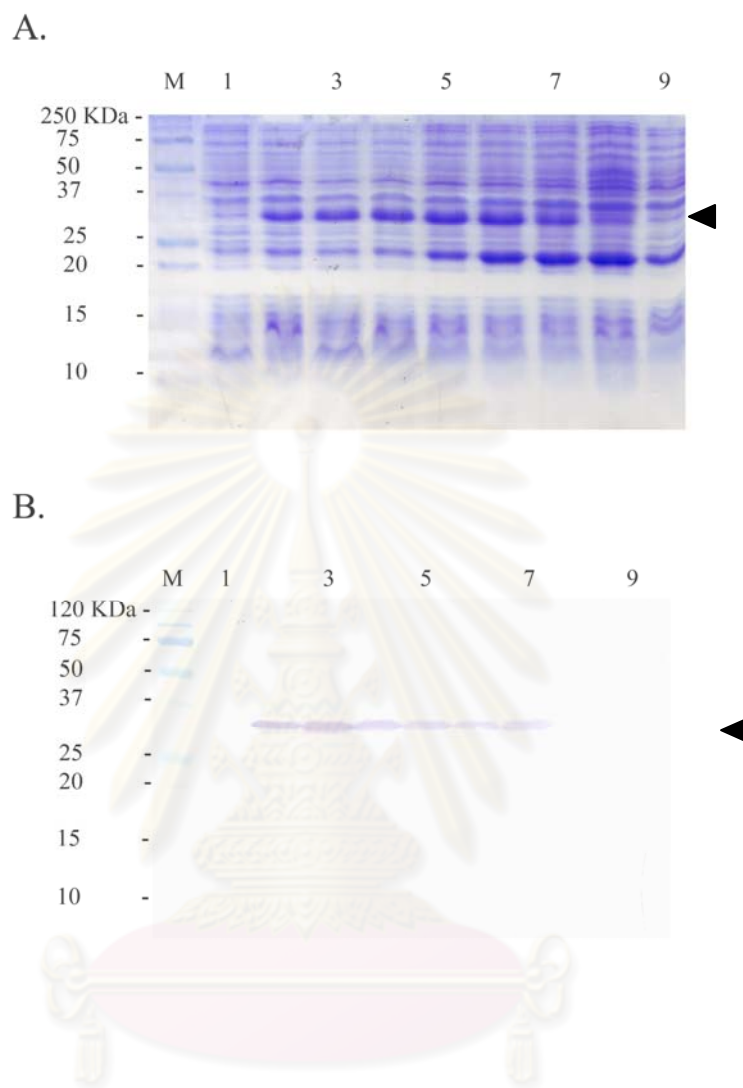


Figure 3.101 SDS-PAGE (A) and Western blot analysis (B) showing *in vitro* expression of rPmFAMeT-s at 0, 1, 2, 6, 12 and 24 hours after induction with 0.4 mM IPTG (lanes 1-7), respectively. A pET15b vector in *E. coli* BL21-CodonPlus (DE3)-RIPL (lane 8) and *E. coli* BL21-CodonPlus (DE3)-RIPL (lane 9) were included as the control.

3.8.3 Cell localization of rPmCOMT, rPmFAMeT-1 and rPMFAMeT-s proteins

Cell localization of rPmCOMT, rPmFAMeT-1 and rPMFAMeT-s proteins was examined. Proteins from the whole cells, soluble and insoluble fractions of cultured recombinant clones were electrophoretically analyzed by 15% SDS-PAGE and Western blot.

All recombinant proteins were greater expressed as the insoluble form than the soluble form when cultured at 37°C (Figs. 3.102, 3.104 and 3.106, respectively). The cultured temperature was then decreased from at 37°C to 25°C. Although these recombinant proteins were more abundantly expressed in the soluble form, the major products were still in the insoluble form (Figs. 3.103, 3.105 and 3.107). Accordingly, the rPmCOMT, PmFAMeT-1 and PmFAMeT-s were purified as the insoluble proteins under the denaturing conditions.

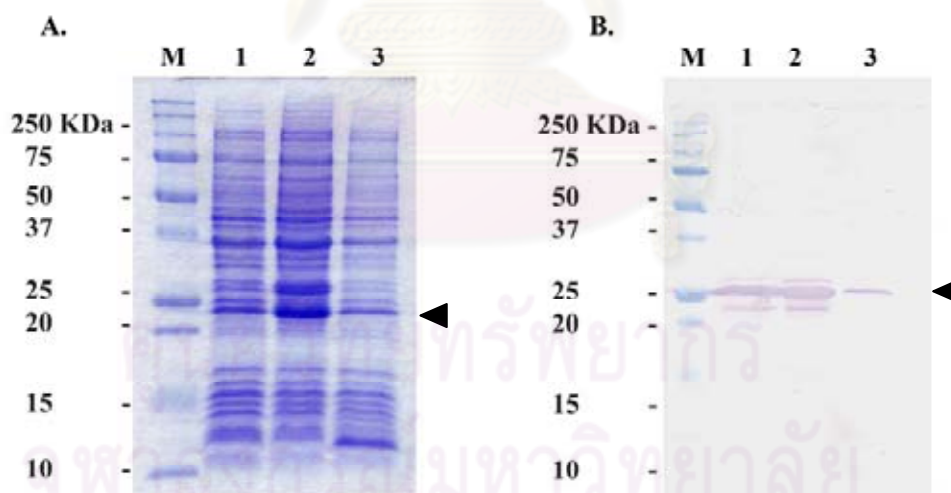


Figure 3.102 SDS-PAGE (A) and Western blot analysis (B) showing *in vitro* expression of a recombinant clone of rPmCOMT cultured at 37°C after induction with 0.4 mM IPTG. Lane 1 = whole cell, lane 2 = insoluble fraction and lane 3 = soluble fraction.

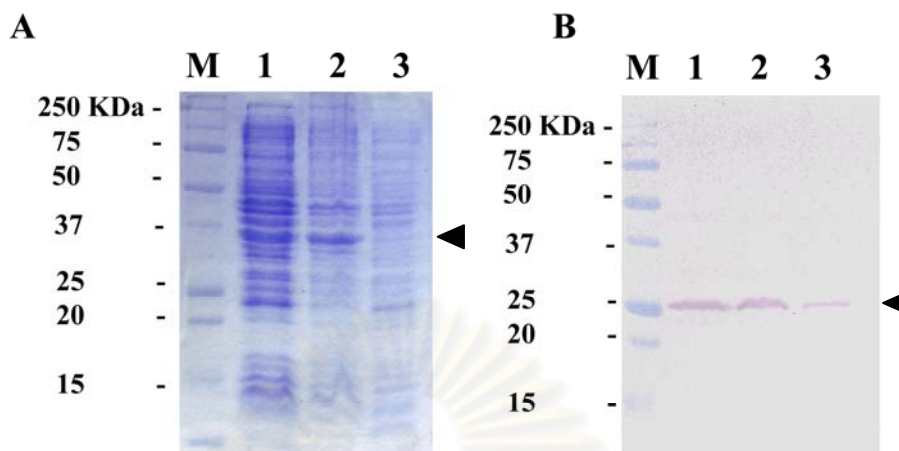


Figure 3.103 SDS-PAGE (A) and Western blot analysis (B) showing *in vitro* expression of a recombinant clone of rPmCOMT cultured at 25°C after induction with 0.4 mM IPTG. Lane 1 = whole cells, lane 2 = insoluble fraction and lane 3 = soluble fraction.

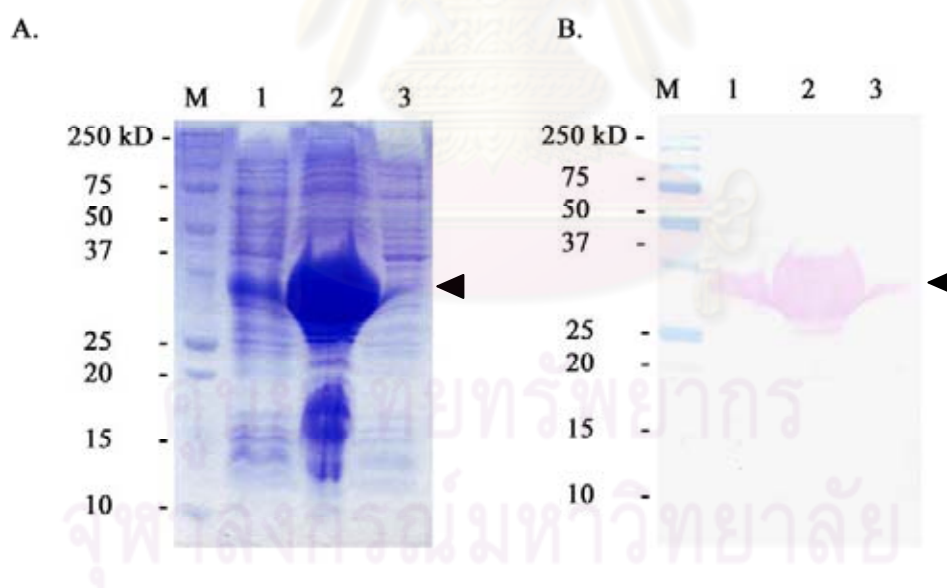


Figure 3.104 SDS-PAGE (A) and Western blot analysis (B) showing *in vitro* expression of a recombinant clone of rPmFAMeT-1 cultured at 37°C after induction with 0.4 mM IPTG. Lane 1 = whole cells, lane 2 = insoluble fraction and lane 3 = soluble fraction.

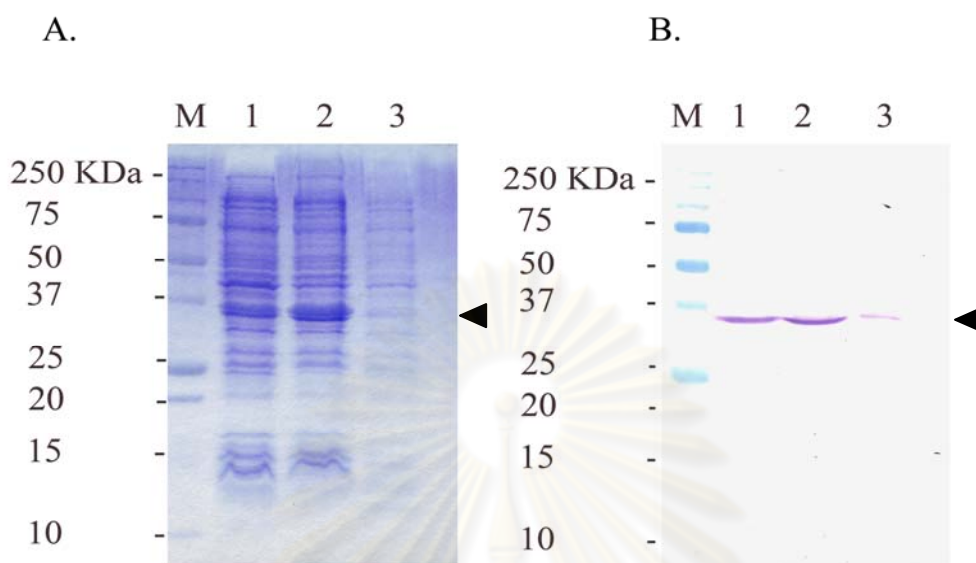


Figure 3.105 SDS-PAGE (A) and Western blot analysis (B) showing *in vitro* expression of a recombinant clone of rPmFAMeT-1 cultured at 25°C after induction with 0.4 mM IPTG. Lane 1 = whole cells, lane 2 = insoluble fraction and lane 3 = soluble fraction.

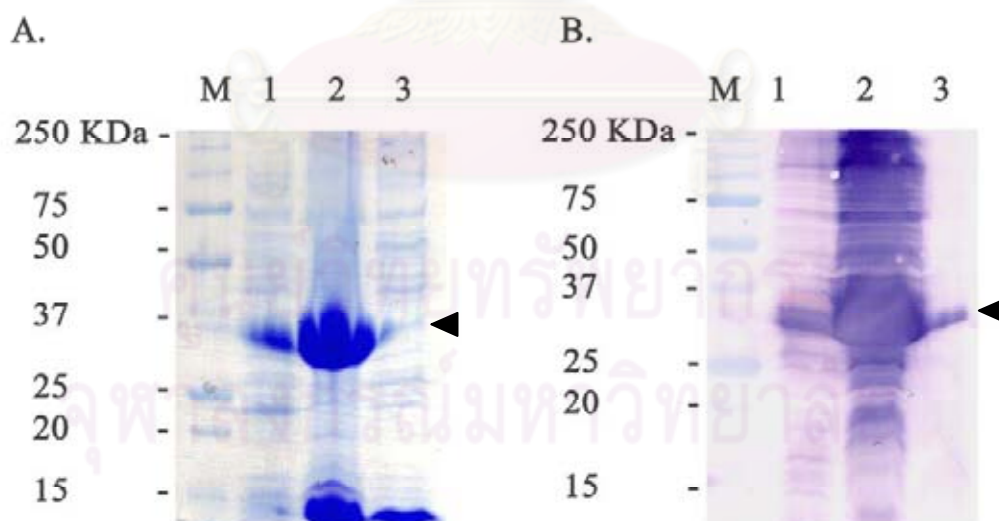


Figure 3.106 SDS-PAGE (A) and Western blot analysis (B) showing *in vitro* expression of a recombinant clone of rPmFAMeT-s cultured at 37°C after induction with 0.4 mM IPTG. Lane 1 = whole cells, lane 2 = insoluble fraction and lane 3 = soluble fraction.

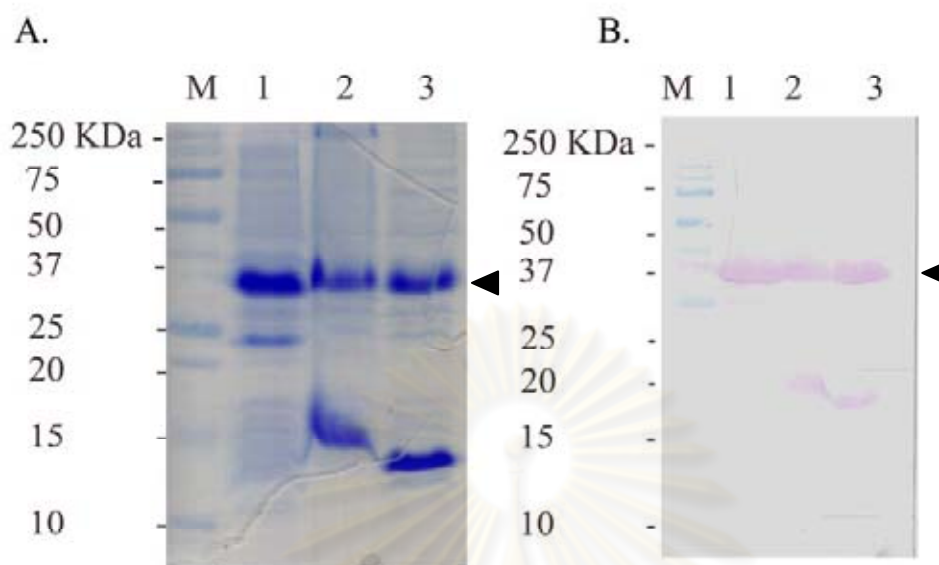


Figure 3.107 SDS-PAGE (A) and Western blot analysis (B) showing *in vitro* expression of a recombinant clone of rPmFAMeT-s cultured at 25°C after induction with 0.4 mM IPTG. Lane 1 = whole cells, lane 2 = insoluble fraction and lane 3 = soluble fraction.

3.8.4 Purification of recombinant protein

The insoluble proteins of all recombinant clones were purified in the denaturing conditions. The cells were washed using 10 ml of the binding buffer (20 mM sodium phosphate, 500 mM NaCl, pH 7.4), sonicated and centrifuged at 14000 rpm for 30 min. The insoluble fraction was loaded into the column and washed with the binding buffer. The recombinant protein was eluted with 6 ml of the elution buffer (20 mM sodium phosphate, 500 mM NaCl, 500 mM imidazole, pH 7.4 and 8M urea). Fractions from the washing and eluting steps were analyzed by 15% SDS-PAGE and western blot analysis. The purified fractions (Figs. 3.108-3.110) were concentrated by ultrafiltration and kept at 4°C (Fig. 3.111). The obtained protein was subjected to polyclonal antibody production in rabbit.

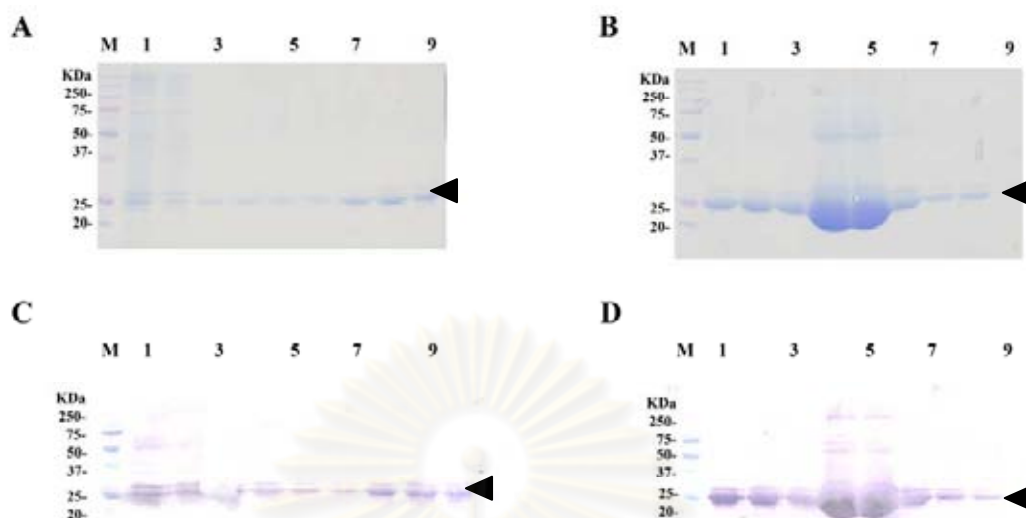


Figure 3.108 SDS-PAGE (A) and Western blot analysis (B) of purified rPmCOMT in the denaturing conditions. The culture was carried at 37 °C and induced with 0.4 mM IPTG for 3 hours. A and C: lane 1 = whole cells, 2 = the insoluble fraction after pass through the column, 2-7 = the first wash fractions, and 8-9 = the second wash fractions, respectively. B and D: lane 1 = the third wash fraction, 2 = the elution fraction, respectively.

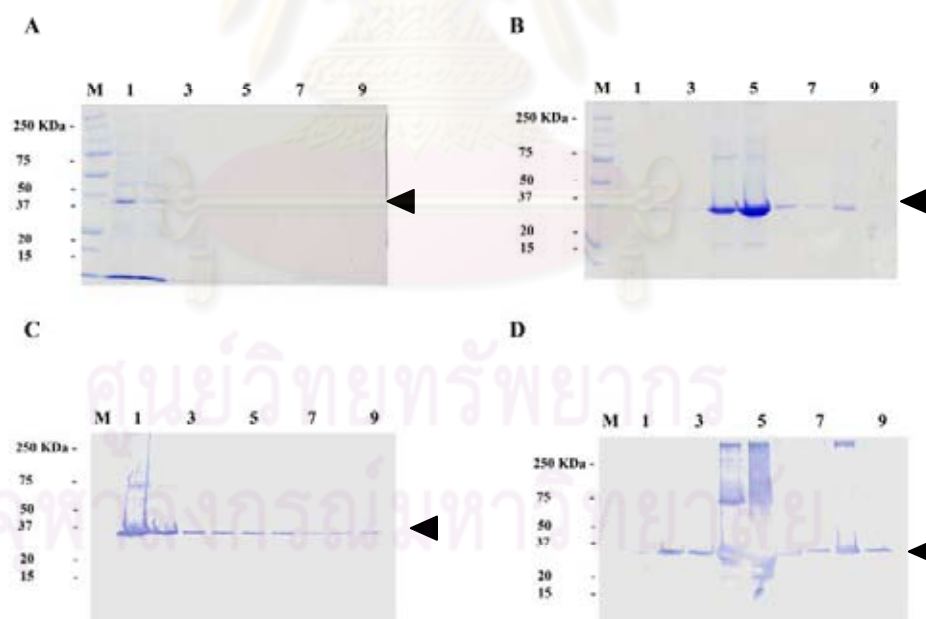


Figure 3.109 SDS-PAGE (A) and Western blot analysis (B) of purified rPmFAMeT-1 in the denaturing conditions. The culture was carried at 37 °C and induced with 0.4 mM IPTG for 3 hours. A and C: lane 1 = whole cells, 2 = the insoluble fraction after pass through the column, 2-7 = the first wash fractions, and 8-9 = the second wash fractions, respectively. B and D: lane 1 = the third wash fraction, 2 = the elution fraction, respectively.

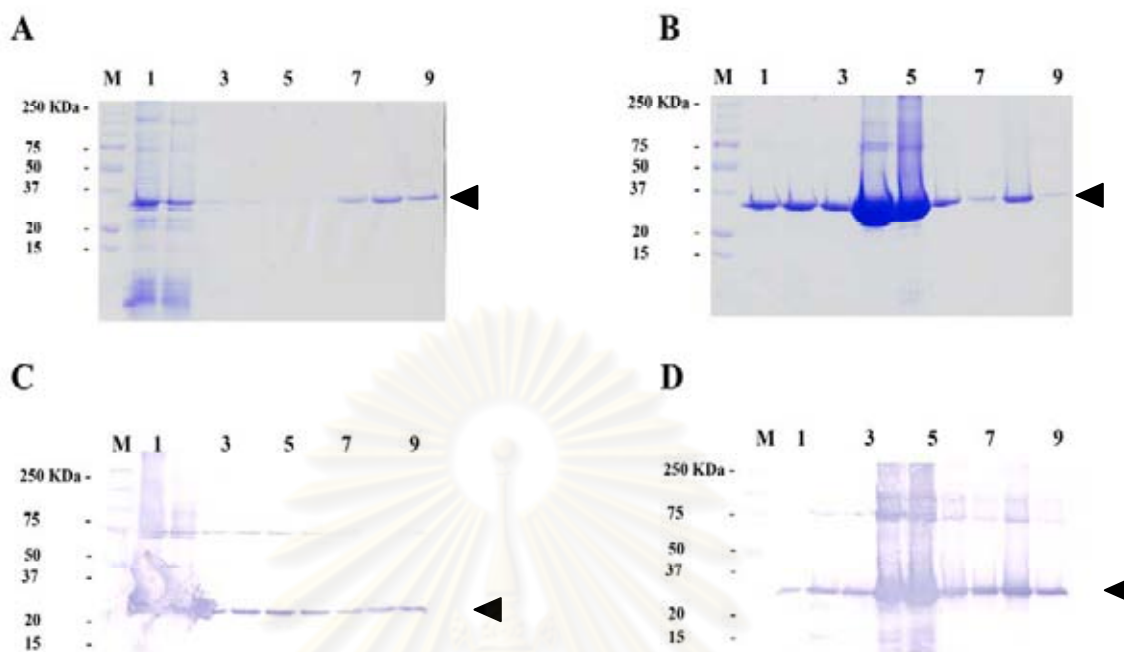


Figure 3.110 SDS-PAGE (A) and Western blot analysis (B) of purified rPmFAMeT-s in the denaturing conditions. The culture was carried at 37 °C and induced with 0.4 mM IPTG for 3 hours. A and C: lane 1 = whole cells, 2 = the insoluble fraction after pass through the column, 2-7 = the first wash fractions, and 8-9 = the second wash fractions, respectively. B and D: lane 1 = the third wash fraction, 2 = the elution fraction, respectively.

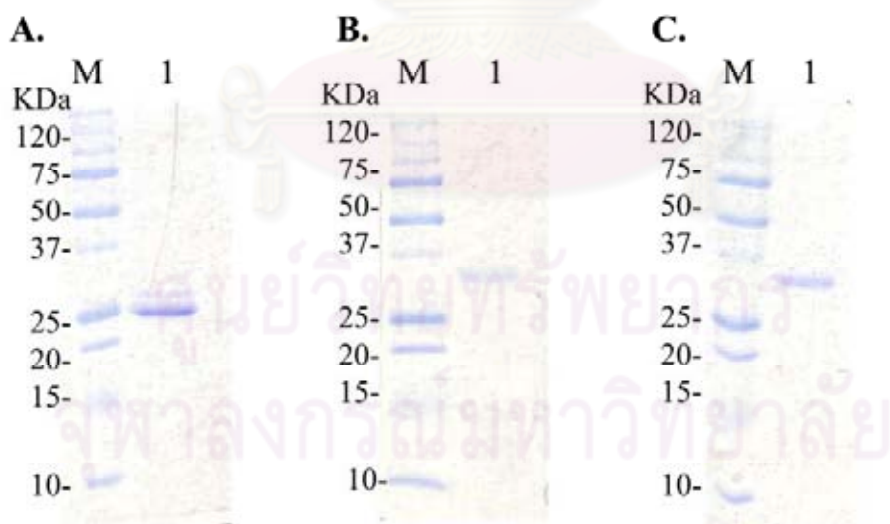


Figure 3.111 SDS-PAGE (A) and Western blot analysis (B) of the insoluble protein fractions of rPmCOMT, rPmFAMeT-s and rPmFAMeT-1 purified in denaturing conditions after culture at 37 °C and induced with 0.4 mM IPTG for 3 hours.

3.8.5 Peptide sequencing of purified rPmCOMT, rPmFAMeT-1 and rPmFAMeT-s

The peptide sequencing was applied to confirm whether the purified proteins were rPmCOMT, rPmFAMeT-1 and rPmFAMeT-s. After size-fractionated, the expected recombinant protein was further analyzed by NanoLC-MS/MS.

Internal peptide sequences of rPmCOMT was SYHNPDPVLVQ YCVNHSLR and IGDGVTLCFKK which significantly matched *O*-methyltransferase of *Fenneropenaeus chinensis* (clone no. HC-H-S01-0684-LF; <http://pmonodon.biotec.or.th>) at 11% of sequence coverage while those of rPmFAMeT-1 were VDTPDVVCCEEER and VGYQSDPFMEWTDPEPWK which significantly matched farnesoic acid *O*-methyltransferase of *P. monodon* (clone no. IN-N-S01-1195-LF) at 13% of sequence coverage. Those of rPmFAMeT-s were VGYQSDPFMEWTDPEPWK which significantly matched farnesoic acid *O*-methyltransferase of *P. monodon* (clone no. IN-N-S01-1195-LF) at 7% of sequence coverage, respectively. Results illustrated that the purified recombinant proteins were the target proteins of this study.

3.8.6 The production of polyclonal antibodies against rPmCOMT, rPmFAMeT-1 and PmFAMeT-s

Anti-PmCOMT, anti-PmFAMeT-1 and anti-PmFAMeT-s polyclonal antibodies were successfully produced in rabbits. The titer of PmFAMeT-s polyclonal antibody (PAb) was high after the third immunization but that of PmFAMeT-1 PAb and PmFAMeT PAb was quite low, thus further antigen administration was required (Tables 3.29-3.31). Rabbits were sacrificed and their serum was collect, filtrated through 0.22 μ M membrane and kept at -20 °C.

Table 3.29 Titers of anti-PmCOMT after the rabbit was immunized rPmCOMT for 4 times

Dilution of serum	Rabbit anti-PmCOMT	
	Pre-immunized serum*	Immunized serum**
1:500	0.052	3.014
1:2000	0.020	2.220
1:8000	0.001	0.955
1:32000	-0.003	0.313

* Pre-immunized serum = serum from normal rabbit

** Immunized serum = serum from rabbit injected with the recombinant protein

Table 3.30 Titers of anti-PmFAMeT-1 after the rabbit was immunized rPmFAMeT-1 for 5 times

Dilution of serum	Rabbit anti PmFAMeT-1	
	Pre-immunized serum*	Immunized serum**
1:500	0.303	1.909
1:2000	0.153	1.021
1:8000	0.091	0.391
1:32000	0.075	0.166

* Pre-immunized serum=serum from normal rabbit

** Immunized serum=serum from rabbit injected with the recombinant protein

Table 3.31 Titers of anti-PmFAMeT-s after the rabbit was immunized rPmFAMeT-s for 3 times

Dilution of serum	Rabbit anti PmFAMeT-s	
	Pre-immunized serum*	Immunized serum**
1:500	0.115	2.392
1:2000	0.027	1.804
1:8000	0.007	0.841
1:32000	0.002	0.292

* Pre-immunized serum=serum from normal rabbit

** Immunized serum=serum from rabbit injected with the recombinant protein

3.8.7 Expression profiles of PmCOMT, PmFAMeT-1 and PmFAMeT-s proteins during ovarian development of *P. monodon*

Non-purified anti-PmCOMT PAb generated the positive signals along with non-specific immunoreactive bands following western blot analysis (data not shown). Therefore, anti-PmCOMT and anti-PmFAMeT-1 PAB were affinity-chromatographically purified.

Anti-PmCOMT PAb revealed a positive band of approximately 24 kDa suggesting no posttranslational modification (i.e. glycosylation) of this non-secretory ovarian protein. More intense signals of PmCOMT were observed in previtellogenic and vitellogenic ovaries than those in cortical rod and mature ovaries of intact *P. monodon* broodstock (Fig. 3.112).



Figure 3.112 Western blotting analysis of anti-PmCOMT PcAb (dilution 1:300, expected MW of 24.1 kDa) using total proteins extracted from ovaries of intact (A) and eyestalk-ablated (B) broodstock of wild *P. monodon*. Ovarian proteins (30 μ g) were size-fractionated by 15% SDS-PAGE.

Lanes 1 = stage I ovaries (GSI = 1.44%); lanes 2-3 = stage II ovaries (GSI = 2.95 and 2.15%, respectively); lanes 4-5, B = stage III ovaries (GSI = 4.62 and 5.37%); lane 6-7 = stage IV ovaries (GSI = 9.36 and 10.41%, respectively). Lanes M = protein standard.

Western blot analysis revealed the positive signals of ovarian PmFAMeT in juveniles and stages I and II but not in stages III and IV ovaries of broodstock. Interestingly, juvenile shrimp possessed either 32 kDa, 37 kDa or both positive bands whereas only a 37 kDa band owing to posttranslational modifications of ovarian FAMeT was only observed in stages I and II ovaries of broodstock.(Fig. 3.113).

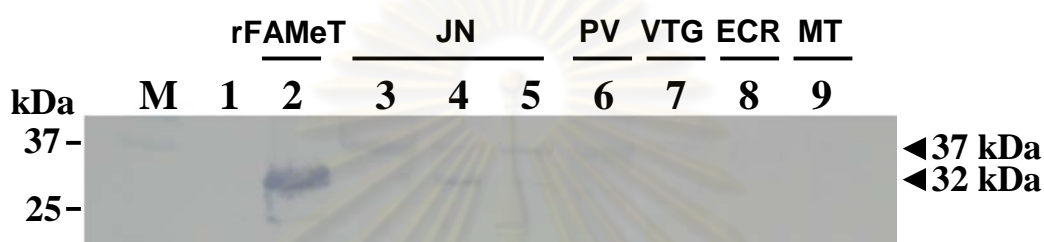


Figure 3.113 Western blot analysis of anti-PmFAMeT-1 PAb (1:300) against total proteins (25 μ g) extracted from ovaries of different stages of *P. monodon*: JN = juveniles, PV = previtellogenic (stage I) ovaries, V = vitellogenic (II) ovaries, CR = cortical rod (III) ovaries, M = mature (IV) ovaries. Lane M: protein standard.

3.9 Localization of all proteins in ovaries of *P. monodon* broodstock

After affinity-chromatographic purification, anti-PmCOMT, anti-PmFAMeT-1 PAb and anti-PmFAMeT-s PAb were used to localize the respective proteins in different stages of ovaries in both intact and eyestalk-ablated *P. monodon* broodstock.

The positive immunohistological signals of PmCOMT were detected in cytoplasm of previtellogenic and vitellogenic oocytes. Nevertheless, the positive signals were observed in cortical rods of stage III (early cortical rod) and IV (mature) oocytes in both intact (Fig. 3.114) and eyestalk-ablated broodstock(Fig. 3.115). However, clearer signals in the latter than the former were noticed. No immunoreactivity was found in ovaries

when incubated with the blocking solution (the negative control) and with the preimmune serum (Figs. 3.114 and 3.115).

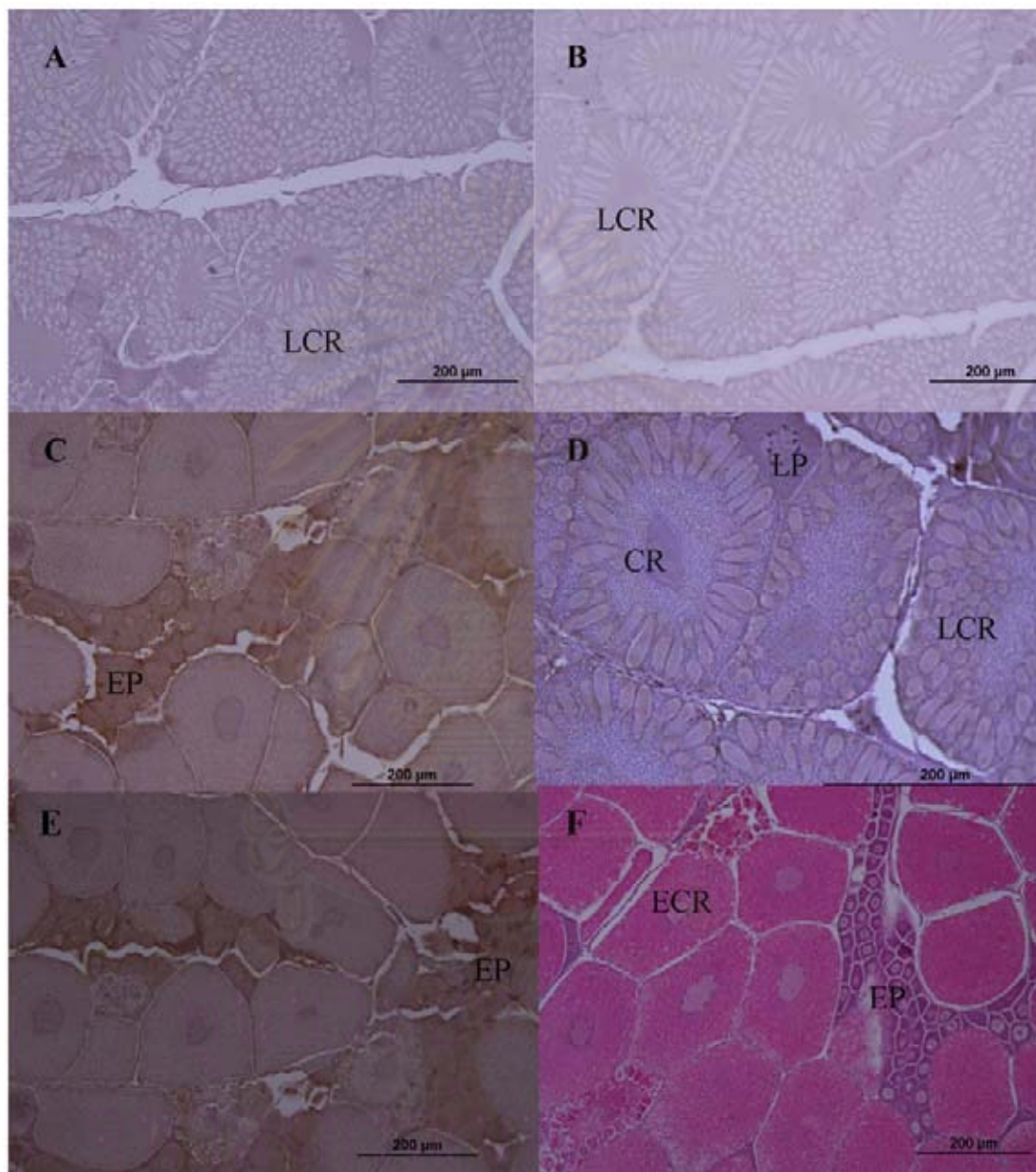


Figure 3.114 Immunohistochemical localization of the PmCOMT protein in ovaries of intact *P. monodon* broodstock (C and D). The blocking solution (A) and preimmune serum (B) were used as the negative control. The conventional HE staining (E) was carried out for identification of oocyte stages.

The anti-PmFAMeT-l PAb and anti-PmFAMeT-s PAb were used to localize the FAMeT protein in ovaries of *P. monodon* broodstock. The weak immunoreactivity was

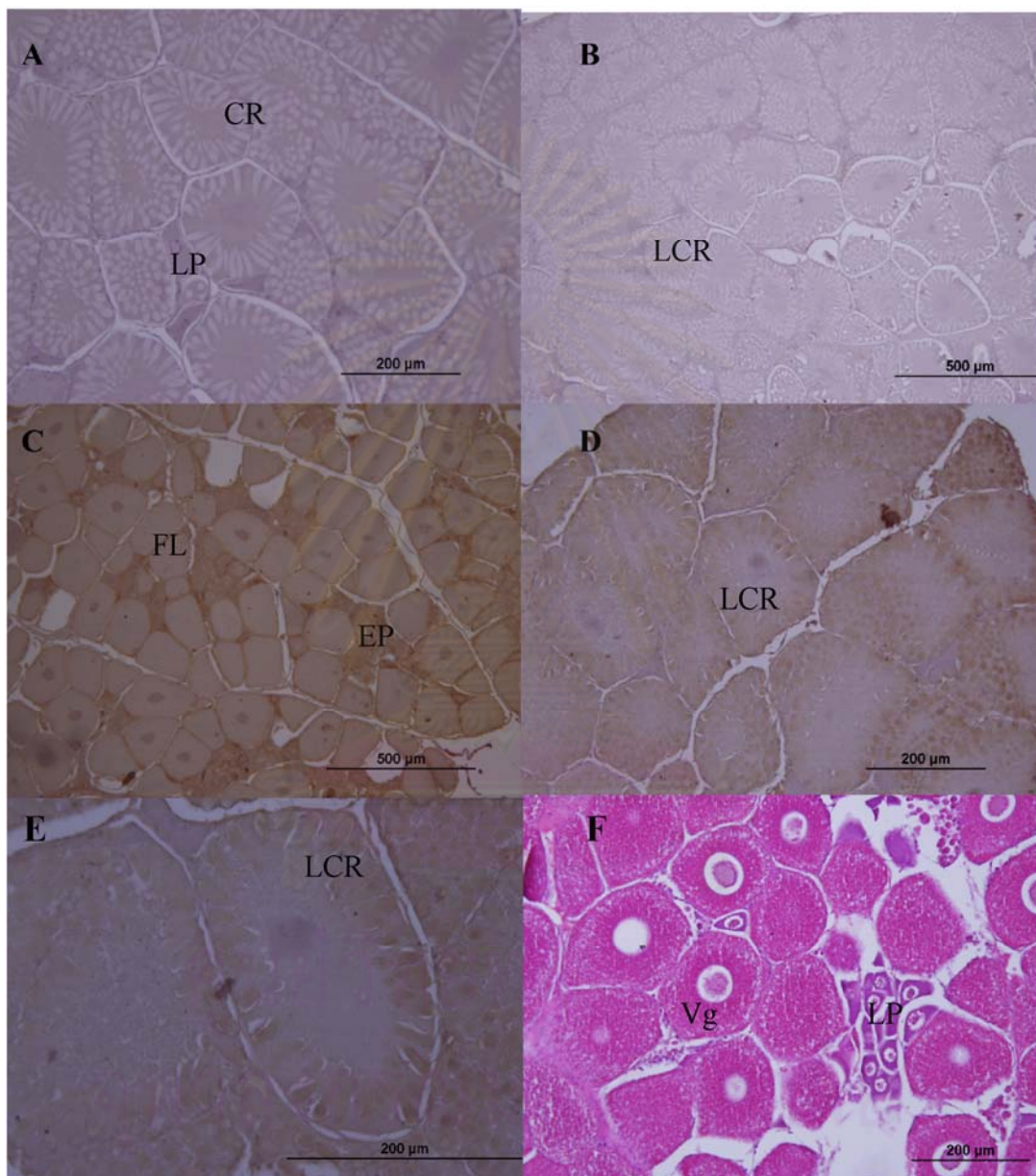


Figure 3.115 Immunohistochemical localization of PmCOMT protein in ovaries of eyestalk-ablated broodstock of *P. monodon* (C-D). The blocking solution (A) and preimmune serum (B) were used as the negative control. The conventional HE staining (E) was carried out for identification of oocyte stages.

observed when anti-PmFAMeT-s PAb was used (Figs 3.116 and 3.117). However, stronger signals were found when anti-PmFAMeT-1 PAb was used (Figs 3.118-3.119).

The positive immunohistochemical signals of PmFAMeT were detected in cortical rods of stages III and IV oocytes in both intact and eyestalk-ablated broodstock of *P. monodon* (Figs 3.118 and 3.119). No immunoreactivity was found in stages I and II oocytes and in ovaries incubated with the blocking solution and the preimmune serum (Figs 3.118 and 3.119).

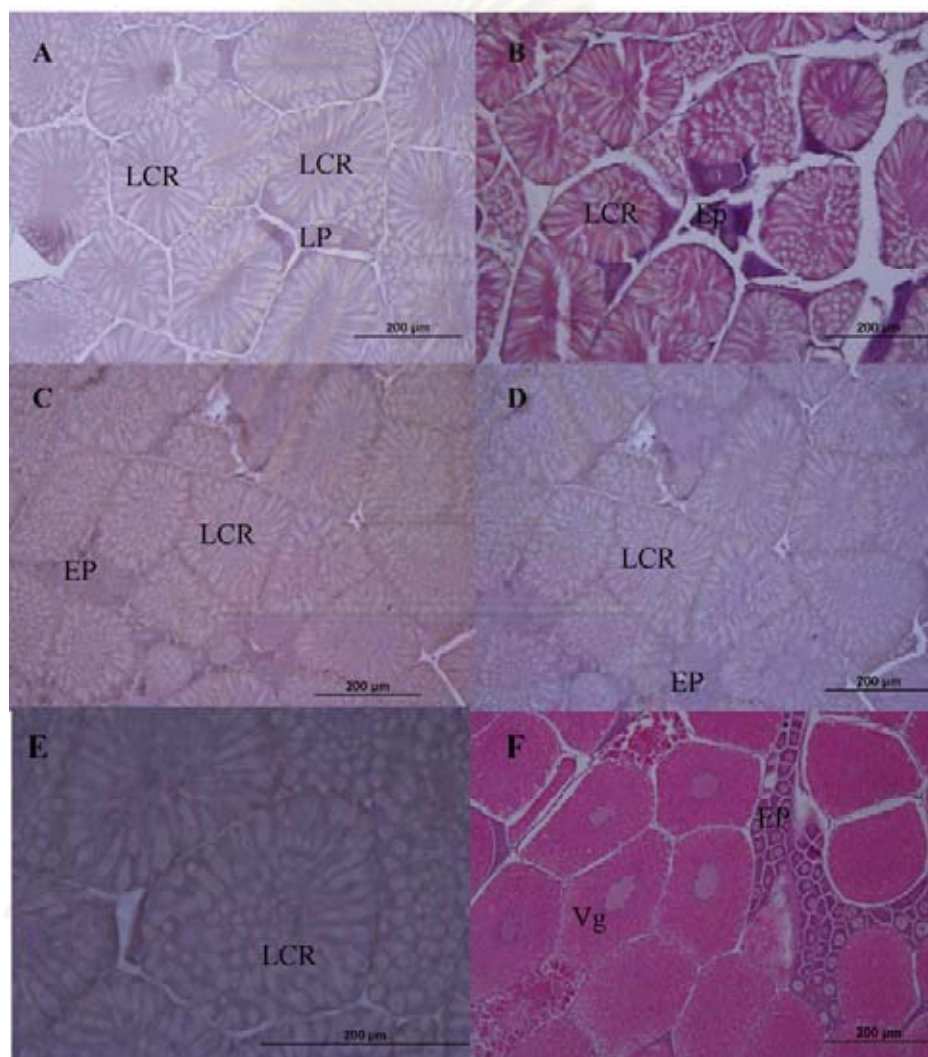


Figure 3.116 Immunohistochemical localization of the PmFAMeT-s protein in ovaries of eyestalk-ablated broodstock of *P. monodon* (C-E). The blocking solution (A) and preimmune serum (B) were used as the negative control. The conventional HE staining (F) was carried out for identification of oocyte stages.

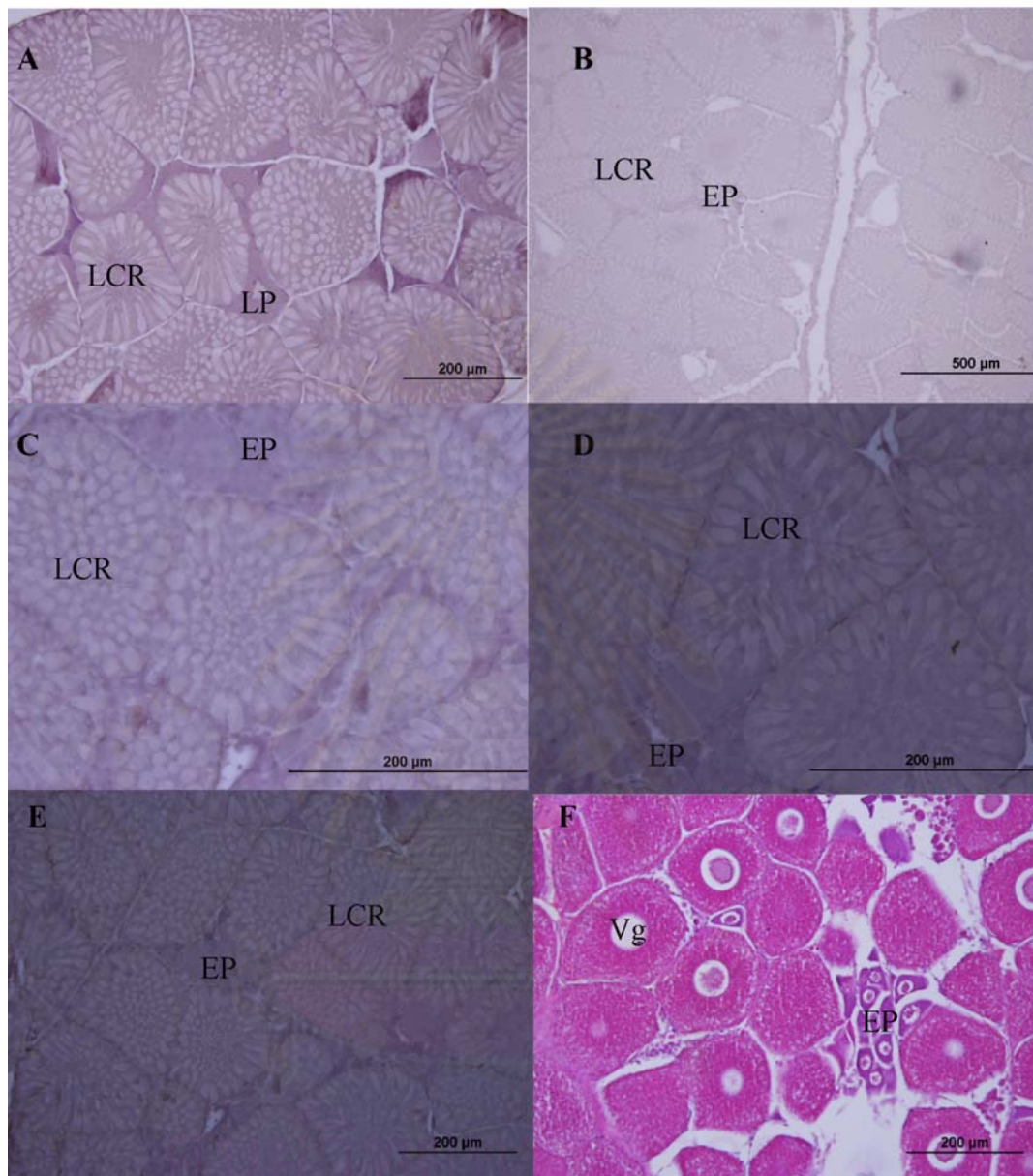


Figure 3.117 Immunohistochemical localization of the PmFAMeT-s protein in ovaries of eyestalk-ablated broodstock of *P. monodon* (C-E). The blocking solution (A) and preimmune serum (B) were used as the negative control. The conventional HE staining (F) was carried out for identification of oocyte stages.

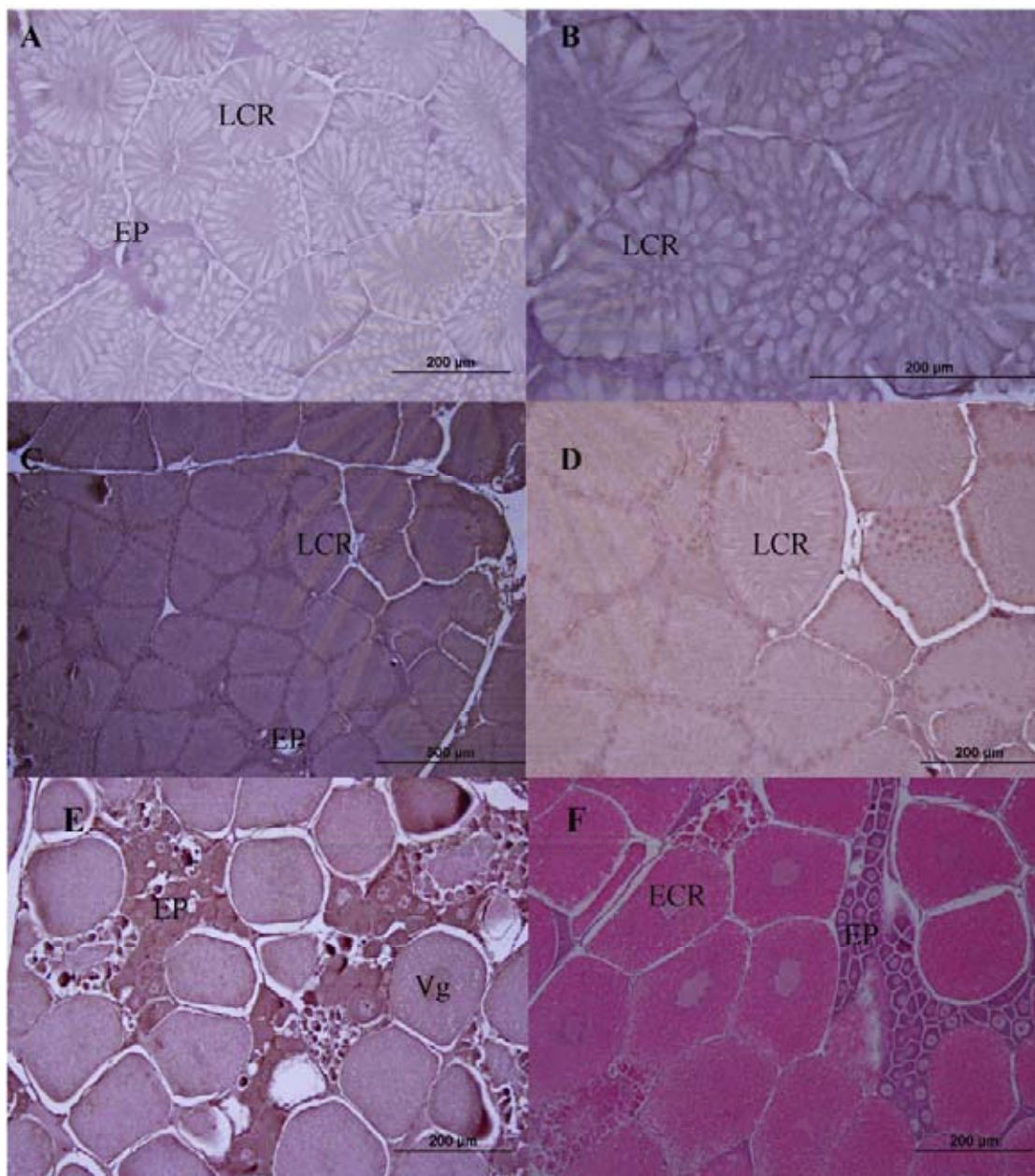


Figure 3.118 Immunohistochemical localization of the PmFAMeT-1 protein in ovaries of intact *P. monodon* broodstock (C-E). The blocking solution (A) and preimmune serum (B) were used as the negative control. The conventional HE staining (F) was carried out for identification of oocyte stages.

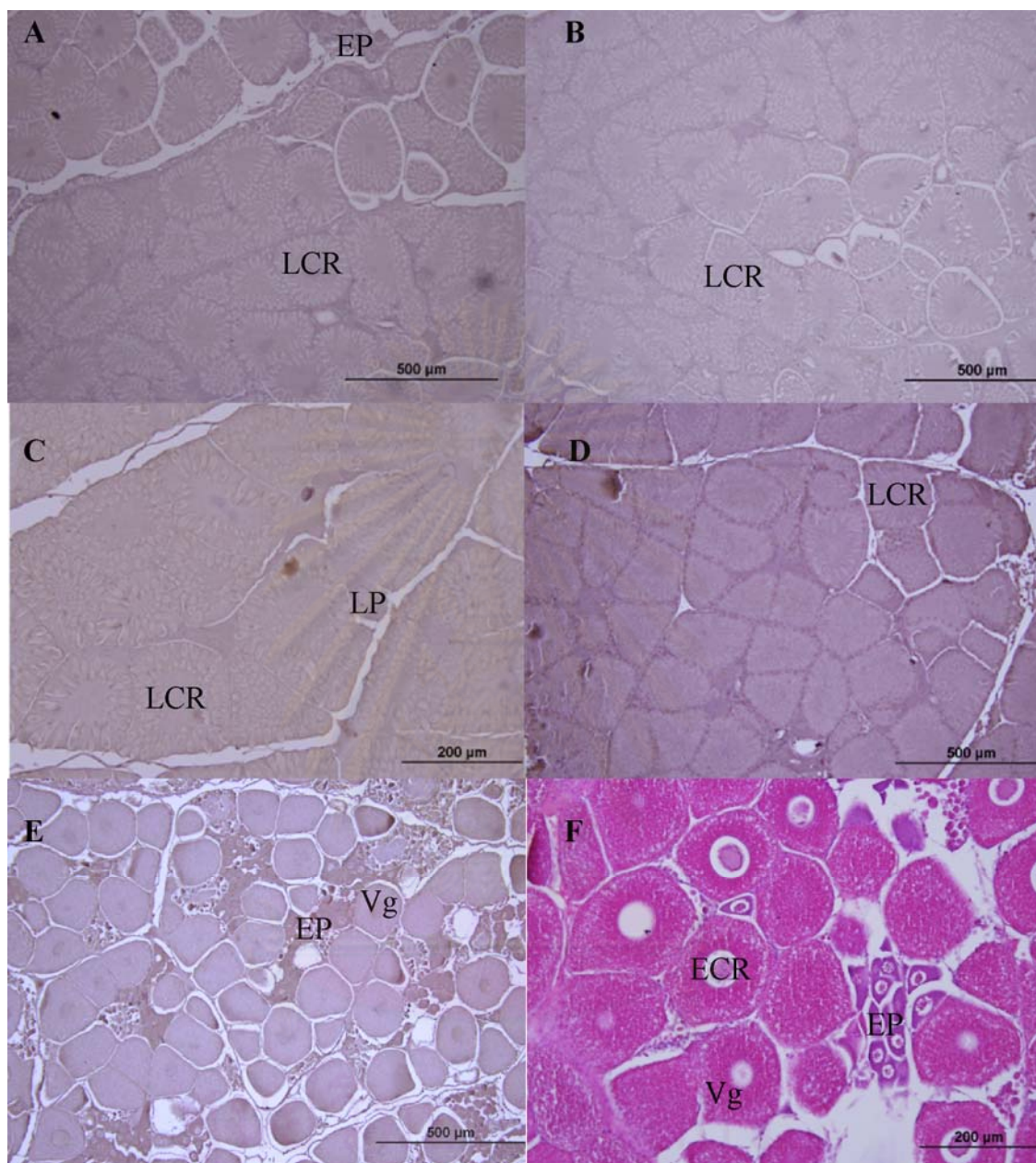


Figure 3.119 Immunohistochemical localization of the PmFAMeT-1 protein in ovaries of eyestalk-ablated broodstock of *P. monodon* (C-E). The blocking solution (A) and preimmune (B) were used as the negative control. The conventional HE staining (F) was carried out for identification of oocyte stages.

CHAPTER IV

DISCUSSION

Isolation and characterization of reproduction-related genes in ovaries of *P. monodon*

Closing life cycle culture of the giant tiger shrimp (*Penaeus monodon*) is crucial to the sustainability of the shrimp industry. However, poor reproductive maturation of captive *P. monodon* females and low quality of spermatozoa of captive males have limited the potential of genetic improvement, which in turn, resulted in remarkably slow domestication and selective breeding programs of *P. monodon* (Withyachumnarnkul et al., 1998; Preechaphol et al., 2007).

Molecular mechanisms and functional involvement of reproduction-related genes and proteins in ovarian development of *P. monodon* is necessary for better understanding of the reproductive maturation of *P. monodon* to resolve the major constraint of this economically important species in captivity (Preechaphol et al., 2007; Klinbunga et al., 2009).

Transcription in germ cells during oogenesis follows carefully regulated programs corresponding to a series of developmental events of oocytes (Grimes, 2004; Qiu and Yamano, 2005; Qui et al., 2005). Recently, genes expressed in the vitellogenic ovaries of *P. monodon* were identified and characterized. A total of 1051 clones from a conventional cDNA library were unidirectionally sequenced from the 5' terminus. The nucleotide sequences of 743 EST (70.7%) significantly matched known genes previously deposited in GenBank (E -value $<10^{-4}$), whereas 308 ESTs (29.3%) were regarded as newly unidentified transcripts (E -value $>10^{-4}$). A total of 559 transcripts (87 contigs and 472 singletons) were obtained after sequence assembly. Several reproduction-related genes including *chromobox protein*, *ovarian lipoprotein receptor*, *progesterin membrane receptor component 1* and *ubiquitin-specific proteinase 9, X chromosome*, were isolated and characterized (Preechaphol et al., 2007).

Subsequently, suppression subtractive hybridization (SSH) libraries between cDNA in stages I (previtellogenic) and III (cortical rod) ovaries of the giant tiger shrimp (*Penaeus monodon*) were established. In all, 452 ESTs were unidirectionally sequenced. Sequence assembly generated 28 contigs and 201 singletons, 109 of which (48.0%) corresponding to known sequences previously deposited in GenBank. Several reproduction-related transcripts were identified.

In order to provide a further insight into the molecular mechanisms involved in the reproductive development and maturation processes of *P. monodon*, the full length cDNA of *O-methyltransferase* (*PmCOMT* and *PmFAMeT*) and ecdysteroid-responsive genes (*PmBr-cZ1* and *PmBr-cZ4*) in *P. monodon* were characterized.

The full length cDNA of *O-methyltransferase* (*OMT*) was first identified in *F. chinensis* (ORF of 666 bp encoding a polypeptide of 221 amino acids). Northern blot and *in situ* hybridization analyses demonstrated that the *OMT* transcripts were constitutively expressed in various tissues and it was up-regulated in hepatopancreas and stomach in shrimp challenged with a mixture of live *Vibrio anguillarum* and *Staphylococcus aureus* suggesting that *OMT* may play multi-functions in physiological processes (Li, D.X. et al., 2006).

In this study, the full length cDNA and genomic DNA of *PmCOMT* was characterized. *PmCOMT* exhibits a relatively high degree of sequence similarity with *catechol-O-methyltransferases domain-containing protein 1* in other species implying the conserved function of this gene family across taxa. Unlike other *P. monodon* genomic DNA sequences (e.g. cyclins A and B, Visudtiphole et al., 2009) previously reported, the exon-intron boundaries of *PmCOMT* did not follow the GT/AG rule. Moreover, the deduced *PmCOMT* lacks a signal peptide and regarded as non-secretory protein in ovaries. *PmCOMT* and *PmFAMeT* from various species (*Homarus americanus*, *Metapenaeus ensis*, *L. vannamei* and *M. japonicus*) were allocated to be different groups of *OMT*. Phylogenetic analysis indicated that both *PmCOMT* and *F. chinensis OMT* are members of *catechol-O-methyltransferase*.

The *PmCOMT* transcripts were expressed in various tissues of broodstock but more abundantly expressed in ovaries and intestine than other tissues. Similar results were found from western blot analysis and a low level of expression was observed in

hemocytes (data not shown). Presumably, PmCOMT may majorly involved in catecholamine degradation of non-steroid producing tissues but contribute in steroidogenesis in ovaries. The actual function of *PmCOMT* in a particular environment needs to be elucidated in shrimp.

Two forms of the full length cDNA of *PmFAMeT* were characterized and reported. *PmFAMeT* exhibits a relatively high degree of sequence similarity with that from other species. Like *FAMeT* in *L. vannamei*, the two isoforms of the deduced PmFAMeT are different according to the presence/absence of a five pentapeptide (Glu-Gly-Arg-Gly-Ser) (Hui et al., 2008). The significance of this pentapeptide insertion within the second CF domain on activity of PmFAMeT-s should be further investigation. Phylogenetic analysis clearly indicated that both *PmFAMeT-l* and *PmFAMeT-s* are closely related to *FAMeT* of other decapod crustaceans and are regarded as members of crustacean *FAMeT* rather than *COMT*.

The deduced PmFAMeT lacks a signal peptide and regarded as non-secretory protein in ovaries. Like, LvFAMeT, tissue distribution analysis revealed constitutive expression of the *PmFAMeT* transcript in various tissues. Western blot analysis revealed a possible post-translational modification of the PmFAMeT protein during ovarian development of *P. monodon* as both the sequence-expected size of 32 kDa and a greater product size of 37 kDa were observed. In addition, the preliminary data on expression of the PmFAMeT protein across various tissues indicated the positive 37 kDa band in pleopods, both 32 and 37 kDa bands in ovaries, eyestalk and epicuticle and only a 32 kDa band in other tissues (data not shown). The wide distribution of PmFAMeT expression may be related to its role in growth and regulation of molting as suggested in *L. vannamei* (Hui et al., 2008).

In addition, two isoforms of the full length cDNA of *PmBr-cZ1* and a single isoform of *PmBr-cZ4* were successfully characterized. The deduced PmBr-cZ1 and PmBr-cZ4 proteins contained BTB domains which are the highly conserved amino-terminal domain and widely distributed the protein-protein interaction motifs found in a family of transcription factors that play critical roles in cellular differentiation, development, and neoplasia (Costoya and Pandolfi, 2001; Lin et al., 2001) and four (for *PmBr cZ1*) or two (for *PmBr cZ4*) ZnF C₂H₂ domains as those of others species. Both *PmBr-cZ1* and *PmBr-cZ4* were more abundantly expressed in ovaries than other

tissues of *P. monodon* broodstock. This indicated that both genes should play an important role on ovarian/oocyte development in *P. monodon*.

Expression of reproduction-related genes during ovarian development of *P. monodon* by semi-quantitative RT-PCR and quantitative real-time PCR

Ovaries are functionally important in reproduction and secretion of hormones for growth and development regulation. Ovarian maturation of *P. monodon* results from rapid synthesis and accumulation of a major yolk protein (vitellin) (Meusy and Payen, 1988; Yano and Hoshino, 2006). Understanding the role of various genes/proteins during ovarian and oocyte development of *P. monodon* may lead to the possible ways to effectively induce ovarian maturation in shrimp.

Quantitative real-time PCR revealed higher expression of *PmCOMT* in ovaries of juveniles than intact wild broodstock suggesting that *PmCOMT* may be necessary for development of premature ovaries of juvenile *P. monodon* and that *PmCOMT* may play a different role during juveniles. *PmCOMT* did not show differential expression profile in ovaries of intact broodstock. Expression of *PmCOMT* during reproductive maturation of intact and eyestalk-ablated *P. monodon* broodstock indicated that *PmCOMT* mRNA is sufficient for ovarian development but a greater level of this transcript may be required during growth and development of juvenile shrimp. *PmCOMT* was comparably expressed in different ages of domesticated juveniles (6 months old) and broodstock (14 and 18 months old).

Expression of total *PmFAMeT* rather than that of *PmFAMeT-l* and *PmFAMeT-s* was examined during ovarian development of intact and eyestalk-ablated *P. monodon*. The ovarian *PmFAMeT* transcript was significantly increased at the final stage (IV) of ovarian development in both intact and eyestalk-ablated broodstock.

The expression level of ovarian *PmFAMeT* of domesticated juveniles and broodstock seemed to be gradually decreased following the cultivation period. This suggested reduced reproductive maturation in domesticated shrimp found in our domestication program at present. The information suggested that *FAMeT* gene products play the important role during the maturation stage of *P. monodon* ovaries.

Eyestalk ablation caused an increase in the mRNA levels of *vitellogenin* and *cortical rod protein* in ovaries of *M. japonicus* (Tsutsui et al., 2005; Okumura et al., 2006). Likewise, the increase in mRNA and earlier up-regulation (vitellogenic, early cortical rod and mature stages) of *PmFAMeT* during ovarian development in eyestalk-ablated female broodstock suggests that gonad inhibiting hormone (GIH; Meusy and Payen, 1988) directly affects *PmFAMeT* transcription. Therefore, the mRNA levels of *PmFAMeT* may be used as the biomarker to reveal degrees of reproductive maturation of *P. monodon*.

The expression level of *PmBr-cZ1* was down-regulated in stage II and III before returned to the normal level at stage IV and after spawning in intact broodstock. Its expression level in stages IV (mature ovaries) was significantly greater than that in stage I (previtellogenic) ovaries and II (vitellogenic) in eyestalk-ablated broodstock. The high levels of expression were also observed in domesticated shrimp (6, 14 and 18 months old). This strongly indicated that the expression profiles of *PmBr-cZ1* can be used to monitor the degrees of reproductive maturation following the effects of hormonal administration and/or maturation diets.

Interesting results were observed from expression profiles of *PmBr-cZ4* during different ovarian stages of intact *P. monodon*. The down-regulation of *PmBr-cZ4* at stage IV ovaries in intact broodstock was observed. In addition, eyestalk ablation significantly reduced its expression levels in comparison with intact shrimp. This implied that lower levels of these gene products may be necessary for the development and final maturation of *P. monodon* oocytes. The findings facilitate the possible use of RNA interference (RNAi) for studying their functional involvement in *P. monodon* ovarian development.

Effects of neurotransmitter, progesterone and ecdysteroid administration on expression of reproduction-related genes in ovaries of *P. monodon*

In *P. monodon*, effects of dopamine on ovarian development have not been reported. Nevertheless, simultaneous injections of 5-HT (25 µg/g body weight) and the dopamine antagonist spiperone (1.5 or 5 µg/g body weight) induced ovarian maturation and spawning in wild *F. stylirostris* and pond-reared *L. vannamei* (Alfaro et al., 2004). Results from this thesis indicated that dopamine administration (10^{-6}

M/shrimp) resulted in significant lower expression of *PmCOMT* in ovaries of juvenile shrimp at 24 hpi ($P < 0.005$) but significant higher expression of *PmFAMeT* in ovaries of juvenile shrimp at 12 hpi ($P < 0.005$) compared to the treatment at 0 hpi. This was unexpected as dopamine should have stimulated the expression of rather *PmCOMT* than *PmFAMeT*. Accordingly, the experiments should be carefully repeated.

Effects of exogenous 5-HT on the reproductive performance of shrimp were reported (Vaca and Alfaro, 2000). 5-HT induced ovarian development of *P. monodon* (Wongprasert et al., 2006) and *M. rosenbergii* (Meeratana et al., 2006) dose dependently. Administration of 5-HT clearly promoted expression of *P. monodon* Ovarian-Specific Transcript (*Pm-OST1*) in ovaries of 5-month-old shrimp. *Pm-OST1* was up-regulated at 12-78 hpi ($P < 0.05$), with the highest expression level observed at 48 hpi ($P < 0.05$) (Klinbunga et al., 2009). Nevertheless, the effects of 5-HT on the expression levels of genes and/or proteins in the ovaries of *P. monodon* broodstock have not been reported.

In this study, effects of 5-HT on expression of *PmCOMT*, *PmFAMeT*, *PmBr-cZ1* and *PmBr-cZ4* in ovaries of 18-month-old *P. monodon* were examined. The injection of 5-HT resulted in increasing of *PmFAMeT* expression for at approximately 50-fold at 1 hpt but it has no effect on expression of other genes. Results clearly suggested that 5-HT plays the upstream effects but not the direct role on stimulation of steroidogenesis in ovaries of *P. monodon*. The molecular effects of 5-HT on *PmFAMeT* gene demonstrate the possible use of 5-HT in place of eyestalk ablation for enhancing ovarian/oocyte development in *P. monodon*.

Interestingly, administration of progesterone had no direct effects on promoting the expression of *PmCOMT*, *PmFAMeT* and *PmBr-cZ1* in ovaries of domesticated 14-month-old *P. monodon* but significantly affects expression of *PmBr-cZ4* at 48 and 72 hpi. The results also indicated that *PmFAMeT* gene products play the upstream effects preceding sex steroid resumption and maturation of ovarian/oocyte development.

Prechaphol et al. (2010) characterized *progesterin membrane receptor component 1* (*Pgmrc1*) of *P. monodon*. The full-length cDNA of *Pgmrc1* was 2015 bp in length containing an ORF of 573 bp corresponding to a polypeptide of 190 amino

acids. Northern blot analysis revealed a single form of *Pgmrc1* in ovaries of *P. monodon*. Quantitative real-time PCR indicated that the expression level of *Pgmrc1* mRNA in ovaries of both intact and eyestalk-ablated broodstock was greater than that of juveniles ($P < 0.05$). *Pgmrc1* was up-regulated in mature (stage IV) ovaries of intact broodstock ($P < 0.05$). Unilateral eyestalk ablation resulted in an earlier up-regulation of *Pgmrc1* since the vitellogenic (II) ovarian stage. Moreover, the expression level of *Pgmrc1* in vitellogenic, early cortical rod and mature (II–IV) ovaries of eyestalk-ablated broodstock was greater than that of the same ovarian stages in intact broodstock ($P < 0.05$). *Pgmrc1* mRNA was clearly localized in the cytoplasm of follicular cells, previtellogenic and early vitellogenic oocytes. Immunohistochemistry revealed the positive signals of the *Pgmrc1* protein in the follicular layers and cell membrane of follicular cells and various stages of oocytes. Therefore, *Pgmrc1* gene products seem to play the important role on ovarian development and may be used as the bioindicator for monitoring progression of oocyte maturation of *P. monodon*.

Progesterin acts as the maturation inducing factor resulting in resuming meiotic maturation of oocyte (Kishimoto, 1999, 2003). The further interesting issue is identification of the appropriate form(s) of progestins that result in the signal transduction pathway in oocytes of *P. monodon*.

The effects of 20E on expression of these genes in ovaries of juvenile *P. monodon* were carried out. The vehicle control (10% ethanol) seems to affect expression levels of *PmCOMT* and results were difficult to be interpreted. In contrast, the expression level of *PmFAMeT* in ovaries of cultured juveniles was obviously affected at 6-24 hpi while *PmBr-cZ1* and *PmBr-cZ4* were up-regulated at 168 hpi. The molecular effects of 5-HT on this expression should be further examined in both wild and domesticated broodstock to evaluate the use of ecdysteroids in combination with serotonin for enhancing ovarian/oocyte development in *P. monodon*.

Localization of *PmCOMT*, *PmFAMeT*, *PmBr-cZ1* and *PmBr-cZ4* transcripts and *PmCOMT* and *PmFAMeT* proteins in oocytes and ovaries of *P. monodon*

In situ hybridization was used to determine the ovarian localization of the mRNAs of reproduction-related genes in this study. *PmCOMT*, *PmFAMeT*, *PmBr-cZ1*

and *PmBr-cZA* were localized in ooplasm of previtellogenic oocytes in all ovarian stages of intact and eyestalk-ablated broodstock. Generally, more intense signals were observed in ovaries of eyestalk-ablated broodstock than intact broodstock. This simply revealed the effects of eyestalk ablation of transcript of examined genes. The finding suggested that these genes should be involved in oogenesis and ovarian development of *P. monodon*. Disappearance of hybridization signals of various genes in ooplasm of more mature stages (vitellogenic, early cortical rod and mature; stages II-IV) of oocytes may be due to significantly increasing oocytes sizes as oogenesis proceeded and low sensitivity of *in situ* hybridization on detecting gene expression per se (Klinbunga et al., 2009).

In situ hybridization signals of *PmFAMeT*, *PmBr-cZ1* and *PmBr-cZA* were not observed in follicular cells and more mature (vitellogenic cortical rod and mature) stages of oocytes. This further indicated cell-type specific expression of these transcripts in ovaries of *P. monodon* broodstock.

Immunohistochemistry gave the interesting issues on the possible translocation of PmCOMT and PmFAMeT proteins during oogenesis in *P. monodon*. The positive immunohistological signals of PmCOMT were detected in cytoplasm of previtellogenic and vitellogenic oocytes. Nevertheless, the positive signals were observed in cortical rods of oocytes in both intact and eyestalk-ablated broodstock. Similarly, the positive signals of PmFAMeT were detected in cortical rods of stages III and IV oocytes in both intact and eyestalk-ablated broodstock of *P. monodon*. It is hypothesized that PmCOMT and PmFAMeT were translated and initially localized in cytoplasm of earlier stages of oocytes before translocated into the cortical rods at the later stages of oogenesis.

***In vitro* expression of rPmFAMeT-l and rPmFAMeT-s proteins and Western blot analysis**

In this study, rPmCOMT, rPmFAMeT-s and rPmFAMeT-l were successfully expressed as the insoluble proteins in *E. coli*. The polyclonal antibodies against these recombinant proteins were successfully produced in rabbit. After affinity-chromatographic purification, anti-PmCOMT PcAb, anti-PmFAMeT-l PcAb and anti-PmFAMeT-s PcAb was used to study expression profiles and localization of a

particular protein by western blot analysis and immunohistochemistry (see above), respectively.

The expression profiles of *PmCOMT* mRNA and protein were slightly different. At the transcriptional level, the *PmCOMT* mRNA was stably transcribed but more intense signals of the PmCOMT protein were observed in previtellogenic and vitellogenic ovaries than those in cortical rod and mature ovaries of intact *P. monodon* broodstock. This implied that *PmCOMT* should be earlier translated since the early stages of ovarian development. The reduction of the translated protein in early cortical rod and mature ovaries suggested that the accumulated *PmCOMT* mRNA in oocytes is probably sufficient to be translated during the late stages of ovarian development in *P. monodon*.

Likewise, the expression profiles of *PmFAMeT* mRNA and protein were clearly different. The PmFAMeT transcripts were more abundantly transcribed during the final maturation of ovarian development. Nevertheless, the PmFAMeT protein was found in juveniles and stages I and II but not in stages III and IV ovaries of broodstock. The disappearance of this protein in more mature stages of ovaries of suggested more rapid translation of the PmFAMeT protein during previtellogenic and vitellogenic stages of ovarian development in *P. monodon*.

In the present study, the reproductive related genes of *P. monodon* were identified. The expression profile of various genes in ovaries of intact and eyestalk-ablated *P. monodon* broodstock implied that several key genes (from the same and/or different pathways) may contribute on ovarian development of *P. monodon*. Functionally analysis of genes and proteins involving ovarian development can be further carried out for better understanding of the reproductive maturation of female *P. monodon* in captivity.

CHAPTER V

CONCLUSIONS

1. The full length cDNAs of *PmCOMT*, *PmFAMeT*, *PmBr-cZl* and *PmBr-cZ4* were successfully characterized. *PmCOMT* and *PmBr-cZ4* was 1176 and 1879 bp in length containing the ORFs of 666 and 1329 bp corresponding to the polypeptides of 221 and 443 amino acids, respectively.
2. Two isoforms of *PmFAMeT* and *PmBr-cZl* were identified. The full length cDNA of *PmFAMeT-l* and *PmFAMeT-s* were 1312 and 1297 bp in length containing the ORFs of 843 and 828 bp corresponding to a protein of 280 and 275 amino acids, respectively. The full length cDNAs of *PmBr-CZl-l* and *PmBr-CZl-s* were 2119 and 1897 bp in length and contained the ORFs of 1443 and 1329 bp corresponding to a polypeptide of 481 and 443 amino acids, respectively.
3. Genomic organization of *PmCOMT* was characterized by genome walk analysis and overlapping PCR. The *PmCOMT* gene contained 3 exons (194, 111 and 361 bp) and 2 introns (143 and 147 bp).
4. Quantitative real-time PCR revealed differential expression of *PmFAMeT*, *PmBr-cZl* and *PmBr-cZ4* but comparable expression of *PmCOMT* during ovarian development of intact broodstock of wild *P. monodon*. Eyestalk ablation resulted in up-regulation of *PmBr-cZl*, down-regulation of *PmFAMeT* but had no effect on the expression level of *PmCOMT* and *PmFAMeT*.
5. Serotonin administration promoted the expression level of *PmFAMeT* in ovaries of 18-month-old shrimp approximately 50 fold at 1 hpi. Administration of 20E in commercially cultured juveniles resulted in the reduced expression level of *PmCOMT* but promoted the expression levels of *PmFAMeT*, *PmBr-cZl* and *PmBr-cZ4*.
6. *In situ* hybridization indicated that *PmFAMeT*, *PmBr-C Zl* and *PmBr-C Z4* was localized only in the cytoplasm of oogonia and previtellogenic oocytes while *PmCOMT* was localized in the cytoplasm of oogonia, previtellogenic oocytes and follicular cells in both intact and eyestalk-ablated broodstock.

7. Recombinant proteins of PmCOMT, PmFAMeT-1 and PmFAMeT-s were successfully expressed *in vitro*. Polyclonal antibodies against these recombinant proteins were produced in rabbit. Western blot analysis indicated that the PmCOMT protein was more preferentially expressed in earlier stages (previtellogenic and vitellogenic ovaries) than that of late stages (early cortical rod and mature ovaries) of ovarian development of *P. monodon*.

8. Immunohistochemistry suggested the translocations of both PmCOMT and PmFAMeT proteins during oogenesis in *P. monodon*. These proteins seemed to be translocated to the cortical rod during the maturation of oocytes.

9. The information suggested that *PmCOMT*, *PmPmFAMeT*, *PmBr-cZ1* and *PmBr-cZ4* play important roles on reproduction of *P. monodon*. In addition, the expression profiles of *PmPmFAMeT*, *PmBr-cZ1* and *PmBr-cZ4* can be used as the biomarker to monitor the reduced degree of ovarian maturation of *P. monodon* as a consequence effects of neurotransmitters, hormones and maturation diets.

References

- Alfaro, J., Zuniga, G., and Komen, J. 2004. Induction of ovarian maturation and spawning by combined treatment of serotonin and a dopamine antagonist, spiperone in *Litopenaeus stylirostris* and *Litopenaeus vannamei*. *Aquaculture* 236:511-522.
- Azevedo, B., A. Cortez, C. Abreu, and Carvalho, F. 2002. Ecdysteroids titres during the reproduction cycle in shrimp *Palaemon serratus* Pennant, 1777. Perfil de ecdisteroides en el ovario del camarón *Palaemon serratus* Pennant, 1777. a lo largo del ciclo reproductor 18:139-143.
- Brown, M.R., D.H. Sieglaff, and H.H. Rees. 2009. Gonadal ecdysteroidogenesis in arthropoda: occurrence and regulation. *Annual review of entomology* 54:105-125.
- Cahansky, A.V., Medesani, D.A. and Rodríguez, E.M. 2008. Induction of ovarian growth in the red claw crayfish, *Cherax quadricarinatus*, by the enkephalinergic antagonist naloxone: In vivo and in vitro studies. *Invertebrate Reproduction and Development* 51:61-67.
- Cardoso, A.M., Barros, C.M.F., Ferrer Correia, A.J., Cardoso, J.M., Cortez, A., Carvalho, F., and Baldaia, L. 1997. Identification of vertebrate type steroid hormones in the shrimp *Penaeus Japonicus* by tandem mass spectrometry and sequential product ion scanning. *Journal of the American Society for Mass Spectrometry* 8:365-370.
- Chan, S.M. 1995. Possible roles of 20-hydroxyecdysone in the control of ovary maturation in the white shrimp *Penaeus vannamei* (Crustacea: Decapoda). *Comparative Biochemistry and Physiology - C Pharmacology Toxicology and Endocrinology* 112:51-59.
- Chan, S.M., Chen, X.G., and Gu, P.L. 1998. PCR cloning and expression of the molt-inhibiting hormone gene for the crab (*Charybdis feriatus*). *Gene* 224:23-33.
- Chang, C.C., Wu, Z.R., Chen, C.S., Kuo, C.M., and Cheng, W. 2007. Dopamine modulates the physiological response of the tiger shrimp *Penaeus monodon*. *Aquaculture* 270:333-342.
- Chen, Y.N., Fan, H.F., Hsieh, S.L., and Kuo, C.M. 2003. Physiological involvement of DA in ovarian development of the freshwater giant prawn, *Macrobrachium rosenbergii*. *Aquaculture* 228:383-395.
- Clark, W.H.J., Yudin, A.I., Lynn, J.W. Griffin, F.J. and Pillai, M.C. 1990. Jelly layer formation in Penaeoidean shrimp eggs. *Biological Bulletin* 178:295-299.

- Clifford, H. C., and Preston, N. P. 2006 Genetic improvement; in Operating Procedures for Shrimp Farming: Global Shrimp OP Survey Results and Recommendations, pp. 73-77. Global Aquaculture Alliance, St. Louis, USA.
- Dubé, F., and Amireault, P. 2007. Local serotonergic signaling in mammalian follicles, oocytes and early embryos. Life Sciences 81:1627-1637.
- Fingerman, M. 1997. Roles of neurotransmitters in regulating reproductive hormone release and gonadal maturation in decapod crustaceans. Invertebrate Reproduction and Development 31:47-54.
- Fong, P.P., Deguchi, R., and Kyojuka, K. 1997. Characterization of serotonin receptor mediating intracellular calcium increase in meiosis-reinitiated oocytes of the bivalve *Ruditapes philippinarum* from Central Japan. Journal of Experimental Zoology 279:89-101.
- Gruntenko, N.E., and Rauschenbach, I.Y. 2008. Interplay of JH, 20E and biogenic amines under normal and stress conditions and its effect on reproduction. Journal of Insect Physiology 54:902-908.
- Gu, P.L., Chu, K.H. and Chan, S.M. 2001. Bacterial expression of the shrimp molt-inhibiting hormone (MIH): Antibody production, immunocytochemical study and biological assay. Cell and Tissue Research 303:129-136.
- Gunamalai, V., Kirubakaran, R. and Subramoniam, T. 2004. Hormonal coordination of molting and female reproduction by ecdysteroids in the mole crab *Emerita asiatica* (Milne Edwards). General and Comparative Endocrinology 138:128-138.
- Gunamalai, V., Kirubakaran, R., and Subramoniam, T. 2006. Vertebrate steroids and the control of female reproduction in two decapod crustaceans, *Emerita asiatica* and *Macrobrachium rosenbergii*. Current Science 90:119-123.
- Hansen, B.H., Altin, D., Hessen, K.M., Dahl, U., Breitholtz, M., Nordtug, T., and Olsen, A.J. 2008. Expression of ecdysteroids and cytochrome P450 enzymes during lipid turnover and reproduction in *Calanus finmarchicus* (Crustacea: Copepoda). General and Comparative Endocrinology 158:115-121.
- Harrison, K. E. (1990) The role of nutrition in maturation, reproduction and embryonic development of decapod crustaceans: A review. J. Shellfish Res. 9: 1-28.
- Huberman, A. 2000. Shrimp endocrinology. A review. Aquaculture 191:191-208.
- Hui, J.H.L., Tobe, S.S., and Chan., S.M. 2008. Characterization of the putative farnesoic acid O-methyltransferase (LvFAMEt) cDNA from white shrimp, *Litopenaeus vannamei*: Evidence for its role in molting. Peptides 29:252-260.

- Jalabert, B. 2005. Particularities of reproduction and oogenesis in teleost fish compared to mammals. Reproduction Nutrition Development 45:261-279.
- Jo, Q.T., Laufer, H., Biggers, W.J., and Kang, H.S. 1999. Methyl farnesoate induced ovarian maturation in the spider crab, *Libinia emarginata*. Invertebrate Reproduction and Development 36:79-85.
- Khamnamtong, B., Thumrunthanakit, S., Klinbunga, S., Aoki, T., Hirono, I., Menasveta, P., 2006. Identification of sex-specific expression markers in the Giant tiger shrimp, *J. Biochem. Mol. Biol.* 39:37-45.
- Kim, Y.K., Kawazoe, I., Jasmani, S., Ohira, T., Wilder, M.N., Kaneko, T., and Aida, K. 2007. Molecular cloning and characterization of cortical rod protein in the giant freshwater prawn *Macrobrachium rosenbergii*, a species not forming cortical rod structures in the oocytes. Comparative Biochemistry and Physiology - B Biochemistry and Molecular Biology 148:184-191.
- Klinbunga, S., Penman, D. J., McAndrew, B. J. and Tassanakajon, A. 1999. Mitochondrial DNA diversity in three populations of the giant tiger shrimp, *Penaeus monodon*. Mar. Biotechnol. 1: 113-121.
- Kruevaisayawan, H., Vanichviriyakit, R., Weerachathanukul, W., Magerd, S., Withyachumnarnkul, B., and Sobhon, P. 2007. Biochemical characterization and physiological role of cortical rods in black tiger shrimp, *Penaeus monodon*. Aquaculture 270:289-298.
- Kuballa, A.V., Guyatt, K., Dixon, B., Thaggard, H., Ashton, A.R., Paterson, B., Merritt, D.J., and Elizur, A. 2007. Isolation and expression analysis of multiple isoforms of putative farnesoic acid O-methyltransferase in several crustacean species. General and Comparative Endocrinology 150:48-58.
- Kuo, C.M., and Lin, W.W. 1996. Changes in morphological characteristics and ecdysteroids during the molting cycle of tiger shrimp, *Penaeus monodon* fabricus. Zoological Studies 35:118-127.
- Kyozuka, K., Deguchi, R., Yoshida, N. and Yamashita, M. 1997. Change in intracellular Ca²⁺ is not involved in serotonin-induced meiosis reinitiation from the first prophase in oocytes of the marine bivalve *Crassostrea gigas*. Developmental Biology 182:33-41.
- Lafont, R., and Mathieu, M. 2007. Steroids in aquatic invertebrates. Ecotoxicology 16:109-130.
- Lago-Lestón, A., Ponce, E., and Muñoz, M.E. 2007. Cloning and expression of hyperglycemic (CHH) and molt-inhibiting (MIH) hormones mRNAs from the

- eyestalk of shrimps of *Litopenaeus vannamei* grown in different temperature and salinity conditions. Aquaculture 270:343-357.
- Laufer, H., Homola, E., and Landau, M. 1991. Hormonal regulation of reproduction in female Crustacea. NOAA Technical Report NMFS 106: 89-98.
- Laufer, H., and Biggers, W.J. 2001. Unifying concepts learned from methyl farnesoate for invertebrate reproduction and post-embryonic development. American Zoologist 41:442-457.
- Laufer, H., Biggers, W.J., and Ahl, J.S.B. 1998. Stimulation of ovarian maturation in the crayfish *Procambarus clarkii* by methyl farnesoate. General and Comparative Endocrinology 111:113-118.
- Limsuwan, C. 2004. Diseases of Pacific white shrimp (*Litopenaeus vannamei*) cultured in Thailand. Proceeding of the JSPS-NRCT International Symposium Joint Seminar 2004: Management of Food Safety in Aquaculture and HACCP. pp. 36-41, Kasetsart University, Thailand.
- Liu, L., H. Laufer, Gogarten, P.J., and Wang, M. 1997. cDNA cloning of a mandibular organ inhibiting hormone from the spider crab *Libinia emarginata*. Invertebrate Neuroscience 3:199-204.
- Marsden, G., Hewitt, D., Boglio, E., Mather, P. and Richardson, N. 2008. Methyl farnesoate inhibition of late stage ovarian development and fecundity reduction in the black tiger prawn, *Penaeus monodon*. Aquaculture 280:242-246.
- Martínez, G., Pérez, M.A., Mettifogo, L., and Wolff, D. 2005. Extracellular Ca²⁺ requirement for serotonin-induced release and meiosis reinitiation from prophase in oocytes of the scallop *Argopecten purpuratus*. Invertebrate Reproduction and Development 47:117-124.
- Martins, J., Ribeiro, K., T. Rangel-Figueiredo, and Coimbra, J. 2007. Reproductive cycle, ovarian development, and vertebrate-type steroids profile in the freshwater prawn *Macrobrachium rosenbergii*. Journal of Crustacean Biology 27:220-228.
- Medina, A., Vila, Y., Mourente, G. and Rodríguez, A. 1996. A comparative study of the ovarian development in wild and pond-reared shrimp, *Penaeus kerathurus* (Forsk., 1775). Aquaculture 148:63-75.
- Meeratana, P., Withyachumnarnkul, B., Damrongphol, P., Wongprasert, K., Suseangtham, A., and Sobhon, P. 2006. Serotonin induces ovarian maturation in giant freshwater prawn broodstock, *Macrobrachium rosenbergii* de Man. Aquaculture 260:315-325.

- Meunpol, O., Iam-Pai, S., Suthikrai, W. and Piyatiratitivorakul, S. 2007. Identification of progesterone and 17 β -hydroxyprogesterone in polychaetes (*Perinereis* sp.) and the effects of hormone extracts on penaeid oocyte development in vitro. *Aquaculture* 270:485-492.
- Mishra, A., and Joy, K.P. 2006a. 2-Hydroxyestradiol-17 β -induced oocyte maturation in catfish (*Heteropneustes fossilis*) involves protein kinase C and its interaction with protein phosphatases. *Comparative Biochemistry and Physiology - A Molecular and Integrative Physiology* 144:416-422.
- Mishra, A., and Joy, K.P. 2006b. 2-Hydroxyestradiol-17 β -induced oocyte maturation: Involvement of cAMP-protein kinase A and okadaic acid-sensitive protein phosphatases, and their interplay in oocyte maturation in the catfish *Heteropneustes fossilis*. *Journal of Experimental Biology* 209:2567-2575.
- Mishra, A., and Joy, K.P. 2006c. HPLC-electrochemical detection of ovarian estradiol-17 β and catecholestrogens in the catfish *Heteropneustes fossilis*: Seasonal and periovulatory changes. *General and Comparative Endocrinology* 145:84-91.
- Mishra, A., and Joy, K.P. 2006d. Involvement of mitogen-activated protein kinase in 2-hydroxyestradiol-17 β -induced oocyte maturation in the catfish *Heteropneustes fossilis* and a note on possible interaction with protein phosphatases. *General and Comparative Endocrinology* 147:329-335.
- Nagaraju, G.P.C. 2007. Is methyl farnesoate a crustacean hormone? *Aquaculture* 272:39-54.
- Nagaraju, G.P.C., Suraj, N.J. and Reddy, P.S. 2003. Methyl farnesoate stimulates gonad development in *Macrobrachium malcolmsonii* (H. Milne Edwards) (Decapoda, Palaemonidae). *Crustaceana* 76:1171-1178.
- Nakatsuji, T., Lee, C.Y., and Watson, R.D. 2009. Crustacean molt-inhibiting hormone: Structure, function, and cellular mode of action. *Comparative Biochemistry and Physiology - A Molecular and Integrative Physiology* 152:139-148.
- Ohira, T., Okumura, T., Suzuki, M., Yajima, Y., Tsutsui, N., Wilder, M.N., and Nagasawa, H. 2006. Production and characterization of recombinant vitellogenesis-inhibiting hormone from the American lobster *Homarus americanus*. *Peptides* 27:1251-1258.
- Okumura, T., Kim, Y.K., Kawazoe, I. Yamano, K., Tsutsui, N. and Aida, K. 2006. Expression of vitellogenin and cortical rod proteins during induced ovarian development by eyestalk ablation in the kuruma prawn, *Marsupenaeus japonicus*. *Comparative Biochemistry and Physiology - A Molecular and Integrative Physiology* 143:246-253.

- Okumura, T., and Sakiyama, K. 2004. Hemolymph levels of vertebrate-type steroid hormones in female kuruma prawn *Marsupenaeus japonicus* (Crustacea: Decapoda: Penaeidae) during natural reproductive cycle and induced ovarian development by eyestalk ablation. Fisheries Science 70:372-380.
- Ongvarrasopone, C., Roshorm, Y., Somyong, S., Pothiratana, C., Petchdee, S., Tangkhabuanbutra, J., Sophasan, S., and Panyim, S. 2006. Molecular cloning and functional expression of the *Penaeus monodon* 5-HT receptor. Biochimica et Biophysica Acta - Gene Structure and Expression 1759:328-339.
- Palacios, E., Racotta, I.S., and Villalejo, M. 2003. Assessment of ovarian development and its relation to mating in wild and pond-reared *Litopenaeus vannamei* shrimp in a commercial hatchery. Journal of the World Aquaculture Society 34:466-477.
- Patio, R., Yoshizaki, G., Thomas, P., and Kagawa, H. 2001. Gonadotropic control of ovarian follicle maturation: The two-stage concept and its mechanisms. Comparative Biochemistry and Physiology - B Biochemistry and Molecular Biology 129:427-439.
- Peixoto, S., Coman, G. Arnold, S., Crocos, P., and Preston, N. 2005. Histological examination of final oocyte maturation and atresia in wild and domesticated *Penaeus monodon* (Fabricius) broodstock. Aquaculture Research 36:666-673.
- Peixoto, S., Wasielesky Jr, W., Martino, R.C., Milach, Â., Soares, R., and Cavalli, R.O. 2008. Comparison of reproductive output, offspring quality, ovarian histology and fatty acid composition between similarly-sized wild and domesticated *Farfantepenaeus paulensis*. Aquaculture 285:201-206.
- Preechaphol, R., Leelatanawit, R., Sittikankeaw, K., Klinbunga, S., Khamnamtong, B., Puanglarp, N., Menasveta, P., 2007. Expressed sequence tag analysis for identification and characterization of sex-related genes in the giant tiger shrimp *Penaeus monodon*. J. Biochem. Mol. Biol. 40:501-510.
- Qiu, G.F., Yamano, K., and Unuma, T. 2005. Cathepsin C transcripts are differentially expressed in the final stages of oocyte maturation in kuruma prawn *Marsupenaeus japonicus*. Comparative Biochemistry and Physiology - B Biochemistry and Molecular Biology 140:171-181.
- Quinitio, E.T., Caballero, R.M., and Gustilo, L. 1993. Ovarian development in relation to changes in the external genitalia in captive *Penaeus monodon*. Aquaculture 114:71-81.
- Quinitio, E.T., Hara, A., Yamauchi, K., and Nakao, S. 1994. Changes in the steroid hormone and vitellogenin levels during the gametogenic cycle of the giant tiger

- shrimp, *Penaeus monodon*. Comparative Biochemistry and Physiology - C Pharmacology Toxicology and Endocrinology 109:21-26.
- Ram, J.L., Fong, P.P., and Kyojuka, K. 1996. Serotonergic mechanisms mediating spawning and oocyte maturation in the zebra mussel, *Dreissena polymorpha*. Invertebrate Reproduction and Development 30:29-37.
- Reddy, P.R., Nagaraju, G.P.C., and Reddy, P.S. 2004. Involvement of methyl farnesoate in the regulation of molting and reproduction in the freshwater crab *Oziotelphusa senex senex*. Journal of Crustacean Biology 24:511-515.
- Richard, D.S., Jones, J.M., Barbarito, M.R., Cerula, S., Detweiler, J.P., Fisher, S.J., Brannigan, D.M., and Scheswohl, D.M. 2001. Vitellogenesis in diapausing and mutant *Drosophila melanogaster*: Further evidence for the relative roles of ecdysteroids and juvenile hormones. Journal of Insect Physiology 47:905-913.
- Richard, D.S., Watkins, N.L., Serafin, R.B., and Gilbert, L.I. 1998. Ecdysteroids regulate yolk protein uptake by *Drosophila melanogaster* oocytes. Journal of Insect Physiology 44:637-644.
- Rodríguez, E.M., López Greco, L.S., Medesani, D.A., Laufer, H., and Fingerman, M. 2002. Effect of methyl farnesoate, alone and in combination with other hormones, on ovarian growth of the red swamp crayfish, *Procambarus clarkii*, during vitellogenesis. General and Comparative Endocrinology 125:34-40.
- Rowley, A.F., Vogan, C.L., Taylor, G.W., and Clare, A.S. 2005. Prostaglandins in non-insectan invertebrates: Recent insights and unsolved problems. Journal of Experimental Biology 208:3-14.
- Sathyanandam, S., Vasudevan, S., and Natesan, M. 2008. Serotonin modulation of hemolymph glucose and crustacean hyperglycemic hormone titers in *Fenneropenaeus indicus*. Aquaculture 281:106-112.
- Senthilkumaran, B., and Joy, K.P. 2001. Perioviulatory changes in catfish ovarian oestradiol-17 β , oestrogen-2-hydroxylase and catechol-O-methyltransferase during GnRH analogue-induced ovulation and in vitro induction of oocyte maturation by catecholestrogens. Journal of Endocrinology 168:239-247.
- Silva Gunawardene, Y.I.N., Tobe, S.S., Bendena, W.G., Chow, B.K.C., Yagi, K.J., and Chan, S.M. 2002. Function and cellular localization of farnesoic acid O-methyltransferase (FAMeT) in the shrimp, *Metapenaeus ensis*. European Journal of Biochemistry 269:3587-3595.
- Soller, M., Bownes, M., and Kubli, E. 1999. Control of oocyte maturation in sexually mature *Drosophila* females. Developmental Biology 208:337-351.

- Spaziani, E.P., Hinsch, G.W. and Edwards, S.C. 1993. Changes in prostaglandin E2 and F2alpha during vitellogenesis in the Florida crayfish *Procambarus paeninsulanus*. Journal of Comparative Physiology - B Biochemical, Systemic, and Environmental Physiology 163:541-545.
- Spaziani, E.P., Hinsch, G.W., and Edwards, S.C. 1995. The effect of prostaglandin E2 and prostaglandin F(2?) on ovarian tissue in the Florida crayfish *Procambarus paeninsulanus*. Prostaglandins 50:189-200.
- Stanley, D. 2006. Prostaglandins and other eicosanoids in insects. Biological significance, 25-44.
- Stricker, S.A., and Smythe, T.L. 2000. Multiple triggers of oocytes maturation in nemertean worms: The role of calcium and serotonin. Journal of Experimental Zoology 287:243-261.
- Stricker, S.A., and Smythe, T.L. 2006a. Differing mechanisms of cAMP- versus seawater-induced oocyte maturation in marine nemertean worms I. The roles of serine/threonine kinases and phosphatases. Molecular Reproduction and Development 73:1578-1590.
- Stricker, S.A., and Smythe, T.L. 2006b. Differing mechanisms of cAMP- versus seawater-induced oocyte maturation in marine nemertean worms II. The roles of tyrosine kinases and phosphatases. Molecular Reproduction and Development 73:1564-1577.
- Styrishave, B., Lund, T., and Andersen, O. 2008. Ecdysteroids in female shore crabs *Carcinus maenas* during the moulting cycle and oocyte development. Journal of the Marine Biological Association of the United Kingdom 88:575-581.
- Subramoniam, T. 2000. Crustacean ecdysteroids in reproduction and embryogenesis. Comparative Biochemistry and Physiology - C Pharmacology Toxicology and Endocrinology 125:135-156.
- Sun, Y.D., Zhao, X.F., Kang, C.J., and Wang, J.X. 2006. Molecular cloning and characterization of Fc-TSP from the Chinese shrimp *Fennerpenaeus chinensis*. Molecular Immunology 43:1202-1210.
- Tan-Fermin, J.D., and Pudadera, R.A. 1989. Ovarian maturation stages of the wild giant tiger prawn, *Penaeus monodon* Fabricius. Aquaculture 66: 229-242.
- Tahara, D., and Yano, I. 2003. Development of hemolymph prostaglandins assay systems and their concentration variations during ovarian maturation in the kuruma prawn, *Penaeus japonicus*. Aquaculture 220:791-800.

- Tahara, D., and Yano, I. 2004. Maturation-related variations in prostaglandin and fatty acid content of ovary in the kuruma prawn (*Marsupenaeus japonicus*). Comparative Biochemistry and Physiology - A Molecular and Integrative Physiology 137:631-637.
- Tierney, A.J., Kim, T., and Abrams, R. 2003. Dopamine in crayfish and other crustaceans: Distribution in the central nervous system and physiological functions. Microscopy Research and Technique 60:325-335.
- Tinikul, Y., Joffre Mercier, A., Soonklang, N., and Sobhon, P. 2008. Changes in the levels of serotonin and dopamine in the central nervous system and ovary, and their possible roles in the ovarian development in the giant freshwater prawn, *Macrobrachium rosenbergii*. General and Comparative Endocrinology 158:250-258.
- Tiu, S.H.K., and Chan, S.M. 2007. The use of recombinant protein and RNA interference approaches to study the reproductive functions of a gonad-stimulating hormone from the shrimp *Metapenaeus ensis*. FEBS Journal 274:4385-4395.
- Treerattrakool, S., Panyim, S., Chan, S.M., Withyachumnarnkul, B., and Udomkit, A. 2008. Molecular characterization of gonad-inhibiting hormone of *Penaeus monodon* and elucidation of its inhibitory role in vitellogenin expression by RNA interference. FEBS Journal 275:970-980.
- Tsukimura, B., Nelson, W.K., and Linder, C.J. 2006. Inhibition of ovarian development by methyl farnesoate in the tadpole shrimp, *Triops longicaudatus*. Comparative Biochemistry and Physiology - A Molecular and Integrative Physiology 144:135-144.
- Tsutsui, N., Ohira, T., Kawazoe, I., Takahashi, A., and Wilder, M.N. 2007. Purification of sinus gland peptides having vitellogenesis-inhibiting activity from the whiteleg shrimp *Litopenaeus vannamei*. Marine Biotechnology 9:360-369.
- Umphrey, H.R., Lee, K.J., Watson, R.D., and Spaziani, E. 1998. Molecular cloning of a cDNA encoding molt-inhibiting hormone of the crab, *Cancer magister*. Molecular and Cellular Endocrinology 136:145-149.
- Wainwright, G., Webster, S.G., Wilkinsoit, M.C., Chung, J.S., and Rees, H.H. 1996. Structure and significance of mandibular organ-inhibiting hormone in the crab, *Cancer pagurus*: Involvement in multihormonal regulation of growth and reproduction. Journal of Biological Chemistry 271:12749-12754.
- Warrier, S.R., Tirumalai, R., and Subramoniam, T. 2001. Occurrence of vertebrate steroids, estradiol 17 β and progesterone in the reproducing females of the mud crab *Scylla serrata*. Comparative Biochemistry and Physiology - A Molecular and Integrative Physiology 130:283-294.

- Wongprasert, K., Asuvapongpatana, S., Poltana, P., Tiensuwan, M., and Withyachumnarnkul, B. 2006. Serotonin stimulates ovarian maturation and spawning in the black tiger shrimp *Penaeus monodon*. Aquaculture 261:1447-1454.
- Yamano, K., Qiu, G.F., and Unuma, T. 2004. Molecular cloning and ovarian expression profiles of thrombospondin, a major component of cortical rods in mature oocytes of penaeid shrimp, *Marsupenaeus japonicus*. Biology of Reproduction 70:1670-1678.
- Yano, I. 1995. Final oocyte maturation, spawning and mating in penaeid shrimp. Journal of Experimental Marine Biology and Ecology 193:113-118.
- Yano, I., and R. Hoshino. 2006. Effects of 17 β -estradiol on the vitellogenin synthesis and oocyte development in the ovary of kuruma prawn (*Marsupenaeus japonicus*). Comparative Biochemistry and Physiology - A Molecular and Integrative Physiology 144:18-23.
- Ye, H., Huang, H., Li, S., and Wang, G. 2008. Immunorecognition of estrogen and androgen receptors in the brain and thoracic ganglion mass of mud crab, *Scylla paramamosain*. Progress in Natural Science 18:691-695.
- Yi, K.K., Tsutsui, N., Kawazoe, I., Okumura, T., Kaneko, T., and Aida, K. 2005. Localization and developmental expression of mRNA for cortical rod protein in kuruma prawn *Marsupenaeus japonicus*. Zoological Science 22:675-680.



APPENDIX

ศูนย์วิทยทรัพยากร
จุฬาลงกรณ์มหาวิทยาลัย

APPENDIX A

Table C1 Raw data and relative expression levels of *PmCOMT* in different ovarian developmental stages of *P. monodon* based on semiquantitative RT-PCR analysis

Sample Groups	Densities of bands		Relative expression levels	Average	STDEV
	<i>EF-1α</i>	<i>PmCOMT</i>			
JNTT1	8249.03	1827.33	0.2215	0.3974	0.1821
JNTT2	6714.92	1738.63	0.2589		
JNTT3	6741.12	3756.57	0.5572		
JNTT4	5515.56	3044.72	0.5520		
BSTT1	7393.83	5431.79	0.7346	0.5595	0.2841
BSTT2	5267.18	4523.89	0.8588		
BSTT3	5113.62	1296.89	0.2536		
BSTT4	5545.39	2169.03	0.3911		
JNOV1	5771.42	20573.11	3.5646	3.2787	0.2695
JNOV2	6856.18	20915.73	3.0506		
JNOV3	6551.97	22623.12	3.4528		
JNOV4	5684.59	17319.34	3.0467		
BSOV1	5710.82	11014.18	1.9286	1.6116	0.4066
BSOV2	7695.28	21628.15	2.8105		
BSOV3	7033.19	14033.82	1.9953		
BSOV4	6255.73	13192.59	2.1088		

Table C2 Raw data and relative expression levels of *PmFAMeT* in different ovarian developmental stages of *P. monodon* based on semiquantitative RT-PCR analysis

Sample Groups	Densities of bands		Relative expression levels	Average	STDEV
	<i>EF-1α</i>	<i>PmFAMeT</i>			
JNTT1	8249.03	1827.33	0.2215	0.3974	0.1821
JNTT2	6714.92	1738.63	0.2589		
JNTT3	6741.12	3756.57	0.5572		
JNTT4	5515.56	3044.72	0.5520		
BSTT1	7393.83	5431.79	0.7346	0.5595	0.2841
BSTT2	5267.18	4523.89	0.8588		
BSTT3	5113.62	1296.89	0.2536		
BSTT4	5545.39	2169.03	0.3911		
JNOV1	5771.42	20573.11	3.5646	3.2787	0.2695
JNOV2	6856.18	20915.73	3.0506		
JNOV3	6551.97	22623.12	3.4528		
JNOV4	5684.59	17319.34	3.0467		
BSOV1	5710.82	11014.18	1.9286	1.6116	0.4066
BSOV2	7695.28	21628.15	2.8105		
BSOV3	7033.19	14033.82	1.9953		
BSOV4	6255.73	13192.59	2.1088		

Table C3 Raw data and relative expression levels of *PmBr-C ZI* in different ovarian developmental stages of *P. monodon* based on semiquantitative RT-PCR analysis

Sample Groups	Densities of bands		Relative expression levels	Average	STDEV
	<i>EF-1α</i>	<i>PmBr-C ZI</i>			
JNTT1	8249.03	1608.72	0.1950	0.2876	0.0711
JNTT2	6714.92	1998.19	0.2975		
JNTT3	6741.12	1953.70	0.2898		
JNTT4	5515.56	2031.05	0.3682		
BSTT1	7393.83	1616.51	0.2186	0.2609	0.0505
BSTT2	5267.18	1329.98	0.2525		
BSTT3	5113.62	1221.83	0.2389		
BSTT4	5545.39	1851.25	0.3338		
JNOV1	5771.42	8110.71	1.4053	1.2458	0.1067
JNOV2	6856.18	8265.27	1.2055		
JNOV3	6551.97	7799.91	1.1904		
JNOV4	5684.59	6720.77	1.1822		
BSOV1	5710.82	7470.56	1.3081	1.0984	0.1748
BSOV2	7695.28	8965.95	1.1651		
BSOV3	7033.19	7111.09	1.0110		
BSOV4	6255.73	5689.67	0.9095		

Table C4 Raw data and relative expression levels of *PmBr-C ZA* in different ovarian developmental stages of *P. monodon* based on semiquantitative RT-PCR analysis

Sample Groups	Densities of bands		Relative expression levels	Average	STDEV
	<i>EF-1α</i>	<i>PmBr-C ZA</i>			
JNTT1	8249.03	1565.10	0.2330	0.1404	0.0795
JNTT2	6714.92	1009.11	0.1496		
JNTT3	6741.12	774.43	0.1401		
JNTT4	5515.56	1002.05	0.1355		
BSTT1	7393.83	741.90	0.1408	0.1012	0.0445
BSTT2	5267.18	410.50	0.0802		
BSTT3	5113.62	269.11	0.0480		
BSTT4	5545.39	5305.15	0.9192		
JNOV1	5771.42	4668.93	0.6809	0.8544	0.3060
JNOV2	6856.18	3680.79	0.5617		
JNOV3	6551.97	7138.42	1.2557		
JNOV4	5684.59	2398.80	0.4200		
BSOV1	5710.82	3964.76	0.5152	0.4509	0.05366
BSOV2	7695.28	3327.16	0.4730		
BSOV3	7033.19	2474.65	0.3955		
BSOV4	6255.73	1565.10	0.2330		

Biography

Mr. Arun Buaklin was born on January 31, 1980 in Sukhothai Province, Thailand. He graduated with the degree of Bachelor of Science (Biotechnology) from Chiang mai University in 2002 and the degree of Master of Science (Biotechnology) at the Program of Biotechnology, Chulalongkorn University in 2006.



ศูนย์วิทยทรัพยากร
จุฬาลงกรณ์มหาวิทยาลัย